A UNITED STATES DEPARTMENT OF COMMERCE PUBLICATION

NBS MONOGRAPH 137

Applications of Waveguide and Circuit Theory to the Development of Accurate Microwave Measurement Methods and Standards

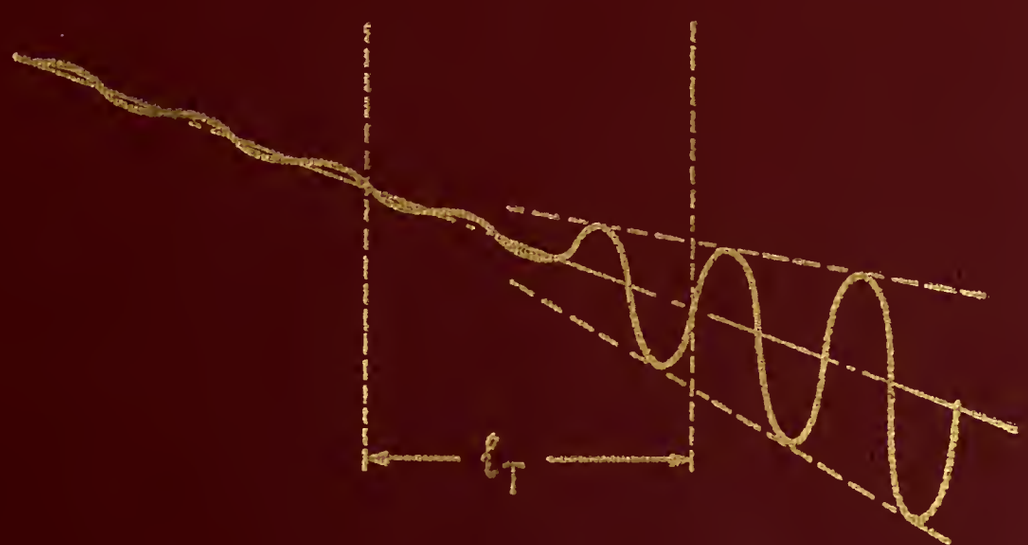

U.S. DEPARTMENT OF COMMERCE
National Bureau of Standards

Applications of Waveguide and Circuit Theory to the Development of Accurate Microwave Measurement Methods and Standards

R. W. Beatty

Institute for Basic Standards
National Bureau of Standards
Boulder, Colorado 80302

U.S. DEPARTMENT OF COMMERCE, Frederick B. Dent, *Secretary*
NATIONAL BUREAU OF STANDARDS, Richard W. Roberts, *Director*

Issued August 1973

Library of Congress Catalog Number: 73-600158

National Bureau of Standards Monograph 137

Nat. Bur. Stand. (U.S.), Monogr. 137, 322 pages (Aug. 1973)

CODEN: NBSMA6

For sale by the Superintendent of Documents, U.S. Government Printing Office, Washington, D.C. 20402
(Order by SD Catalog No. C13.44:137). Price $5.20. Stock Number 0303–01169

Contents

ABSTRACT

The basic theory and analytical methods used in the development of accurate microwave measurement methods and standards are presented.

Developments at the U.S. National Bureau of Standards during 1948-1968 are described in which the above theory and analytical methods were applied.

These developments were in the fields of power, impedance, attenuation and phase shift, and led to the establishment of National Standards and calibration methods at frequencies from about 300 MHz to 30 GHz.

Key words: Attenuation definitions; attenuation measurement; barretter mount efficiency; coaxial connectors; impedance measurement; microwave network theory; mismatch errors; phase shift-measurement; power measurement; reflectometers; waveguide joints; waveguide theory.

PREFACE

The purpose of this monograph is to show how microwave waveguide and circuit theory was formulated and applied to the development of accurate measurement methods and standards at the U.S. National Bureau of Standards.

The topics of power, impedance, attenuation, and phase shift standards and measurement techniques have been selected for discussion. Appropriate research papers by the author and his associates have been partially revised and updated for the above purposes. In addition, new material, especially on attenuation definitions, has been included.

It is not possible here to present a complete history of NBS research in this area, nor to accurately describe the present state-of-the-art. However, an attempt has been made to put the work in perspective by giving references to previous and subsequent NBS pertinent research.

It is intended that this monograph will indicate the character and extent of the research which must be performed in order to develop accurate microwave measurement methods and standards at the highest level. It is hoped that the collected works and discussions will be helpful and stimulating to other workers in the same general field.

ACKNOWLEDGMENTS

This NBS monograph is a partially revised version of a doctoral thesis presented to the Department of Electronic Engineering of the University of Tokyo, Tokyo, Japan. It describes research done partly while the author was an employee of the U.S. National Bureau of Standards (NBS) since 1948 and partly while a guest worker in 1970-71 with the Electrotechnical Laboratory (ETL) Tanashi Branch, Tanashi, Tokyo, Japan.

Thus, the author is indebted to personnel of NBS, ETL, and the University of Tokyo in completing the work. The work could not have been accomplished without the approval and encouragement of Dr. Lewis M. Branscomb, Former Director of NBS, and Dr. Fusao Mori, Director of ETL. The support at NBS of Dr. Ernest Ambler, Director of the Institute for Basic Standards (IBS), Mr. Bascom W. Birmingham, Deputy Director, IBS at Boulder, Colorado, and Dr. Raymond C. Sangster, Chief, Electromagnetics Division, is gratefully acknowledged. At ETL, the strong support of Dr. Kenjiro Sakurai, Chief of the Radio- and Opto-Electronics Division, Dr. Hideo Yamanaka, Chief of the Opto-Electronics Section, Mr. Ryunosuke Ishige, Chief of the Radio Electronics Section, Dr. Hiroshi Kashiwagi, of the Laser Section, and Dr. Toshio Nemoto is most gratefully acknowledged. At the University of Tokyo, the counsel and supervision received from Prof. Sogo Okamura, Faculty of Engineering, Department of Electronic Engineering, was especially helpful, and essential for the completion of the work.

The help of many co-workers and associates at NBS and elsewhere in stimulating and carrying out the research is acknowledged as follows: Dr. David M. Kerns, Senior Research Scientist at NBS, associate of the author since 1948 and leading NBS specialist in electromagnetic theory for rf measurement, taught courses, wrote tutorial and research papers laying solid foundations upon which many of the NBS microwave standards are based, and stimulated the author's work through many helpful discussions. His influence and assistance are particularly strong in the theoretical portion of this monograph. Much of the material in chapter 2 is derived from his part 1 of our book (see list of references: Kerns and Beatty, 1967), and sections 2.3c(2), 2.3d, and 2.3e are taken directly from his writings. Dr. Glenn F. Engen, a co-worker since 1954, contributed to the research on tuned reflectometers, attenuation from power measurements, and measurements of connector reflections and losses. Mr. Wilbur J. Anson contributed to the work on impedance standards and the hybrid reflectometer. Mr. William E. Little, Mr. B. C. Yates, and Mr. G. E. Fentress contributed to the research on impedance standards, intrinsic attenuation, and the

measurement of small losses. Dr. George E. Schafer (now at the U.S. Army Electronics Proving Ground, Fort Huachuca, Arizona) was closely associated with the author in carrying out the research on phase shift standards.

Mr. A. C. MacPherson (now at the U.S. Naval Research Laboratory, Anacostia, D.C.) contributed to the work on mismatch errors in microwave power measurements and Mr. Frank Reggia (now at the Harry Diamond Laboratories, Washington D.C.) contributed to the research on the measurement of barretter mount efficiency.

Discussions with Dr. Bruno O. Weinschel of Weinschel Engineering Co., Gaithersburg, Md., stimulated and influenced the research on attenuation definitions. Dr. Paul F. Wacker's review of the theoretical portions was very helpful.

Finally, the author is especially grateful to Mrs. Anne Y. Rumfelt who carefully and thoroughly read the manuscript and made many helpful suggestions and corrections. Miss Sharon Foote, Mrs. Florence M. Indorf, and Miss Janet Becker typed the manuscript and put it into proper form for the NBS Publications Section.

APPLICATIONS OF WAVEGUIDE AND CIRCUIT THEORY TO THE DEVELOPMENT OF ACCURATE MICROWAVE MEASUREMENT METHODS AND STANDARDS

R. W. Beatty

National Bureau of Standards

Boulder, Colorado

The basic theory and analytical methods used in the development of accurate microwave measurement methods and standards are presented.

Developments at the U.S. National Bureau of Standards during 1948-1968 are described in which the above theory and analytical methods were applied.

These developments were in the fields of power, impedance, attenuation and phase shift, and led to the establishment of National Standards and calibration methods at frequencies from about 300 MHz to 30 GHz.

Key words: Attenuation definitions; attenuation measurement; barretter mount efficiency; coaxial connectors; impedance measurement; microwave network theory; mismatch errors, phase shift measurement; power measurement; reflectometers; waveguide joints; waveguide theory.

1. Introduction

1.1. General

This monograph presents a formulation of waveguide and circuit theory with selected applications to the development of accurate measurement methods and standards. A portion of the research at the U.S. National Bureau of Standards by the author and co-workers during the period 1948-1968 is described.

Although considerable work had been done prior to 1948 in the field of microwave measurements at the M.I.T. Radiation Laboratory and other laboratories, much remained to be accomplished before U.S. radio frequency and microwave standards and calibration services could be established.

The theory of waveguides and of microwave circuits needed to be re-examined and the foundations exposed and strengthened. The quantities to be measured needed to be precisely defined, and the conditions under which the theory remains valid needed to be clearly stated. New and refined measurement techniques and standards needed to be developed. Errors needed to be analyzed and limits of uncertainty evaluated.

In the following, the above points are illustrated with specific examples. In Chapters 2 and 3, respectively, a formulation of waveguide and circuit theory is given which is slanted towards measurement applications. Selected applications are given in Chapters 4 through 7, respectively, for the topics of power, impedance, attenuation, and phase shift.

1.2. Theory

Waveguide and circuit theory is presented in Chapters 2 and 3, respectively. Although this theory must be considered well-known, it has previously not been as clearly presented in a form convenient for measurement applications. Greater attention is paid to fundamental aspects of the theory, the assumptions made, and the conditions required for validity.

The waveguide theory of Chapter 2 applies mainly to lossless,[1] uniform cylindrical waveguides of arbitrary cross-section. A rigorous and general treatment of this subject has been published (Kerns and Beatty, 1967). Much of the same material is presented in this monograph, from a somewhat less general point of view, but with specific applications in mind.

First, the basic terms "waveguide junction," "waveguide leads," "terminal surface" and "terminal variables" are defined in section 2.1. Two sets of terminal variables are discussed in section 2.2. One set consists of quantities v and i which are generalizations of voltage and current. The other set are the complex amplitudes a and b of the traveling waves which interfere to give rise to the generalized voltage and current. These terminal variables are related to the waveguide fields corresponding to a given mode in a given waveguide.

The theory of waveguides leading to modal equations is based upon assumptions of uniform, cylindrical waveguide geometry, and freedom from dissipative loss and from leakage. As shown in Chapter 2 the transverse fields for a given mode can each be resolved into two components; one in the complex plane, and one vector (space) component. The complex components denoted by the letters v and i are regarded as generalizations of voltage and current. Under certain conditions, they may be made to coincide with actual voltage and current in transmission lines.

---

[1] The case of small losses is not treated in Chapter 2, but is illustrated in a later example (sec. 5.3).

It further develops that these variables may be referred to a given terminal surface in a waveguide which is part of a waveguide junction (a microwave network or circuit). When so referred, they may be regarded as terminal variables, similar to the familiar terminal variables "voltage" and "current" encountered in lumped element network theory. It follows that conventional network theory may be applied to the analysis of microwave circuits involving waveguides.

Power and impedance normalization are discussed and normalization factors are defined. The consequences of some specific choices of these factors are explored and a scheme for suppressing them for convenience in manipulating circuit equations is given. The concept of "characteristic impedance" is clarified.

General power relationships for waveguide junctions are examined and the realizability conditions (including lossnessness) are precisely stated. In addition, the reciprocity condition is given in matrix form. Finally, representation of sources by terminal variables and impedances or reflection coefficients is discussed together with the simple, but important, equations for joining together elements of waveguide circuits.

Following the presentation of the general theory, special theory for two-arm waveguide junctions (2-ports) is developed in Chapter 3, along lines considered useful for analysis of measurement circuits. Some theory for 3-ports and 4-ports is also developed.

Special emphasis is given to the use of scattering coefficients and they are used in developing equations for many basic concepts. For example, efficiency, mismatch loss, substitution loss, transducer loss, insertion loss, and attenuation of a 2-port network are all carefully defined and equations given. The concepts of phase difference and phase shifts associated with a 2-port are introduced. Transmission phase shift, insertion phase shift, and differential phase shift are defined. Analytical tools based upon the cascading of 2-port networks and upon the transformation of reflection coefficient by a 2-port network are presented.

The realizability, reciprocity, and lossless conditions on the scattering coefficients of 3-port networks are given. Scattering matrices for circuit elements such as directional couplers and circulators are given. Finally, the basic circuit used in many measurement applications, consisting of a source, a 3-port network, a detector, and load, is analyzed and equations are presented.

1.3. Applications

In Chapters 4 through 7, applications of the theory and analytical techniques to the development of accurate measurement methods and standards are given.

The mismatch errors in the calibration and use of microwave power meters were originally quite large. Application of the foregoing theory led to the reduction of these errors and made possible the evaluation of limits of uncertainty as stated in the calibration reports. In 4.2, the analysis and pertinent equations are presented.

In 4.3, the development of an improved method for measuring efficiencies of barretter mounts is described. This work resulted in the first accurate determination of efficiencies of coaxial barretter mounts. The analysis in terms of scattering and reflection coefficients was found useful in later developments.

Applications to impedance or reflection coefficient measurement techniques and standards are discussed in Chapter 5. The adjustable sliding termination described in 5.2 is an improvement on previous designs. It employs a simple resistive strip which can rotate and move relative to a short-circuit, in such a way as to produce reflection coefficients ranging from zero to nearly unity. The entire termination is designed to be slid inside a waveguide so that the phase of the reflection coefficient can be varied. This has proven to be a useful tool in measurement applications.

In section 5.3, formulas, graphs, and conductivity data are presented to aid any laboratory in designing and evaluating impedance standards consisting of quarter-wavelength short-circuited sections of coaxial line or rectangular waveguide. All standard sizes are covered over a frequency range from 200 MHz to 330 GHz.

A number of interesting circuits yielding squared VSWR response are analyzed in 5.4. An even more useful development is "magnified response." It permits very sensitive measurements of small reflection coefficients or of small differences between impedances which are almost equal. The application of these techniques to a modified phasable load method of impedance measurement is indicated.

The adjustment of tuners for some impedance measurement applications is described in 5.5. The use of tuners led to the development of the tuned reflectometer, which, together with the quarter-wavelength short-circuit standard, became the most accurate calibration technique for reflection coefficient standards.

An interesting variation of the tuned reflectometer is described in 5.6. It consists of constructing a tuned reflectometer using rectangular waveguide components, except for the output waveguide, which is coaxial. One then slides loads in the coaxial section and adjusts the tuners belonging to the rectangular waveguide instruments. Once adjusted, it is used to measure reflection coefficients of coaxial terminations and devices.

The tuned reflectometer is also used to measure the reflections and losses of waveguide joints or coaxial connectors by a sensitive technique described in 5.7.

There are many applications of microwave circuit theory to attenuation measurements as discussed in Chapter 6. The subject of attenuation definitions is discussed at some length in 6.2. Circuit theory is used to clearly show different results from different definitions. Precise definitions suitable for highly accurate measurement applications are formulated and the conditions of measurement are tightly specified.

The error due to mismatch often causes the greatest uncertainty in attenuation measurements. Mismatch effects in cascade-connected attenuators are analyzed in 6.3 and mismatch errors in measuring fixed and variable attenuators are treated in 6.4. Usually, only the magnitudes of the reflection coefficients of the circuits and the attenuators are measured or estimated when evaluating mismatch errors. Of course, the phases are also involved, but it is assumed that they can take on any value, and the limits of error are calculated, assuming the most unfavorable conditions. Actually, the realizability conditions limit the range over which reflection coefficient phases can vary. Thus the limits of error calculated by the above method may be too conservative in some cases. In 6.5, it is shown that the effect of realizability on error limit calculations is practically unimportant except for low-loss attenuators, below, say 1 decibel.

In most analytical techniques, an attenuator is represented by a simple 2-port network. However, this model gives no information regarding the effect of imperfections of connectors or adapters. A more complicated model is required, and this is discussed fully in 6.6.

In sections 6.7 and 6.8, techniques for measuring attenuation are described. The first makes use of the theory of linear fractional transformation of reflection coefficient. The second technique is a simple measurement of power ratio, but is refined to give unprecedented accuracy. Circuit theory is applied to evaluate small mismatch errors which contribute to the uncertainty of the measurement.

The measurement of small attenuations, such as losses in waveguide joints and in short sections of waveguide, by a 2-channel nulling method is described in section 6.9. A circuit for producing known, very small changes of attenuation or phase shift is described in section 6.10.

The topic of phase shift measurements and standards at microwave frequencies was long neglected. In section 7.2, phase shift equations for 2-ports are presented. The development of the tuned reflectometer made possible one form of microwave phase shift standard. The phase of the reflectometer output signal is made to closely track the position of a short-circuit sliding in a precision waveguide. Phase measurements then reduce to a measurement of frequency and of mechanical displacements and dimensions. The errors in such a standard were analyzed in 7.3.

A modification of the tuned reflectometer circuit was developed using two short-circuits sliding in waveguides of slightly different widths in order to produce known, small phase shifts. This is the basic principle of the differential phase shifter described in 7.4.

Finally, the definitions of phase shift of various terminal variables are analyzed and equations are derived in 7.2. The concept of an ideal phase shifter is examined. This section, together with 3.10, gives a number of basic phase shift equations useful in the analysis of phase shift measuring circuits.

1.4. Conclusions and References

In section 8, it is concluded that the foregoing applications of the theory demonstrate its usefulness in developing accurate standards and measurement methods. The steps in the development include precise definitions of the quantities to be measured, development and evaluation of accurate standards and measuring techniques, and the analysis and evaluation of errors.

A list of references, arranged alphabetically by the name of the senior author, is given in section 9. The references not only support the work described but indicate later work which extended or superseded the earlier work.

2. Basic Theory of Waveguide Junctions

2.1. Definitions

a. Waveguide Junctions

A "waveguide junction" is not simply a junction where some waveguides come together and are joined where their walls intersect. The term has a broader meaning but includes such simple junctions. For purposes of analysis, a waveguide junction is considered to be an idealized representation of a given actual electromagnetic device to which access is provided by means of waveguides.

Such a waveguide junction is linear and has uniform, lossless, cylindrical waveguide leads which may be of arbitrary cross-section. It does not leak, or, in other words, electromagnetic energy enters and leaves only thru waveguide leads.

In general, sources may be present inside the junction and there may be attenuated modes present in the waveguide leads. However, in this monograph, these possibilities are both excluded from consideration.

b. Terminal Surfaces and Terminal Variables

The outer boundaries of a waveguide junction are perfectly conducting surfaces which prevent the flow of electromagnetic energy except inside the waveguide leads. The waveguide junction may be considered to terminate somewhere inside the waveguide leads at terminal surfaces which may be arbitrarily chosen. For convenience, they are usually chosen to be planes perpendicular to the waveguide axes.

In order to provide a convenient measure of the flow of electromagnetic energy in the waveguide leads, quantities such as v and i are defined which are derived from the transverse electric and magnetic fields at the terminal surfaces. These quantities are called "terminal variables" and usually a set of two suffices to characterize the flow of energy in a given mode in a given waveguide lead. If more than one mode is propagating in a given waveguide lead, there is a different set of terminal variables associated with each mode.

2.2. v, i, a and b for Waveguide[1]

a. Introduction

It is convenient to define quantities denoted as v and i for waveguide that behave in a similar way to voltage and current in lumped circuit element networks. Then it becomes possible to apply conventional circuit theory to the analysis of waveguide junctions and circuits.

The quantities called v and i are derived from the transverse components E_t and H_t of the electric and magnetic complex vector field amplitudes corresponding to a given waveguide mode. For example, E_t is written as the product of two factors, v and e^0. The factor v is complex and represents the time variation and phase of the field. The factor e^0 is a vector function which gives the relative strength and direction of the field in the waveguide (i.e., the mode pattern).

If there is more than one mode propagating in the waveguide, then a different v and i are obtained corresponding to each mode (also a different e^0 and h^0).

We write expressions for E_t and H_t in terms of complex and vector potential functions and then obtain v, i, e^0 and h^0 in terms of them. In order to make v and i behave like voltage and current, it is necessary to examine power and wave impedance relationships and then define power and impedance normalization constants W_0 and Z_0. The consequences of choosing these constants in different ways are discussed. For example, by a suitable choice of Z_0, v and i can be made to coincide with actual voltage and current in a coaxial waveguide operating in the TEM-mode (transmission line).

b. Basic Derivation of v, i, e^0 and h^0

For a given mode at a given terminal surface in a waveguide, we resolve E_t and H_t into factors as follows:

$$E_t = v\, e^0, \text{ and}$$

$$H_t = i\, h^0, \tag{2.1}$$

where v and i are complex and contain the information representing sinusoidal time variation in the complex plane, and e^0 and h^0 contain information about the relative magnitudes and directions of the transverse field components. We call v and i

[1]The principal concepts and conditions underlying the definitions of these symbols are given in Kerns (1967).

respectively, generalized voltage and current, and we call e^0 and h^0 the basis fields for a given waveguide mode.

Since E_t and H_t may be expressed in terms of complex and vector potential functions, it is also possible to express, v, i, e^0 and h^0 in terms of these functions as will be shown.

c. Complex and Vector Potential Functions

Let the axis of the waveguides be the z-axis and let the direction of propagation be the +z-direction. Waveguide field equations may be derived from Hertz potentials of the form

$$\Pi = f \phi e_z, \tag{2.2}$$

where f is a function only of the transverse coordinates, ϕ is a function only of z, e_z is the unit vector in the +z-direction, and Π satisfies the vector wave equation

$$\nabla^2\Pi + k^2\Pi = 0, \text{ where } k^2 = \omega^2\mu\varepsilon. \tag{2.3}$$

We obtain a scalar wave equation

$$\nabla^2 f + K^2 f = 0, \tag{2.4}$$

where the solutions for f depend upon the boundary conditions corresponding to a given waveguide. We also obtain a one-dimensional wave equation in ϕ whose solution is

$$\phi = Ae^{-\gamma z} + Be^{\gamma z}, \tag{2.5}$$

where the propagation constant $\gamma = \alpha + j\beta$.

For TM (transverse magnetic) fields it can be shown (Kerns and Beatty, 1967) that

$$E = \nabla\times\nabla\times\Pi = \phi'\nabla f + K^2 f\phi e_z$$

$$H = j\omega\varepsilon\nabla\times\Pi = j\omega\varepsilon\phi(\nabla f\times e_z), \tag{2.6}$$

and for TE (transverse electric) fields,

$$E = -j\omega\mu\nabla\times\Pi = -j\omega\mu\phi(\nabla g\times e_z)$$

$$H = \nabla\times\nabla\times\Pi = \phi'\nabla g + K^2 g\phi e_z, \tag{2.7}$$

where g has been used instead of f because it is subject to different boundary conditions.

Some examples of f and g functions for certain waveguide cross-sections follow.

For rectangular waveguide of width a and height b, application of the boundary conditions yields (Kerns and Beatty, 1967);

For TM-modes

$$f_{mn} = \sin\left(\frac{m\pi x}{a}\right) \sin\left(\frac{n\pi y}{b}\right)$$

$$K_{mn}^2 = \left(\frac{m\pi}{a}\right)^2 + \left(\frac{n\pi}{b}\right)^2. \tag{2.8}$$

For TE-modes

$$g_{mn} = \cos\left(\frac{m\pi x}{a}\right) \cos\left(\frac{n\pi y}{b}\right)$$

$$K_{mn}^2 = \left(\frac{m\pi}{a}\right)^2 + \left(\frac{n\pi}{b}\right)^2. \tag{2.9}$$

For the TEM-mode in coaxial waveguide in which ρ denotes the radial coordinate, we obtain

$$f = C_1 \ln \rho + C$$

$$K^2 = 0 \tag{2.10}$$

In general, we can write for the transverse field components in the case of TM-modes

$$E_t = \phi' \nabla f = v e^0$$

$$H_t = j\omega\varepsilon\phi(\nabla f \times e_z) = i h^0, \tag{2.11}$$

where $v \propto \phi'$, $e^0 \propto \nabla f$, $i \propto j\omega\varepsilon\phi$, and $h^0 \propto (\nabla f \times e_z)$.

The corresponding relationships for TE-modes are

$$E_t = -j\omega\mu\phi(\nabla g \times e_z) = v e^0$$

$$H_t = \phi' \nabla g = i h^0, \tag{2.12}$$

where $v \propto -j\omega\mu\phi$, $e^0 \propto (\nabla g \times e_z)$, $i \propto \phi'$, and $h^0 \propto \nabla g$.

The constants of proportionality are to be determined, and will be done so in the most convenient manner in the following.

d. Power and Impedance Normalization

Consider the relationships for power P, (integral of Poynting's vector across the terminal surface) and wave impedance Z_w in terms of E_t and H_t. We write the following

$$P = \mathrm{Re}(W), \text{ where} \tag{2.13}$$

$$W = \frac{1}{2} \int E_t \times \bar{H}_t \cdot e_z \, ds, \text{ or} \tag{2.14}$$

$$W = (\bar{i}v)\,\frac{1}{2}\int e^0 \times h^0 \cdot e_z \, ds, \text{ or} \tag{2.15}$$

$$W = (\bar{i}v) \cdot W_0, \tag{2.16}$$

$$\text{where } W_0 = \frac{1}{2}\int e^0 \times h^0 \cdot e_z \, ds. \tag{2.17}$$

W_0 is a power normalizing constant to be chosen for convenience. For example, if i and v denote root-mean-square (rms) complex amplitudes, it is convenient to choose $W_0 = 1$, so that $P = \mathrm{Re}(\bar{i}v)$. Once the value of W_0 has been chosen, it fixes the product $|e^0 h^0|$ for a given mode in a waveguide.

Next, we write the following expression for the wave impedance Z_w for a given mode in a given waveguide

$$Z_w = \frac{e_z \times E_t^+}{H_t^+} = \frac{v^+}{i^+} \cdot \frac{e_z \times e^0}{h^0} = Z_0 \, Z_w^0 \tag{2.18}$$

In this expression, E_t^+ and H_t^+ are the transverse components of the electric and magnetic field waves traveling in the +z-direction, v^+ and i^+ are the corresponding traveling waves of "voltage" and "current," Z_w^0 is the "wave impedance" of the basis fields e^0 and h^0, and Z_0 is an impedance normalization constant.

It can be seen that Z_0 is proportional to the wave impedance Z_w, and the constant of proportionality $1/Z_w^0$ is real (since e^0 and h^0 are not complex) and dimensionless (since Z_w and Z_0 have the dimensions of ohms). Note that the dimensions of W_0, Z_0, v and i can be chosen in several different ways, but the choice used here is considered to be the most convenient for use in circuit analysis.

e. Examples of Waveguide v and i

(1) TEM-mode in Coaxial Waveguide

The familiar coaxial waveguide operating in the TEM-mode (transmission line mode) is an interesting example of convenient choices of normalizing constants W_0 and Z_0. Depending upon how they are chosen, v and i can be made to coincide with actual voltage and current in the transmission line. This is shown as follows. It has been shown (Kerns and Beatty, 1967) that the potential function f for the TEM-mode in coaxial waveguide is of the form [see eq. (2.10)]

$$f = C_1 \ln \rho + C,$$

where the cylindrical coordinates ρ, θ, and z apply, and the radii a and b, with $b > a$, are used. Following eq. (2.11), let

$$e^0 = f = \frac{1}{\rho} C_1 e_\rho$$

$$h^0 = C_3(f \times e_z) = \frac{1}{\rho} C_2 e_\theta \tag{2.19}$$

In the above equation, e_z, e_ρ, and e_θ are unit vectors and $C_2 = C_3 C$.

The power normalization factor W_0 is

$$W_0 = \frac{1}{2} \int_S e^0 \times h^0 \cdot e_z \, ds = \frac{C_1 C_2}{2} \int_a^b \frac{2\pi\rho}{\rho^2} \, d\rho = \pi C_1 C_2 \ell n \frac{b}{a} \tag{2.20}$$

The relationship involving the impedance normalization factor Z_0 is

$$\frac{Z_w}{Z_0} = \frac{1}{Z_0}\sqrt{\frac{\mu}{\varepsilon}} = \frac{e_z \times e^0}{h^0} = \frac{C_1}{C_2} \tag{2.21}$$

Solving for C_1 and C_2, we obtain

$$C_1 = \sqrt{\sqrt{\frac{\mu}{\varepsilon}} \cdot \frac{W_0}{\pi Z_0 \ell n \frac{b}{a}}} \tag{2.22}$$

$$C_2 = \sqrt{\frac{W_0 Z_0}{\pi\sqrt{\frac{\mu}{\varepsilon}} \ell n \frac{b}{a}}} \tag{2.23}$$

Now consider the actual rms voltage V and current I in the transmission line in terms of their line integral definitions.

$$V = \frac{1}{\sqrt{2}} \int_a^b E_t \cdot d\ell = v\left(\frac{1}{\sqrt{2}} \int_a^b e^0 \cdot e_\rho \, d\rho\right), \text{ or}$$

$$V = v\sqrt{\sqrt{\frac{\mu}{\varepsilon}} \frac{W_0}{2\pi Z_0} \ell n \frac{b}{a}}, \quad \text{and} \tag{2.24}$$

$$I = \frac{1}{\sqrt{2}} \oint H_t \cdot d\ell = i\left(\frac{1}{\sqrt{2}} \int_0^{2\pi} h^0 \cdot e_\theta \rho \cdot d\theta\right), \text{ or}$$

$$I = i\sqrt{\frac{2\pi Z_0 W_0}{\sqrt{\frac{\mu}{\varepsilon}} \ell n \frac{b}{a}}} \tag{2.25}$$

It is apparent from inspection of eqs. (2.24) and (2.25) that we can obtain the convenient relationships $V = v$ and $I = i$ if we put $W_0 = 1$ and

$$Z_0 = \sqrt{\frac{\mu}{\varepsilon}} \frac{1}{2\pi} \ln \frac{b}{a}. \tag{2.26}$$

This is the well-known equation for the "characteristic impedance" of the coaxial line. Although this represents the most convenient choice for Z_0, other choices would be possible in which $v \neq V$ and $i \neq I$. (This fact is not so well-known.)

If Z_0 is chosen as above, it involves only the radii of the line and the properties μ and ε of the medium inside the line. For a given line operating in the TEM mode, there is only one value of Z_0 and thus, it is "characteristic" of that line. The name "characteristic impedance" is apt in this case.

However, when modes higher than the TEM are considered, in coaxial waveguide as well as other types of waveguide, the term "characteristic impedance" is less appropriate. In these cases, there is a v and i associated with each mode, but the line integrals of E_t and H_t depend upon the path and there is no single convenient choice of W_0 and or of Z_0.

If one chooses Z_0 for a given mode in a given waveguide, then Z_0 is "characteristic" of that mode in that waveguide for that choice. However, since different choices might be found convenient for different purposes, Z_0 is in the broad sense simply a normalization constant and is not really "characteristic" of either the waveguide or the mode.[2]

(2) TE_{10} Mode in Rectangular Waveguide

Proceeding as in the previous section, we can obtain expressions for e^0 and h^0 starting with eq. (2.9) and applying eqs. (2.12), (2.17), and (2.18). They are

$$e^0 = 2\sqrt{\frac{Z_w}{Z_0} \cdot \frac{W_0}{ab}} \left[\sin\left(\frac{\pi x}{a}\right)\right] e_y$$

$$h^0 = -2\sqrt{\frac{Z_0}{Z_w} \cdot \frac{W_0}{ab}} \left[\sin\left(\frac{\pi x}{a}\right)\right] e_x \tag{2.27}$$

Again, we consider some line integral definitions of "voltage" V, and "current" I, which are arbitrary in that we choose the path of integration. Suppose that we

[2]It is considered that if Z_0 were to be characteristic of a given waveguide, then there could be only one value of Z_0 for that waveguide. Similarly, if Z_0 were to be characteristic of a given mode, then there could be only one value of Z_0 for that mode.

choose V to be the line integral of electric field along the center of the waveguide cross-section which bisects the wide dimension. Then

$$V = \int_0^b (E_t)_{max} \cdot e_y \, dy = v \int_0^b (e^0)_{max} \cdot e_y \, dy, \text{ or}$$

$$V = v\left\{2b\sqrt{\frac{Z_w}{Z_0} \cdot \frac{W_0}{ab}}\right\}. \tag{2.28}$$

If we choose $W_0 = 1$ and $Z_0 = 4(b/a)Z_w$, then $V = v$.

Now suppose that I is the total current in one of the wide walls. Then

$$I = -\int_0^a H_t \cdot e_x \, dx = -i \int_0^a h^0 \cdot e_x \, dx, \text{ or}$$

$$I = i\left\{\frac{4a}{\pi}\sqrt{\frac{Z_0}{Z_w} \cdot \frac{W_0}{ab}}\right\}. \tag{2.29}$$

If we again choose W_0 and Z_0 as above, we find that

$$I = i\left(\frac{8}{\pi}\right). \tag{2.30}$$

We would find it more convenient if I were to equal i. This can be arranged by redefining I. Suppose that the new I, or I_n represents the current in a strip of width w, instead of the current in the entire wall. Let the strip be centered in the waveguide wall. It can then be shown that $I_n = i$ when $w \cong 0.406a$, where a is the total width of the wall.

If, on the other hand, we were to choose $Z_0 = \left(\frac{\pi}{4}\right)^2 \frac{b}{a} Z_w$ then I = i. We could then redefine V to be the line integral over a shorter path. If the path length were approximately 0.393b, then the new V would equal v.

In the above redefining of V and I, we could not take V larger than the line integral of E_t over the full height of the waveguide, and we could not take I larger than the current in the total width of the widest wall. Thus, the limits between which Z_0 may be chosen to obtain simultaneously V = v and I = i are

$$4 \frac{b}{a} Z_w \geq Z_0 \geq \left(\frac{\pi}{4}\right)^2 \frac{b}{a} Z_w, \tag{2.31}$$

where

$$Z_w = \frac{377}{\sqrt{1 - \left(\frac{f_c}{f}\right)^2}} \sqrt{\frac{\mu_r}{\varepsilon_r}} \text{ ohms}. \tag{2.32}$$

In the above expression, f is the operating frequency, f_c is the cutoff frequency, and μ_r and ε_r are respectively the relative permeability and the relative permittivity.

The above example illustrates the arbitrary nature of the choice of W_0 and Z_0 and shows some of the consequences of various choices.

f. Traveling Wave Amplitudes a and b

Another convenient set of terminal variables are the voltage traveling wave amplitudes a and b. They are related to v and i by

$$\begin{cases} V = a + b \\ Z_0 i = a - b \end{cases} \qquad \begin{cases} a = \frac{1}{2}(v + Z_0 i) \\ b = \frac{1}{2}(v - Z_0 i) \end{cases} \tag{2.33}$$

The power and impedance (or reflection coefficient) relationships are

$$P = W_0 \mathrm{Re}(\bar{i}v) = W_0 \mathrm{Re}\left[\frac{1}{Z_0}(\bar{a}-\bar{b})(a+b)\right] = \frac{W_0}{Z_0}\left(|a|^2 - |b|^2\right) \tag{2.34}$$

$$\frac{b}{a} = \frac{v - Z_0 i}{v + Z_0 i} = \frac{Z - Z_0}{Z + Z_0}, \tag{2.35}$$

where $Z = \frac{v}{i}$. Let

$$\Gamma_w = \frac{Z_w - Z_0}{Z_w + Z_0} = \frac{(Z_w/Z_0) - 1}{(Z_w/Z_0) + 1} = \frac{Z_w^0 - 1}{Z_w^0 + 1} \tag{2.36}$$

Note that if Z_0 is in ohms, Z_w^0, the wave impedance of the basis fields, is a normalized impedance and is dimensionless.

g. Other Traveling Wave Amplitudes

Two other sets of traveling wave amplitudes will be mentioned. They are sometimes called power waves, since they have the dimensions of the square root of power.

One set of traveling wave amplitudes is very simply related to a and b and is used to suppress W_0 and Z_0 from the power and impedance relations. This can be convenient when carrying through a complicated analysis. The suppressed constants can be reinserted after the analysis has been completed, if desired.

If we define a new set of terminal variables

$$a' = a\sqrt{\frac{W_0}{Z_0}}, \quad \text{and} \quad b' = b\sqrt{\frac{W_0}{Z_0}}, \tag{2.37}$$

then the power relationship is simply

$$P = |a'|^2 - |b'|^2, \tag{2.38}$$

and there is no change in the reflection coefficient

$$\frac{b'}{a'} = \frac{b}{a} \tag{2.39}$$

Then

$$\begin{aligned} v &= \sqrt{\frac{Z_0}{W_0}}\,(a' + b') \\ \sqrt{W_0 Z_0}\; i &= a' + b' \end{aligned} \qquad \left\{ \begin{aligned} a' &= \frac{1}{2}\sqrt{\frac{W_0}{Z_0}}\,(v + Z_0 i) \\ b' &= \frac{1}{2}\sqrt{\frac{W_0}{Z_0}}\,(v - Z_0 i) \end{aligned} \right. \tag{2.40}$$

Another set of terminal variables is used in the analysis of transistor circuits, for example, and is defined as follows (Kerns, 1967).

$$\left\{ \begin{aligned} a_m &= \frac{1}{2}\,\frac{1}{\sqrt{R_m}}\,(v_m + Z_m i_m) \\ b_m &= \frac{1}{2}\,\frac{1}{\sqrt{R_m}}\,(v_m - \overline{Z}_m i_m), \end{aligned} \right. \tag{2.41}$$

in which Z_m is the impedance terminating port m.

The existence of different sets of terminal variables each designated as a and b is sometimes confusing and can lead to errors if the basic definitions are not clearly understood.

2.3. Parameter Matrices

a. Impedance and Admittance Matrices

The sets of simultaneous linear equations relating the pairs of terminal variables of a waveguide junction can be written compactly in matrix form. For example, for a total number N of propagated modes, we define the column matrices

$$v = \begin{pmatrix} v_1 \\ v_2 \\ \cdot \\ \cdot \\ \cdot \\ v_N \end{pmatrix}, \quad \text{and} \quad i = \begin{pmatrix} i_1 \\ i_2 \\ \cdot \\ \cdot \\ \cdot \\ i_N \end{pmatrix}, \tag{2.42}$$

We can then write the set of equations relating the v's and i's in matrix form

$$v = Zi, \quad \text{or} \quad i = Yv, \tag{2.43}$$

where

$$Z = \begin{pmatrix} Z_{11} & Z_{12} & \cdots & Z_{1N} \\ Z_{21} & Z_{22} & \cdots & Z_{2N} \\ \cdot & \cdot & & \cdot \\ \cdot & \cdot & & \cdot \\ Z_{N1} & Z_{N2} & \cdots & Z_{NN} \end{pmatrix},$$

and Y is the inverse of Z. The above Z and Y matrices are called the impedance and admittance matrices, respectively.

b. The Scattering Matrix

If we consider the terminal variables a and b in a similar way, we obtain

$$b = Sa, \tag{2.44}$$

where S is the scattering matrix. It has elements similar to those of the above impedance matrix, and the elements are called scattering coefficients.

Since there are several sets of terminal variables denoted by the letters a and b, it happens that there are also different scattering matrices denoted by the letter S. For example, the coefficients in the scattering matrix used to relate power waves (Bodway, 1967) are sometimes called "S-parameters."

This situation can cause confusion. In order to distinguish between different scattering matrices, it is necessary to examine the definitions of the terminal variables that they relate.

In this monograph, the scattering matrix will relate the complex voltage wave amplitudes a and b as defined in eq. (2.33).

The relationships connecting Z, Y, and S, are written in matrix equations as follows

$$Z = (1 + S)(1 - S)^{-1} \; Z_0 = Y^{-1} \tag{2.45}$$

$$(ZZ_0^{-1} - 1)(ZZ_0^{-1} + 1)^{-1} = S = (1 - Z_0Y)(1 + Z_0Y)^{-1} \tag{2.46}$$

c. Power

(1) General

The total complex power input to a waveguide junction is by extension of eq. (2.16), in matrix notation

$$W = i^{*}W_0v, \tag{2.47}$$

where * denotes the Hermitian conjugate and

$$W_0 = \begin{pmatrix} W_{01} & 0 & -- & 0 \\ 0 & W_{02} & -- & 0 \\ - & - & -- & - \\ 0 & 0 & -- & W_{0N} \end{pmatrix}.$$

It can be shown that

$$W = i^*W_0Zi = v^*Y^*W_0v, \text{ and} \tag{2.48}$$

$$P = \mathrm{Re}(W) = a^*(W_0Z_0^{-1} - S^*W_0Z_0^{-1})a. \tag{2.49}$$

(2) Realizability Conditions

A waveguide junction is said to be "realizable" if its Z, Y, and X are such that $\mathrm{Re}(W) \geq 0$ for arbitrary v or i. The conditions thus placed on Z, Y, and S are the "realizability conditions" for passive waveguide junctions.

Consider the impedance matrix Z, and define $H_Z = \frac{1}{2}(W_0Z + Z^*W_0)$. Note that H_Z is Hermitian ($H_Z^* = H_Z$). Since

$$\mathrm{Re}(W) \equiv \mathrm{Re}(i^*W_0Zi) \equiv i^*H_Zi, \tag{2.50}$$

conditions on Re(W) are equivalent to conditions on the matrix of the Hermitian form i^*H_Zi.

We now distinguish (Kerns and Beatty, 1967) three cases of realizability, according to whether the dissipation in the junction is positive for every non-zero i, for only some i, or for no i.

(a) "Strict realizability": $\mathrm{Re}(W) > 0$ for every non-zero i. In this case the Hermitian matrix H_Z and the associated form are said to be "positive definite" (or, sometimes, "strictly positive"). A useful criterion for this case is: a Hermitian matrix is positive definite if and only if all its principal minors are positive.[3]

(b) "Semi-realizability": $\mathrm{Re}(W) \geq 0$ for every i and $\mathrm{Re}(W) = 0$ for some non-zero i. In this case H_Z and the associated form are said to be "positive semi-definite"; a criterion for this case is: a Hermitian matrix is positive semi-definite if and only if it is singular and all its principal minors are nonnegative (Mirsky, 1955).

[3]For a proof of this theorem see Mirsky (1955). A "principal minor" of a matrix A is a minor whose diagonal is part of the diagonal of A. Thus a principal minor is obtained by selecting rows and columns with the same sets of indices. Special cases of the principal minors of A are the diagonal elements of A and the determinant of A.

(c) "Losslessness": $\mathrm{Re}(W) = 0$ for every i. For this case it is easily shown directly that H_Z must be the (N×N) zero matrix.

For the admittance matrix Y and for the scattering matrix S, the matrices corresponding to H_Z are $H_Y = \frac{1}{2}(W_0 Y + Y^* W_0)$ and $H_S = (W_0 Z_0^{-1} - S^* W_0 Z_0^{-1} S)$, respectively.

Realizability conditions for Z, Y, and S may be summarized as follows: Realizability requires the matrices H_Z, H_Y, and H_S to be positive definite, positive semi-definite, or zero, according as case a, b, or c applies.

At this point it is observed that certain simplifications may be obtained in the above analysis and results by suitable choices of normalization. For example, if W_0 is a scalar matrix (i.e. a scalar multiple of the unit matrix), it cancels out in the statement of realizability conditions for Z and Y; similarly, if $W_0 Z_0^{-1}$ is a scalar matrix, it cancels out in the statements pertaining to S (see table 2-1).

Table 2-1. Realizability and reciprocity conditions under simplifying normalizations.

	Z (W_0 SCALAR, Z_0 ARBITRARY)	Y (W_0 SCALAR, Z_0 ARBITRARY)	S ($W_0 Z_0^{-1}$ SCALAR)
REALIZABILITY	Z+Z*PD, PSD, OR 0.	Y+Y*PD, PSD, OR 0.	1-S*SPD, PSD, OR 0.
RECIPROCITY	$\tilde{Z} = Z$	$\tilde{Y} = Y$	$\tilde{S} = S$

NOTE: 1. PD = POSITIVE DEFINITE, PSD = POSITIVE SEMI-DEFINITE.
2. RECIPROCITY MAY OF COURSE HOLD SIMULTANEOUSLY WITH ANY CASE OF REALIZABILITY.

d. Reciprocity

Provided that the parameters μ, ε (which may be complex) are symmetric tensors (which may reduce to scalars) it can be shown that (Kerns, 1949a)

$$\sum_{m=1}^{n} \int_{S_m} (E' \times H'' - E'' \times H') \cdot n_m \, dS = 0, \tag{2.51}$$

where E', H', and E", H" denote any two electromagnetic fields (of the same frequency) that can exist in the given waveguide junction. From eqs. (2.1) and (2.17) it follows that eq. (2.51) is equivalent to

$$\tilde{i}'' W_0 v' - \tilde{i}' W_0 v'' \equiv 0, \tag{2.52}$$

where the ~ denotes the transpose of a matrix.

To find the consequences of eq. (2.52) for Z, Y, we first insert $v' = Zi'$, $v'' = Zi''$. After taking the transpose of the second term, we obtain

$$\tilde{i}''(W_0 Z - \tilde{Z} W_0) i' = 0,$$

which implies

$$W_0 Z - \tilde{Z} W_0 = 0, \tag{2.53}$$

since i', i'' are arbitrary. Since $Z = Y^{-1}$ (and $\tilde{Z} = \tilde{Y}^{-1}$), the relation

$$W_0 Y - \tilde{Y} W_0 = 0 \tag{2.54}$$

is an immediate consequence of eq. (2.53).

To find the conditions imposed on S we use eq. (2.33) and find from eq. (2.52)

$$\tilde{a}'' Z_0^{-1} W_0 b' - \tilde{a}' Z_0^{-1} W_0 b'' \equiv 0.$$

Hence, using $b = Sa$, we must have

$$Z_0^{-1} W_0 S - \tilde{S} Z_0^{-1} W_0 = 0. \tag{2.55}$$

The reciprocity conditions eq. (2.52) and eq. (2.55) may be simplified by appropriate choice of normalizations, and it happens that the appropriate choices are the same as in the case of the realizability conditions considered above. Table (2-1) furnishes a summary of all these relations in simplified form.

e. Sources; Joining Equations

(1) General

We have already noted that our basic expression for the power input contributed by one waveguide mode, $W_a = \bar{i}_a v_a$ (for $W_a^0 = 1$), is of the same form as the expression for input power at a pair of terminals in an alternating-current network. We shall now consider two further fundamental relations that are required to establish the basis of the application of equations of the form of network equations to waveguide problems.

(2) Sources

For simplicity consider a waveguide "junction" having just one waveguide lead, in which just one mode propagates. We choose a terminal surface and consider the terminal variables v_1, i_1. We assume that the junction is linear (from an external

point of view) but not necessarily passive. The most general linear relation connecting v_1 and i_1 can be written

$$v_1 = Z_{g1} i_1 + v_{g1} \tag{2.56}$$

or

$$i_1 = Y_{g1} v_1 + i_{g1}, \tag{2.57}$$

where Z_{g1}, Y_{g1}, v_{g1}, i_{g1} are constants. The presence of sources may be manifested in these equations in two ways: in the inhomogeneity of the equations (i.e. $v_{g1} \neq 0$) or in a violation of the realizability condition as applied to Z_{g1} and Y_{g1}. The latter possibility means for these 1×1 matrices $\mathrm{Re}(Z_{g1}) < 0$ and $\mathrm{Re}(Y_{g1}) < 0$, as may be seen in table (2-1). It should be observed that eq. (2.56) and eq. (2.57) respectively represent versions of Thevenin's and Norton's theorems.

Alternatively, we may describe the source in terms of the terminal variables b_1, a_1. The most general linear relation connecting these variables may be written

$$b_1 = S_{g1} a_1 + b_{g1}, \tag{2.58}$$

where S_{g1} and b_{g1} are constants characterizing the source. This might be called Kerns' theorem, after D. M. Kerns. The equation states that the general emergent wave b_1 is the sum of the wave b_{g1} that would be emitted into a non-reflecting load and the reflected portion of the incident wave a_1. From table (2-1) we see that violation of the realizability condition for the 1×1 scattering matrix S_{g1} means $|S_{g1}| > 1$.

(3) Joining Equations

Suppose that a waveguide lead of one system is to be connected to a waveguide lead of another system. We assume that the terminal surfaces associated with each system have been so located that they coincide when the connection is made (fig. 2-1). The transverse components of E, H on the common terminal surface S are then given by the equations

$$E_t = \sum v_a e_a^0,$$

$$H_t = \sum i_a h_a^0, \tag{2.59}$$

associated with the one system and also by the equations

$$E_t' = \sum v_a' e_a^{0\prime},$$

$$H_t' = \sum i_a' h_a^{0\prime}, \tag{2.60}$$

associated with the other. We assume

$$e_a^0 = e_a^{0\prime}; \tag{2.61}$$

this implies

$$h_a^0 = -h_a^{0\prime}, \tag{2.62}$$

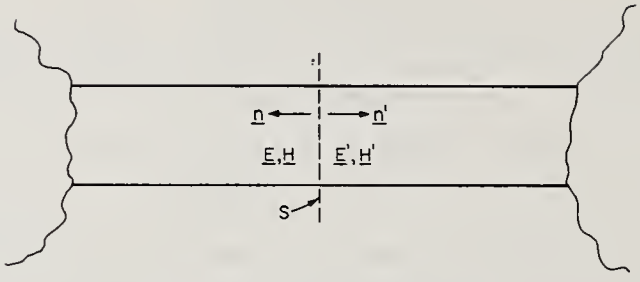

Figure 2-1. Coincident terminal surfaces.

since $n = -n'$. For the electromagnetic fields corresponding to eqs. (2.59) and (2.60) to be continued properly across S, it is necessary and sufficient that $E_t \equiv E_t'$, $H_t \equiv H_t'$. This means that it is in turn necessary and sufficient that

$$\begin{aligned} v_a &= v_a' \\ i_a &= -i_a' \end{aligned} \tag{2.63}$$

for each mode involved. These are the joining equations of waveguide theory. They are of exactly the same form as the equations in circuit theory that describe the joining of two pairs of terminals. To verify this, consider that the terminal pairs shown in figure 2-2 are to be joined.

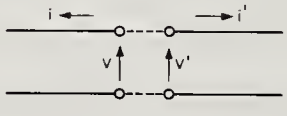

Figure 2-2. An "equivalent circuit" for joining.

With the sign conventions indicated in figure 2-2, circuit theory obviously requires $v = v'$, $i = -i'$. (The sign conventions are determined by eq. (2.62) together with the choice of n_m as the inward normal on S_m.)

In the equations that characterize a waveguide junction, such as the matrix equation $v = Zi$, the number of variables is twice the number of equations. In a waveguide junction characterized by a set of N equations, the electromagnetic state has N degrees of freedom. However, if loads or sources[4] are connected at all terminal surfaces and the joining equations are applied, the number of equations becomes equal to the number of unknowns in the system. Thus, except for special cases where the equations are not all independent, the terminal variables (and hence the electromagnetic state) become determinate.

[4]A passive waveguide junction possessing just one waveguide lead (multimode or not) is termed a "load" or a "termination"; if not passive, it is termed a "source."

3. Introductory Network Analysis

3.1. Linear Network Parameters

a. Introduction

It has been shown in the previous section that network equations developed for alternating current networks consisting of distinct circuit elements may also be used in waveguide problems in which distinct circuit elements do not exist as lumped elements, but are distributed in space.

These network equations are briefly reviewed as a point of departure to reintroduce scattering coefficients and other parameters used to relate wave amplitudes.

b. Terminal Variables

It is customary to provide access to a network by means of terminals, and in most cases, these are grouped in pairs. We can have input terminal pairs to which sources are connected to feed energy into a network, and we can have output terminal pairs to which loads or terminations are connected to absorb or reflect energy emerging from the network. Usually, there is a terminal pair to which a detector is connected, especially in circuits used for measurement purposes.

The voltage v across a given pair of terminals, and the current i flowing into one terminal (and out of the other) are the terminal variables in common use. The relationship between the terminal variables at one terminal pair and those at another terminal pair is determined by the characteristics of the network. If all of the network elements are linear, the relationship is given by a set of linear equations, having coefficients which are independent of the terminal variables. These coefficients are called network parameters.

c. Network Parameters

It is possible to obtain more than one set of parameters for a given network, depending upon how the terminal variables are selected at the terminals. Three frequently encountered sets of parameters for a two-terminal pair network (four-pole, or 2-port) are shown in figure 3-1.

The equations defining the parameters are given in three forms. The first form is the usual set of two simultaneous linear equations. The second form is the corresponding matrix equation. The last form is the short form of the matrix equation, where the matrices are indicated by single letters.

Figure 3-1. Representation of a fourpole (2-port)

$$\begin{cases} v_1 = Z_{11}i_1 + Z_{12}i_2 \\ v_2 = Z_{21}i_1 + Z_{22}i_2 \end{cases} \quad \begin{pmatrix} v_1 \\ v_2 \end{pmatrix} = \begin{pmatrix} Z_{11} & Z_{12} \\ Z_{21} & Z_{22} \end{pmatrix} \begin{pmatrix} i_1 \\ i_2 \end{pmatrix}; \quad v = Zi. \tag{3.1}$$

$$\begin{cases} i_1 = Y_{11}v_1 + Y_{12}v_2 \\ i_2 = Y_{21}v_1 + Y_{22}v_2; \end{cases} \quad \begin{pmatrix} i_1 \\ i_2 \end{pmatrix} = \begin{pmatrix} Y_{11} & Y_{12} \\ Y_{21} & Y_{22} \end{pmatrix} \begin{pmatrix} v_1 \\ v_2 \end{pmatrix}; \quad i = Yv. \tag{3.2}$$

$$\begin{cases} v_1 = Av_2 - Bi_2 \\ i_1 = Cv_2 - Di_2; \end{cases} \quad \begin{pmatrix} v_1 \\ i_1 \end{pmatrix} = \begin{pmatrix} A & B \\ C & D \end{pmatrix} \begin{pmatrix} v_2 \\ -i_2 \end{pmatrix} \tag{3.3}$$

The above matrices are called respectively the impedance matrix, the admittance matrix, and the ABCD matrix (general circuit parameters). The ABCD matrix may also be called the v and i cascading matrix.

d. Complex Wave Amplitudes a and b

Access to a waveguide junction is provided by means of waveguide leads. Terminal surfaces chosen in the waveguide leads form part of the outer boundary of the waveguide junction. The amplitude a of the voltage wave incident on the junction and the amplitude b of the voltage wave emerging from the junction at each such terminal surface are one type of terminal variables in common use. The terminal surfaces where energy may enter or emerge from a waveguide junction are also called ports.

e. Parameters Associated with a and b

It is possible to define many sets of parameters relating a and b for a given waveguide junction. Three of these sets of parameters for a 2-port network are shown in figure 3-2, and defined in eqs. (3.4), (3.5), and (3.6).

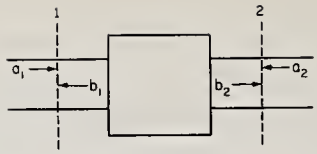

Figure 3-2. Representation of a 2-port waveguide junction with terminal surfaces and terminal variables a and b.

$$\begin{cases} b_1 = S_{11}a_1 + S_{12}a_2 \\ b_2 = S_{21}a_1 + S_{22}a_2; \end{cases} \quad \begin{bmatrix} b_1 \\ b_2 \end{bmatrix} = \begin{bmatrix} S_{11} & S_{12} \\ S_{21} & S_{22} \end{bmatrix} \begin{bmatrix} a_1 \\ a_2 \end{bmatrix}; \quad b = Sa \tag{3.4}$$

$$\begin{cases} a_1 = g_{11}b_1 + g_{12}b_2 \\ a_2 = g_{21}b_1 + g_{22}b_2; \end{cases} \quad \begin{bmatrix} a_1 \\ a_2 \end{bmatrix} = \begin{bmatrix} g_{11} & g_{12} \\ g_{21} & g_{22} \end{bmatrix} \begin{bmatrix} b_1 \\ b_2 \end{bmatrix}; \quad a = gb \tag{3.5}$$

$$\begin{cases} b_1 = r_{11}a_2 + r_{12}b_2 \\ a_1 = r_{21}a_2 + r_{22}b_2 \end{cases} \quad \begin{bmatrix} b_1 \\ a_1 \end{bmatrix} = \begin{bmatrix} r_{11} & r_{12} \\ r_{21} & r_{22} \end{bmatrix} \begin{bmatrix} a_2 \\ b_2 \end{bmatrix} \tag{3.6}$$

The coefficients in the above equations are called scattering, gathering, and cascading coefficients, respectively.

f. Other Terminal Variables

Another set of terminal variables v and i can be used with waveguide junctions. They are generalizations of voltage and current and can actually represent transmission line voltages and currents in cases where only the TEM-mode propagates. The parameters relating v and i for waveguide junctions are called by the same names as the corresponding ones relating voltage and current. Still other terminal variables could be defined by forming linear combinations of the ones already mentioned. However, terminal variables other than v and i, and a and b have not been widely used.

g. Network Equivalent to a Waveguide Junction

A network which shares an identical set of parameters with a waveguide junction is said to be equivalent to that junction. Such equivalence may hold at only one frequency at which the parameters are defined, or in the less usual case, might hold over a range of frequencies.

For example, the parameters relating the terminal variables v and i for a waveguide junction may be identical with those which relate voltage and current for a network. In this case, the impedance matrices would certainly be identical. It follows that all of the other parameter matrices would be the same as the corresponding ones for the equivalent network. This is true because each set of parameters relating terminal variables is linearly related to each other set.

Occasionally some difficulty may arise in identifying equivalent networks if, for example, we are given a scattering matrix for a waveguide junction and find that the impedance matrix does not exist (the elements may be infinitely large).

An example is the following, in which the equivalent circuit is a single series impedance Z_1 as shown in figure 3-3.

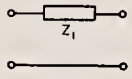

Figure 3-3. A fourpole having a single series element.

By inspection, the admittance matrix is

$$Y = \frac{1}{Z_1}\begin{pmatrix} 1 & -1 \\ -1 & 1 \end{pmatrix}.$$

It follows from eq. (2.46) that the corresponding scattering matrix is

$$S = \frac{1}{Z_1 + (Z_{01} + Z_{02})}\begin{pmatrix} Z_1 - (Z_{01} - Z_{02}) & 2Z_{01} \\ 2Z_{02} & Z_1 + (Z_{01} - Z_{02}) \end{pmatrix}. \qquad (3.7)$$

If we choose $Z_{01} = Z_{02} = Z_0$, then

$$S = \frac{1}{(Z_1/Z_0) + 2}\begin{pmatrix} (Z_1/Z_0) & 2 \\ 2 & (Z_1/Z_0) \end{pmatrix}. \qquad (3.8)$$

Application of eq. (2.45) in order to obtain an impedance matrix will reveal that each of the elements is infinite. It is then said that the impedance matrix does not exist.

3.2. The Scattering Matrix

a. General Remarks

The scattering matrix has an appropriate name as we can see from the example below.

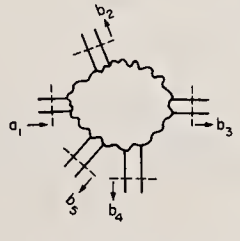

Figure 3-4. Representation of a multi-arm waveguide junction with energy incident in arm 1.

As shown in figure 3-4, a wave of amplitude a_1 entering the waveguide junction in arm 1 is scattered, and some of the energy is transmitted to each of the other arms of the junction. (For simplicity, it has been assumed that the other arms have nonreflecting terminations so that there are no reflected waves in these arms.) The coefficients in the linear equations relating the amplitudes of the emergent waves (the b's) to the amplitudes of the incident waves (the a's) are called the scattering coefficients. The matrix of these coefficients is called the scattering matrix which was defined more formally in eq. (2.44).

In general some scattering will also occur as a result of reflection. Since scattering involves both transmission and reflection of energy, it is to be expected that the scattering coefficients will be of two kinds; transmission coefficients and reflection coefficients. This will be illustrated clearly in the case of two-arm waveguide junctions (2-ports), to be discussed.

Much of the theory of two-arm waveguide junctions may be applied to waveguide junctions with more than two arms, as will be shown below. Consider a waveguide junction having n arms, all of which are terminated by non-reflecting loads except the p^{th} and q^{th} arms. This requires that all incident wave amplitudes vanish except for a_p and a_q. The scattering equation b = Sa for the waveguide junction then reduces to

$$\begin{cases} b_p = S_{pp}a_p + S_{pq}a_q \\ b_q = S_{qp}a_p + S_{qq}a_q, \end{cases} \tag{3.9}$$

considering only the emergent waves in the p^{th} and q^{th} arms. This is of the same form as that for a two-arm waveguide junction, so that one can for example determine S_{pp}, S_{pq}, S_{qp}, and S_{qq} by the same techniques developed for determining S_{11}, S_{12}, S_{21}, and S_{22} of two-arm junctions, to be described.

b. Scattering Coefficients of a Two-Arm Waveguide Junction

Consider a two-arm waveguide junction with a source connected to arm 1 and a load connected to arm 2. The reflection coefficient of the load is designated by Γ_L as shown in figure 3-5. The reflection coefficient of a load is defined to be the ratio of the amplitude of the wave reflected from that load to the amplitude of the wave incident upon it.

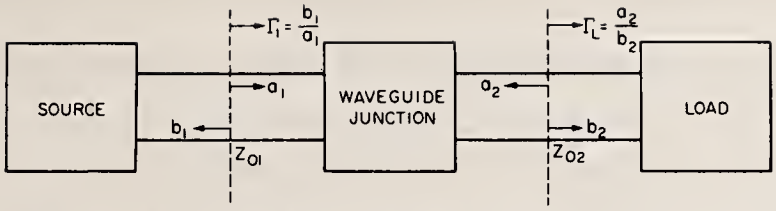

Figure 3-5. A two-arm waveguide junction connected between a source and a load.

Referring to eq. (3.4) it can be seen that the input reflection coefficient Γ_1 can be written

$$\Gamma_1 = S_{11} + \frac{S_{12}S_{21}\Gamma_L}{1 - S_{22}\Gamma_L} = \frac{(S_{12}S_{21} - S_{11}S_{22})\Gamma_L + S_{11}}{1 - S_{22}\Gamma_L}. \tag{3.10}$$

Note that if there is no reflection from the load ($\Gamma_L = 0$), the only source of reflection is within the waveguide junction, and

$$\left(\frac{b_1}{a_1}\right)_{a_2=0} = (\Gamma_1)_{\Gamma_L=0} = S_{11}. \tag{3.11}$$

Therefore S_{11} is the reflection coefficient "observed looking into" arm 1 with arm 2 terminated in a non-reflecting load. We can say that S_{11} characterizes the reflecting property of the waveguide junction for energy entering arm 1.

A similar argument with the above roles of arms 1 and 2 reversed will show that S_{22} is the reflection coefficient "observed looking into" arm 2 with arm 1 terminated in a non-reflecting load. Thus, the scattering coefficients S_{11} and S_{22} are reflection coefficients. We can generalize on the basis of previous remarks about eq. (3.9) that any scattering coefficient of the form S_{pq} is a reflection coefficient if $p = q$.

It can be shown conversely that when $p \neq q$, the scattering coefficient S_{pq} is a transmission coefficient. If the transmission coefficient is defined as the ratio of the amplitude b_2 of the wave emerging from arm 2 to the amplitude a_1 of the wave incident in arm 1, when a non-reflecting load is connected to arm 2, then inspection of eq. (3.4) shows that

$$\left(\frac{b_2}{a_1}\right)_{a_2=0} = S_{21}. \tag{3.12}$$

A similar argument applies to S_{12}, and extension to S_{pq} is straightforward.

c. Effects of Moving Terminal Surfaces

The scattering coefficients of a given waveguide junction have been defined in terms of wave amplitudes at certain arbitrarily selected terminal surfaces. If new terminal surfaces are chosen, a new set of scattering coefficients will then apply. Since only a simple change was made in the waveguide junction, one would hope for a simple relationship between the new and old sets of scattering coefficients. That this is the case may be shown as follows. Consider the new set of wave amplitudes and scattering coefficients to be denoted by primes.

It is well known that a wave traveling along a uniform section of waveguide experiences attenuation and phase delay as it progresses. If, as in figure 3-6, a wave traveling to the right has an amplitude a_1' at terminal surface 1', it will have an amplitude $a_1 = a_1' e^{-\gamma \ell_1}$ at terminal surface 1. Similarly, a wave traveling to the left having an amplitude b_1 at terminal surface 1 will have an amplitude $b_1' = b_1 e^{-\gamma \ell_1}$ at terminal surface 1'. Here we regard ℓ_1 only as a distance between two terminal surfaces, considered as always positive, since we have not set up any conventions of positive and negative displacement in this case.

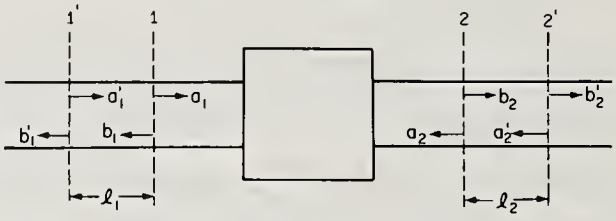

Figure 3-6. Changes of locations of terminal surfaces from 1 and 2 to 1′ and 2′.

Assuming that the waveguide leads are lossless, their propagation constants (γ's) will be $j\beta_1$ and $j\beta_2$, and the following relationships will hold:

$$a_1 = a_1' e^{-j\beta_1 \ell_1}, \quad b_1' = b_1 e^{-j\beta_1 \ell_1}$$

$$a_2 = a_2' e^{-j\beta_2 \ell_2}, \quad b_2' = b_2 e^{-j\beta_2 \ell_2}. \tag{3.13}$$

We apply the definitions of S_{11} and S_{21} as in eqs. (3.11) and (3.12) to S_{11}' and S_{21}', obtaining

$$S_{11}' = S_{11} e^{-j2\beta_1 \ell_1} \quad \text{and} \quad S_{21}' = S_{21} e^{-j(\beta_1 \ell_1 + \beta_2 \ell_2)}. \tag{3.14}$$

Interchanging subscripts 1 and 2 yields

$$S_{22}' = S_{22} e^{-j2\beta_2 \ell_2} \quad \text{and} \quad S_{12}' = S_{12} e^{-j(\beta_2 \ell_2 + \beta_1 \ell_1)}. \tag{3.15}$$

No such simple relationship would be obtained with impedances and admittances, and this is one important advantage of using scattering coefficients.

If we now designate the original set of terminal surfaces and scattering coefficients by primes, eqs. (3.14) and (3.15) will still hold, but we will want to solve them for S_{11}, S_{12}, S_{21}, and S_{22}. Upon doing this, it will be found that the algebraic sign of the exponents will be positive instead of negative. The effect of shifting a terminal surface to a new position in either direction should now be evident.

3.3. Reciprocity, Realizability, and Losslessness for 2-Ports

The relationships derived for waveguide junctions in general will be specialized to apply to 2-ports. The meanings of these relationships in terms of energy flow will be examined later.

In the following, the usual symbol Z_0 will be used to designate the normalizing impedance of the propagating mode (usually only one in each waveguide lead), and an additional subscript will be added to designate the particular waveguide lead of the waveguide junction (these waveguide leads are often identical, but are sometimes quite different from one another).

The power normalization matrix W_0 will be taken equal to the unit matrix so that it will disappear from the following equations. This is felt to be justified because it seldom happens that we need to choose W_0 otherwise, and if we do, we can refer back to sections 2.2 and 2.3.

We will carry through the Z_0 normalization factor because it is more often useful. Cases continue to occur where the waveguide arms of a junction are not identical and we do not wish to choose all of the Z_0's equal.

a. Reciprocity

In terms of the scattering coefficients it has been shown that the reciprocity condition is given by eq. (2.55). Assuming that the power normalization matrix is the unit matrix, we have

$$Z_0^{-1}S = \tilde{S}Z_0^{-1}. \tag{3.16}$$

Performing the indicated multiplication for the 2×2 matrices, we obtain

$$\begin{pmatrix} \frac{S_{11}}{Z_{01}} & \frac{S_{12}}{Z_{01}} \\ \frac{S_{21}}{Z_{02}} & \frac{S_{22}}{Z_{02}} \end{pmatrix} = \begin{pmatrix} \frac{S_{11}}{Z_{01}} & \frac{S_{21}}{Z_{02}} \\ \frac{S_{12}}{Z_{01}} & \frac{S_{22}}{Z_{02}} \end{pmatrix} \tag{3.17}$$

The resulting condition on the scattering coefficients is

$$S_{12}Z_{02} = S_{21}Z_{01}. \tag{3.18}$$

It is often stated that reciprocity implies the equality of S_{12} and S_{21} but it is seen that this is true only[1] when Z_{01} and Z_{02} are equal. It is not always convenient or appropriate to choose them equal, so the correct relationship above should be kept in mind.

b. Strict Realizability

The condition of strict realizability, discussed in section 2.3, excludes losslessness, and is given by the following matrix inequality

$$\mathrm{Re}(W) = a^* H_S a > 0, \text{ for arbitrary } a \neq 0,$$

$$\text{where } H_S = W_0 Z_0^{-1} - S^* W_0 Z_0^{-1} S, \tag{3.19}$$

as in eq. (2.49). This condition requires that H_S be positive definite, which in turn requires that all of the principal minors of H_S be positive. However, it is not necessary to show that all of the principal minors are positive, since this follows automatically if one shows that the leading minors are positive. The leading minors are the ones which progressively include the elements on the principal diagonal, starting at upper left.

The equation for H_S for 2×2 matrices, assuming that W_0 is the unit matrix, is

$$H_S = \begin{bmatrix} \dfrac{1 - |S_{11}|^2}{Z_{01}} - \dfrac{|S_{21}|^2}{Z_{02}} & -\left(\dfrac{\bar{S}_{11}S_{12}}{Z_{01}} + \dfrac{\bar{S}_{21}S_{22}}{Z_{02}}\right) \\ -\left(\dfrac{\bar{S}_{12}S_{11}}{Z_{01}} + \dfrac{\bar{S}_{22}S_{21}}{Z_{02}}\right) & \dfrac{1 - |S_{22}|^2}{Z_{02}} - \dfrac{|S_{12}|^2}{Z_{01}} \end{bmatrix}. \tag{3.20}$$

Thus, strict realizability requires that

$$\frac{Z_{01}}{Z_{02}} \cdot \frac{|S_{21}|^2}{1 - |S_{11}|^2} < 1,$$

$$\frac{Z_{02}}{Z_{01}} \cdot \frac{|S_{12}|^2}{1 - |S_{22}|^2} < 1,$$

---

[1] If new terminal variables are employed such that $S'_{12} = S_{12}\sqrt{(Z_{02}/Z_{01})}$ and $S'_{21} = S_{21}\sqrt{(Z_{01}/Z_{02})}$, then reciprocity requires $S'_{12} = S'_{21}$. See section 2.2.g.

and

$$\left(\frac{1 - |S_{11}|^2}{Z_{01}} - \frac{|S_{21}|^2}{Z_{02}}\right)\left(\frac{1 - |S_{22}|^2}{Z_{02}} - \frac{|S_{12}|^2}{Z_{01}}\right)$$

$$- \left|\frac{\bar{S}_{11}S_{12}}{Z_{01}} + \frac{\bar{S}_{21}S_{22}}{Z_{02}}\right|^2 > 0. \qquad (3.21)$$

On testing a scattering matrix to see whether it corresponds to a strictly realizable waveguide junction, only two of the above inequalities need to be considered; the last one, and either of the remaining ones. It is noteworthy that the first two inequalities involve the magnitudes but not the phases of the scattering coefficients, while the third inequality involves both magnitudes and phases.

c. Losslessness

While a lossless waveguide junction is not actually obtainable in practice, one can approach this condition closely, and it is therefore important. The assumption of lossless waveguide leads which has been made, is of comparable importance. It has been stated, in section 2.3, that losslessness requires H_S to be zero, which requires each element of H_S to vanish. This yields the following restraints upon the scattering coefficients:

$$\frac{Z_{01}}{Z_{02}} = \frac{1 - |S_{11}|^2}{|S_{21}|^2} = \frac{|S_{12}|^2}{1 - |S_{22}|^2} = -\frac{\bar{S}_{11}S_{12}}{\bar{S}_{21}S_{22}} = -\frac{\bar{S}_{12}S_{11}}{\bar{S}_{22}S_{21}}. \qquad (3.22)$$

It can be shown that an equivalent and more revealing set of restraints on the scattering equations is the following:

$$|S_{11}| = |S_{22}| = S,$$

$$Z_{01}|S_{21}| = Z_{02}|S_{12}| = \sqrt{[Z_{01}Z_{02}(1-S^2)]},$$

and

$$\psi_{12} + \psi_{21} = \psi_{11} + \psi_{22} \pm (2n - 1)\pi, \qquad (3.23)$$

where ψ_{pq} is the phase of S_{pq} and n is an integer.

It is interesting to note that the condition of losslessness implies a partial symmetry in that $|S_{11}| = |S_{22}|$, and a partial reciprocity in that $Z_{01}|S_{21}| = Z_{02}|S_{12}|$. One, also notes that this condition requires every element of H_S to vanish, while the strict realizability condition requires that all of the principal minors be greater than zero. Therefore, one should not in general simply replace the inequality signs in eq. (3.21) by equals signs to convert to the lossless condition.

3.4. Power and Efficiency

A two-arm waveguide junction is often connected between a source of energy and a load as shown in figure 3-7.

This arrangement shown in figure 3-7 is frequently encountered in measurement systems. The rate of energy flow into the junction P_1 equals the incident power P_{I1} minus the reflected power P_{R1}.

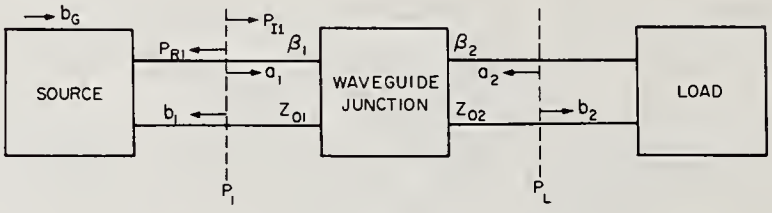

Figure 3-7. Diagram of a simple waveguide system with energy flowing from left to right, with net powers P_1 and P_L and with incident and reflected powers P_{I1} and P_{R1}.

The rate of energy dissipation in the load is P_L, and the rate of energy dissipation in the waveguide junction is $P_1 - P_L$. The efficiency η_1 of the waveguide junction is defined to be the ratio of P_L to P_1. An expression for the efficiency is developed as follows: The net power P_1 crossing terminal surface 1 to the right is

$$P_1 = P_{I1} - P_{R1}, \tag{3.24}$$

where the incident power $P_{I1} = |a_1|^2/Z_{01}$, and the reflected power $P_{R1} = |b_1|^2/Z_{01}$, and therefore

$$P_1 = \frac{|a_1|^2}{Z_{01}} (1 - |\Gamma_1|^2), \tag{3.25}$$

where $\Gamma_1 = b_1/a_1$.

Similarly, the net power P_L absorbed by the load is

$$P_L = \frac{|b_2|^2}{Z_{02}} (1 - |\Gamma_L|^2), \tag{3.26}$$

where $\Gamma_L = a_2/b_2$.

The efficiency η_1 of the waveguide junction when energy is fed into arm 1 is

$$\eta_1 = \frac{P_L}{P_1} = \frac{Z_{01}}{Z_{02}} \cdot \left|\frac{b_2}{a_1}\right|^2 \cdot \frac{1 - |\Gamma_L|^2}{1 - |\Gamma_1|^2}. \tag{3.27}$$

Substituting eq. (3.10) for Γ_1, and solving eq. (3.4) for the ratio of b_2 to a_1, one obtains

$$\eta_1 = \frac{Z_{01}}{Z_{02}} \cdot \frac{|S_{21}|^2(1 - |\Gamma_L|^2)}{|1 - S_{22}\Gamma_L|^2 - |(S_{12}S_{21} - S_{11}S_{22})\Gamma_L + S_{11}|^2}. \tag{3.28}$$

The efficiency is seen to be not only a property of the waveguide junction, but also of the reflection coefficient Γ_L of the load. In the special case of a non-reflecting load,

$$[\eta_1]_{a_2=0} = \frac{Z_{01}}{Z_{02}} \cdot \frac{|S_{21}|^2}{1 - |S_{11}|^2}. \tag{3.29}$$

If the positions of the source and the load with respect to the waveguide junction were to be reversed, it is apparent that the expressions for the efficiency η_2 would be of the same form, but with subscripts 1 and 2 interchanged. Thus

$$\eta_2 = \frac{Z_{02}}{Z_{01}} \cdot \frac{|S_{12}|^2(1 - |\Gamma_L|^2)}{|1 - S_{11}\Gamma_L|^2 - |(S_{12}S_{21} - S_{11}S_{22})\Gamma_L + S_{22}|^2}, \tag{3.30}$$

and

$$[\eta_2]_{a_1=0} = \frac{Z_{02}}{Z_{01}} \cdot \frac{|S_{12}|^2}{1 - |S_{22}|^2} \tag{3.31}$$

It is interesting to compare eqs. (3.29) and (3.31) with the inequalities eq. (3.21). The first two inequalities simply state that the efficiency of a strictly realizable waveguide junction is less than unity for two conditions. The first condition assumes that energy enters arm 1 and there is no reflection from the load on arm 2. The second condition is similar except that 1 and 2 are interchanged.

3.5. Representation of the Source

If we consider a source connected to arm 1 of a waveguide junction as in figure 3-7, it is possible to show in a number of ways that

$$a_1 = b_G + b_1\Gamma_G, \tag{3.32}$$

where a_1 is the amplitude of the wave in arm 1 incident upon the junction, b_G is the amplitude of the wave that the generator would emit to a non-reflecting load,[2] b_1 is the amplitude of the wave reflected from the junction in arm 1, and Γ_G is the reflection coefficient of the source. It is considered desirable to build confidence in this relationship by giving alternate derivations, since it is widely used in circuit analysis.

a. From Linear Relation for Source and Joining Equations

For convenience, the wave amplitudes referred to in eq. (2.58) will be primed,

[2]It is assumed here that the generator is unaffected by load changes. This is not true in general, but is approximately true if isolation or buffering is employed between the active source and terminal surface No. 1.

and b_{g1} and S_{g1} become respectively b_G and Γ_G. Then the diagram of figure 3-8 represents the situation when a source is joined to arm 1 of a waveguide junction.

The joining equations are evidently

$$a_1 = b_1',$$

$$b_1 = a_1', \tag{3.33}$$

and

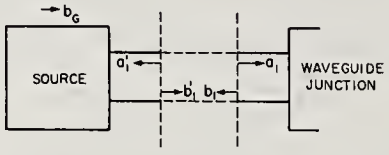

Figure 3-8. Representation of a waveguide junction connected to a source of energy.

Substituting these into the modified eq. (2.58) yields eq. (3.32). Note that the a's and b's of eq. (3.32) are chosen in different directions than in section 2.3.e.

b. From a Constant Voltage Generator

If we postulate a constant voltage source as shown in figure 3-9 and relate a and b to v and i in the usual manner, it is found that eq. (3.32) can again be obtained.

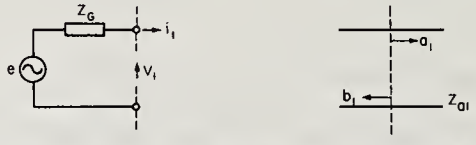

Figure 3-9. A constant voltage generator with a waveguide output having either terminal variables v_1 and i_1 or a_1 and b_1.

The steps are as follows:

$$v_1 = e - i_1 Z_G,$$

$$a_1 + b_1 = e - \frac{Z_G}{Z_{01}}(a_1 - b_1) = e - \frac{1 + \Gamma_G}{1 - \Gamma_G}(a_1 - b_1),$$

$$2a_1(1 - \Gamma_1\Gamma_G) = e(1 - \Gamma_G),$$

$$a_1 = \frac{1}{1 - \Gamma_1\Gamma_G} \cdot \left\{\frac{e}{2}(1 - \Gamma_G)\right\} \tag{3.34}$$

We define b_G as the amplitude of the emergent wave from the generator (a_1) when a non-reflecting load is connected ($\Gamma_1 = 0$). Thus

$$b_G = \frac{e}{2}(1 - \Gamma_G). \tag{3.35}$$

Then it follows that

$$a_1 = \frac{b_G}{1 - \Gamma_1\Gamma_G} \tag{3.36}$$

or

$$a_1 = b_G + b_1\Gamma_G. \tag{3.32}$$

c. Summation of Wave Reflections

Supposing that a wave amplitude b_G emerges from the generator, one can consider the multiple reflections that take place as shown in figure 3-10.

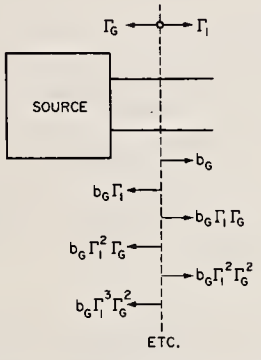

Figure 3-10. Representation of multiple reflections at a terminal surface in the waveguide connected to an energy source.

The sum of wave amplitudes reflected toward the generator is

$$b_1 = b_G\Gamma_1[1 + (\Gamma_G\Gamma_1) + (\Gamma_G\Gamma_1)^2 + \ldots],$$

or

$$b_1 = \frac{b_G\Gamma_1}{1 - \Gamma_G\Gamma_1}, \quad \text{or} \quad b_1 = \frac{b_G b_1}{a_1 - \Gamma_G b_1}$$

or

$$a_1 = b_G + b_1\Gamma_G, \tag{3.32}$$

3.6. Net Power and Available Power

a. Net Power to a Waveguide Junction

Suppose that a source is connected to a waveguide junction as shown in figure 3-7. The net power delivered to the junction is

$$P_1 = \frac{|a_1|^2}{Z_{01}}(1 - |\Gamma_1|^2) = \frac{|b_G|^2}{Z_{01}} \cdot \frac{1 - |\Gamma_1|^2}{|1 - \Gamma_G\Gamma_1|^2}. \tag{3.37}$$

The components of this power associated with the incident and reflected waves are respectively

$$P_{I1} = \frac{|b_G|^2}{Z_{01}} \cdot \frac{1}{|1 - \Gamma_G\Gamma_1|^2},$$

and

$$P_{R1} = \frac{|b_G|^2}{Z_{01}} \cdot \frac{|\Gamma_1|^2}{|1 - \Gamma_G\Gamma_1|^2}. \tag{3.38}$$

It is sometimes erroneously assumed that the incident power from a generator is always independent of the load. However one can see from the above equation that this can be true only if the generator is non-reflecting, or $\Gamma_G = 0$.

b. Available Power from Generator

It is seen above that the net, incident, and reflected power from a generator all depend upon the reflection coefficient Γ_1 of the effective load terminating the generator. It is well known that the net power will be maximum when the load impedance is the complex conjugate of the generator impedance, or when

$$Z_1 = \overline{Z}_G. \tag{3.39}$$

This condition in terms of the corresponding reflection coefficients (remembering that Z_{01} is real for lossless waveguide leads) is

$$\Gamma_1 = \overline{\Gamma}_G. \tag{3.40}$$

The net power output from the source under this condition is termed the available power P_A, and is obtained by substituting eq. (3.40) into eq. (3.37), as follows:

$$P_A = \frac{|b_G|^2}{Z_{01}} \cdot \frac{1}{1 - |\Gamma_G|^2}. \tag{3.41}$$

The components of the available power associated with the incident and reflected waves respectively are

$$P_{AI} = \frac{|b_G|^2}{Z_{01}} \cdot \frac{1}{(1 - |\Gamma_G|^2)^2} = \frac{P_A}{1 - |\Gamma_G|^2},$$

and

$$P_{AR} = \frac{|b_G|^2}{Z_{01}} \cdot \frac{|\Gamma_G|^2}{(1 - |\Gamma_G|^2)^2} = P_A \frac{|\Gamma_G|^2}{1 - |\Gamma_G|^2}. \tag{3.42}$$

Compare these to the net power P_0 delivered to a non-reflecting load,

$$P_0 = \frac{|b_G|^2}{Z_{01}}. \tag{3.43}$$

Thus P_0 is generally less than P_A except when the generator is non-reflecting ($\Gamma_G = 0$), and then they are the same.

3.7. Mismatch Loss

a. Mismatch Loss in General

We define mismatch loss L_M as the ratio in decibels of the power P_M absorbed by a matched load to the power P_{MM} absorbed by a mismatched load, when these loads are alternately connected to the same source (generator), or

$$L_M = 10 \log_{10} \frac{P_M}{P_{MM}}. \tag{3.44}$$

It is necessary to understand what is meant by the terms "match" and "mismatch," and their meanings will be discussed later.

One sees that the above mismatch loss is simply a special case of the ratio of the powers absorbed by two different loads which are alternately connected to the same generator. If the load initially connected has a reflection coefficient ${}^{i}\Gamma_1$, the load finally connected has a reflection coefficient ${}^{f}\Gamma_1$, and the generator has a reflection coefficient Γ_G, the ratio expessed in decibels is

$$L_C = 10 \log_{10} \left(\left| \frac{1 - \Gamma_G {}^{f}\Gamma_1}{1 - \Gamma_G {}^{i}\Gamma_1} \right|^2 \frac{1 - |{}^{i}\Gamma_1|^2}{1 - |{}^{f}\Gamma_1|^2} \right) = 10 \log_{10} \frac{{}^{i}P_1}{{}^{f}P_1} \tag{3.45}$$

and is called (Beatty, 1964a) the comparison loss. An expression of this form is widely used (Beatty and MacPherson, 1953) in the analysis of mismatch errors in power measurements.

If one is given ${}^{i}P_1$ expressed in decibels referred to some convenient level, one subtracts L_C in order to obtain ${}^{f}P_1$. Supposing that the load initially connected were matched and the load finally connected were mismatched, then eq. (3.45) reduces to eq. (3.44), which gives the power loss in decibels due to mismatch.

b. Meaning of Mismatch

The term "mismatch" implies that other than matched conditions exist. This is clear enough, but there are various interpretations of the term "match." In a manner of speaking, one impedance is said to match another when the two are identical.

Thus, a load that matches a given generator yields the condition

$$Z_1 = Z_G \quad \text{or} \quad \Gamma_1 = \Gamma_G.$$

However, the concept of a conjugate match is well established and the conditions are given by eqs. (3.39) and (3.40).

One could argue that a conjugate match is really a mismatch since the two impedances involved are not exactly equal to each other. The resistive components are equal, but the reactive components have opposite sign. However, the word "matched" is commonly used to mean adapted, fit, or suited. For example, a married couple are said to be well matched if they complement each other. Thus the word "matched" can have various meanings other than "equal." In precise work, we must be careful that we understand just what meaning is implied.

It is said that a load matches a waveguide when its impedance equals the characteristic impedance of the waveguide, or $Z_1 = Z_{01}$ and $\Gamma_1 = 0$. If Z_{01} is real, then this type of non-reflecting match or Z_0 match may be equivalent to a conjugate match, providing that the impedance Z_G of the generator feeding the waveguide also equals Z_{01}. However, if Z_{01} is complex, a non-reflecting or Z_0 match will not in general result in maximum power absorbed in the load, although there will be no reflection of energy back towards the generator.

One should be aware that other types of impedance matching have been defined in addition to those above, so that the terms "match" and "mismatch" should be used with care. A load that is matched in one sense, may be mismatched in another.

c. Conjugate Mismatch Loss

A generator delivers its available power P_A when terminated in a load which provides a conjugate match as mentioned above. When a different load terminates the generator, the net power delivered, P_1, is less. The ratio of P_A to P_1, expressed[3] in decibels, is the conjugate mismatch loss M_C:

$$M_C = 10 \log_{10} \frac{P_A}{P_1} = 10 \log_{10} \frac{|1 - \Gamma_G \Gamma_1|^2}{(1 - |\Gamma_G|^2)(1 - |\Gamma_1|^2)}. \tag{3.46}$$

The conjugate mismatch loss M_C cannot be negative, since P_A is either equal to or greater than P_1. In the simple case when the generator is non-reflecting ($\Gamma_G = 0$), the conjugate mismatch loss reduces to

$$[M_C]_{\Gamma_G=0} = 10 \log_{10} \left(\frac{1}{1 - |\Gamma_1|^2} \right). \tag{3.47}$$

One sometimes finds this expression given for mismatch loss without the statement that it requires a non-reflecting generator to be correct.

[3]This follows from eqs. (3.37) and (3.41).

d. The Z_0 Mismatch Loss

When a transmission line or waveguide is terminated in such a way that there are no reflected waves, the impedance of the termination equals or matches the characteristic impedance of the transmission line or waveguide. If the generator were to have the same impedance, then maximum net power would be delivered to the load, assuming of course that there were no losses in between. If one were then to connect a different load, there would be less power delivered, and a mismatch loss would result. The expression for mismatch loss would be eq. (3.47).

However, the generator is not always non-reflecting so that the Z_0 mismatch loss is

$$M_{Z_0} = 10 \log_{10} \frac{P_0}{P_1} = 10 \log_{10} \frac{|1 - \Gamma_G \Gamma_1|^2}{1 - |\Gamma_1|^2}. \tag{3.48}$$

It is possible for this expression to become negative (when $P_1 > P_0$), but this can occur only when $\Gamma_G \neq 0$.

e. Difference Between Conjugate and Z_0 Mismatch Losses

It has been observed that the conjugate mismatch loss and the Z_0 mismatch loss are the same when the generator is non-reflecting, and are given by eq. (3.47). In general, however, these two quantities are not the same and their difference is given by

$$M_C - M_{Z_0} = 10 \log_{10} \frac{P_A}{P_0} = 10 \log_{10} \frac{1}{1 - |\Gamma_G|^2}. \tag{3.49}$$

This is the ratio expressed in decibels of the available power from the generator to the power which would be absorbed by a non-reflecting load connected to that generator.

3.8. Transmission Properties of 2-Ports

Enough theory has already been developed to enable calculation of the net power transmitted through a 2-port. For example, the net power input to arm 1 may be calculated from eq. (3.37) and the net power output to a load connected to arm 2 is then obtained from eq. (3.28) for the efficiency. In terms of b_G and Γ_G, the scattering coefficients of the 2-port, Z_{02}, and the reflection coefficient Γ_L of the load, the net power transmitted to the load is

$$P_L = \frac{|b_G|^2}{Z_{02}} \cdot \frac{|S_{21}|^2 (1 - |\Gamma_L|^2)}{|(1 - S_{11}\Gamma_G)(1 - S_{22}\Gamma_L) - S_{12}S_{21}\Gamma_G\Gamma_L|^2}. \tag{3.50}$$

It is often desirable to compare the transmission properties on two 2-ports, and this problem has given rise to the concept of substitution loss which will be defined. The allied concepts of transducer loss, insertion loss, and attenuation are special cases of substitution loss, as will be shown.

In the following, unless otherwise stated, it will be assumed that the generator connects to arm number 1 of the 2-port and the load connects to arm number 2. This will allow a simpler notation. It then follows that a reversal of these connections will require a reversal of the subscripts 1 and 2 in the equations.

a. Substitution Loss

If one 2-port is removed from between a given generator and load, and another 2-port is substituted in its place, the net powers absorbed by the load under the initial and final conditions will have the following ratio, expressed in decibels:

$$L_S = 10 \log_{10} \frac{i_{P_L}}{f_{P_L}} = 20 \log_{10} \left| \frac{i_{S_{21}}[(1 - f_{S_{11}}\Gamma_G)(1 - f_{S_{22}}\Gamma_L) - f_{S_{12}} f_{S_{21}}\Gamma_G\Gamma_L]}{f_{S_{21}}[(1 - i_{S_{11}}\Gamma_G)(1 - i_{S_{22}}\Gamma_L) - i_{S_{12}} i_{S_{21}}\Gamma_G\Gamma_L]} \right|, \quad (3.51)$$

where the front superscripts i and f denote initial and final conditions, respectively, and it has been assumed that the act of substituting one 2-port for the other does not change the characteristics of either the generator or the load.

The above expression applies to cases in which the two arms of the waveguide are dissimilar, and/or have different propagating modes, as well as to the more usual case in which they are identical and the same mode propagates in each.

The substitution loss L_S, as defined above may range from $-\infty$ to $+\infty$, and upon assuming negative values, could be regarded as a gain, rather than a loss. This continues to hold true even when we exclude "active" 2-ports such as amplifiers, for the final 2-port might be a better transducer than the initial 2-port.

The substitution loss may be restricted to positive values by specifying certain characteristics for the initial 2-port, or for the generator and the load, as will be discussed later.

Actually, the substitution loss most closely corresponds to what one can measure, since even if initially no 2-port device is placed between generator and load, one must still have a joint or connector. When very accurate measurements are to be made, it is not permissible to neglect the reflection and dissipative loss of the connector (Beatty, 1964), so that it must be considered as the initial waveguide junction. As shown in figure 3-11, one always measures the substitution loss, even when the initial waveguide junction consists only of a connector.

A step attenuator, in which one attenuator is removed and another inserted in its place, is an excellent example of the need for the concept of substitution loss. This concept may also be applied to the case of a smoothly variable attenuator which may be regarded as though one removes an initial attenuator (corresponding to the initial setting) and substitutes in its place another attenuator (corresponding to the final setting) even though one does not physically remove the variable attenuator from the circuit. Thus it is analytically equivalent to a step attenuator, and the substitution loss concept applies.

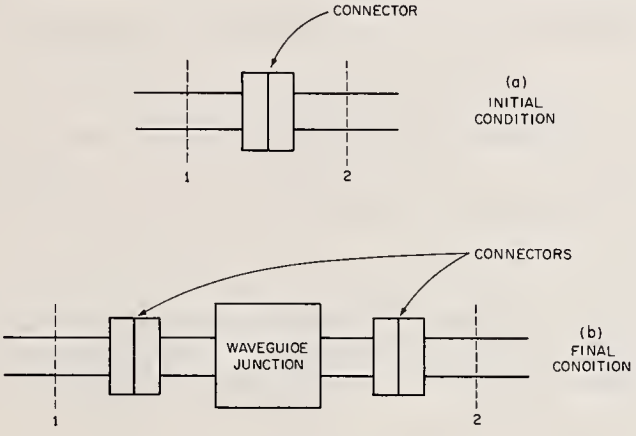

Figure 3-11. Insertion of a waveguide junction into a waveguide system. (a) Initial condition—one connector pair. (b) Final condition—waveguide junction core and two connector pairs.

b. Transducer Loss

As a special case of substitution loss, consider that the initial waveguide junction is a perfect transducer and transmits all of the available generator power P_A to the load. In order to do this the perfect transducer must not only be lossless, but must transform the load impedance to the complex conjugate of the generator impedance. The substitution loss is then obtained from eqs. (3.41) and (3.50) and is called the transducer loss:

$$L_T = 10 \log_{10} \frac{P_A}{P_L} = 10 \log_{10} \times \left(\frac{Z_{02}}{Z_{01}} \frac{|(1 - S_{11}\Gamma_G)(1 - S_{22}\Gamma_L) - S_{12}S_{21}\Gamma_G\Gamma_L|^2}{|S_{21}|^2(1 - |\Gamma_G|^2)(1 - |\Gamma_L|^2)} \right). \quad (3.52)$$

It follows from the above equation that the transducer loss of a passive 2-port cannot be negative. It is a measure of how closely the performance of the 2-port approaches that of a perfect transducer connected between a given generator and load.

Although the transducer loss is felt to be a useful concept, any attempts to measure transducer loss will be in error by the amount by which the initial 2-port fails to be a perfect transducer, unless the transducer loss of the initial 2-port can be closely estimated, and added to the observed loss.

Like substitution loss, transducer loss may apply to 2-ports having dissimilar arms, and/or dissimilar propagating modes in each arm. It cannot be used to specify a property of a 2-port since Γ_G and Γ_L are involved in eq. (3.52).

c. Insertion Loss

Another special case of substitution loss is the insertion loss.[4] Here it is assumed that the initial 2-port is a perfect connector or adapter, which has no dissipative loss and introduces no reflection or phase shift. The initial power is given by eq. (3.37) substituting Γ_L for Γ_1, and the final power is given by eq. (3.50), so that the insertion loss is

$$L_1 = 10 \log_{10} \frac{i_{P_L}}{f_{P_L}} = 10 \log_{10} \left[\frac{Z_{02}}{Z_{01}} \cdot \frac{|(1 - S_{11}\Gamma_G)(1 - S_{22}\Gamma_L) - S_{12}S_{21}\Gamma_G\Gamma_L|^2}{|S_{21}(1 - \Gamma_G\Gamma_L)|^2} \right] \quad . \quad (3.53)$$

It is apparent that the insertion loss is normally positive, but could be negative; for example, in the case where the load does not provide a conjugate match to the generator, and the 2-port which is inserted is lossless and does provide a conjugate match.

The idealized initial condition of a perfect connector may perhaps be more closely approached in practice than the initial condition of perfect transducer, and hence the insertion loss may be more accurately measured than the transducer loss. Neither can be used in general to specify the characteristics of a 2-port, since generator and load characteristics affect both. However, they both become equivalent in the case of non-reflecting generator and load to be discussed below.

d. Attenuation[5] or Characteristic Insertion Loss

A concept which is useful for specification of a characteristic of a 2-port is its attenuation, which is the transducer loss or the insertion loss of the 2-port

---

[4] In the IRE definition of Insertion Loss see p. 75 of IRE Dictionary (1961), the definition is "fuzzy" because nothing is said about the initial connector which is opened to insert the device.

[5] See section 6.2 for further discussion of definitions of attenuation.

when placed in a non-reflecting system. Making the substitution $\Gamma_G = \Gamma_L = 0$ in eq. (3.52) or eq. (3.53) yields

$$A = 10 \log_{10}\left(\frac{Z_{02}}{Z_{01}} \cdot \frac{1}{|S_{21}|^2}\right). \tag{3.54}$$

In attempting to measure the attenuation of a 2-port, one should note that errors will be produced by any failure to meet the assumed initial conditions, and the condition of a non-reflecting system. The actual quantity measured will be the substitution loss, and the error may be analyzed by comparison of eqs. (3.54) and (3.51).[6]

In the special but often encountered case in which arms 1 and 2 of the 2-port are identical, it is convenient to choose $Z_{01} = Z_{02}$, and its attenuation is

$$[A]_{Z_{01}=Z_{02}} = 20 \log_{10} \frac{1}{|S_{21}|}. \tag{3.55}$$

It is apparent that $|S_{21}|$ may be determined by measuring the attenuation of the 2-port, provided that we specify Z_{01} and Z_{02}. Similarly, $|S_{12}|$ may be determined by connecting the generator to arm 2 and the load to arm 1.

The attenuation of a waveguide junction[7] for energy traveling into arm 2 and out of arm 1 is

$$A_2 = 10 \log_{10}\left(\frac{Z_{01}}{Z_{02}} \cdot \frac{1}{|S_{12}|^2}\right). \tag{3.56}$$

The difference between the "forward" and "backward" attenuations is

$$A_2 - A_1 = 20 \log_{10}\left|\frac{Z_{01}S_{21}}{Z_{02}S_{12}}\right|. \tag{3.57}$$

It is interesting to note that a waveguide junction which satisfies the reciprocity condition ($Z_{01}S_{21} = Z_{02}S_{12}$) has the same "forward" and "backward" attenuations. This is one test for reciprocity, but is not a sufficient condition, since it tells nothing about the phase relationship between S_{12} and S_{21}.

e. Components of Losses

It is convenient and instructive to separate the substitution loss and its derivatives into components, one associated with the dissipation of energy, and the other with mismatch.

---

[6] A detailed error analysis is given later in sections 6.4, 6.5, and 6.6.

[7] One can specify the attenuation between any two arms of a multiport having all of its arms terminated in some specified manner to passive loads.

The net power transmitted to the load equals the input power multiplied by the efficiency of the 2-port. If the available power from the generator is given, then the input power to the 2-port may be obtained from the conjugate mismatch loss. Thus two quantities, (1) the conjugate mismatch loss and (2) the efficiency, are sufficient to determine the power absorbed by the load, if the available power from the generator is given. (1) is associated with mismatch, and (2) is associated with the dissipation of energy.

It is evident that substitution of another 2-port for the initial one will cause a change of power absorbed by the load, and that the change will be equal to the changes of (1) and (2) above. Thus the substitution loss may be written

$$L_S = ({}^{f}M_C - {}^{i}M_C) + 10 \log_{10}\left(\frac{i_\eta}{f_\eta}\right) = (L_S)_M + (L_S)_D. \tag{3.58}$$

Referring to eq. (3.46) we can write

$$(L_S)_M = 10 \log_{10}\left(\left|\frac{1 - \Gamma_G {}^{f}\Gamma_1}{1 - \Gamma_G {}^{i}\Gamma_1}\right|^2 \cdot \frac{1 - |{}^{i}\Gamma_1|^2}{1 - |{}^{f}\Gamma_1|^2}\right), \tag{3.59}$$

and referring to eq. (3.28), we can write

$$(L_S)_D = 10 \log_{10}\left(\left|\frac{{}^{i}S_{21}}{{}^{f}S_{21}} \cdot \frac{1 - {}^{f}S_{22}\Gamma_L}{1 - {}^{i}S_{22}\Gamma_L}\right|^2 \cdot \frac{1 - |{}^{f}\Gamma_1|^2}{1 - |{}^{i}\Gamma_1|^2}\right), \tag{3.60}$$

where Γ_1 is given by eq. (2.12).

The substitution loss is obtained by adding eqs. (3.59) and (3.60), which yields

$$L_S = 20 \log_{10}\left|\frac{{}^{i}S_{21}}{{}^{f}S_{21}} \cdot \frac{1 - {}^{f}S_{22}\Gamma_L}{1 - {}^{i}S_{22}\Gamma_L} \cdot \frac{1 - \Gamma_G {}^{f}\Gamma_1}{1 - \Gamma_G {}^{i}\Gamma_1}\right|. \tag{3.61}$$

It is apparent that substitution of eq. (3.10) into eq. (3.61) will yield eq. (3.51), verifying that eq. (3.61) does represent the substitution loss.

The components of transducer loss may be obtained by appropriate specialization of eq. (3.58) and are

$$[L_T]_M = 10 \log_{10} \frac{|1 - \Gamma_G\Gamma_1|^2}{(1 - |\Gamma_G|^2)(1 - |\Gamma_1|^2)}, \tag{3.62}$$

and

$$[L_T]_D = 10 \log_{10} \frac{1}{\eta_1}, \tag{3.63}$$

where η_1 is given by eq. (3.28).

Similarly the components of insertion loss are

$$[L_1]_M = 10 \log_{10}\left(\left|\frac{1 - \Gamma_G\Gamma_1}{1 - \Gamma_G\Gamma_L}\right|^2 \cdot \frac{1 - |\Gamma_L|^2}{1 - |\Gamma_1|^2}\right). \tag{3.64}$$

and

$$[L_1]_D = 10 \log_{10} \frac{1}{\eta}. \tag{3.65}$$

Finally, the components of attenuation are

$$[A]_M = 10 \log_{10} \frac{1}{1 - |S_{11}|^2}, \tag{3.66}$$

and

$$[A]_D = 10 \log_{10}\left(\frac{Z_{02}}{Z_{01}} \cdot \frac{1 - |S_{11}|^2}{|S_{21}|^2}\right). \tag{3.67}$$

Comparison of eq. (3.67) with eq. (3.29) shows that the component of attenuation associated with dissipation may also be written

$$[A_1]_D = 10 \log_{10} \frac{1}{[\eta_1]_{a_2=0}}. \tag{3.68}$$

3.9. Maximum Transmitted Power

The conditions for maximum transmission of power to a load are given with reference to figure 3-12, in which two lossless tuners are shown connected one on each side of the waveguide junction.

First, the maximum power available from the generator must be obtained at the input to the waveguide junction. The conjugate match $\Gamma_A = \overline{\Gamma}_G$ must be obtained by adjustment of the tuner T_V, and the generator will then deliver maximum power. Since T_V is lossless, maximum power will be obtained in arm 1 of the waveguide junction, and the conjugate match $\Gamma_1 = \overline{\Gamma}_B$ will apply there.

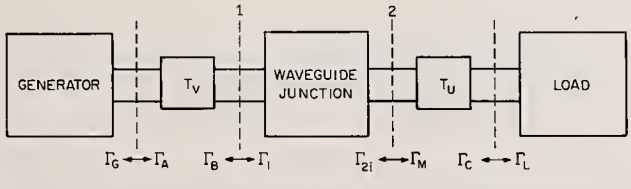

Figure 3-12. Two lossless tuners attached to waveguide junction in order to obtain maximum power to load.

Second, maximum power must be obtained at the output arm of the wavguide junction, arm 2. This will occur when $\Gamma_M = \overline{\Gamma}_{2i}$, where Γ_{2i} is the reflection coefficient of the equivalent generator at that terminal surface. Under this condition, it is evident that the efficiency of the waveguide junction is maximum. It is also evident that since T_U is lossless, the condition $\Gamma_L = \overline{\Gamma}_C$ will also apply.

In practice, adjustment of tuners in the above sequence would not produce the maximum transmission of power with only one adjustment of each, since the second adjustment would in general upset the conditions achieved by the first adjustment.[8] Rather, a series of adjustments converging upon the desired condition might be necessary.

a. Maximum Efficiency

The efficiency of a two-arm waveguide junction was seen to depend upon Γ_L, the reflection coefficient of the load. With the load terminating arm 2 of the 2-port, the efficiency η_1 is given by eq. (3.28). One expects that the efficiency would have a maximum value η_{1M} for a particular value Γ_M of the reflection coefficient of the load.

The following problem is often of interest. Given the characteristics of the waveguide junction (for example, the scattering coefficients and the characteristic impedances of the waveguide leads) calculate Γ_M and η_{1M}. The solutions will be given, one based upon analysis of eq. (3.28), and the other based upon the maximum power considerations discussed previously.

(1) Gradient of Efficiency

According to eq. (3.28), efficiency is a function of Γ_L, which is complex, and one can plot contours of efficiency in the Γ_L-plane. Maxima and minima will occur when the gradient of η_1 vanishes.

The gradient of η_1 is

$$\nabla \eta_1 = \vec{e}_{|\Gamma_L|} \frac{\partial \eta_1}{\partial |\Gamma_L|} + \vec{e}_{\psi_L} \frac{1}{|\Gamma_L|} \cdot \frac{\partial \eta_1}{\partial \psi_L}. \tag{3.69}$$

[8]There are special cases in which the second adjustment would not upset the first. For example, when the waveguide junction is an isolator.

Both components of the gradient vanish at a maximum point. In order for the ψ_L-component of the gradient to vanish,

$$0 = \frac{\partial \eta_1}{\partial \psi_L}$$

$$= \frac{-2Z_{01}|S_{21}|^2(1-|\Gamma_L|^2)|\Gamma_L|[|S_{22}|\sin(\psi_{22}+\psi_L) + |S_{12}S_{21}-S_{11}S_{22}||S_{11}|\sin(\psi_U-\psi_{11}+\psi_L)]}{Z_{02}[|1-S_{22}\Gamma_L|^2-|(S_{12}S_{21}-S_{11}S_{22})\Gamma_L+S_{11}|^2]^2}. \tag{3.70}$$

where ψ_U is the phase angle of $(S_{12}S_{21} - S_{11}S_{22})$. It vanishes when

$$\left|\frac{S_{22}}{(S_{12}S_{21} - S_{11}S_{22})S_{11}}\right| = \frac{\sin(\psi_{11} - \psi_U - \psi_M)}{\sin(\psi_{22} + \psi_M)}, \tag{3.71}$$

where ψ_M is the phase of Γ_M. The solution of eq. (3.71) for ψ_M gives the argument of the reflection coefficient of the load for the maximum efficiency point. This solution is independent of $|\Gamma_M|$.

In a similar way, it can be shown that the $|\Gamma_L|$-component of the gradient vanishes when

$$A|\Gamma_L|^2 - B|\Gamma_L| + A = 0, \tag{3.72}$$

where

$$A = |S_{22}| \cos(\psi_{22} + \psi_M) + |(S_{12}S_{21} - S_{11}S_{22})S_{11}| \cos(\psi_{11} - \psi_U - \psi_M),$$

and

$$B = (1 - |S_{11}|^2 + |S_{22}|^2 - |S_{12}S_{21} - S_{11}S_{22}|^2).$$

Note that ψ_M has been substituted for ψ_L in A.

The solution for Γ_M is then

$$\Gamma_M = \frac{B}{2A}\left\{1 \mp \sqrt{\left[1 - \left(\frac{2A}{B}\right)^2\right]}\right\} e^{j\psi_M}. \tag{3.73}$$

Substitution of Γ_M for Γ_L in eq. (3.28) will then give η_{1M}, the maximum efficiency:

$$\eta_{1M} = \frac{Z_{01}}{Z_{02}} \frac{|S_{21}|^2(1 - |\Gamma_M|^2)}{|1 - S_{22}\Gamma_M|^2 - |(S_{12}S_{21} - S_{11}S_{22})\Gamma_M + S_{11}|^2}. \tag{3.74}$$

(2) Maximum Efficiency from Maximum Power Considerations

Referring to figure 3-13,

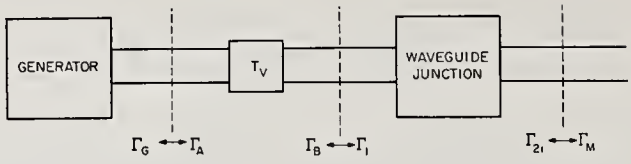

Figure 3-13. Generator, tuner, and waveguide junction.

the conditions for maximum power transmission (and maximum efficiency) are

$$\Gamma_1 = \overline{\Gamma}_B, \tag{3.75}$$

and

$$\Gamma_M = \overline{\Gamma}_{2i}. \tag{3.76}$$

Rewriting eqs. (3.75) and (3.76)

$$\overline{\Gamma}_B = \Gamma_1 = \frac{(S_{12}S_{21} - S_{11}S_{22})\Gamma_M + S_{11}}{1 - S_{22}\Gamma_M}, \tag{3.77}$$

and

$$\Gamma_M = \overline{\Gamma}_{2i} = \frac{(\overline{S}_{12}\overline{S}_{21} - \overline{S}_{11}\overline{S}_{22})\overline{\Gamma}_B + \overline{S}_{22}}{1 - \overline{S}_{11}\overline{\Gamma}_B}. \tag{3.78}$$

We can eliminate $\overline{\Gamma}_B$ and obtain a quadratic equation with variable Γ_M:

$$a\Gamma_M^2 - B\Gamma_M + \overline{a} = 0, \tag{3.79}$$

where

$$a = S_{22} + \overline{S}_{11}(S_{12}S_{21} - S_{11}S_{22}),$$

and

$$B = 1 - |S_{11}|^2 + |S_{22}|^2 - |S_{12}S_{21} - S_{11}S_{22}|^2.$$

The solution of eq. (3.79) is

$$\Gamma_M = \frac{B}{2a}\left\{1 \pm \sqrt{\left[1 - \left(\frac{2|a|}{B}\right)^2\right]}\right\}. \tag{3.80}$$

The expression for maximum efficiency is then

$$\eta_{1M} = \frac{Z_{01}}{Z_{02}} \frac{|S_{21}|^2(1 - |\Gamma_M|^2)}{|1 - S_{22}\Gamma_M|^2 - |(S_{12}S_{21} - S_{11}S_{22})\Gamma_M + S_{11}|^2}. \tag{3.74}$$

Since the complex Γ_M can be obtained from eq. (3.79), one can also separately find the magnitude and phase of Γ_M as follows. If we multiply eq. (3.79) by $e^{-j\psi_M}$, we obtain

$$ae^{j\psi_M}|\Gamma_M|^2 - B|\Gamma_M| + \bar{a}e^{-j\psi_M} = 0. \tag{3.81}$$

Taking the real part, we obtain

$$A|\Gamma_M|^2 - B|\Gamma_M| + A = 0.$$

which is of the same form as eq. (3.72), and taking the imaginary part of eq. (3.81), we obtain

$$\left|\frac{S_{22}}{S_{11}(S_{12}S_{21} - S_{11}S_{22})}\right| = -\frac{\sin(\psi_U + \psi_M - \psi_{11})}{\sin(\psi_{22} + \psi_M)}. \tag{3.71}$$

Thus the two solutions for Γ_M are seen to be equivalent. However, the minimum loss method yields the complex value of Γ_M from solution of eq. (3.79) while the vanishing of the gradient method requires first a calculation of ψ_M, then a calculation of $|\Gamma_M|$ by eqs. (3.71) and (3.73).

b. Minimum Transducer Loss

The following problem is of some interest in connection with maximum transmission of power. Suppose that the lossless tuners T_U and T_V are connected as shown in figure 3-12 and adjusted to give maximum transmission of power. Under these conditions, the transducer loss of the resulting waveguide junction (including the tuners) is minimum. What is the value in terms of the characteristics of the original waveguide junction?

It is apparent that the component of transducer loss associated with mismatch as given by eq. (3.62) is zero. Thus the minimum transducer loss is given by eq. (3.63), where η is the efficiency of the resulting waveguide junction. However, since tuners T_U and T_V are lossless, the efficiency is also that of the original waveguide junction. Under the above condition of maximum transmission of power, this efficiency is a maximum η_M, and hence the minimum transducer loss is

$$[L_T]_M = 10 \log_{10} \frac{1}{\eta_M}. \tag{3.82}$$

It has not been assumed in this instance that Γ_G and Γ_L vanish, hence we cannot conclude that resulting waveguide junction is non-reflecting, and in general, it will not fulfill this condition.

c. Intrinsic Attenuation

The minimum attenuation of a 2-port, obtained by adjusting tuners connected as shown in figure 3-12, is by definition (Beatty, 1964c) the minimum transducer loss under the conditions of non-reflecting generator and load ($\Gamma_G = \Gamma_L = 0$). It is given by eq. (3.82) and may be called the intrinsic attenuation for reasons similar to those given above.

The resulting composite waveguide junction including the tuners is non-reflecting (a bilateral Z_0 match), since the conjugate match condition exists at both input and output terminal surfaces, and the generator and load are non-reflecting. Re-writing eq. (3.82)

$$A_I = 10 \log_{10} \frac{1}{\eta_M}, \tag{3.83}$$

3.10. Phase Shift

a. Relative Phase

A quantity such as voltage, current, or voltage wave amplitude which varies sinusoidally at a fixed frequency f may be represented by a complex quantity

$$u = Ae^{j(\omega t+B)} = Ae^{j\theta}. \tag{3.84}$$

The phase of u at any instant of time t is

$$\theta = \arg u = \omega t + B. \tag{3.85}$$

where $\omega = 2\pi f$.

Since we cannot tell absolutely when t was equal to zero, B cannot be absolutely determined and thus phase is always relative. The phase θ may be expressed in degrees, radians, or cycles.

We choose the convention that the angle θ is positive when measured counterclockwise in the complex plane, and we choose u as above (not $u = Ae^{-j\theta}$).

b. Shift of Phase by a 2-Port[9]

We are interested in different kinds of relative phase or phase shift. For example, we may observe the phase of the output voltage[10] of a 2-port relative to the

[9]See Kerns and Beatty (1967), and Beatty (1964d). In this monograph, phase shift is positive if it is a phase advance (lead) and negative if it is a phase delay (lag). However, it should be noted that the term "phase shift" is often used to denote the absolute magnitude of a phase difference, and is then always positive.

[10]Other quantities, such as current or electric wave amplitude may also be of interest.

phase of the output from a signal source, which is padded or isolated and phase locked to an oscillator of stable frequency. If the 2-port changes, the relative phase of the output voltage may be shifted to a different value. The phase shift is

$$\Delta\theta = {}^{f}\theta - {}^{i}\theta, \tag{3.86}$$

where front superscripts i and f denote respectively the initial and final values of the relative phase of the output voltage.

c. Different Kinds of Phase Shift of 2-Ports

Three kinds of phase shift associated with 2-ports are illustrated in figure 3-14.

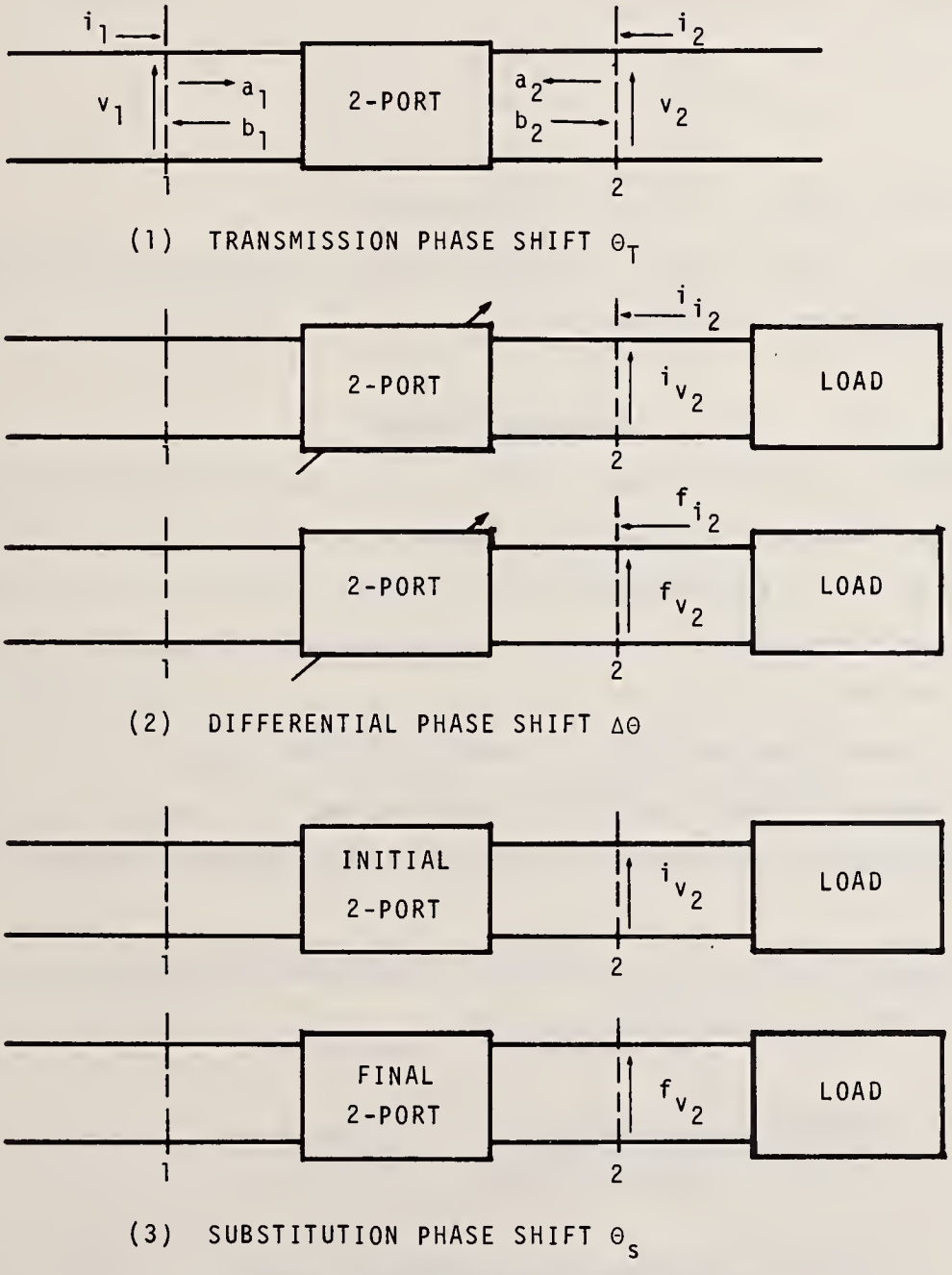

Figure 3-14. Three kinds of phase shift associated with a 2-port.

They are:

(1) Transmission Phase Shift

$$\theta_T = \arg\left(\frac{b_2}{a_1}\right);\ \arg\left(\frac{v_2}{v_1}\right);\ \arg\left(\frac{i_2}{i_1}\right). \tag{3.87}$$

This is similar to transmission loss.

(2) Differential Phase Shift

$$\Delta\theta = \arg\left(\frac{f_{b_2}}{i_{b_2}}\right) = \arg\left(\frac{f_{v_2}}{i_{v_2}}\right) = \arg\left(\frac{f_{i_2}}{i_{i_2}}\right). \tag{3.88}$$

This is similar to incremental attenuation.

(3) Substitution Phase Shift, Including Insertion Phase Shift

$$\theta_S = \arg\left(\frac{f_{b_2}}{i_{b_2}}\right);\ \arg\left(\frac{f_{v_2}}{i_{v_2}}\right);\ \arg\left(\frac{f_{i_2}}{i_{i_2}}\right). \tag{3.89}$$

This is similar to substitution loss or to insertion loss.

Further discussion of this topic, including equations for various phase shifts of 2-ports is presented later in section 7.2.

3.11. Cascading 2-Ports

In the analysis of measuring systems, it is often necessary to determine the properties of a 2-port composed of a number of cascade-connected 2-ports. Consider the following problem. Given the scattering coefficients of each of two individual 2-ports, determine the scattering coefficients of the composite 2-port which results when these 2-ports are cascade-connected. This problem may be reduced to three steps: (1) conversion of the scattering matrices of each unit to cascading matrices, (2) multiplication in sequence of these cascading matrices, and (3) conversion of the resulting cascading matrix to the scattering matrix of the composite waveguide junction.

To illustrate and provide the basis for these procedures, consider the cascade connection of two 2-ports as shown in figure 3-15.

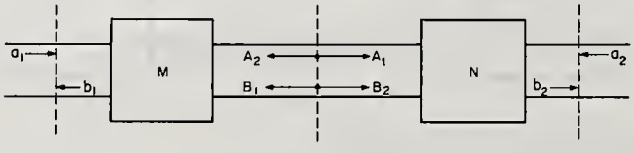

Figure 3-15. Cascade connection of two 2-ports.

The scattering matrices of M and N are

$$m = \begin{pmatrix} m_{11} & m_{12} \\ m_{21} & m_{22} \end{pmatrix} \quad \text{and} \quad n = \begin{pmatrix} n_{11} & n_{12} \\ n_{21} & n_{22} \end{pmatrix}. \tag{3.90}$$

The corresponding cascading matrices relate the wave amplitudes as follows:

$$\begin{pmatrix} b_1 \\ a_1 \end{pmatrix} = \begin{pmatrix} M_{11} & M_{12} \\ M_{21} & M_{22} \end{pmatrix} \begin{pmatrix} A_2 \\ B_2 \end{pmatrix} = M \begin{pmatrix} A_2 \\ B_2 \end{pmatrix},$$

and

$$\begin{pmatrix} B_1 \\ A_1 \end{pmatrix} = \begin{pmatrix} N_{11} & N_{12} \\ N_{21} & N_{22} \end{pmatrix} \begin{pmatrix} a_2 \\ b_2 \end{pmatrix} = N \begin{pmatrix} a_2 \\ b_2 \end{pmatrix}. \tag{3.91}$$

The joining equations are

$$A_2 = B_1 \quad \text{and} \quad A_1 = B_2. \tag{3.92}$$

Thus,

$$\begin{pmatrix} b_1 \\ a_1 \end{pmatrix} = MN \begin{pmatrix} a_2 \\ b_2 \end{pmatrix} = R \begin{pmatrix} a_2 \\ b_2 \end{pmatrix}, \tag{3.93}$$

where R is the cascading matrix of the composite waveguide junction. The relationship between the scattering matrix S and the cascading matrix is as follows:

$$R = \frac{1}{S_{21}} \begin{pmatrix} (S_{12}S_{21} - S_{11}S_{22}) & S_{11} \\ -S_{22} & 1 \end{pmatrix}, \tag{3.94}$$

and

$$S = \frac{1}{r_{22}} \begin{pmatrix} r_{12} & (r_{11}r_{22} - r_{12}r_{21}) \\ 1 & -r_{21} \end{pmatrix}. \tag{3.95}$$

For the example above,

$$R = \begin{pmatrix} (M_{11}N_{11} + M_{12}N_{21}) & (M_{11}N_{12} + M_{12}N_{22}) \\ (M_{21}N_{11} + M_{22}N_{21}) & (M_{21}N_{12} + M_{22}N_{22}) \end{pmatrix}. \tag{3.96}$$

In terms of the scattering coefficients,

$$\begin{cases} r_{11} = [(m_{12}m_{21} - m_{11}m_{22})(n_{12}n_{21} - n_{11}n_{22}) - m_{11}m_{22}] \dfrac{1}{m_{21}n_{21}}, \\ r_{12} = [m_{11}(1 - m_{22}n_{11}) - m_{12}m_{21}n_{11}] \dfrac{1}{m_{21}n_{21}}. \\ r_{21} = [-n_{22}(1 - m_{22}n_{11}) - m_{22}n_{12}n_{21}] \dfrac{1}{m_{21}n_{21}}, \text{ and} \\ r_{22} = (1 - m_{22}n_{11}) \dfrac{1}{m_{21}n_{21}}. \end{cases} \tag{3.97}$$

Using eq. (3.95), we obtain the scattering coefficient of the composite waveguide junction in terms of those of the two cascaded units as follows:

$$\begin{cases} S_{11} = m_{11} + \dfrac{m_{12}m_{21}n_{11}}{1 - m_{22}n_{11}} \\ S_{12} = \dfrac{n_{12}m_{12}}{1 - n_{11}m_{22}}, \\ S_{21} = \dfrac{m_{21}n_{21}}{1 - m_{22}n_{11}}, \text{ and} \\ S_{22} = n_{22} + \dfrac{n_{12}n_{21}m_{22}}{1 - n_{11}m_{22}}. \end{cases} \tag{3.98}$$

3.12. Cascading Coefficients

The cascading coefficients are of special interest not only in analysis of cascaded 2-ports, but are also the coefficients of the equation for the transformation of reflection coefficient by a 2-port. Rewriting eq. (3.10) we obtain

$$\Gamma_1 \equiv \frac{r_{11}\Gamma_L + r_{12}}{r_{21}\Gamma_L + r_{22}}. \tag{3.99}$$

Inspection of eq. (3.94) reveals that the following equation holds

$$r_{11}r_{22} - r_{12}r_{21} = \frac{S_{12}}{S_{21}}. \tag{3.100}$$

Referring to eq. (3.18), it is seen that the reciprocity condition on the cascading coefficients is

$$r_{11}r_{22} - r_{12}r_{21} = \frac{Z_{01}}{Z_{02}}. \tag{3.101}$$

The lossless condition on these coefficients are as follows:

$$\begin{cases} |r_{12}| = |r_{21}|; \quad |r_{11}| = |r_{22}|; \\ |r_{11}r_{22} - r_{12}r_{21}| = \dfrac{Z_{01}}{Z_{02}}; \quad \text{and} \\ \phi_{12} + \phi_{21} = \phi_{11} + \phi_{22} \pm 2n\pi, \end{cases} \tag{3.102}$$

where n is an integer and ϕ_{pq} is the argument of r_{pq}.

In terms of the cascading coefficients, the efficiency η_1 can be written

$$\eta_1 = \frac{Z_{01}}{Z_{02}} \cdot \frac{1 - |\Gamma_L|^2}{|r_{21}\Gamma_L + r_{22}|^2 - |r_{11}\Gamma_L + r_{12}|^2}. \tag{3.103}$$

3.13. Transformation of Reflection Coefficients

A 2-port with arm 2 terminated in a load having a reflection coefficient Γ_L has an input (arm 1) reflection coefficient of

$$\Gamma_1 = \frac{(S_{12}S_{21} - S_{11}S_{22})\Gamma_L + S_{11}}{1 - S_{22}\Gamma_L} = \frac{a\Gamma_L + b}{c\Gamma_L + d}. \tag{3.104}$$

The reflection coefficient Γ_L is said to be transformed to a reflection coefficient Γ_1 by the 2-port. An equation of the form of eq. (3.104) is called a linear fractional transformation. Many properties of the linear fractional transformation from the theory of complex variables[11] can be applied to the theory of waveguide junctions. A few of the simpler properties will be reviewed and applications to some types of microwave measurements will become apparent.

a. Simpler Transformations

It is helpful in visualizing transformations of a complex quantity Γ_L to another complex quantity Γ_1 to draw the two complex planes, and plot corresponding points. Thus we might have the following transformations illustrated in figure 3-16.

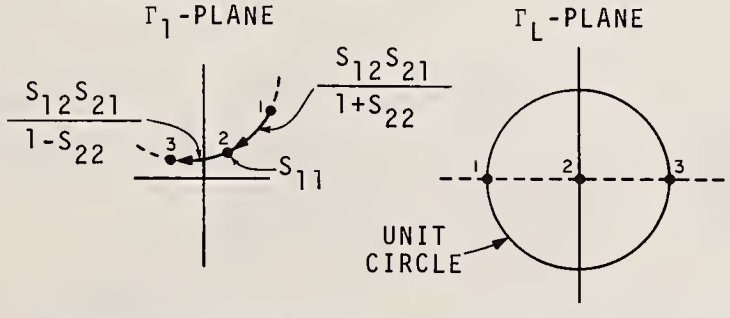

Figure 3-16. Transformation of three points from Γ_L-plane to Γ_1-plane.

1. $\Gamma_1 = \frac{-a + b}{-c + d} = S_{11} - \frac{S_{12}S_{21}}{1 + S_{22}}$; $\Gamma_L = -1$.

2. $\Gamma_1 = \frac{b}{d} = S_{11}$; $\Gamma_L = 0$.

[11] There is a wealth of literature on this subject and only a few examples are listed (Deschamps, 1953), (Storer, et al., 1953, and (Mathis, 1954).

$$3. \qquad \Gamma_1 = \frac{a + b}{c + d} = S_{11} + \frac{S_{12}S_{21}}{1 - S_{22}}; \qquad \Gamma_L = +1. \tag{3.105}$$

A well-known property of the linear fractional transformation is that circles in the Γ_L-plane transform to circles (different ones) in the Γ_1-plane. Since three distinct points determine a circle, one can draw the Γ_1-circle corresponding to a given Γ_L-circle by transforming just three distinct points of the Γ_L-circle. In figure 3.16 the real axis in the Γ_L-plane (a circle of infinite radius) has been transformed into a circle in the Γ_1-plane.

b. The Sliding Termination

A termination sliding inside a uniform, lossless waveguide will cause the reflection coefficient Γ_L at a fixed terminal surface in the waveguide to vary in phase, but not in magnitude. Thus a circular locus of Γ_L is produced, with its center on the origin.

The corresponding circular locus of Γ_1 can be found by applying eq. (3.104), but it is simpler to use the following form of eq. (3.10):

$$\Gamma_1 - S_{11} = \frac{S_{12}S_{21}}{\frac{1}{|\Gamma_L|} e^{-j\psi_L} - S_{22}}. \tag{3.106}$$

The variation of ψ_L by sliding the termination changes only one term. Proceeding one step at a time, we can determine the corresponding variation of Γ_1 as shown in figure 3-17.

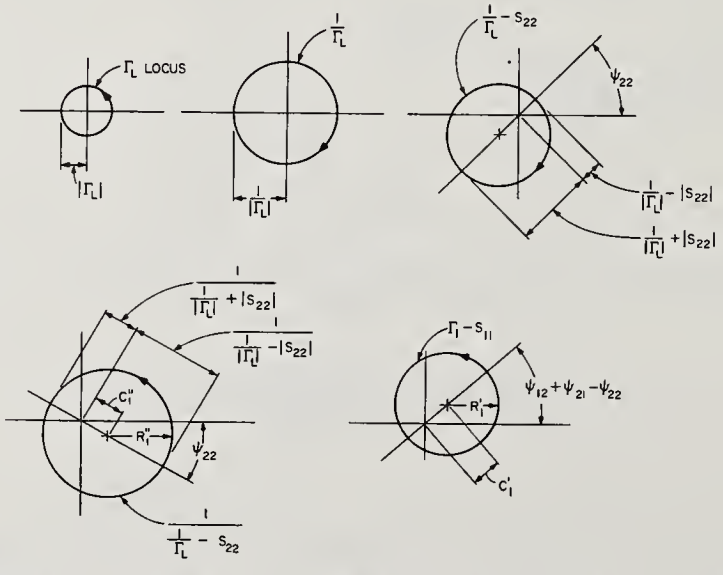

Figure 3-17. Steps in the transformation of a Γ_L-circle to a $(\Gamma_1 - S_{11})$-circle.

From figure 3-17 it is evident that the radius of the $(\Gamma_1 - S_{11})$-circle, and also of the Γ_1-circle of figure 3-18 is $R_1''|S_{12}S_{21}|$, or

$$R_1 = R_1' = \frac{1}{2}\left(\frac{1}{\frac{1}{|\Gamma_L|} + |S_{22}|} + \frac{1}{\frac{1}{|\Gamma_L|} - |S_{22}|}\right)|S_{12}S_{21}| = \frac{|S_{12}S_{21}\Gamma_L|}{1 - |S_{22}\Gamma_L|^2}. \qquad (3.107)$$

The distance from the origin to the center of the $(\Gamma_1 - S_{11})$-circle is

$$|C_1'| = |S_{12}S_{21}|\left(R_1'' - \frac{1}{\frac{1}{|\Gamma_L|} + |S_{22}|}\right) = \frac{|S_{12}S_{21}S_{22}\Gamma_L^2|}{1 - |S_{22}\Gamma_L|^2} = R_1|S_{22}\Gamma_L|. \qquad (3.108)$$

The Γ_1-circle is shown in figure 3-18.

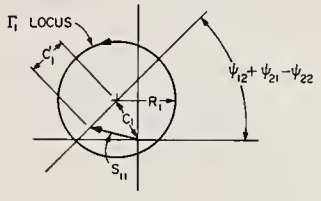

Figure 3-18. The Γ_1-circle corresponding to a Γ_L-circle centered on the origin.

c. Significance of the Radius of the Γ_1-Circle

Under certain conditions, the radius R_1 of the Γ_1-circle equals the efficiency $[\eta_2]_{a_1=0}$ of the waveguide junction. These conditions are

1. $|\Gamma_L| = 1$ (a sliding short circuit).
2. $Z_{01}S_{21} = Z_{02}S_{12}$ (the reciprocity condition).

When these conditions are satisfied,

$$R_1 = \frac{Z_{02}}{Z_{01}}\frac{|S_{12}|^2}{1 - |S_{22}|^2} = [\eta_2]_{a_1=0}. \qquad (3.109)$$

The component of attenuation associated with dissipation $[A_2]_D$ is related to the radius of the Γ_1-circle as follows:

$$[A_2]_D = 10 \log_{10}\frac{1}{R_1}. \qquad (3.110)$$

Note that the attenuation component $[A_2]_D$ corresponds to energy flowing into arm 2 and out of arm 1, while the Γ_1-circle corresponds to energy flowing in the opposite direction.

A similar result is obtained if the sliding short-circuit is in arm 1, and R_2 is the radius of the Γ_2-circle, as follows:

$$[A_1]_D = 10 \log_{10} \frac{1}{R_2}. \tag{3.111}$$

d. Displacement of Center from Origin

The center of the Γ_1-circle is displaced from the origin by the vector representing the complex quantity $C_1 = S_{11} + C_1'$, where $|C_1'|$ is given by eq. (3.108) and C_1 is directed at the angle $\psi_{12} + \psi_{21} - \psi_{22}$ as shown in figure 3-18.

It is apparent that the Γ_1-circle will be concentric with the origin if the waveguide junction is non-reflecting ($S_{11} = S_{22} = 0$). We have then

$$[C_1]_{S_{11}=S_{22}=0} = 0 \quad \text{and} \quad [R_1]_{S_{11}=S_{22}=0} = |S_{12}S_{21}\Gamma_L|. \tag{3.112}$$

Also, for a non-reflecting waveguide junction, for which reciprocity holds, and $|\Gamma_L| = 1$,

$$[A]_{S_{11}=S_{22}=0} = 10 \log_{10} \frac{1}{[R]_{S_{11}=S_{22}=0}}. \tag{3.113}$$

In this case it makes no difference which is the direction of energy flow through the waveguide junction.

The possibility of other conditions for which the Γ_1-circle might be concentric with the origin exists. For example, if C_1' and S_{11} are equal and opposite,

$$\psi_{11} + \psi_{22} = \psi_{12} + \psi_{21} \pm (2n - 1)\pi,$$

and

$$|S_{11}| = \frac{|S_{12}S_{21}S_{22}\Gamma_L^2|}{1 - |S_{22}\Gamma_L|^2}. \tag{3.114}$$

e. Locus of Γ_1 for Γ_L Real

If Γ_L is restricted to real values, the locus of Γ_1 is a circle. This condition may be closely approximated in practice by varying the bias current of a barretter in a microwave power mount,[12] for example.

[12]This technique is based upon a method originated by Kerns (1949b). See also, Beatty and Reggia (1955).

Referring to eq. (3.106) we again proceed step-by-step to obtain the circular locus of Γ_1 as shown in figure 3-19.

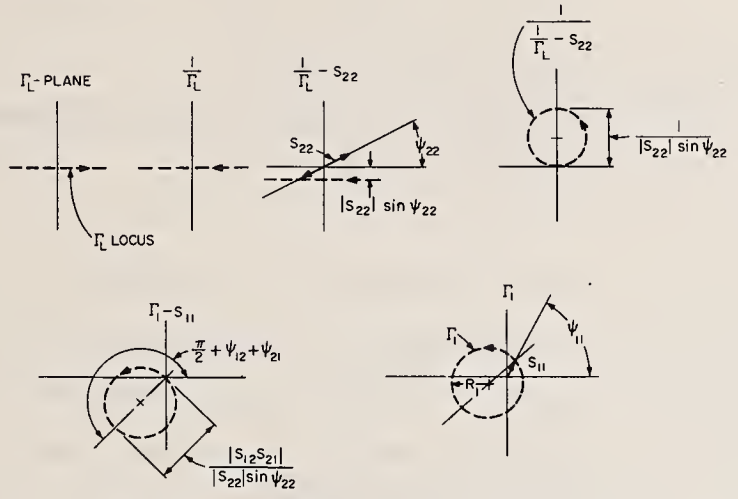

Figure 3-19. Steps in the transformation of real Γ_L to a Γ_1-circle.

It can be seen from inspection of figure 3-19 that

$$R_1 = \frac{|S_{12}S_{21}|}{2|S_{22}| \sin \psi_{22}}, \tag{3.115}$$

and that the center of the Γ_1-circle is located at

$$C_1 = S_{11} + R_1 e^{j(\pi/2 + \psi_{12} + \psi_{21})}. \tag{3.116}$$

f. Other Γ_1-Circles

It is possible to obtain a circular locus of Γ_1 by means other than those mentioned. For example, a non-reflecting generator and variable phase shifter could be connected so as to vary the phase of a_2, while a fixed non-reflecting generator operating at the same frequency is connected to arm 1. In this case,

$$\Gamma_1 = \frac{b_1}{a_1} = S_{11} + S_{12} \frac{a_2}{a_1}. \tag{3.117}$$

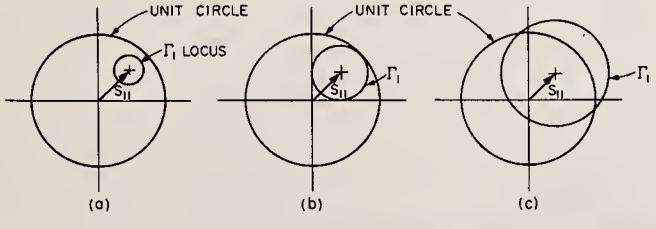

Figure 3-20. Possible Γ_1-circles obtained by varying phase of a_1.

Depending upon the ratio of $|a_2|$ to $|a_1|$, we could have the loci for Γ_1 shown in figure 3-20.

Similarly,

$$\Gamma_2 = \frac{b_2}{a_2} = S_{22} + S_{21}\frac{a_1}{a_2}, \tag{3.118}$$

and corresponding circular loci may be obtained for Γ_2.

Such loci may be used in measurements of scattering coefficients of non-reciprocal and active 2-ports (Altschuler, 1962).

3.14. The Linear Fractional Transformation

Instead of the transformation of reflection coefficients by a 2-port as in eq. (3.104), we are sometimes concerned with the transformation of a complex quantity w to the Z-plane in which the coefficients and the variables w and Z can be assigned any appropriate values to correspond to a given physical problem. We consider

$$Z = \frac{aw + b}{cw + d}, \tag{3.119}$$

where Z is the dependent, and w the independent complex variable, and $a = Ae^{j\alpha}$, $b = Be^{j\beta}$, $c = Ce^{j\gamma}$, and $d = De^{j\delta}$.

Two cases are of special interest, one in which the magnitude of w remains constant and its phase ψ_w, varies, and the other the converse, i.e. the phase ψ_w remains constant, and $|w|$ varies.

a. Constant $|w|$, Variable ψ_w

It is helpful to write eq. (3.119) in the following form

$$Z = \frac{a}{c} - \frac{(ad - bc)/cd}{(c/d)w + 1}, \tag{3.120}$$

and to let $e = Ee^{j\varepsilon} = (ad - bc)/cd$.

One can proceed step-by-step, as was done in a previous section, and arrive at the diagram of figure 3-21 to represent the transformation.

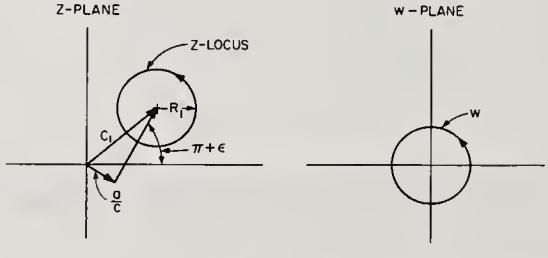

Figure 3-21. Transformation of a w-circle centered on the origin to a Z-circle.

The arrows on the circles correspond to increasing ψ_w, the phase angle of w. The radius R_1 of the Z-circle is

$$R = \frac{|cdew|}{|d|^2 - |cw|^2}, \tag{3.121}$$

and the position C_1 of the center of the circle is at

$$C_1 = \frac{a}{c} - \frac{|d^2e|}{|d|^2 - |cw|^2} e^{j\varepsilon}. \tag{3.122}$$

b. Constant ψ_w, Variable $|w|$

It is helpful to write eq. (3.119) in the following form.

$$Z = \frac{a}{c} - \frac{[(ad - bc)/c^2]e^{-j\psi_w}}{|w| + (d/c)e^{-j\psi_w}}, \tag{3.123}$$

and to let $p = Pe^{j\rho} = (ad - bc)/c^2$.

Step-by-step procedures will yield the diagram of figure 3-22 to represent the transformation.

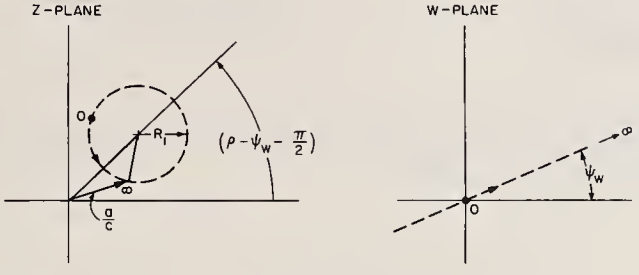

Figure 3-22. Transformation of a w-line thru the origin to a Z-circle.

The arrows on the circles correspond to increasing $|w|$. The radius R_1 of the Z-circle is

$$R_1 = \frac{|p|}{2|d/c| \sin(\delta - \gamma - \psi_w)}, \tag{3.124}$$

and the position C_1 of the center of the circle is

$$C_1 = \frac{a}{c} + R_1 e^{j(\rho - \psi_w - \pi/2)} \tag{3.125}$$

c. Invariance of Cross-Ratio

The following property of the linear transformation has measurement applications and is therefore of interest.

What is called the "cross ratio" or "anharmonic ratio" is invariant under a linear fractional transformation.[13] This is illustrated in figure 3-23 and eq. (3.126).

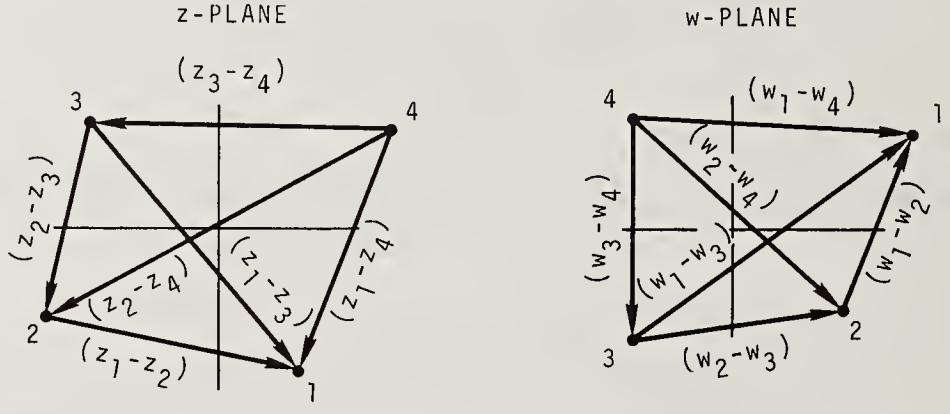

Figure 3-23. Four points in the w-plane transformed into four other points in the z-plane.

$$\frac{Z_1 - Z_2}{Z_2 - Z_3} \cdot \frac{Z_3 - Z_4}{Z_4 - Z_1} = \frac{W_1 - W_2}{W_2 - W_3} \cdot \frac{W_3 - W_4}{W_4 - W_1}. \tag{3.126}$$

An application of this property is given in section 3.15j.

---

[13] See for example, Townsend (1915).

3.15. 3-Ports or Waveguide Junctions Having Three Arms

a. Introduction

There are many physical forms which may be represented by a waveguide junction having three arms, with a single mode propagating in each arm.

In some cases, a physical form having only two arms may be represented by a 3-port. For example, if one of the arms consists of cylindrical waveguide of circular cross-section, two orthogonal modes may propagate in this arm, and it may be represented by two arms, each having a single mode.

In other cases, a physical form having more than three arms may be represented by a 3-port. For example, a four-arm junction such as a directional coupler with one arm terminated and not available for connection, may be represented by a 3-port. Similarly, if the frequency of operation is below the dominant mode cutoff frequency for all but three of the arms, then it may be represented by a 3-port (assuming that each of the three remaining arms has single mode propagation).

b. Realizability Conditions

The general condition for strict realizability as given in section 2.3c(2)(a) applies, that is the Hermitian matrices H_Z, H_Y, or H_S are positive definite. Considering only $H_S = Z_0^{-1} - S^*Z_0^{-1}S$, in which the power normalizing matrix has been chosen as the unit matrix, we have

$$H_S = \begin{pmatrix} S_{H_{11}} & S_{H_{12}} & S_{H_{13}} \\ S_{H_{21}} & S_{H_{22}} & S_{H_{23}} \\ S_{H_{31}} & S_{H_{32}} & S_{H_{33}} \end{pmatrix}, \tag{3.127}$$

where

$$S_{H_{11}} = \frac{1 - |S_{11}|^2}{Z_{01}} - \frac{|S_{21}|^2}{Z_{02}} - \frac{|S_{31}|^2}{Z_{03}},$$

$$S_{H_{12}} = -\left(\frac{\overline{S}_{11}S_{12}}{Z_{01}} + \frac{\overline{S}_{21}S_{22}}{Z_{02}} + \frac{\overline{S}_{31}S_{32}}{Z_{03}}\right),$$

$$S_{H_{13}} = -\left(\frac{\overline{S}_{11}S_{13}}{Z_{01}} + \frac{\overline{S}_{21}S_{23}}{Z_{02}} + \frac{\overline{S}_{31}S_{33}}{Z_{03}}\right),$$

$$S_{H_{21}} = -\left(\frac{\overline{S}_{12}S_{11}}{Z_{01}} + \frac{\overline{S}_{22}S_{21}}{Z_{02}} + \frac{\overline{S}_{32}S_{31}}{Z_{03}}\right),$$

$$S_{H_{22}} = -\frac{|S_{12}|^2}{Z_{01}} + \frac{1 - |S_{22}|^2}{Z_{02}} - \frac{|S_{32}|^2}{Z_{03}},$$

$$S_{H_{23}} = -\left(\frac{\overline{S}_{12}S_{13}}{Z_{01}} + \frac{\overline{S}_{22}S_{23}}{Z_{02}} + \frac{\overline{S}_{32}S_{33}}{Z_{03}}\right),$$

$$S_{H_{31}} = -\left(\frac{\overline{S}_{13}S_{11}}{Z_{01}} + \frac{\overline{S}_{23}S_{21}}{Z_{02}} + \frac{\overline{S}_{33}S_{31}}{Z_{03}}\right),$$

$$S_{H_{32}} = -\left(\frac{\overline{S}_{13}S_{12}}{Z_{01}} + \frac{\overline{S}_{23}S_{22}}{Z_{02}} + \frac{\overline{S}_{33}S_{32}}{Z_{03}}\right),$$

and

$$S_{H_{33}} = -\frac{|S_{13}|^2}{Z_{01}} - \frac{|S_{23}|^2}{Z_{02}} + \frac{1 - |S_{33}|^2}{Z_{03}}. \tag{3.128}$$

In order for H_S to be positive definite, all of the principal minors must be positive, although it is only necessary to show that all of the leading principal minors are positive. The latter condition is as follows:

$$S_{H_{11}} > 0,$$

$$S_{H_{11}}S_{H_{22}} - S_{H_{12}}S_{H_{21}} > 0,$$

and

$$\det H_S > 0. \tag{3.129}$$

It then follows that

$$S_{H_{22}} > 0,$$

$$S_{H_{33}} > 0,$$

and

$$S_{H_{22}}S_{H_{33}} - S_{H_{23}}S_{H_{32}} > 0,$$

$$S_{H_{11}}S_{H_{33}} - S_{H_{13}}S_{H_{31}} > 0. \tag{3.130}$$

These conditions state that the net power input to the waveguide junction must be positive for whatever excitation is chosen, or that for some excitation, some energy is absorbed by the junction. For example, consider a source connected to arm 1 and non-reflecting loads to arms 2 and 3. The power input to the junction is

$$P_{in} = \frac{|a_1|^2 - |b_1|^2}{Z_{01}} = |a_1|^2 \left\{\frac{1 - |S_{11}|^2}{Z_{01}}\right\}, \tag{3.131}$$

and the power output is

$$P_{out} = \frac{|b_2|^2}{Z_{02}} + \frac{|b_3|^2}{Z_{03}} = |a_1|^2 \left\{\frac{|S_{21}|^2}{Z_{02}} + \frac{|S_{31}|^2}{Z_{03}}\right\}. \tag{3.132}$$

If power is absorbed in the junction, then

$$P_{in} - P_{out} > 0,$$

or

$$|a_1|^2 \left\{\frac{1 - |S_{11}|^2}{Z_{01}} - \frac{|S_{21}|^2}{Z_{02}} - \frac{|S_{31}|^2}{Z_{03}}\right\} > 0,$$

or

$$\frac{1 - |S_{11}|^2}{Z_{01}} - \frac{|S_{21}|^2}{Z_{02}} - \frac{|S_{31}|^2}{Z_{03}} > 0,$$

or

$$S_{H_{11}} > 0. \tag{3.133}$$

Each of the other conditions corresponds to a different excitation and it can be shown that any excitation can be synthesized as a combination of those implied by the first condition stated, i.e. the leading principal minors of H_S must be positive.

c. Conditions for Losslessness

A large class of 3-ports have very little loss, and the properties of lossless waveguide junctions apply to a good degree of approximation in most of these cases.

These properties are concisely stated as in section 2.3c(2)(c) by saying that all of the elements of H_S vanish. There are nine elements, but the off-diagonal elements at the top are the conjugates of the opposite off-diagonal elements at the bottom and give no additional information when set equal to zero. Hence, we have just six lossless conditions as follows:

$$\frac{1 - |S_{11}|^2}{Z_{01}} - \frac{|S_{21}|^2}{Z_{02}} - \frac{|S_{31}|^2}{Z_{03}} = 0,$$

$$- \frac{\overline{S}_{11}S_{12}}{Z_{01}} - \frac{\overline{S}_{21}S_{22}}{Z_{02}} - \frac{\overline{S}_{31}S_{32}}{Z_{03}} = 0,$$

$$- \frac{|S_{12}|^2}{Z_{01}} + \frac{1 - |S_{22}|^2}{Z_{02}} - \frac{|S_{32}|^2}{Z_{03}} = 0,$$

$$- \frac{\overline{S}_{11}S_{13}}{Z_{01}} - \frac{\overline{S}_{21}S_{23}}{Z_{02}} - \frac{\overline{S}_{31}S_{33}}{Z_{03}} = 0,$$

$$- \frac{|S_{13}|^2}{Z_{01}} - \frac{|S_{23}|^2}{Z_{02}} + \frac{1 - |S_{33}|^2}{Z_{03}} = 0,$$

$$- \frac{\overline{S}_{12}S_{13}}{Z_{01}} - \frac{\overline{S}_{22}S_{23}}{Z_{02}} - \frac{\overline{S}_{32}S_{33}}{Z_{03}} = 0. \qquad (3.134)$$

These conditions state that the net power input to a lossless waveguide junction must be zero for any combination or excitations chosen, or that no energy is absorbed within the junction.

As in the case of the 2-port, the conditions obtained directly from $H_S = 0$ are not necessarily in the most useful form, and other ones may be derived.

For example, consider the lossless condition $H_S = Z_0^{-1} - S^*Z_0^{-1}S = 0$ in a slightly different form:

$$S^*Z_0^{-1}S = Z_0^{-1},$$

$$S^* = Z_0^{-1}S^{-1}Z_0 = Z_0^{-1}\frac{\text{adj } S}{\det S}Z_0. \qquad (3.135)$$

Equating corresponding elements and taking the magnitude of each side of the equations, we obtain for a typical element, say S_{21}:

$$|S_{21}| = \frac{1}{|\det S|}\frac{Z_{02}}{Z_{01}}|S_{12}S_{33} - S_{13}S_{32}|. \qquad (3.136)$$

It is possible to show that $|\det S| = 1$ as follows. We make use of the following general rules which apply to determinants:

1. det (AB) = det A det B
2. det (transpose of A) = det A
3. det A* = det (transpose of $\overline{A}$).

The following steps then lead to the desired result.

$$\det(Z_0^{-1}) = \det(S^*)\ \det(Z_0^{-1})\ \det(S),$$

$$1 = \det(S^*)\ \det(S) = (\det S)^*\ (\det S) = |\det S|^2,$$

Therefore

$$|\det S| = 1. \tag{3.137}$$

The equations obtained by equating corresponding elements of the above matrices are

$$|S_{11}| = |S_{22}S_{33} - S_{23}S_{32}|, \qquad |S_{12}| = \frac{Z_{01}}{Z_{02}}\,|S_{21}S_{33} - S_{23}S_{31}|,$$

$$|S_{13}| = \frac{Z_{01}}{Z_{03}}\,|S_{21}S_{32} - S_{22}S_{31}|, \quad |S_{21}| = \frac{Z_{02}}{Z_{01}}\,|S_{12}S_{33} - S_{13}S_{32}|,$$

$$|S_{22}| = |S_{11}S_{33} - S_{13}S_{31}|, \qquad |S_{23}| = \frac{Z_{02}}{Z_{03}}\,|S_{11}S_{32} - S_{12}S_{31}|,$$

$$|S_{31}| = \frac{Z_{03}}{Z_{01}}\,|S_{12}S_{23} - S_{13}S_{22}|, \quad |S_{32}| = \frac{Z_{03}}{Z_{02}}\,|S_{11}S_{23} - S_{13}S_{21}|,$$

and

$$|S_{33}| = |S_{11}S_{22} - S_{12}S_{21}|. \tag{3.138}$$

They are useful in proving some of the theorems for lossless 3-ports to follow.

d. Reciprocity

A straightforward application of eq. (2.55) yields the reciprocity conditions for 3-ports which are

$$\begin{aligned} S_{21}Z_{01} &= S_{12}Z_{02}, \\ S_{31}Z_{01} &= S_{13}Z_{03}, \\ S_{32}Z_{02} &= S_{23}Z_{03}. \end{aligned} \tag{3.139}$$

e. Symmetry[14]

There are many types of symmetry possible. For example, consider symmetrically constructed H-plane and E-plane tees. If arm 3 is the branching arm and the terminal surfaces in arms 1 and 2 are chosen symmetrically, the conditions on the scattering

[14] Techniques for the analysis of symmetrical waveguide junctions are given in Kerns (1951).

coefficients are as follows: For the H-plane tee,

$$S_{11} = S_{22}, \quad S_{12} = S_{21},$$
$$S_{13} = S_{31} = S_{23} = S_{32}. \tag{3.140}$$

For the E-plane tee,

$$S_{11} = S_{22}, \quad S_{12} = S_{21}$$
$$S_{32} = S_{23} = -S_{13} = -S_{31}. \tag{3.141}$$

The symmetrical Y structures exhibit a higher order of symmetry, and non-reciprocal devices such as circulators may possess symmetry. Each type of symmetry yields a set of constraints upon the scattering coefficients. It is possible to have electrical symmetry without physical symmetry, but this is not usually encountered.

f. 3-Port, One Arm Terminated

A 3-port with one arm terminated in a load so that only two arms are available for connection to sources and loads is essentially a 2-port. The parameters of the 2-port may be found in terms of the 3-port and the reflection coefficient of the fixed termination.

If the load of reflection coefficient Γ_{L3} terminates arm 3, then $a_3 = \Gamma_{L3} b_3$, and the scattering equations for the 3-port are

$$b_1 = {}^3S_{11}a_1 + {}^3S_{12}a_2 + {}^3S_{13}\Gamma_{L3}b_3,$$
$$b_2 = {}^3S_{21}a_1 + {}^3S_{22}a_2 + {}^3S_{23}\Gamma_{L3}b_3,$$
$$b_3 = {}^3S_{31}a_1 + {}^3S_{32}a_2 + {}^3S_{33}\Gamma_{L3}b_3, \tag{3.142}$$

where the front superscript identifies the scattering coefficient as that of the 3-port. Solving to obtain the scattering equations of the 2-port, we obtain

$$b_1 = \left({}^3S_{11} + \frac{{}^3S_{13}\,{}^3S_{31}\Gamma_{L3}}{1 - {}^3S_{33}\Gamma_{L3}} \right) a_1 + \left({}^3S_{12} + \frac{{}^3S_{13}\,{}^3S_{32}\Gamma_{L3}}{1 - {}^3S_{33}\Gamma_{L3}} \right) a_2,$$
$$b_2 = \left({}^3S_{21} + \frac{{}^3S_{23}\,{}^3S_{31}\Gamma_{L3}}{1 - {}^3S_{33}\Gamma_{L3}} \right) a_1 + \left({}^3S_{22} + \frac{{}^3S_{23}\,{}^3S_{32}\Gamma_{L3}}{1 - {}^3S_{33}\Gamma_{L3}} \right) a_2. \tag{3.143}$$

It is seen that if either the load is non-reflecting ($\Gamma_{L3} = 0$) or the third arm is decoupled ($S_{23} = S_{31} = 0$) the scattering coefficients of the 2-port become those of the 3-port or

$${}^2S_{11} = {}^3S_{11}, \; {}^2S_{12} = {}^3S_{12}, \; {}^2S_{21} = {}^3S_{21}, \text{ and } {}^2S_{22} = {}^3S_{22}. \tag{3.144}$$

g. Non-Reciprocal 3-Ports

An interesting non-reciprocal 3-port is the circulator, which is shown in two forms in figure 3-24.

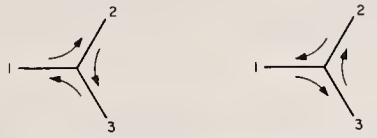

Figure 3-24. Schematic diagrams for lossless, non-reciprocal 3-port circulators.

The scattering matrix corresponding to the ideal forms of the two circulators shown in figure 3-24 are

$$S = \begin{pmatrix} 0 & 0 & 1 \\ 1 & 0 & 0 \\ 0 & 1 & 0 \end{pmatrix}, \quad S = \begin{pmatrix} 0 & 1 & 0 \\ 0 & 0 & 1 \\ 1 & 0 & 0 \end{pmatrix}. \tag{3.145}$$

The ideal circulator is lossless (S*S = 1).

h. The Directional Coupler, 3-Port

Actually, directional couplers are often considered as a class of lossless 4-ports, but if one arm is internally terminated so as to be not available for connection, it is then a 3-port. As shown in figure 3-25 the side arm (arm 3) to which detectors may be connected couples mainly to the incident wave in arm 1. The coupling ratio is the ratio of the incident input power to the power coupled out to a non-reflecting detector, when the main arm of the coupler is terminated by a non-reflecting load.

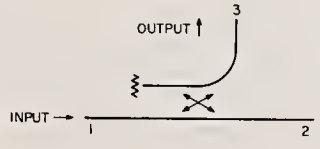

Figure 3-25. Schematic diagram for a directional coupler connected as a 3-port.

When $a_2 = a_3 = 0$ (non-reflecting loads), the coupling is

$$C = 10 \log_{10} \left| \frac{a_1}{b_3} \right|^2 \frac{Z_{03}}{Z_{01}} = 10 \log_{10} \left\{ \frac{Z_{03}}{|S_{31}|^2 Z_{01}} \right\}, \tag{3.146}$$

or if the 3-port is a reciprocal one,

$$C = -10 \log_{10} |S_{13} S_{31}|. \tag{3.147}$$

Another important property of the directional coupler is the ratio of the emergent power coupled out for a given incident power input to arm 1, to the power coupled out for the same incident power to arm 2, assuming non-reflecting loads on all arms except those connected to sources. This ratio expressed in decibels is called the directivity D. It may be written

$$D = 10 \log_{10} \left(\left(\frac{|f_{b_3}|^2}{|a_1|^2} \cdot \frac{Z_{01}}{Z_{03}} \right)_{a_2=a_3=0} \left(\frac{|a_2|^2}{|b_{b_3}|^2} \cdot \frac{Z_{03}}{Z_{02}} \right)_{a_1=a_3=0} \right), \tag{3.148}$$

where f_{b_3} indicates coupling to the "forward" wave, and b_{b_3} indicates coupling to the "backward" wave, the amplitudes a_1 of the forward, and a_2 of the backward wave being equal. It follows then that the directivity is

$$D = 10 \log_{10} \left(\frac{Z_{01}}{Z_{02}} \cdot \left| \frac{S_{31}}{S_{32}} \right|^2 \right), \tag{3.149}$$

or if the 3-port is a reciprocal one, the directivity can be written

$$D = 10 \log_{10} \left| \frac{S_{13} S_{31}}{S_{23} S_{32}} \right|. \tag{3.150}$$

In case that $Z_{01} = Z_{02} = Z_{03}$, reciprocity implies that $S_{31} = S_{13}$, and $S_{32} = S_{23}$, or

$$D = 20 \log_{10} \left| \frac{S_{31}}{S_{32}} \right|. \tag{3.151}$$

It may be more convenient to measure the power transmitted through the main arm than the incident power. The directivity might then be defined as the ratio of emergent powers coupled out of the side arm for the same powers transmitted through the main arm. This would lead to an equation for directivity similar to eq. (3.149) except that the ratio of Z_{02} to Z_{01} would appear in place of the ratio of Z_{01} to Z_{02}.

Note that the ideal circulator is similar to a directional coupler for which the coupling ratio is unity and the directivity infinite. Thus the ideal circulator couples all of the energy out of the main arm into the side arm.

Two representations for ideal 3-port directional couplers are shown in figure 3-26.

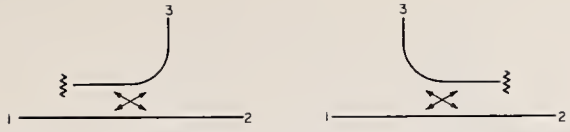

Figure 3-26. Schematic diagrams for ideal 3-port directional couplers.

The scattering matrices corresponding to the 3-ports shown are

$$S = \begin{bmatrix} 0 & \sqrt{(1-c^2)} & c \\ \sqrt{(1-c^2)} & 0 & 0 \\ c & 0 & 0 \end{bmatrix}, \tag{3.152}$$

$$S = \begin{bmatrix} 0 & \sqrt{(1-c^2)} & 0 \\ \sqrt{(1-c^2)} & 0 & c \\ 0 & c & 0 \end{bmatrix}. \tag{3.153}$$

Observe that the scattering matrix of an ideal 3-port directional coupler is not unitary. Although ideal in concept, it contains an internal termination and is not lossless.

i. Solution of the Scattering Equations for b_3

A number of measurement systems can be represented by a 3-port connected in a system as shown in figure 3-27.

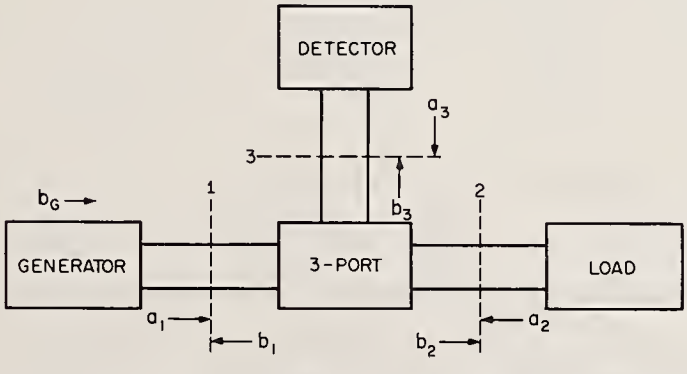

Figure 3-27. A 3-port connected in a system representative of many measurement systems.

In analyzing the system, one is often interested in solving for b_3, the amplitude of the wave incident upon the detector. This is conveniently done by writing the scattering equations for the 3-port, applying the terminal plane relationships imposed by the generator and load, and solving the resulting equations. A solution containing determinants is conveniently obtained using Cramer's rule.

The scattering equations are

$$b_1 = S_{11}a_1 + S_{12}a_2 + S_{13}a_3,$$
$$b_2 = S_{21}a_1 + S_{22}a_2 + S_{23}a_3,$$
$$b_3 = S_{31}a_1 + S_{32}a_2 + S_{33}a_3. \tag{3.154}$$

The terminal plane relationships to be applied are

$$a_1 = b_G + b_1\Gamma_G,$$
$$a_2 = b_2\Gamma_L,$$
and
$$a_3 = b_3\Gamma_D, \tag{3.155}$$

where Γ_G, Γ_L and Γ_D denote reflection coefficients of the generator, load, and detector, respectively.

The equations to be solved are

$$-b_G = -(1 - S_{11}\Gamma_G)a_1 + S_{12}\Gamma_G\Gamma_L b_2 + S_{13}\Gamma_G\Gamma_D b_3,$$
$$0 = S_{21}a_1 - (1 - S_{22}\Gamma_L)b_2 + S_{23}\Gamma_D b_3,$$
$$0 = S_{31}a_1 + S_{32}\Gamma_L b_2 - (1 - S_{33}\Gamma_D)b_3. \tag{3.156}$$

The solution for b_3 is

$$b_3 = \frac{\begin{vmatrix} -(1-S_{11}\Gamma_G) & S_{12}\Gamma_G\Gamma_L & -b_G \\ S_{21} & -(1-S_{22}\Gamma_L) & 0 \\ S_{31} & S_{32}\Gamma_L & 0 \end{vmatrix}}{\begin{vmatrix} -(1-S_{11}\Gamma_G) & S_{12}\Gamma_G\Gamma_L & S_{13}\Gamma_G\Gamma_D \\ S_{21} & -(1-S_{22}\Gamma_L) & S_{23}\Gamma_D \\ S_{31} & S_{32}\Gamma_L & -(1-S_{33}\Gamma_D) \end{vmatrix}} \tag{3.157}$$

or

$$b_3 = -b_G \frac{\begin{vmatrix} S_{21} & -(1-S_{22}\Gamma_L) \\ S_{31} & S_{32}\Gamma_L \end{vmatrix}}{\begin{vmatrix} -(1-S_{11}\Gamma_G) & S_{12}\Gamma_G\Gamma_L & S_{13}\Gamma_G\Gamma_D \\ S_{21} & -(1-S_{22}\Gamma_L) & S_{23}\Gamma_D \\ S_{31} & S_{32}\Gamma_L & -(1-S_{33}\Gamma_D) \end{vmatrix}}. \tag{3.158}$$

When one wishes to see the effect on b_3 of variations in Γ_L, the following form is useful:

$$b_3 = -b_G \frac{\begin{vmatrix} S_{21} & S_{22} \\ S_{31} & S_{32} \end{vmatrix}\Gamma_L + S_{31}}{\begin{vmatrix} -(1-S_{11}\Gamma_G) & S_{12}\Gamma_G & S_{13}\Gamma_G\Gamma_D \\ S_{21} & S_{22} & S_{23}\Gamma_D \\ S_{31} & S_{32} & -(1-S_{33}\Gamma_D) \end{vmatrix}\Gamma_L - \begin{vmatrix} (1-S_{11}\Gamma_G) & S_{13}\Gamma_G\Gamma_D \\ S_{31} & (1-S_{33}\Gamma_D) \end{vmatrix}}. \tag{3.159}$$

Note that the above equation has the form of eq. (3.104) the linear fractional transformation of reflection coefficient. Therefore the results of sections 3.13 and 3.14 are applicable.

A further simplification of the above equation may be made as follows. Let

$$K = \frac{\begin{vmatrix} S_{21} & S_{22} \\ S_{31} & S_{32} \end{vmatrix}}{S_{31}}, \tag{3.160}$$

$$\Gamma_{2i} = \frac{\begin{vmatrix} -(1-S_{11}\Gamma_G) & S_{12}\Gamma_G & S_{13}\Gamma_G\Gamma_D \\ S_{21} & S_{22} & S_{23}\Gamma_D \\ S_{31} & S_{32} & -(1-S_{33}\Gamma_D) \end{vmatrix}}{\begin{vmatrix} (1-S_{11}\Gamma_G) & S_{13}\Gamma_G\Gamma_D \\ S_{31} & (1-S_{33}\Gamma_D) \end{vmatrix}}, \tag{3.161}$$

and

$$C = b_G \frac{S_{31}}{\begin{vmatrix} (1-S_{11}\Gamma_G) & S_{13}\Gamma_G\Gamma_D \\ S_{31} & (1-S_{33}\Gamma_D) \end{vmatrix}}. \tag{3.162}$$

Then[15]

$$b_3 = -C \frac{K\Gamma_L + 1}{\Gamma_{2i}\Gamma_L - 1} = C \frac{1 + K\Gamma_L}{1 - \Gamma_{2i}\Gamma_L} = CK \frac{\frac{1}{K} + \Gamma_L}{1 - \Gamma_{2i}\Gamma_L}. \tag{3.163}$$

It can be seen by reference to eq. (3.151) that in case the 3-port represents a directional coupler, the parameter K is approximately equal to its directivity ratio, assuming that S_{22} is small and $S_{21} \simeq 1$.

The parameter Γ_{2i} can be shown as follows to be the internal reflection coefficient of the equivalent generator at terminal surface 2. One recalls an application of Thevenin's theorem in which the internal impedance of a constant voltage source may be determined by considering the inactive source and measuring the impedance "looking back" into its output terminals. In a similar manner, the internal reflection coefficient Γ_{2i} is obtained by "looking back" at terminal surface 2 with the generator inactive. We then have the following conditions on terminal surfaces 1, 2, and 3:

$$\begin{aligned} a_1 &= b_1\Gamma_G, \\ a_3 &= b_3\Gamma_D, \\ b_2 &= a_2\Gamma_{2i}. \end{aligned} \tag{3.164}$$

[15] This result appeared in a number of papers, for example: Beatty and Kerns (1958); Beatty (1959); Engen and Beatty (1959); and Anson (1961).

The equations to be solved are

$$\begin{aligned} 0 &= -(1 - S_{11}\Gamma_G)b_1 + S_{12}a_2 + S_{13}\Gamma_D b_3, \\ b_2 &= S_{21}\Gamma_G b_1 + S_{22}a_2 + S_{23}\Gamma_D b_3, \\ 0 &= S_{31}\Gamma_G b_1 + S_{32}a_2 - (1 - S_{33}\Gamma_D)b_3. \end{aligned} \tag{3.165}$$

Solving for a_2 we obtain

$$a_2 = b_2 \frac{\begin{vmatrix} (1-S_{11}\Gamma_G) & S_{13}\Gamma_D \\ S_{31}\Gamma_G & (1-S_{33}\Gamma_D) \end{vmatrix}}{\begin{vmatrix} -(1-S_{11}\Gamma_G) & S_{12} & S_{13}\Gamma_D \\ S_{21}\Gamma_G & S_{22} & S_{23}\Gamma_D \\ S_{31}\Gamma_G & S_{32} & -(1-S_{33}\Gamma_D) \end{vmatrix}}. \tag{3.166}$$

It can be seen that the Γ_{2i} of eqs. (3.161) and (3.166) is the same as the Γ_{2i} of eq. (3.164), and hence Γ_{2i} has the interpretation given above.

The short form of eq. (3.163) is useful in reflectometer theory. It is interesting to observe that the ratio of b_3 to b_4 for a 4-port connected as a reflectometer can also be put into this form (Engen and Beatty, 1959).

j. Measurement of Reflection Coefficient Γ_u with general 3-Port

The response b_3 of a 3-port connected as in figure 3-27 is given by eq. (3.163), and is a linear fractional transformation. We can use the property of invariance of the cross-ratio in measuring the reflection coefficient Γ_u of an unknown load as follows (Beatty, 1972b).

Connect in sequence 3 different loads having known reflection coefficients Γ_1, Γ_2, and Γ_3 to port 2 of the 3-port, measuring the corresponding values of $b_3 = V_1$, V_2, and V_3 (measure both magnitude and phase). Then connect the unknown load and measure V_u corresponding to Γ_u.

We can deduce from eq. (3.126) that

$$\frac{V_1 - V_2}{V_2 - V_3} \cdot \frac{V_3 - V_u}{V_u - V_1} = \frac{\Gamma_1 - \Gamma_2}{\Gamma_2 - \Gamma_3} \cdot \frac{\Gamma_3 - \Gamma_u}{\Gamma_u - \Gamma_1}. \tag{3.167}$$

Solving for Γ_u, we obtain

$$\Gamma_u = \frac{\Gamma_3 + r\Gamma_1}{1 + r},$$

where

$$r = \frac{\Gamma_2 - \Gamma_3}{\Gamma_1 - \Gamma_2} \cdot \frac{V_1 - V_2}{V_2 - V_3} \cdot \frac{V_3 - V_u}{V_u - V_1}. \tag{3.168}$$

a. The Directional Coupler

An ideal directional coupler is a lossless 4-port having a scattering matrix which can be put into the form in eq. (3.169). To obtain this form, one uses a numbering scheme as shown in figure 3-28 and chooses terminal surfaces appropriately:

$$S = \begin{Vmatrix} 0 & j\sqrt{(1-c^2)} & 0 & c \\ j\sqrt{(1-c^2)} & 0 & c & 0 \\ 0 & c & 0 & j\sqrt{(1-c^2)} \\ c & 0 & j\sqrt{(1-c^2)} & 0 \end{Vmatrix}. \tag{3.169}$$

It may be shown[16] that any non-reflecting lossless reciprocal 4-port has a scattering matrix that can be put in this form and is potentially a directional coupler.

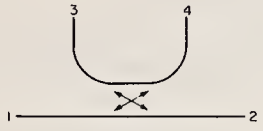

Figure 3-28. Schematic diagram of a 4-port directional coupler.

Suppose that arm 4 is internally terminated so that $a_4 = \Gamma_T b_4$, and that only the remaining three arms are available for connection. The scattering equations of the resulting 3-port are then as follows:

$$\begin{cases} b_1 = c^2\Gamma_T a_1 + j\sqrt{(1 - c^2)}\,a_2 + jc\sqrt{(1 - c^2)}\,\Gamma_T a_3 \\ b_2 = j\sqrt{(1 - c^2)}\,a_1 + 0 + ca_3 \\ b_3 = jc\sqrt{(1 - c^2)}\,\Gamma_T a_1 + ca_2 - (1 - c^2)\Gamma_T a_3. \end{cases} \tag{3.170}$$

The directivity of this coupler is

$$D = 10 \log_{10} \left| \frac{{}^3S_{23}}{{}^3S_{13}} \right|^2 = 10 \log_{10} \frac{1}{(1 - c^2)|\Gamma_T|^2}. \tag{3.171}$$

It is seen that the directivity is strongly influenced by the termination. The directivity is infinite for a non-reflecting termination but decreases as the reflection from the termination is increased.

The coupling of this coupler is

$$C = -10 \log_{10} |S_{23}S_{32}| = 20 \log_{10} \frac{1}{c}. \tag{3.172}$$

[16] See, for example, vol. 8 of MIT Rad. Lab. Series, Principles of Microwave Circuits, edited by Montgomery, Dicke, and Purcell (McGraw-Hill, New York, N.Y., 1948).

It is seen that the coupling is unaffected by the termination, providing that we have an ideal 4-port directional coupler to begin with, as was assumed above. Also, the vanishing of ${}^3S_{22}$ is unaffected. A non-zero Γ_T does affect ${}^3S_{11}$, ${}^3S_{33}$, and the directivity, however.

b. The Magic Tee

A magic tee is usually envisioned as an E-H tee having appropriate internal tuning elements, adjusted to provide a non-reflecting 4-port. Its external appearance is as shown in figure 3-29. A magic tee can be regarded as a lossless reciprocal

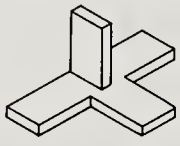

Figure 3-29. External appearance of a magic tee.

4-port having a scattering matrix of a directional coupler with a coupling factor of $c = 1/\sqrt{2}$, or a coupling C of approximately 3 decibels. It is shown schematically in figure 3-30.

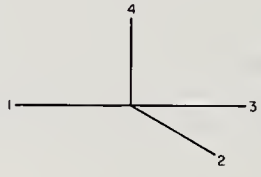

Figure 3-30. Schematic diagram of an E-H tee.

The corresponding scattering matrix is as follows:

$$S = \frac{1}{\sqrt{2}} \begin{pmatrix} 0 & j & 0 & 1 \\ j & 0 & 1 & 0 \\ 0 & 1 & 0 & j \\ 1 & 0 & j & 0 \end{pmatrix}. \tag{3.173}$$

This can be put into a different form by choosing different numbers for the arms, and by moving the terminal surfaces in two of the arms. Moving the terminal surfaces in arms 2 and 3 a quarter-wavelength outwards gives

$$S = \frac{1}{\sqrt{2}} \begin{pmatrix} 0 & 1 & 0 & 1 \\ 1 & 0 & -1 & 0 \\ 0 & -1 & 0 & 1 \\ 1 & 0 & 1 & 0 \end{pmatrix}. \tag{3.174}$$

Reversing the numbering of arms 2 and 3 gives

$$S = \frac{1}{\sqrt{2}} \begin{pmatrix} 0 & 0 & 1 & 1 \\ 0 & 0 & -1 & 1 \\ 1 & -1 & 0 & 0 \\ 1 & 1 & 0 & 0 \end{pmatrix}. \tag{3.175}$$

This is the usual form of the scattering matrix of a magic tee.

The magic tee can be used as a phase shifter and as an isolating power divider, among its other uses. In its application as a phase shifter, sliding short-circuits are placed in opposite arms, say arms 2 and 4 of figure 3-30. We then examine b_3 relative to a_1 to observe phase shifting properties. The appropriate scattering equation is

$$b_3 = -\frac{1}{\sqrt{2}} (b_2 e^{j\theta_2} - b_4 e^{j\theta_4}), \tag{3.176}$$

where θ_2 and θ_4 relate to the positions of the sliding short-circuits in arms 2 and 4. But $b_2 = b_4 = a_1/\sqrt{2}$, if arm 3 is terminated by a non-reflecting load so that $a_2 = 0$. Therefore,

$$\frac{b_3}{a_1} = -\frac{1}{2} (e^{j\theta_2} - e^{j\theta_4}). \tag{3.177}$$

If the short circuits are initially positioned so that $e^{j\theta_2} - e^{j\theta_4} = 2$, they can then have their motions ganged so that this phase addition is preserved as they are moved to change the phase of b_3 relative to a_1 without changing the amplitude. In order to accomplish this, both short-circuits must move in the same direction with respect to the center of the magic tee.

In its application as an isolating power divider to form 2 channels, the magic tee has one arm, say arm 3 terminated by a non-reflecting load, and the source is connected to arm 1. The power divides between arms 2 and 4 just as though two identical generators were connected to arms 2 and 4. If Γ_G is the reflection coefficient of the generator connected to arm 1, then the reflection coefficients of the equivalent generators for arms 2 and 4 are also Γ_G.

4. Power

4.1. Introduction

Two research topics are described in this chapter. In section 4.2., the analysis of mismatch errors (Beatty and MacPherson, 1953) in the calibration and use of microwave power meters is presented.

In section 4.3, the measurement of barretter mount efficiency by an improved version (Beatty and Reggia, 1955) of the impedance variation method (Kerns, 1949b) is described, errors are analyzed, and experimental results are given.

4.2. Mismatch Errors

a. Introduction

In waveguide circuits, it is often required to determine the power delivered to a matched, or non-reflecting load, by a signal source. Assuming that the power meter correctly indicates the power absorbed, it often will not give the desired result because of mismatch.[1]

This point is illustrated by the following example, which is taken from p. 130 of Griesheimer (1947), where the results were incorrect. A signal source delivers power to a load according to

$$P_1 = \frac{|b_G|^2}{Z_{01}} \frac{1 - |\Gamma_1|^2}{|1 - \Gamma_G\Gamma_1|^2}. \tag{3.37}$$

If we assume that the signal source delivers 100 mW to a non-reflecting ($\Gamma_1 = 0$) load, and that this is the desired result, then

$$\frac{|b_G|^2}{Z_{01}} = 100 \text{ mW}.$$

If a power meter having a VSWR of 1.4, or $|\Gamma_1| = 1/6$, reads correctly the power absorbed, and the generator is non-reflecting ($\Gamma_G = 0$), then

$$[P_1]_{\Gamma_G=0} = 100\left(1 - \frac{1}{36}\right) = 97.2 \text{ mW}.$$

The power meter reads 2.8% lower than the desired value. Now if the signal source also has a VSWR of 1.4 (but still delivers 100 mW to a matched load) the

[1] See section 3.7b for a discussion of the meaning of "mismatch." In this monograph the term "mismatch" generally denotes a departure from the Z_0-match, or non-reflecting condition.

power delivered to the power meter depends upon the phase of $\Gamma_G\Gamma_1$ according to eq. (3.37) and lies between the limits

$$92.0 \text{ mW} \leq [P_1]_{|\Gamma_G|=|\Gamma_1|=1/6} \leq 102.9 \text{ mW}.$$

Thus the power meter can indicate 2.9% above the desired value or 8% below it.

Although this effect was known (Hand and Schrock, 1951), the analysis of the error had not been published before 1953 and quoted error limits were often incorrect. The error could be quite large when the generator mismatch was large, which was often the case when generators were insufficiently padded or isolated. Subsequently, more attention was paid to achieving a source match (Engen, 1958; Beatty and Fentress, 1971). If the source is well matched, then a correction can be calculated if one knows the VSWR of the power meter.

Application of the theory of section 3.7 and particularly of eq. (3.45) to various circuit arrangements employed in the calibration and use of power meters is given in the following discussion. The presentation is a slightly revised version of Beatty and MacPherson (1953), which first presented equations and results which are still useful today.

b. Calibration of Power Meters

(1) General Discussion

A power meter is calibrated by comparing its indicated power with the power it actually absorbs. Best accuracy of calibration is obtained by avoiding the use of secondary standards, attenuators or directional couplers and comparing the meter directly with a reference standard which may be a bolometric or calorimetric device. This may be done by alternate connection of the meter and the standard to a stable source or by the use of certain power splitting devices enabling simultaneous comparison, or by a combination of methods. Power splitting devices having a power ratio of unity have the advantage that geometric symmetry is possible, permitting precise mechanical construction which leads to a corresponding excellence of electrical symmetry.

The end result of a power meter calibration is often a correction factor f which is used to convert the meter reading R_M to the power P_M aborbed by the meter

($P_M = fR_M$). The correction factor f may be obtained in terms of observed quantities:

$$f = \frac{P_M}{R_M} = \left(\frac{P_M}{P_S}\right)\frac{P_S}{R_M} = (K)\frac{P_S}{R_M} \tag{4.1}$$

where P_S represents the power absorbed by the standard power measuring device. Alternatively, a calibration factor K_b is defined (Larson, 1962) for bolometric power mounts employing dc substitution. It is the ratio of the substituted dc power P_{bm} in the bolometer element to the microwave power P_{Im} incident upon the bolometer mount. In the event that P_{bm} equals R_M above, then f of eq. (4.1) equals the reciprocal of the effective efficiency η_e, and

$$K_b = \eta_e(1 - |\Gamma_M|^2) = \frac{1 - |\Gamma_M|^2}{f}, \tag{4.2}$$

where Γ_M is the reflection coefficient of the power meter. Calibration factors have also been defined for bolometer units (bolometer mount with bolometer element installed) in combination with directional couplers (Desch and Larson, 1963).

All of these calibration factors are related and can be determined from measured power ratios. In the following, it is assumed that the ratio P_S to R_M can be determined and that we are concerned only with the deviation from unity of the factor K of eq. (4.1). It is normally unity except as affected by mismatches and deviations from ideal properties of any power dividing devices that may be used.

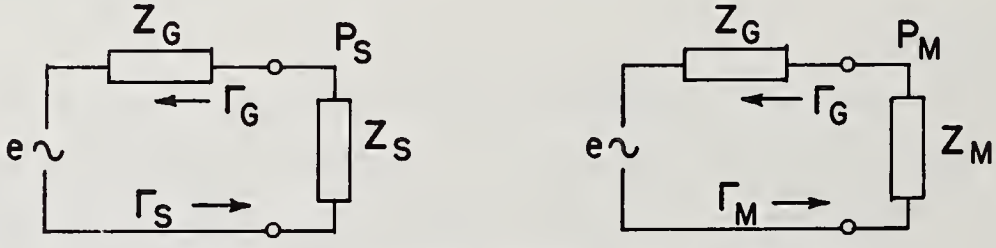

Figure 4-1. Alternate connection to stable source.

(2) Method 1 -- Alternate Connection to a Stable Power Source

The power meter and the standard are alternately connected to a stable generator as shown in figure 4-1. The generator output is padded to prevent the change in loading from affecting its amplitude or frequency. The ratio of the powers absorbed by the meter and the standard is[2]

$$K_1 = \frac{P_M}{P_S} = \left|\frac{1 - \Gamma_G\Gamma_S}{1 - \Gamma_G\Gamma_M}\right|^2 \cdot \frac{1 - |\Gamma_M|^2}{1 - |\Gamma_S|^2} \tag{4.3}$$

[2]This is a direct application of the theory of comparison loss developed in section 3.7a, eq. (3.45).

where Γ_G, Γ_S, and Γ_M are the voltage reflection coefficients respectively of the generator, the standard, and the power meter, measured at the place of connection.[3]

It is convenient to measure the voltage standing wave ratio (VSWR or ρ) corresponding[4] to the magnitude of Γ. Assuming that the worst phase combinations can exist in eq. (4.3);

$$\frac{\rho_M}{\rho_S}\left(\frac{\rho_G\rho_S + 1}{\rho_G + \rho_M}\right)^2 \geq K_1 \geq \frac{\rho_M}{\rho_S}\left(\frac{\rho_G + \rho_S}{\rho_G\rho_M + 1}\right)^2 . \tag{4.4}$$

In a specific example, if $\rho_G = 4.0$, $\rho_S = 1.05$, and $\rho_M = 1.25$, K_1 lies between 0.84 and 1.17, a mismatch error between -16 and +17 percent if K_1 is erroneously taken to be unity.

The range of error can be reduced by "matching back" toward the generator, making Γ_G vanish. In this case, eq. (4.3) becomes:

$$K_1' = \frac{1 - |\Gamma_M|^2}{1 - |\Gamma_S|^2} = \frac{\rho_M}{\rho_S}\left(\frac{\rho_S + 1}{\rho_M + 1}\right)^2 . \tag{4.5}$$

With $\rho_S = 1.05$ and $\rho_M = 1.25$ as before, $K_1' = 0.99$, and the mismatch error is -1 percent.

Caution must be used in attempts to further reduce the mismatch error by matching the power meter input. If an adjustable transformer is used for this purpose, the loss in the transformer itself will cause an error which cannot be readily evaluated. Only transformers with known loss can be safely used for this purpose.

(3) Method 2 -- Comparison Using T-Junctions

(a) Simultaneous Comparison: The generator is connected to the center arm (No. 3) of a symmetrical T-junction as shown in figure 4-2. The standard and the power meter are connected to the other two arms (arms 1 and 2, respectively).

---

[3] It is evident that K_1 equals unity if $\Gamma_M = \Gamma_S$, a condition which may be recognized by a method described by MacPherson and Kerns (1950).

[4] $|\Gamma| = (\rho - 1)/(\rho + 1)$.

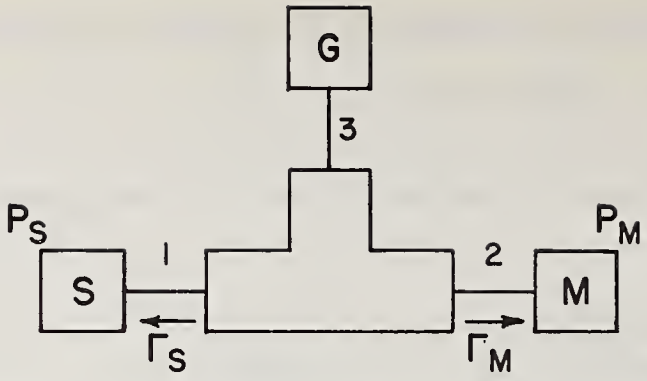

Figure 4-2. T-junction comparison.

It can be shown that equal power will be delivered to the standard and the meter by a symmetrical T providing that their impedances are identical. A high degree of symmetry can be achieved by precise mechanical design and construction and by special techniques, such as electroforming. The degree of symmetry achieved may in some cases exceed the accuracy with which it can be measured. In the general case, however, in which asymmetry must be taken into account, the ratio of powers absorbed by the meter and the standard is.[5]

$$K_2 = \frac{P_M}{P_S} = \left|\frac{S_{23}}{S_{13}}\right|^2 \cdot \left|\frac{1 - \left(S_{11} - \frac{S_{13}}{S_{23}} S_{12}\right)\Gamma_S}{1 - \left(S_{22} - \frac{S_{23}}{S_{13}} S_{12}\right)\Gamma_M}\right|^2 \cdot \frac{1 - |\Gamma_M|^2}{1 - |\Gamma_S|^2}. \tag{4.6}$$

The coefficients of the form $S_{m,n}$ are the scattering coefficients of the T. These scattering coefficients are either voltage reflection coefficients ($m = n$), or voltage transmission coefficients ($m \neq n$), and can be measured[6] with a standing-wave machine.

It is possible to obtain the magnitudes of the coefficients in eq. (4.6) from VSWR measurements and calculate the limits of K_2 as the phases are permitted to vary. Assuming that the T is symmetrical and lossless, K_2 lies between the limits:

$$\rho_M \rho_S \geq K_2 \geq \frac{1}{\rho_M \rho_S}. \tag{4.7}$$

Specifically; if $\rho_S = 1.05$, and $\rho_M = 1.25$, K_2 lies between 0.76 and 1.31, an error between -24 and +31 percent.

[5]This equation follows from the scattering equations (eq. (3.153)) of a three-arm junction.

[6]See section 4.2e.

(b) Alternate Connection to T-Junction: The generator is connected to the center arm (No. 3) of a T-junction as shown in figure 4-3. An uncalibrated power monitor is connected to one arm (No. 1) and the generator output is adjusted to maintain a constant indication of the monitor. The meter and the standard are alternately connected to the other arm (No. 2).

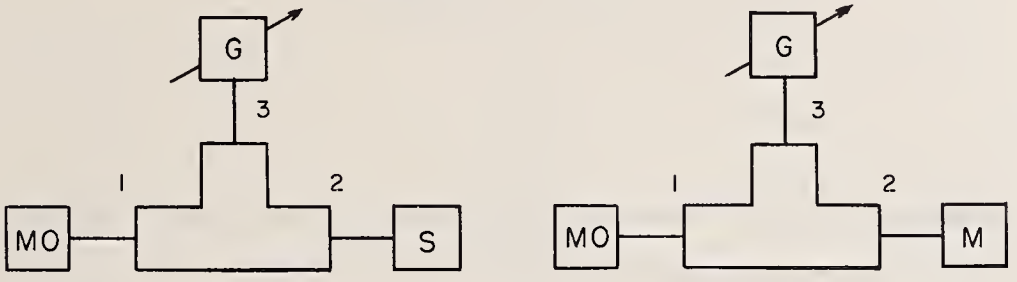

Figure 4-3. Alternate connection to a T junction.

The ratio of powers absorbed by the meter and the standard from these conditions, applying eq. (4.6), is

$$K_3 = \frac{P_M}{P_S} = \frac{P_M}{P_{MO}} \cdot \frac{P_{MO}}{P_S} = \left| \frac{1 - \left(S_{22} - \frac{S_{23}}{S_{13}} S_{12} \right) \Gamma_S}{1 - \left(S_{22} - \frac{S_{23}}{S_{13}} S_{12} \right) \Gamma_M} \right|^2 \cdot \frac{1 - |\Gamma_M|^2}{1 - |\Gamma_S|^2}. \qquad (4.8)$$

Comparison of this equation with eq. (4.6) shows that the effect of asymmetry of the T has been reduced by this method. In the case of a symmetrical lossless T, the limits of K_3 as determined from measurements of the magnitudes of the coefficients are the same as the limits of K_2, as expressed in eq. (4.7),

$$\rho_M \rho_S \geq K_3 \geq \frac{1}{\rho_M \rho_S}. \qquad (4.9)$$

(4) Method 3 -- Comparison Using Magic T

(a) Simultaneous Comparison: The standard and the power meter are connected to the symmetrical arms (numbers 1 and 2, respectively) of a magic T[7] as shown in figure 4-4.

[7]A conventional waveguide magic T may be defined as a four-arm junction having the form shown in figure 4-4 which is symmetrical, lossless, and matched looking in each arm.

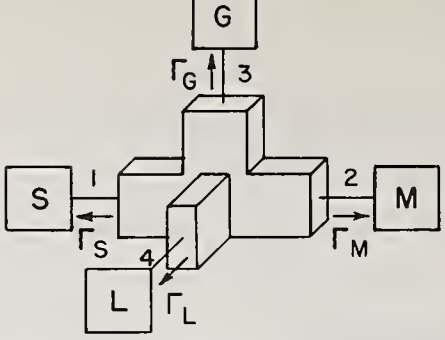

Figure 4-4. Magic T comparison.

A generator and matched load are connected to the other arms (numbers 3 and 4, respectively). It can be shown that equal power will be delivered to the standard and the meter by a symmetrical magic T provided that their impedances are identical. But in the general case in which the asymmetry and mismatch are taken into account the ratio of powers absorbed by the meter and the standard is,[8]

$$K_4 = \frac{P_M}{P_S} = \left| \frac{ab - cd\Gamma_L}{bg - df\Gamma_L\Gamma_M} \right|^2 \cdot \frac{1 - |\Gamma_M|^2}{1 - |\Gamma_S|^2} \tag{4.10}$$

where:

$$a = S_{23}(1 - S_{11}\Gamma_S) + S_{12}S_{13}\Gamma_S$$
$$b = S_{13}(1 - S_{44}\Gamma_L) + S_{14}S_{34}\Gamma_L$$
$$c = S_{34}(1 - S_{11}\Gamma_S) + S_{13}S_{14}\Gamma_S$$
$$d = S_{14}S_{23} - S_{13}S_{24}$$
$$f = S_{12}S_{34} - S_{13}S_{24}$$
$$g = S_{13}(1 - S_{22}\Gamma_M) + S_{12}S_{23}\Gamma_M.$$

The scattering coefficients of the magic T can be measured[9] with a standing-wave machine or the ideal[10] values can be used if the losses in the T are sufficiently small, the internal matching is sufficiently good, and the mechanical construction is sufficiently precise.

If the four-arm junction is an ideal magic T having properly chosen reference planes, $S_{11} = S_{22} = S_{33} = S_{44} = S_{12} = S_{34} = 0$, and $S_{14} = -S_{24} = S_{13} = S_{23}$.

It is possible to simplify eq. (4.10) in several ways. For example, if it is assumed that the load is perfectly matched ($\Gamma_L = 0$), eq. (4.10) reduces to eq. (4.6).

[8]This equation follows from the scattering equations of a four-arm junction.

[9]See for example section 4.2e.

[10]See eq. (3.172).

If in addition some of the properties of an ideal magic T are substituted in this equation ($S_{11} = S_{22} = S_{12} = 0$, and $|S_{13}| = |S_{23}|$), it reduces to eq. (4.5). A nomogram representing eq. (4.5) is shown in figure 4-5.

$$K = \frac{\rho_m}{\rho_s}\left(\frac{\rho_s + 1}{\rho_m + 1}\right)^2, \quad \rho_G = 1.0$$

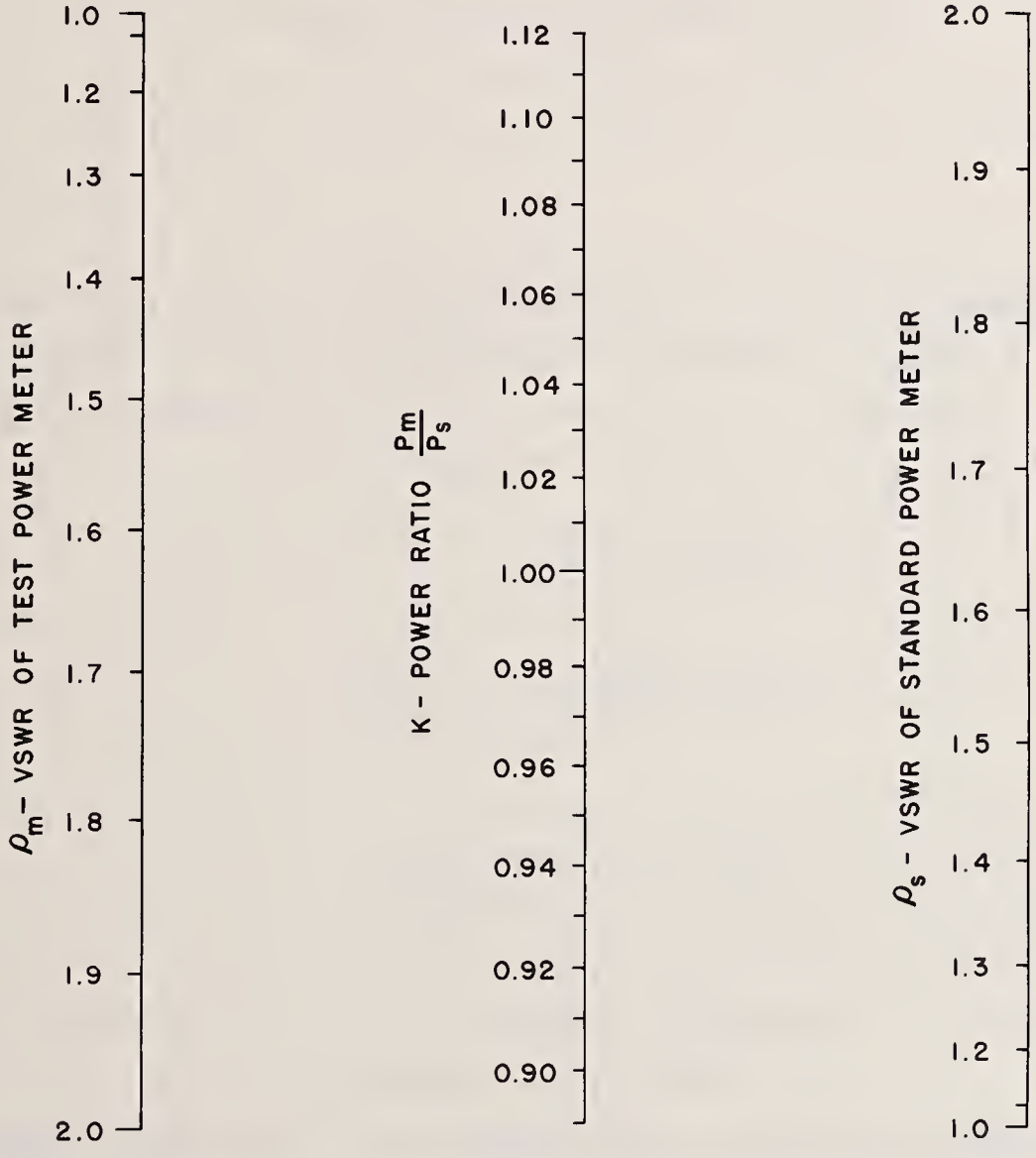

Figure 4-5. Mismatch effect in the calibration of power meters.

(b) Alternate Connection to Magic T: The generator and a load are connected to the symmetrical arms (numbers 3 and 4, respectively) of a magic T as shown in figure 4-6.

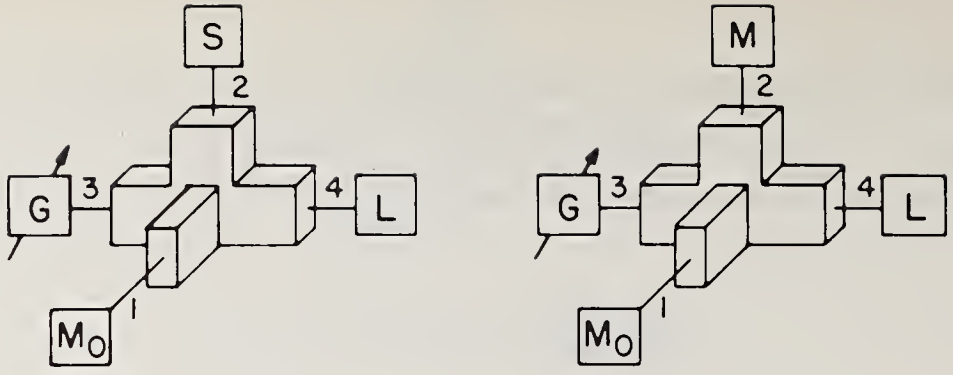

Figure 4-6. Alternate connection to a magic T.

An uncalibrated power monitor is connected to arm No. 1 and the meter and standard are alternately connected to arm No. 2. The generator output is adjusted to maintain a constant indication of the monitor. The ratio of powers absorbed by the meter and the standard is:

$$K_5 = \frac{P_M}{P_S} = \frac{P_M}{P_{MO}} \cdot \frac{P_{MO}}{P_S}$$

$$K_5 = \left|\frac{b\,g' - df\Gamma_L\Gamma_S}{b\,g - df\Gamma_L\Gamma_M}\right|^2 \cdot \frac{1 - |\Gamma_M|^2}{1 - |\Gamma_S|^2} \qquad (4.11)$$

where:

$$b = S_{13}(1 - S_{44}\Gamma_L) + S_{14}S_{34}\Gamma_L$$
$$g' = S_{13}(1 - S_{22}\Gamma_S) + S_{12}S_{23}\Gamma_S$$
$$d = S_{14}S_{23} - S_{13}S_{24}$$
$$f = S_{12}S_{34} - S_{13}S_{24}$$
$$g = S_{13}(1 - S_{22}\Gamma_M) + S_{12}S_{23}\Gamma_M.$$

If the load is matched ($\Gamma_L = 0$), eq. (4.11) reduces to eq. (4.8). It is evident that the asymmetry effect is generally less in the alternate connection method than in the simultaneous comparison method. If the magic T is very nearly ideal, substitution of some of its properties ($S_{12} = S_{22} = 0$) into eq. (4.8) reduces it to eq. (4.5). For a perfect magic T.

$$\frac{P_M}{P_S} = \frac{1 - |\Gamma_M|^2}{1 - |\Gamma_S|^2} = \frac{\rho_M}{\rho_S}\left(\frac{\rho_S + 1}{\rho_M + 1}\right)^2. \qquad (4.5)$$

c. Discussion of Calibration Methods

The alternate connection of the meter and the standard to the same generator is a simple and flexible method which can be employed with waveguide or coaxial line. No auxiliary power dividing equipment is required and the mismatch error is relatively small and can be easily evaluated from VSWR measurements if the generator is matched. The generator must remain stable in power output and frequency during the calibration and must be padded to prevent oscillator pulling caused by changes in loading.

The use of a power divider permits simultaneous comparison of the meter and the standard. This reduces the necessity for padding the oscillator and the stability requirements are not as great.

If the degree of symmetry is low, the mismatch and asymmetry error may be reduced by using the alternate connection method with a power monitor. The generator padding and stability requirements are increased and it is necessary to provide a smoothly adjustable generator output.

Symmetrical three-arm T's are commercially available in waveguide and coaxial line. Because of the center conductor, the coaxial T involves additional difficulties of construction not encountered in the waveguide T. The mismatch error can be evaluated from measurements of the parameters of the T. The range of mismatch error, even with a perfect T, is greater than that obtained by alternate connection of the meter and the standard to a matched generator.

Symmetrical waveguide magic T's are commercially available but magic T's or hybrid circuits in coaxial line are not readily obtainable. Carefully constructed waveguide magic T's make excellent power dividers for power meter calibration, permitting simultaneous comparison with no more mismatch error than is encountered with alternate connection to a matched generator. If asymmetry is appreciable, it can be determined from measurements of the T parameters.

The effect of asymmetry can be reduced by using the alternate connection method with a power monitor.

A magic T can also be used to accurately compare two impedances (MacPherson and Kerns, 1950). If one impedance is adjustable, the two can be made equal. Applying this principle to power meter calibration, the impedances of the meter and the standard can sometimes be made nearly equal, permitting a reduction in the mismatch error.

d. Use of Power Meters

(1) General Remarks

If the power to be measured is within the range of the power meter, a direct measurement can be made. If the power is greater, a calibrated device such as an attenuator or directional coupler is used in such a way that a known fraction of the power is measured by the power meter.

(2) Direct Measurement

In the direct measurement of the power that a given generator will deliver to a given load, the power meter is simply substituted for the load. This is the same situation encountered in the alternate connection of two power meters to a stable source. If the meter and the load are nearly matched,[11] it is often erroneously assumed that the power measured by the meter is the same as that delivered to the load. Assuming that the generator is well padded, the ratio of powers absorbed by the load and the power meter is given by eq. (4.3) with an appropriate change in subscripts

$$K_6 = \frac{P_L}{P_M} = \left|\frac{1 - \Gamma_G\Gamma_M}{1 - \Gamma_G\Gamma_L}\right|^2 \cdot \frac{1 - |\Gamma_L|^2}{1 - |\Gamma_M|^2}. \tag{4.12}$$

In this expression the reflection coefficients of the generator, meter, and load are designated as Γ_G, Γ_M, and Γ_L, respectively. If the power meter reading is assumed to be correct, it is multiplied by the factor K_6 to obtain the power that the generator will deliver to the load. It is apparent that eq. (4.12) and eq. (4.3) are of the same form and that the limits of K_6 are:

$$\frac{\rho_L}{\rho_M}\left(\frac{\rho_G + \rho_M}{\rho_G\rho_L + 1}\right)^2 \leq K_6 \leq \frac{\rho_L}{\rho_M}\left(\frac{\rho_G\rho_M + 1}{\rho_G + \rho_L}\right)^2. \tag{4.13}$$

In a specific example, taking $\rho_G = 4.0$, $\rho_M = 1.05$, and $\rho_L = 1.25$, K_6 lies between 0.84 and 1.17, a mismatch error of between -16 and +17 percent.

If the generator is matched, the mismatch error in the previous example is approximately -1 percent.

---

[11] The Z_0-match, or the non-reflecting condition is the desired condition.

(3) Use of Calibrated Attenuator

If a calibrated attenuator is used to extend the range of power meter as shown in figure 4-7, the measured power is normally multiplied by the attenuator ratio to obtain the power available to the load. If the error of mismatch is taken into

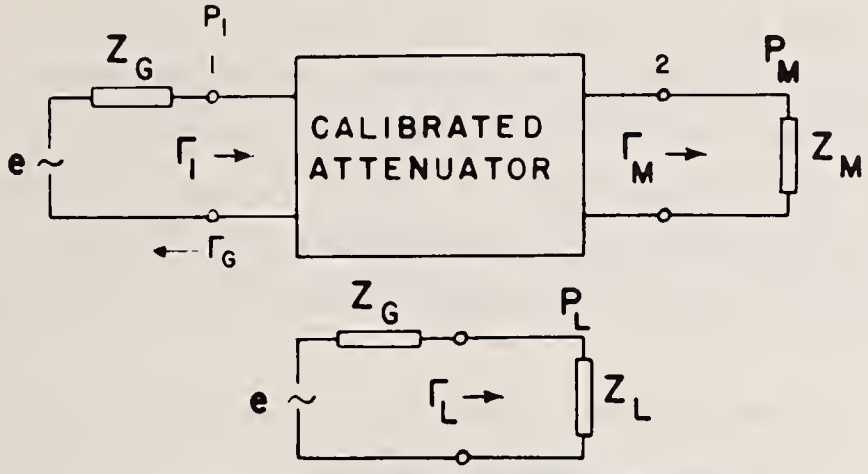

Figure 4-7. Use of calibrated attenuator.

account, the previous result is multiplied by a correction factor K_7 to obtain the power delivered to the load when it is connected directly to the generator. The factor K_7 is given by[12]

$$K_7 = \frac{P_L}{P_M R_A} = \left| \frac{1 - \Gamma_G \Gamma_1}{1 - \Gamma_G \Gamma_L} (1 - S_{22}\Gamma_M) \right|^2 \frac{1 - |\Gamma_L|^2}{1 - |\Gamma_M|^2}. \tag{4.14}$$

In eq. (4.14) the reflection coefficients of the generator, load, and meter are denoted by Γ_G, Γ_L, and Γ_M, respectively. The scattering coefficients of the attenuator are denoted by $S_{m,n}$ and Γ_1 represents the input voltage reflection coefficient of the attenuator with its output connected to the power meter. From the scattering equations for a reciprocal two terminal-pair network,

$$\Gamma_1 = S_{11} + \frac{S_{12}^2 \Gamma_M}{1 - S_{22}\Gamma_M}, \tag{4.15}$$

and the attenuation in decibels is:

$$A_T = 10 \log_{10} R_A = 10 \log_{10} \left| \frac{1}{S_{12}} \right|^2. \tag{4.16}$$

[12]This equation follows from eq. (4.12) and the scattering equations of a two-port.

If only the VSWR's are measured corresponding to the reflection coefficients of eq. (4.14), the limits of K_7 are:

$$4\,\frac{\rho_L}{\rho_M}\left[\frac{(\rho_G\rho_1 + 1)(\rho_{22}\rho_M + 1)}{(\rho_G + \rho_L)(\rho_{22} + 1)(\rho_1 + 1)}\right]^2 \geq K_7 \geq 4\,\frac{\rho_L}{\rho_M}\left[\frac{(\rho_G + \rho_1)(\rho_{22} + \rho_M)}{\rho_G\rho_L + 1)(\rho_{22} + 1)(\rho_1 + 1)}\right]^2. \qquad (4.17)$$

In a specific example, taking $\rho_G = 2.0$, $\rho_M = 1.20$, $\rho_L = 1.1$, $\rho_{22} = 1.20$ and $\rho_1 = 1.25$, K_7 lies between 0.89 and 1.14, a mismatch error between -11 and +14 percent.

If desired, the error may be evaluated by measuring the reflection coefficients appearing in eq. (4.14). The measured value of Γ_1 may be checked by measuring the scattering coefficients of the attenuator and substituting in eq. (4.15). Inspection of eqs. (4.15) and (4.16) shows that Γ_1 approximately equals S_{11} if the attenuation is large.

If the attenuator is reflection-free ($S_{11} = S_{22} = 0$), eq. (4.14) reduces to:

$$K_7' = \left|\frac{1 - \Gamma_G\Gamma_1}{1 - \Gamma_G\Gamma_L}\right|^2 \frac{1 - |\Gamma_L|^2}{1 - |\Gamma_M|^2} \qquad (4.18)$$

and eq. (4.15) reduces to:

$$\Gamma_1' = S_{12}{}^2\Gamma_M. \qquad (4.19)$$

In a specific example, taking $\rho_G = 2.0$, $\rho_M = 1.20$, $\rho_L = 1.1$, and $\rho_1 = 1.019$ (10 dB attenuator), K_7' lies between 0.970 and 1.046, a mismatch error between -3 and +5 percent.

If the generator is matched ($\Gamma_G = 0$), eq. (4.18) reduces to:

$$K_7'' = \frac{1 - |\Gamma_L|^2}{1 - |\Gamma_M|^2} = \frac{\rho_L}{\rho_M}\left[\frac{\rho_M + 1}{\rho_L + 1}\right]^2. \qquad (4.20)$$

Assuming that $\rho_L = 1.1$ and $\rho_M = 1.20$, K_7'' equals 1.007, representing a mismatch error of less than 1 percent.

(4) Use of Directional Couplers

(a) Temporarily Inserted: A directional coupler is often used to extend the range of power meters as shown in figures 4-8 and 4-9. In figure 4-8, the coupler is temporarily inserted between the generator and load and the power is measured with a power meter. The measured power is normally multiplied by the coupler ratio to

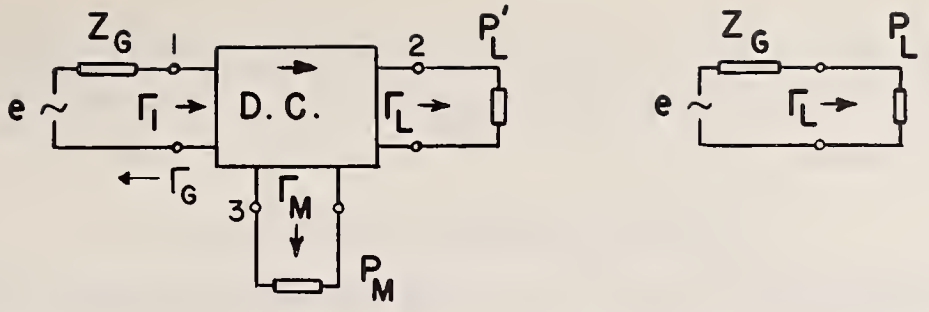

Figure 4-8. Temporary insertion of directional coupler.

obtain the power available to the load. If the effect of mismatch is taken into account, the previous result is multiplied by a correction factor K_8 to obtain the power delivered to the load when it is connected directly to the generator. The factor K_8 is given by:[13]

$$K_8 = \frac{P_L}{P_M R_{CO}} = \left|\frac{1 - \Gamma_G\Gamma_1}{1 - \Gamma_G\Gamma_L}\right|^2 \cdot |S_{13}|^2 \cdot \left|\frac{S_{12}(1 - S_{33}\Gamma_M) + S_{13}S_{23}\Gamma_M}{S_{23}(\Gamma_1 - S_{11}) + S_{12}S_{13}}\right|^2 \frac{1 - |\Gamma_L|^2}{1 - |\Gamma_M|^2}. \tag{4.21}$$

In eq. (4.21) the reflection coefficients of the generator, meter, and load are denoted by Γ_G, Γ_M, and Γ_L, respectively. The input reflection coefficient of the directional coupler connected as shown in figure 4-8 is Γ_1. The scattering coefficients of the coupler are designated by $S_{m,n}$. The coupling, C, and directivity D, are defined in the usual manner:

$$\begin{cases} C = 10 \log_{10} R_{CO} = 10 \log_{10}\left|\frac{1}{S_{13}}\right|^2 \\ D = 10 \log_{10}\left|\frac{S_{13}}{S_{23}}\right|^2. \end{cases} \tag{4.22}$$

It can be shown by a solution of the scattering equations for a three-arm junction that the reflection coefficient Γ_1 is:

$$\Gamma_1 = S_{11} + \frac{S_{12}^2\Gamma_L}{(1 - S_{22}\Gamma_L) - \frac{S_{13}(1 - S_{22}\Gamma_L) + S_{12}S_{23}\Gamma_L}{S_{12}(1 - S_{33}\Gamma_M) + S_{13}S_{23}\Gamma_M} S_{23}\Gamma_M} + \frac{S_{13}^2\Gamma_M}{(1 - S_{33}\Gamma_M) - \frac{S_{12}(1 - S_{33}\Gamma_M) + S_{13}S_{23}\Gamma_M}{S_{13}(1 - S_{22}\Gamma_L) + S_{12}S_{23}\Gamma_L} S_{23}\Gamma_L}. \tag{4.23}$$

[13]The derivation of this equation is straightforward, starting from the scattering equations of a three-arm junction. See eq. (3.153).

If the directional coupler can be considered to be perfect, having infinite directivity ($S_{23} = 0$) and being reflection-free ($S_{11} = S_{22} = S_{33} = 0$), the above equations simplify, eq. (4.23) reducing to:

$$\Gamma_1' = S_{11} + S_{12}^2\Gamma_L + S_{13}^2\Gamma_M \tag{4.24}$$

and eq. (4.21) reducing to eq. (4.18). If in addition the generator is matched ($\Gamma_G = 0$), eq. (4.20) applies.

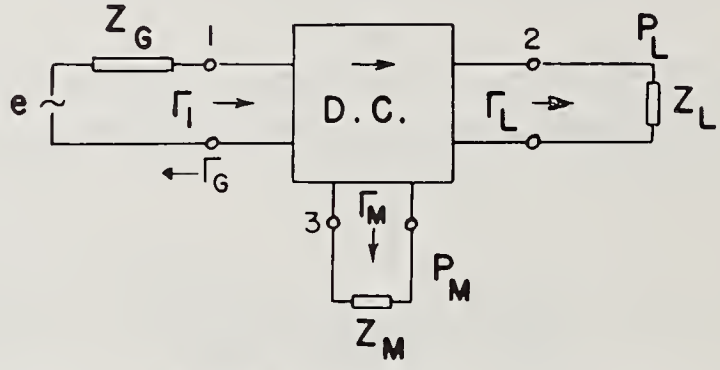

Figure 4-9. Permanent installation of directional coupler.

(b) Permanently Installed: A directional coupler is often permanently installed between the generator and the load as shown in figure 4-9. The power delivered to the load is normally obtained by multiplying the power meter reading by the coupler ratio. If mismatch is present, it is necessary to multiply this result by a correction factor K_9. This factor is given by:[14]

$$K_9 = \frac{P_L}{P_M R_{CO}} = |S_{13}|^2 \left| \frac{S_{12}(1 - S_{33}\Gamma_M) + S_{13}S_{23}\Gamma_M}{S_{13}(1 - S_{22}\Gamma_L) + S_{12}S_{23}\Gamma_L} \right| \frac{1 - |\Gamma_L|^2}{1 - |\Gamma_M|^2}. \tag{4.25}$$

Note that $K_9 = 1$ when $|\Gamma_L| = |\Gamma_M| = 0$, and $|S_{12}| = 1$. If the directional coupler can be considered to be perfect ($S_{11} = S_{22} = S_{33} = S_{23} = 0$) and the coupling is loose ($S_{12} = 1$), eq. (4.25) reduces to eq. (4.20)

In a specific example let $\rho_L = 1.5$ and $\rho_M = 1.25$. A directional coupler is used having a directivity of 25 decibels, a coupling of 20 decibels and reflections in each arm producing a VSWR less than 1.1. Assuming the worst phase conditions, the limits of error calculated from eq. (4.25) are approximately -8 and +2 percent.

If the directional coupler is assumed to be perfect in the same example, the error calculated from eq. (4.20) is approximately -3 percent.

[14]The derivation is similar to that for eq. (4.21).

If these examples can be considered typical, it is evident that the simplified equation cannot be used to evaluate the mismatch error unless the directional coupler is very nearly perfect and the degree of mismatch is small.

e. Measurement of Scattering Coefficients

A reciprocal network having n-terminal pairs and a scattering matrix S is shown in figure 4-10. The scattering coefficients are of the general form $S_{p,q}$ where p and

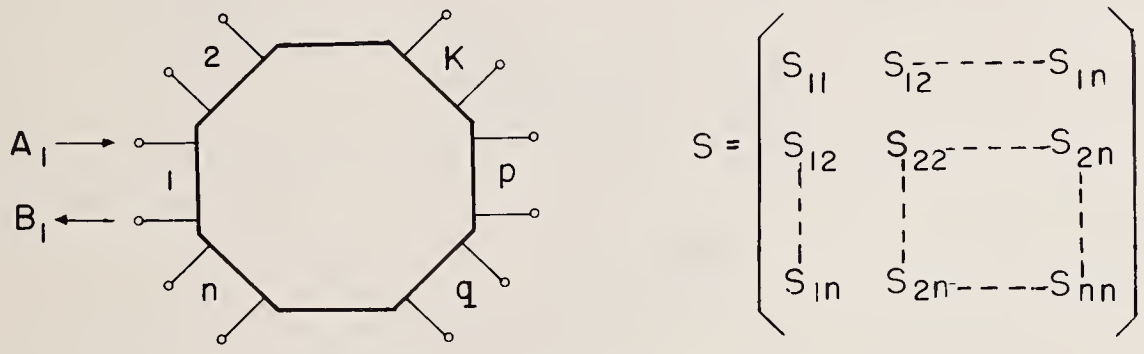

Figure 4-10. Network having n-terminal pairs.

q are integers, each denoting a given terminal pair. It is assumed that reciprocity holds in the form $S_{pq} = S_{qp}$.

If p = q = K, the voltage reflection coefficient S_{KK} is measured at the K^{th} terminal pair with all other terminal pairs connected to reflection-free loads.

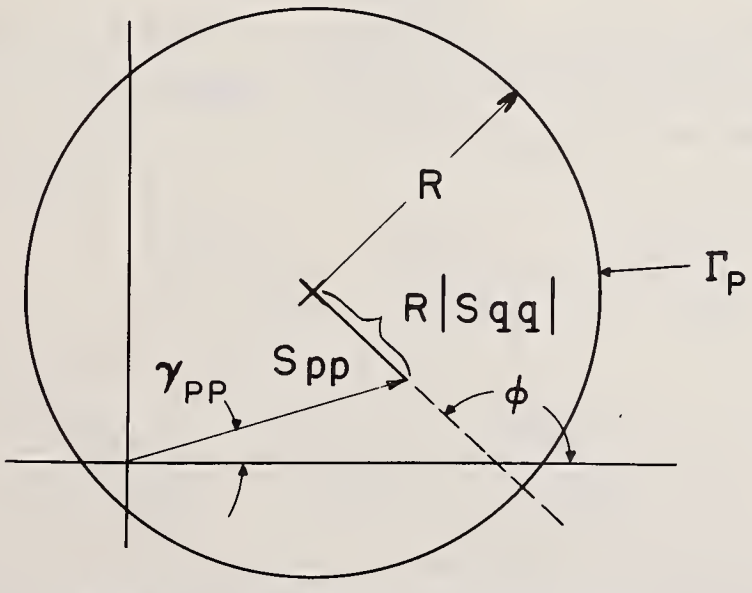

Figure 4-11. Reflection coefficient circle.

If $p \neq q$, the voltage transmission coefficient S_{pq} is measured in the following way. The q^{th} terminal pair is connected to a variable reactance. All other terminal pairs with the exception of the p^{th} pair are connected to reflection-free loads.

The input reflection coefficient Γ_p is measured for various reactances at q. The locus of the measured points is a circle as shown in figure 4-11. Assuming that reciprocity holds in the form $S_{pq} = S_{qp}$, the magnitude and phase of S_{pq} are:

$$|S_{pq}|^2 = R\{1 - |S_{qq}|^2\}$$

$$\gamma_{pq} = \frac{1}{2}(\phi + \gamma_{qq}). \tag{4.26}$$

A short derivation follows:

If A and B denote the incident and reflected voltage waves at a pair of terminals p and q,

$$\begin{cases} B_p = S_{pp}A_p + S_{pq}A_q \\ B_q = S_{qp}A_p + S_{qq}A_q. \end{cases} \tag{4.27}$$

Let

$$\frac{A_q}{B_q} = \epsilon^{j\theta}.$$

Then

$$\frac{A_q}{A_p} = \frac{S_{qp}}{e^{-j\theta} - S_{qq}} \tag{4.28}$$

and:

$$\Gamma_p = \frac{B_p}{A_p} = S_{pp} + S_{pq}\frac{A_q}{A_p} = S_{pp} + \frac{S_{pq}^2}{\epsilon^{-j\theta} - S_{qq}}. \tag{4.29}$$

A variation of θ represents a change in the reactance connected to terminal pair q. As shown in figure 4-12, the magnitude of the vector quantity $(\Gamma_p - S_{pp})$ goes through maximum and minimum values as θ changes.

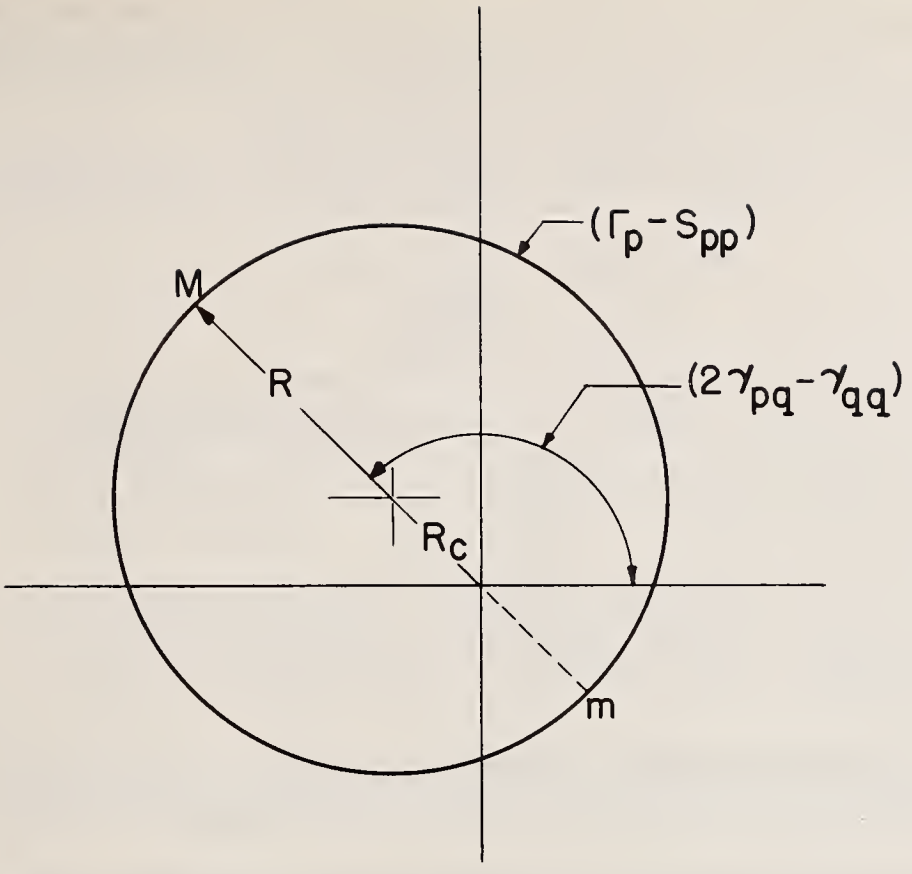

Figure 4-12. Translated reflection coefficient circle.

At these points M and m,

$$(\Gamma_p - S_{pp})_M = \frac{|S_{pq}|^2}{1 - |S_{qq}|} e^{j(2\gamma_{pq} - \gamma_{qq})} \tag{4.30}$$

$$(\Gamma_p - S_{pp})_m = \frac{|S_{pq}|^2}{1 + |S_{qq}|} e^{j(2\gamma_{pq} - \gamma_{qq} \pm \pi)}. \tag{4.31}$$

The radius of the circle is:

$$R = \frac{1}{2}\left(\frac{|S_{pq}|^2}{1 - |S_{qq}|} + \frac{|S_{pq}|^2}{1 + |S_{qq}|}\right) = \frac{|S_{pq}|^2}{1 - |S_{qq}|^2}. \tag{4.32}$$

The distance to the center of the circle is:

$$R_C = \frac{1}{2}\left(\frac{|S_{pq}|^2}{1 - |S_{qq}|} - \frac{|S_{pq}|^2}{1 + |S_{qq}|}\right) = \frac{|S_{pq}|^2}{1 - |S_{qq}|^2} |S_{qq}| = R|S_{qq}|. \tag{4.33}$$

Denoting the phase angle $(2\gamma_{pq} - \gamma_{qq})$ by ϕ, the diagram of figure 4-12 can be drawn.

An alternate method of measuring the scattering coefficients of an n-terminal pair network is as follows. Referring to figure 4–10, the scattering coefficients S_{pp}, S_{pq}, and S_{qq} are determined by terminating terminal pair q in three different

loads having voltage reflection coefficients Γ_{L_1}, Γ_{L_2}, and Γ_{L_3}, and measuring the corresponding input voltage reflection coefficients Γ_1, Γ_2, and Γ_3 at terminal pair p with all other terminal pairs terminated in matched loads.

Solving the three equations for input voltage reflection coefficient of the form

$$\Gamma = S_{pp} + \frac{S_{pq}^2 \Gamma_L}{1 - S_{qq}\Gamma_L}, \tag{4.34}$$

the following expressions are obtained for the scattering coefficients.

$$S_{pp} = \frac{\Gamma_{L_1}\Gamma_{L_2}\Gamma_3(\Gamma_1 - \Gamma_2) + \Gamma_{L_2}\Gamma_{L_3}\Gamma_1(\Gamma_2 - \Gamma_3) + \Gamma_{L_3}\Gamma_{L_1}\Gamma_2(\Gamma_3 - \Gamma_1)}{\Gamma_{L_1}\Gamma_{L_2}(\Gamma_1 - \Gamma_2) + \Gamma_{L_2}\Gamma_{L_3}(\Gamma_2 - \Gamma_3) + \Gamma_{L_3}\Gamma_{L_1}(\Gamma_3 - \Gamma_1)} \tag{4.35}$$

$$S_{qq} = - \frac{\Gamma_{L_1}(\Gamma_2 - \Gamma_3) + \Gamma_{L_2}(\Gamma_3 - \Gamma_1) + \Gamma_{L_3}(\Gamma_1 - \Gamma_2)}{\Gamma_{L_1}\Gamma_{L_2}(\Gamma_1 - \Gamma_2) + \Gamma_{L_2}\Gamma_{L_3}(\Gamma_2 - \Gamma_3) + \Gamma_{L_3}\Gamma_{L_1}(\Gamma_3 - \Gamma_1)} \tag{4.36}$$

$$S_{pq}^2 = - \frac{(\Gamma_1 - \Gamma_2)(\Gamma_2 - \Gamma_3)(\Gamma_3 - \Gamma_1)(\Gamma_{L_1} - \Gamma_{L_2})(\Gamma_{L_2} - \Gamma_{L_3})(\Gamma_{L_3} - \Gamma_{L_1})}{(\Gamma_{L_1}\Gamma_{L_2}(\Gamma_1 - \Gamma_2) + \Gamma_{L_2}\Gamma_{L_3}(\Gamma_2 - \Gamma_3) + \Gamma_{L_3}\Gamma_{L_1}(\Gamma_3 - \Gamma_1)]^2}. \tag{4.37}$$

Extension to the non-reciprocal case is straightforward. One replaces S_{pq}^2 by $S_{pq}S_{qp}$, and $2\gamma_{pq}$ is replaced by $\gamma_{pq} + \gamma_{qp}$.

4.3. Barretter Mount Efficiency Measurement

a. Introduction

As mentioned in the introduction to Chapter 4, the impedance variation method of measuring barretter mount efficiency was developed by Kerns (1949b). At first, accuracy was poor (10-20%) because impedances could not be accurately measured in coaxial and rectangular waveguide.

In the following section, a method is described which is based upon Kerns' work, but avoids the measurement of impedance. The accuracy is estimated to be better than ± 1.6% (see table 4-2). The work described here was performed in 1953-54 and was followed with further refinements.[15] The work on microwave power measurements is well covered in a survey article (Rumfelt and Elwell, 1967).

[15] Tuned reflectometer techniques (Engen, 1961) were applied to measure efficiencies of barretter mounts in rectangular waveguide with improved accuracy (0.5%). These techniques were used at frequencies where the more accurate (0.2%) microcalorimeter methods had not yet been applied. Finally a method was developed (Engen, 1966) to accurately (1.4%) transfer the calibration of a bolometer mount in rectangular waveguide to one having a coaxial output.

Although the method described below is presently not in use at NBS, it illustrates the application of microwave circuit theory to the development of accurate measurement techniques. The description of the method begins with a discussion of the definition of bolometer mount efficiency.

The efficiency, η, of a bolometer mount is defined as the ratio of the power dissipated in the bolometer element to the power input to the bolometer mount. If the power dissipated in the bolometer element, P_b, can be accurately determined, the power input, P_I, to the bolometer mount is

$$P_I = \frac{P_b}{\eta}. \tag{4.38}$$

P_b is usually measured by substitution techniques in which it is customary to reduce the audio or dc bolometer bias power (after the rf power is applied) until the bolometer resistance returns to its original operating value. It is assumed that the change in bolometer resistance caused by the rf power is identical to the change in resistance caused by an equal amount of af or dc power P_d. The validity of this assumption has been treated (Carlin and Sucher, 1952), (Adams and Desch, 1968), (Jarvis and Adams, 1968), (Adams and Jarvis, 1969), for Wollaston wire bolometers cooled by convection. Based upon this analysis, Carlin and Sucher concluded that "Wollaston wire bolometers, when properly designed and mounted, afford a means of measuring cw power over a frequency range extending to the millimeter wavelength region, with an accuracy approaching that of low-frequency measurements." It should be noted, however, that under less favorable conditions the substitution error for convection-cooled Wollaston wire bolometers may be appreciable (let us say greater than 0.5 percent) at frequencies above the estimated limit of 3,000 MHz, depending upon the length and mounting of the bolometer element.

If the ratio of P_b to P_d is K_s,

$$P_I = \frac{K_s}{\eta} P_d. \tag{4.39}$$

It is possible to estimate the limits of K_s for a specific Wollaston wire bolometer from the calculated curves of Carlin and Sucher (1952).

An impedance method of determining bolometer mount efficiency has been described by Kerns (1949b). Unfortunately, relatively small errors in the required impedance measurements can lead to a large error (10-20%) in the efficiency as determined by this method.

A modification of Kerns' method will be described, in which the direct measurement of impedance is avoided, permitting the efficiencies of tunable bolometer mounts to be obtained with increased accuracy (1.6%). Efficiencies of untuned bolometer mounts can thereby be obtained with very little loss in accuracy from voltage ratio measurements.

b. Impedance Method

In the impedance method of determining efficiency the bolometer mount is thought of as replaced by an equivalent two-terminal-pair network terminated in the bolometer resistance. As shown in figure 4-13, the input impedance (of the equivalent network) corresponding to each of three different bolometer resistances is obtained.

The normal operating resistance of the bolometer is designated as R_2. The efficiency for this condition may be calculated from the following expression deduced from Kerns (1949), involving the three terminating resistances w_1, w_2, and w_3 and the three corresponding input impedances Z_1, Z_2, and Z_3,

$$\text{Efficiency } (\eta)_{w_2=R_2} = \frac{R_2}{\mathrm{Re}Z_2}\left|\frac{(Z_2 - Z_1)(Z_3 - Z_2)(w_3 - w_1)}{(Z_3 - Z_1)(w_2 - w_1)(w_3 - w_2)}\right| \tag{4.40}$$

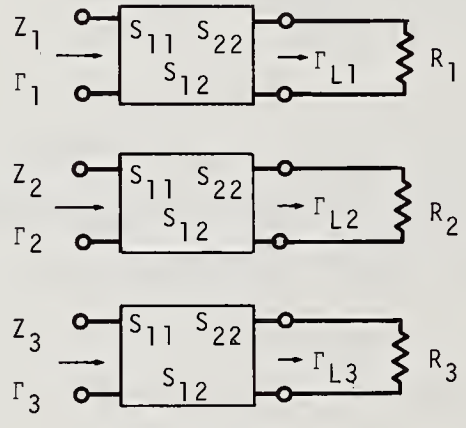

$$\Gamma_1 = S_{11} + \frac{S_{12}^2\Gamma_{L1}}{1-S_{22}\Gamma_{L1}}$$

$$\Gamma_2 = S_{11} + \frac{S_{12}^2\Gamma_{L2}}{1-S_{22}\Gamma_{L2}}$$

$$\Gamma_3 = S_{11} + \frac{S_{12}^2\Gamma_{L3}}{1-S_{22}\Gamma_{L3}}$$

$$\eta_{R=R_2} = \frac{|S_{12}|^2\left\{1-|\Gamma_{L2}|^2\right\}}{|1-S_{22}\Gamma_{L2}|^2-|S_{11}(1-S_{22}\Gamma_{L2})+S_{12}^2\Gamma_{L2}|^2}$$

Figure 4-13. Efficiency of a two-terminal-pair network (terminated in a resistance R_2) determined from three measurements of input impedance or reflection coefficient.

An equivalent expression for the efficiency can be obtained[16] in terms of the voltage reflection coefficients corresponding to the above terminating resistances and input impedances.

$$\text{Efficiency } (\eta)_{R=R_2} = \left| \frac{(\Gamma_2 - \Gamma_1)(\Gamma_3 - \Gamma_2)(\Gamma_{L3} - \Gamma_{L1})}{(\Gamma_3 - \Gamma_1)(\Gamma_{L2} - \Gamma_{L1})(\Gamma_{L3} - \Gamma_{L2})} \right| \frac{1 - |\Gamma_{L2}|^2}{1 - |\Gamma_2|^2}, \qquad (4.41)$$

where Γ denotes an input, and Γ_L a terminating reflection coefficient.

If the bolometer forms one arm of a Wheatstone bridge, it is convenient to adjust the bolometer resistances R_1, R_2, and R_3 to predetermined values. If the factor containing the real parameters Γ_{L1}, Γ_{L2}, and Γ_{L3} is denoted by C, eq. (4.41) becomes

$$\eta = \frac{C}{1 - |\Gamma_2|^2} \left| \frac{(\Gamma_2 - \Gamma_1)(\Gamma_3 - \Gamma_2)}{\Gamma_3 - \Gamma_1} \right|, \qquad (4.42)$$

where

$$C = \{1 - |\Gamma_{L2}|^2\} \left| \frac{\Gamma_{L3} - \Gamma_{L1}}{(\Gamma_{L2} - \Gamma_{L1})(\Gamma_{L3} - \Gamma_{L2})} \right| = \frac{2R_2(R_3 - R_1)}{(R_2 - R_1)(R_3 - R_2)},$$

and

$$\Gamma_L = \frac{R_L - Z_0}{R_L + Z_0},$$

Where Z_0 is an arbitrary real impedance.

It is generally true that the factor C can be more accurately determined than the other factors in eq. (4.42), because C is a function of resistances determined by dc measurement.

The reflection coefficients Γ_1, Γ_2, and Γ_3 occur in difference terms of eq. (4.42), with the unfortunate result that a given error in measuring individual reflection coefficients may produce a much larger error in the calculated efficiency.

For example, if C = 19.92, $\Gamma_1 = 0.0676$, $\Gamma_2 = 0$, and $\Gamma_3 = 0.174\, e^{j61\pi/60}$, the efficiency is approximately 97 percent. An error of only ± 1 percent in measuring the voltage standing-wave ratios

$$\left\{ \text{VSWR} = \frac{1 + |\Gamma|}{1 - |\Gamma|} \right\} \text{ corresponding to } |\Gamma_1| \text{ and } |\Gamma_3|$$

can produce an error of approximately ± 6 percent in the calculated efficiency.

---

[16] Equation (4.41) can be obtained by simultaneous solution of the equations appearing in figure 4-13, which are based upon the scattering equations of a two-terminal-pair network. See section 3.1e, eq. (3.4).

In order to reduce this error in efficiency to the more useful value of ± 1 percent, it would be necessary in the example to make VSWR measurements to an accuracy better than approximately ± 0.2 percent. It is apparent that the determination of efficiency by this method places rather severe requirements on the accuracy of UHF or microwave impedance measurements.

c. Improved Method

It is possible to avoid the direct measurement of impedance of tunable bolometer mounts having a high efficiency (above approximately 90%) and thereby increase the accuracy of the efficiency determination.

Assuming that the bolometer mount can be made reflection-free ($\Gamma_2 = 0$) by an appropriate tuning adjustment when the bolometer is operating at its normal rated resistance, R_2, eq. (4.42) becomes

$$\eta = C\left|\frac{\Gamma_1\Gamma_3}{\Gamma_1 - \Gamma_3}\right|. \tag{4.43}$$

If, in addition, the bolometer mount has a high efficiency, it can be assumed with small error (as discussed later) that the vectors representing Γ_1 and Γ_3 terminate on a straight line passing through the origin. The efficiency is

$$\eta = C\left|\frac{\Gamma_1\Gamma_3}{|\Gamma_1| \pm |\Gamma_3|}\right|. \tag{4.44}$$

The plus sign is used if the vectors representing Γ_1 and Γ_3 terminate on opposite sides of the origin, and the negative sign is used if they terminate on the same side.

Bolometer resistances R_1 and R_3 should be chosen above and below R_2 in order to obtain the greatest possible spread. In this case the vectors representing Γ_1 and Γ_3 terminate on opposite sides of the origin, and

$$\eta = C\,\frac{|\Gamma_1\Gamma_3|}{|\Gamma_3| + |\Gamma_1|} = \frac{C}{2}\,\frac{(\rho_1 - 1)(\rho_3 - 1)}{\rho_1\rho_3 - 1}, \tag{4.45}$$

where ρ represents the VSWR corresponding to $|\Gamma|$.

Instead of measuring ρ_1 and ρ_3, more accurate results may be obtained by measuring the relative voltage output of a loosely coupled, properly positioned fixed probe.

A simplified representation of a slotted section and probe is shown in figure 4-14. It is seen that the voltage, E_P, (in waveguide of rectangular cross section operating in the dominant mode, E_P corresponding to the strength of the transverse electric field) is a function of the reflection coefficients of the generator, probe, and load referred to the probe position. From inspection of the equivalent circuit

$$E_P = E_G \frac{(1 - \Gamma_G)(1 + \Gamma_P)(1 + \Gamma_L)}{(1 + \Gamma_G)(1 - \Gamma_P)(1 + \Gamma_L) + 2(1 + \Gamma_P)(1 - \Gamma_G\Gamma_L)}, \tag{4.46}$$

in which the subscripts G, P, and L, refer to the generator, probe, and load, respectively.

By means of a matching transformer following the generator, it is possible to make Γ_G vanish. In this case,

$$E_P = E_G \frac{1}{y_P + \frac{2}{1 + \Gamma_L}}, \tag{4.47}$$

where $y_P = (1 - \Gamma_P)(1 + \Gamma_P)$.

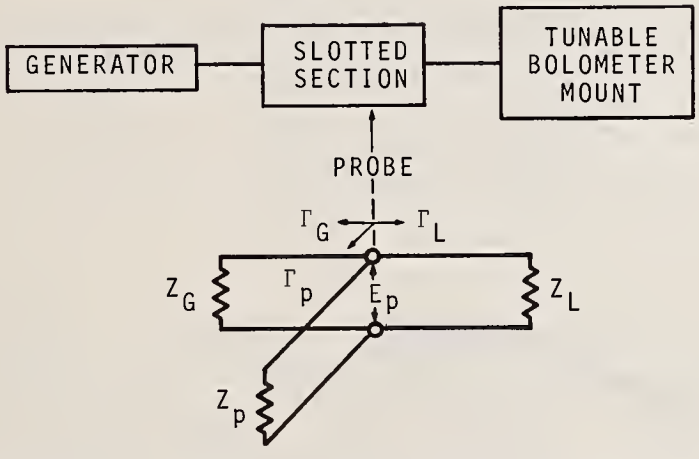

Figure 4-14. Simplified block diagram of measuring apparatus and an equivalent circuit representation.

If in addition, the probe is loosely coupled ($y_P \simeq 0$),

$$E_P \simeq \frac{E_G}{2}(1 + \Gamma_L). \tag{4.48}$$

If the probe is located at a position where its response is maximum when the bolometer resistance is R_1, E_{P1} is proportional to $(1 + |\Gamma_1|)$. With the probe fixed in that position, the bolometer resistance is changed to R_2 and then R_3, observing the probe response,

$$\begin{aligned} E_{P1} &= k(1 + |\Gamma_1|) \\ E_{P2} &= k \\ E_{P3} &\simeq k(1 - |\Gamma_3|). \end{aligned} \tag{4.49}$$

Defining the ratios K_1 and K_3 as follows,

$$K_1 = \frac{E_{P1}}{E_{P2}} = 1 + |\Gamma_1|$$

$$K_3 = \frac{E_{P3}}{E_{P2}} \simeq 1 - |\Gamma_3|, \tag{4.50}$$

the efficiency may be written

$$\eta = C \frac{(E_{P1} - E_{P2})(E_{P2} - E_{P3})}{E_{P2}(E_{P1} - E_{P3})} = C \frac{(K_1 - 1)(1 - K_3)}{K_1 - K_3}. \tag{4.51}$$

A correction to eq. (4.51), to compensate for failure of the assumption that the vectors representing Γ_1 and Γ_3 are colinear, can be made if the other sources of error are neglected for the moment. Let the ratio of η given by eq. (4.43) to that given by eq. (4.51) be

$$\zeta_1 = \left| \frac{\Gamma_1 \Gamma_3}{\Gamma_1 - \Gamma_3} \right| \frac{(K_1 - K_3)}{(K_1 - 1)(1 - K_3)}. \tag{4.52}$$

If the angular difference between Γ_1 and Γ_3, as shown in figure 4-15, is

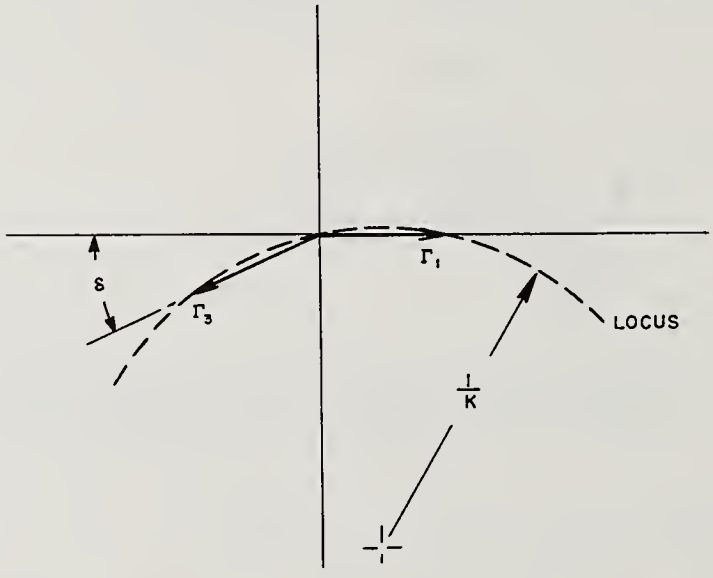

Figure 4-15. Diagram illustrating curvature of input reflection coefficient locus for resistive termination of bolometer mount.

$\pi + \delta$, where $\delta \leq 0.1$, it can be shown that

$$|\Gamma_3| \simeq (1 - K_3)(1 + \delta^2/2K_3),$$

$$|\Gamma_3 - \Gamma_1| \simeq (K_1 - K_3)\left\{1 + \delta^2 \frac{K_1(1 - K_3)^2}{2K_3(K_1 - K_3)^2}\right\},$$

and

$$\zeta_1 \simeq 1 + \delta^2 \frac{(K_1 - 1)(K_1 - K_3^2)}{2K_3(K_1 - K_3)^2}. \tag{4.53}$$

The angular difference, δ, is simply related to the curvature, K, of the locus of the reflection coefficient. This locus may be determined by measuring the input reflection coefficient (referred to the fixed position of the probe) as the bolometer resistance is varied. The expression relating K and δ is

$$\delta \simeq \frac{K}{2}(K_1 - K_3) \qquad (\delta \leq 0.1). \tag{4.54}$$

Equation (4.53) may be written in terms of K:

$$\zeta_1 \simeq 1 + K^2 \frac{(K_1 - 1)(K_1 - K_3^2)}{8K_3}. \tag{4.55}$$

A graph representing the percentage correction according to eq. (4.55) is shown in figure 4-16.

Another correction to eq. (4.51) is based upon the fact that there may be appreciable losses between the fixed probe position and the bolometer mount input. The efficiency of a length of line or waveguide having a known attenuation is shown in figure 4-17. If the line or guide section is not uniform, the efficiency must be

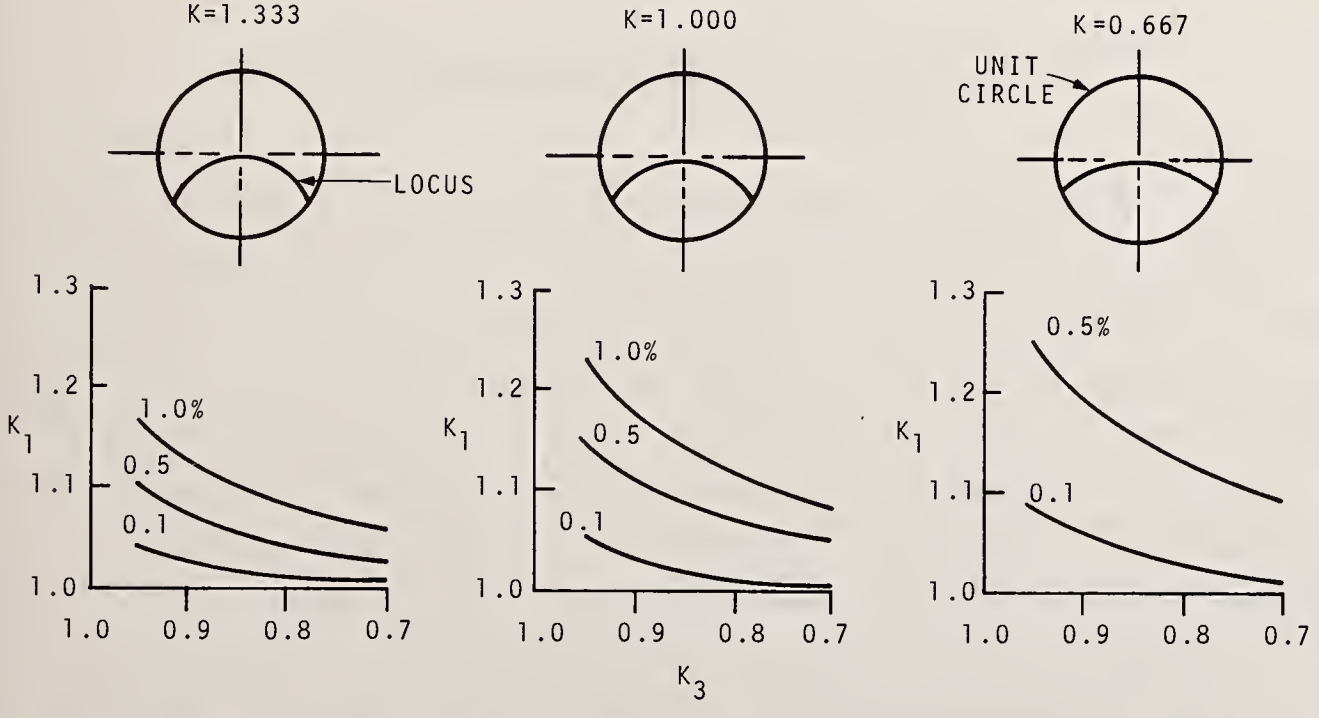

Figure 4-16. Percentage correction to efficiency corresponding to curvature of reflection coefficient locus for three values of curvature.

determined by other means, such as measuring the bolometer mount efficiency with another identical slotted section inserted between the bolometer mount and the measuring slotted section. If the efficiency of that portion of the circuit between the fixed probe position and the bolometer mount input is η_{P-B}, the efficiency of the bolometer mount, applying the above corrections is

$$\eta = \frac{C}{\eta_{P-B}} \left| \frac{(K_1 - 1)(1 - K_3)}{K_1 - K_3} \right| \left\{ 1 + K^2 \frac{(K_1 - 1)(K_1 - K_3^2)}{8K_3} \right\}. \qquad (4.56)$$

It is seen that both corrections increase the efficiency over the value obtained in eq. (4.51).

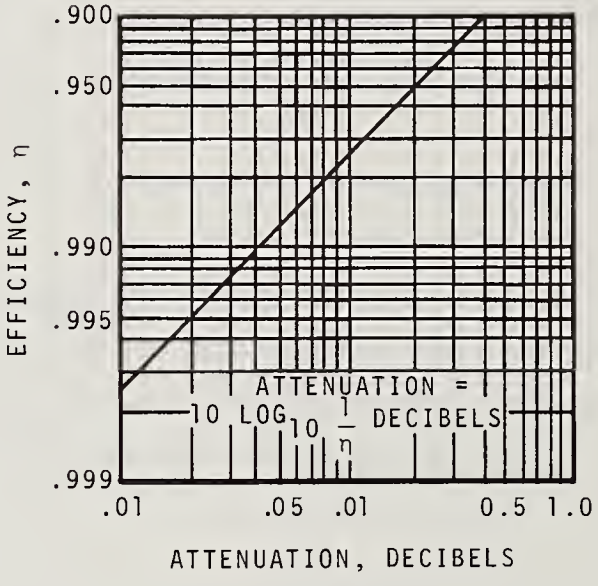

Figure 4-17. Efficiency of a symmetrical, matched attenuator (or a length of uniform line) terminated in a reflection-free load.

The method just described is applicable to tunable bolometer mounts (adjusted for no reflection when $R = R_2$), in which the bolometer element can be represented by a resistance terminating the bolometer mount. (Barretters are generally suitable, but there is evidence that thermistors do not fulfill this condition).

The efficiency of tunable bolometer-mount assemblies, including matching transformers, can also be measured by this method. After the efficiency of a tunable bolometer-mount assembly has been determined, at a specified operating frequency, the efficiency of another tunable or untuned bolometer mount or assembly can be obtained by comparing the power readings of the two mounts when alternately connected to a stable, well-padded generator. Assuming that the power dissipated in

the element can be accurately measured by dc substitution techniques (See Chapter 3 of Ginzton, 1957), and letting the subscripts A and B refer to the two mounts,

$$\eta_A P_A = P_{Ad}$$
$$\eta_B P_B = P_{Bd}, \tag{4.57}$$

where η is the efficiency, P is the input power, and P_d is the power dissipated in the bolometer element.

If Γ_B is the input reflection coefficient of the bolometer mount whose efficiency is to be determined, and we assume that $\Gamma_A = 0$, the ratio of powers aborbed by the two bolometer mounts or assemblies, (assuming a matched generator) is

$$\frac{P_A}{P_B} = \frac{1}{1 - |\Gamma_B|^2} = \frac{(\rho_B + 1)^2}{4\rho_B}. \tag{4.58}$$

The efficiency of the second bolometer mount is

$$\eta_B = \frac{P_A}{P_B}\frac{P_{Bd}}{P_{Ad}}\ \eta_A = \frac{(\rho_B + 1)^2}{4\rho_B}\frac{P_{Bd}}{P_{Ad}}\eta_A, \tag{4.59}$$

where ρ_B is the VSWR corresponding to $|\Gamma_B|$.

An error in measuring ρ_B will cause an error in determining η_B, but fortunately the error is small in most practical cases. For example, if ρ_B is determined to be 1.20 with an accuracy of ± 2 percent, the corresponding error in η_B is approximately ± 0.2 percent.

d. Discussion of Errors

An accurate knowledge of the efficiency of bolometer mounts used for microwave power measurement is essential to accurate power measurement. For this reason, it is felt that a detailed discussion of the error in measuring efficiency is desirable.

Certain sources of error appear to be common to most measurements at high frequency. Among these are instability of oscillators and amplifiers, unwanted frequency modulation (FM), spurious amplitude modulation (AM) and harmonics in the generator output, pulling of the oscillator by changes in loading, erratic or unknown detector characteristics, errors in measuring the detector output, impedance mismatches at junctions, and mechanical instability of the components. Error from these sources is minimized by careful instrumentation and the use of recognized good practice in measurement techniques. For example, the stability of electronic equipment is improved by using voltage-stabilized power supplies, phase locking the frequency, and by avoiding large ambient temperature variations. Oscillator pulling is minimized by the use of nonreciprocal transmission-line elements or attenuator pads

with at least 20-dB attenuation. Unwanted FM is reduced by careful modulation practices or by the use of high-Q transmission cavities to attenuate undesired side bands. Parasitic oscillations, causing spurious AM, can be eliminated by usual procedures, e.g., damping, shielding; and minimizing feedback. Low-pass filters are used to reduce the harmonic output of generators. Detectors can be calibrated before use or the need for known detector characteristics may be avoided by use of calibrated attenuators. Matching transformers can be used to reduce impedance mismatches, and careful attention to reducing movement of the components will reduce mechanical instability.

After the above precautions are taken, observations should be made to verify the desired conditions. For example, the generator output can be observed with a spectrum analyzer to verify the reduction in unwanted FM and spurious AM. The oscillator-output amplitude and frequency can be monitored during load changes to observe pulling, and the detector output can be monitored with a continuous recorder to observe system stability.

Additional sources of error, which can be minimized by careful instrumentation and experimental procedure, are instability of the bolometer bias supply, inaccuracy of resistance measurement, mechanical irregularities in the slotted section and traveling probe, excessive coupling, and incorrect position of the probe. The use of heavy-duty, low-discharge storage batteries or solid state voltage reference sources will generally provide a stable bias supply.

Resistances R_1, R_2, and R_3 are measured at direct current and assumed to be the same at UHF or microwaves. It was pointed out by Kerns (1949), and can be seen from eq. (4.42), that even if the dc resistances are multiplied by a constant real factor, there will be no error in efficiency. The effect of random errors in resistance measurement upon the efficiency is the same as the random errors in VSWR measurements, discussed in section b. It was seen that an error in VSWR between the limits ± 0.2 percent will produce an error in efficiency between the limits of approximately ± 1 percent.

Resistance measurements between 100 and 300 ohms can be made with an accuracy of approximately ± 0.05 percent with a good Wheatstone bridge. The corresponding error in efficiency would be approximately ± 0.25 percent.

The choice of a slotted section and traveling probe is important in adjusting Γ_G and Γ_2 for minimum value, and in approximating the assumed uniform, lossless line or waveguide.

The error caused by excessive probe coupling is difficult to evaluate analytically (see eqs. (4.46) and (4.47)). However, it is possible to determine experimentally when the probe is sufficiently decoupled by making a series of efficiency measurements, each with a diminishing value of probe coupling. When there is no further appreciable change in the measured efficiency, the probe has been sufficiently withdrawn. Another method of checking the effect of probe coupling consists in making two efficiency measurements, one with the probe set to the position for maximum response corresponding to a bolometer resistance R_1, and the other with the probe set to the position for maximum response when the bolometer resistance is R_3. If nothing else is changed, the two probe positions are separated by approximately $\lambda/4$, so that the phase of the reflection from the load as seen at the probe position differs by approximately 180 degrees in the two cases. An example of this method is given in table 4-1, where it is assumed that the average of the two efficiency measurements closely approximates the correct efficiency with the probe sufficiently decoupled. This assumption was found to be valid for small variations in efficiency.

It is possible to evaluate the effect of certain sources of error analytically. The error in measurement of the relative voltage output of the probe, the incorrect positioning of the probe, the generator and load mismatch, and the curvature of the input reflection coefficient locus can be taken into account if the resulting error in the efficiency is small.

If ε_1, ε_2, and ε_3 are the errors made in measuring the probe relative voltages E_{P1}, E_{P2}, and E_{P3}, respectively, the error in efficiency from this source alone is approximately

$$\varepsilon \simeq \frac{-1}{K_1 - K_3}\left[\frac{K_1(1 - K_3)}{(K_1 - 1)}(\varepsilon_1 - \varepsilon_2) + \frac{K_3(K_1 - 1)}{(1 - K_3)}(\varepsilon_2 - \varepsilon_3)\right]. \tag{4.60}$$

If the individual errors lie within the range indicated by $|\varepsilon_1| = |\varepsilon_2| = |\varepsilon_3| \leq \varepsilon'$, the maximum error in efficiency would be less than

$$\varepsilon = \pm \frac{2K_1(1 - K_3)}{(K_1 - 1)(K_1 - K_3)}\varepsilon' \text{ or } \varepsilon = \pm \frac{2K_3(K_1 - 1)}{(1 - K_3)(K_1 - K_3)}\varepsilon', \tag{4.61}$$

whichever is largest. A graph of this relationship is shown in figure 4-18. Using a 200-ohm barretter, the limiting values of K_1 and K_3 were determined to be approximately 1.33 and 0.75. Referring to figure 4-18, with ε' assumed equal to ± 0.1 percent, the error in efficiency would be less than ± 0.4 percent. As this is a random error, improved accuracy can be obtained by averaging the results of a number of measurements.

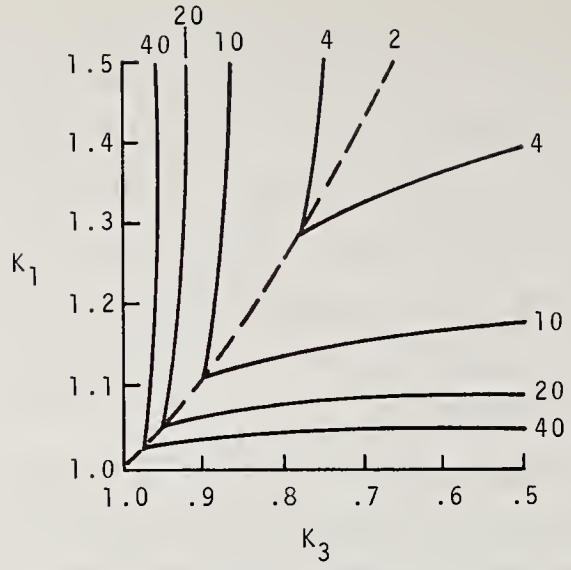

Figure 4-18. Factor by which the random error in measuring the relative output voltage of the probe is multiplied in order to obtain the corresponding error in efficiency.

An analysis of the error in efficiency caused by generator and load mismatch, curvature of the reflection coefficient locus, and incorrect probe position yields, after some manipulation, a correction factor to apply to eq. (4.51). It is

$$\zeta_2 \simeq \left\{1 + \left[\left(\frac{1-K_3}{K_1-K_3}\right)\frac{\alpha^2}{2K_1} + \left(\frac{K_1-1}{K_1-K_3}\right)\frac{(\delta+\alpha)^2}{2K_3} + \frac{\delta^2}{2}\frac{(K_1-1)(1-K_3)}{(K_1-K_3)^2} + \frac{(1-K_1K_3)}{(K_1-1)(1-K_3)}|\Gamma_2|\cos\psi_2\right.\right.$$
$$\left. - \frac{1}{(K_1-1)}|\Gamma_2|\cos(\psi_2-\alpha) + \frac{1}{(1-K_3)}|\Gamma_2|\cos(\psi_2-\delta-\alpha) - \frac{K_1(1-K_3)}{(K_1-K_3)}|\Gamma_G|\cos(\psi_G+\alpha)\right.$$
$$\left.\left. - \frac{K_3(K_1-1)}{(K_1-K_3)}|\Gamma_G|\cos(\psi_G+\delta+\alpha)\right]\right\} \tag{4.62}$$

where ψ and ψ_2 are the angular arguments of Γ_G and Γ_2, respectively, and α represents twice the angular error ($2\beta\Delta\ell$) in setting the probe to its correct position. ($\Delta\ell$ is the distance the probe position is in error.)

In the derivation of eq. (4.62) approximations were made (very small higher-order terms were neglected), assuming that $|\Gamma_G| < 0.005$, $|\Gamma_2| < 0.005$, $\delta < 0.1$, and $\alpha < 0.1$. The magnitude of the error represented by eq. (4.62) can be illustrated by considering some of the sources of error separately. For example, if $\delta = \alpha = 0$,

$$\zeta_2 \simeq 1 - |\Gamma_G|\cos\psi_G + |\Gamma_2|\cos\psi_2. \tag{4.63}$$

If $|\Gamma_G| = |\Gamma_2| = 0.005$, the total mismatch error lies between the limits ± 1 percent.

If $\Gamma_G = \Gamma_2 = 0$,

$$\zeta_2 \simeq 1 + \frac{1}{2(K_1 - K_3)}\left[\left(\frac{1 - K_3}{K_1}\right)\alpha^2 + \left(\frac{K_1 - 1}{K_3}\right)(\delta + \alpha)^2 + \frac{(K_1 - 1)(1 - K_3)}{(K_1 - K_3)}\delta^2\right]. \qquad (4.64)$$

A graph of the effect of changing the probe position upon the calculated efficiency is shown in figure 4-19 for $K_1 = 1.0676$, $K_3 = 0.826$, and $\delta = 5°$.

If $\Gamma_G = \Gamma_2 = \alpha = 0$, eq. (4.62) reduces to eq. (4.53), as represented by figure 4-16.

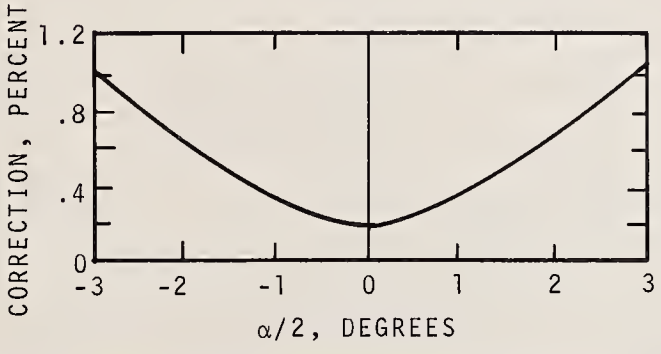

Figure 4-19. Effect of varying probe position upon the efficiency correction according to equation (4.64).

e. Experimental Results

The efficiencies of two commercially available bolometer mounts were measured at 600, 1,000, 2,000, and 3,000 MHz. The efficiency of a commercially available tunable bolometer mount (A) was measured first, and then the efficiency of a commercially available bolometer mount (B) was determined from comparative power measurements. The data obtained in a typical measurement of the efficiency of a bolometer mount is shown in table 4-1. It was found that the efficiency of the tunable bolometer mount remained at approximately 96 percent over the above frequency range, while the efficiency of mount B decreased with rising frequency, as shown in figure 4-20. Because only one of each of the two types of mounts was investigated, the measured efficiencies are not necessarily representative of these types of bolometer mounts.

Table 4-1. Typical efficiency measurement at 1,000 MHz.

K	R_1 = 150 ohms		R_1 = 250 ohms	
	R_a	E_{pa}	R_a	E_{pa}
1----------	150.0	1.270	250.0	1.277
2----------	200.0	1.119	200.0	1.155
3----------	250.0	1.000	150.0	1.000

IN EACH CASE, THE PROBE WAS IN POSITION FOR MAXIMUM RESPONSE WHEN $R = R_1$.

$C = 16.00$ (CALCULATED FROM eq (4))

$\eta = 0.946$ (MEASURED WHEN R_1 = 150 ohm)

$\eta = 0.916$ (MEASURED WHEN R_1 = 250 ohm)

$\eta = 0.948$ (AVERAGE OF ABOVE TWO VALUES)

$\eta_{P-B} = 0.988$ (MEASURED)

$C_1 = 1.002$ (CORRECTION FOR LOCUS CURVATURE)

$\eta_\lambda = 0.962$ ((MOUNT A) CALCULATED FROM eq (18))

$P_{Ad} = 0.807$ mw,

$P_{Bd} = 0.823$ mw,

$\rho_B = 1.020$ (MEASURED)

$\eta_B = 0.981$ ((MOUNT B) CALCULATED FROM eq (21)).

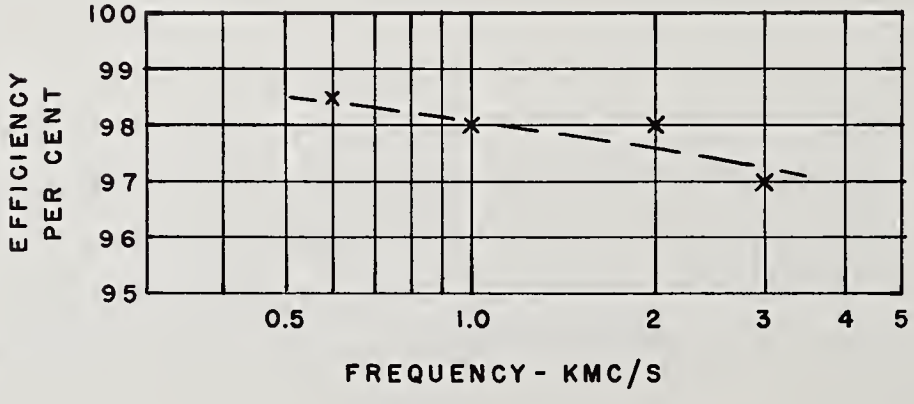

Figure 4-20. Measured efficiency of a coaxial bolometer mount B.

Table 4-2. Estimate of limits of error in a single efficiency measurement.

PRINCIPAL SOURCES OF ERROR	APPROXIMATE LIMITS OF ERROR IN EFFICIENCY
	%
MEASUREMENT OF ηP-B	±0.5
MEASUREMENT OF PROBE VOLTAGE	± .4
MEASUREMENT OF RESISTANCES	± .2
GENERATOR MISMATCH	± .1
LOAD MISMATCH	± .1
ESTIMATED LIMITS OF ERROR IN SINGLE EFFICIENCY MEASUREMENT OF TUNABLE BOLOMETER MOUNT	±1.3
MEASUREMENT OF POWER	±0.2
MEASUREMENT OF VSWR	± .1
ESTIMATED LIMITS OF ERROR IN SINGLE EFFICIENCY MEASUREMENT OF UNTUNED BOLOMETER MOUNT	±1.6

An approximate evaluation of the error in measuring efficiency is given in table 4-2. It represents an estimate of the limits of error in a single measurement of efficiency. The actual error can be considerably less than this, if the effect of random errors is reduced by averaging the results of a number of measurements. A further reduction of error could be obtained by use of better equipment and imrpoved measuring techniques.

f. Conditions for Linear Γ_1-Locus

It will be shown that the locus of the input voltage reflection coefficient of a lossless, tuned, linear, passive, two-terminal-pair network terminated in loads having real reflection coefficients is a straight line passing through the origin.

The lossless condition requires that[17]

$$|S_{11}| = |S_{22}| = S$$

$$|S_{12}|^2 = 1 - |S_{11}|^2 = 1 - |S_{22}|^2 \equiv 1 - S^2$$

$$2\psi_{12} = \psi_{11} + \psi_{22} \pm \pi, \tag{4.65}$$

where ψ represents the angular argument of a scattering coefficient.

[17] See section 3.3c, and assume $Z_{01} = Z_{02}$.

The input reflection coefficient of a reciprocal two-terminal-pair network terminated in a load having a real reflection coefficient $|\Gamma_L|$, is from eq. (3.10),

$$\Gamma = S_{11} + \frac{S_{12}^2|\Gamma_L|}{1 - S_{22}|\Gamma_L|}. \tag{4.65}$$

Because the network is matched ($\Gamma = 0$) when terminated in a load having a reflection coefficient Γ_{L2},

$$S_{11} = - \frac{S_{12}^2|\Gamma_{L2}|}{1 - S_{22}|\Gamma_{L2}|}. \tag{4.66}$$

Combining eq. (4.65) and eq. (4.67),

$$Se^{j\psi_{11}} = S^2|\Gamma_{L2}|e^{j(\psi_{11}+\psi_{22})} - (1 - S^2)|\Gamma_{L2}|e^{j2\psi_{12}} \tag{4.67}$$

or

$$Se^{j\psi_{11}} = |\Gamma_{L2}|e^{j(\psi_{11}+\psi_{22})}. \tag{4.68}$$

It is evident that $S = |\Gamma_{L2}|$ and $\psi_{22} = 0$ for the above lossless, tuned, two-terminal-pair network. Substituting the results of eq. (4.65) and eq. (4.68) in eq. (4.66), the input reflection coefficient is

$$\Gamma = \frac{|\Gamma_{L2}| - |\Gamma_L|}{1 - |\Gamma_{L2}\Gamma_L|} e^{j\psi_{11}} \tag{4.69}$$

As $|\Gamma_L|$ varies, the locus of Γ is a straight line passing through the origin.

It should be noted that the above conditions imposed upon the network (lossless, matched input when terminated in a load having the real reflection coefficient Γ_{L2}) are sufficient to produce a linear input reflection coefficient locus passing through the origin, but are not necessary. The amount of locus curvature is not necessarily an indication of the amount of loss, because it is possible to obtain a straight line locus with a lossy network having $\psi_{22} = 0$.

5. Impedance-Reflection Coefficient

5.1. Introduction

The accurate measurement of impedance or of reflection coefficient is easier in rectangular waveguide of convenient dimensions (such as 0.4" x 0.9" inside, or WR-90) than in coaxial waveguide. Rigid, high-quality components are readily available, and the absence of a center conductor and supporting insulators makes it easy to slide terminations inside a rectangular waveguide.

The development of an adjustable sliding termination for rectangular waveguide is described in section 5.2. It is an improvement over previous designs and has proven useful in adjusting tuned reflectometers and in other measurement applications.

The quarter wavelength short-circuited section of waveguide is the most accurately known standard of reflection coefficient. It nominally has a reflection coefficient of unity, but due to wall losses, is a bit smaller. If the conductivity of the metal walls is known, the magnitude of the reflection coefficient can be calculated to very good accuracy. The absence of current flow across the joint minimizes dissipative loss in the waveguide joint. In other types of standards, this loss causes an error which is difficult to evaluate. The short-circuited section should be made from a single block of metal in order to eliminate any other joint losses. In section 5.3, formulas, graphs and conductivity data are presented to aid in designing, constructing, and evaluating the above type of reflection coefficient standard.

Research on different kinds of waveguide junctions for use in impedance measurements is described in section 5.4. It was found that adjustment of a tuner in one type of waveguide junction produced a squared VSWR response instead of the usual VSWR response. The use of directional couplers was found to give magnified response. (The ratio of maximum to minimum detector output equals k times the VSWR, where k is the magnifying factor.) By use of a tuner, the magnification factor can be varied and made as large as desired.

Applications of tuners in circuits for the measurement of reflection coefficient are described in section 5.5. A tuner was used to magnify the response of a phasable load reflectometer, and to magnify the difference between two loads alternately connected to a reflectometer. Finally, a reflectometer with two tuners was investigated and analyzed. This form of reflectometer, when used with a quarter wavelength short-circuit impedance standard has provided the basis for present-day calibrations of impedance standards at the U.S. National Bureau of Standards.

As was mentioned above, accurate impedance measurements are more difficult in coaxial line than in rectangular waveguide. Accordingly, the hybrid reflectometer, described in section 5.6, was developed. It consists almost completely of rectangular waveguide components except for the output section of waveguide, (which is coaxial) and the sliding loads, which must slide inside a section of coaxial line. Coaxial quarter wavelength short-circuit impedance standards are used. A waveguide-to-coaxial adapter connects the rectangular and the coaxial portions together. The hybrid principle makes it easy to adapt the existing tuned reflectometer for measurements in various types of waveguide other than those having rectangular or coaxial cross section.

Reflectometer tuning and sliding load techniques were developed to measure small reflections and losses in waveguide joints. The theory and technique are described in section 5.7, and experimental results are given for WR-90 (X-band) waveguide joints.

5.2. Adjustable Sliding Termination

a. Introduction

The adjustable sliding termination (A.S.T.) using a resistive vane which can rotate and slide relative to a sliding short-circuit in rectangular waveguide (Beatty, 1957), is particularly useful for fine tuning of reflectometers, as well as other applications. The design is applicable to lowest TE modes in uniconductor waveguides but is not readily adaptable to other forms such as coaxial line.

There are many measurement situations where a sliding load, having low reflections, is useful. One having high reflections, such as a sliding short-circuit is also useful. A sliding load which can be adjusted over a wide range of reflection coefficients,[1] ranging from zero to nearly unity, is even more useful.

For example, in tuning a reflectometer, one tunes for high directivity of the directional coupler by reducing the cyclical variations of the side arm output as the load is slid inside the output waveguide. If the load is adjustable, a more sensitive tuner adjustment is possible, because one can simultaneously approach a

[1] A resistive vane fastened to a rotating and sliding short-circuit in circular waveguide has been described (deRonde, 1957), and proposed as a variable standard of reflection coefficient. It is not possible to obtain complete cancellation of reflections, however.

"flat" response and zero response. It is possible by this technique to obtain effective directivities in excess of 100 decibels and thereby increase the accuracy of reflection coefficient measurements.

The adjustable sliding termination described here is superior in performance to previous ones. It can be adjusted for completely zero reflection as well as almost total reflection. It is simple in design and construction.

An adjustable sliding termination for rectangular waveguide was described by Grantham (1951). Several years later, a similar termination was produced commercially. That termination differed from its predecessor in details of construction of the dissipative element and the reflecting antenna. Both terminations were designed primarily to provide minimum reflection and could not be adjusted over a wide range. The commercial termination has a range of 1.005 to 1.15 in VSWR. The principle of the double slug tuner was used (Ellenwood and Ryan, 1953) to obtain an adjustable sliding termination with a somewhat greater range. An adjustable sliding termination having a wide range was described by Kato and Sakai (1955), but it was not possible to adjust this termination for cancellation of its reflections.

b. Principle of Operation

As shown in the diagram of figure 5-1, this termination slides inside a rectangular waveguide and consists of a short-circuiting piston to which is attached a dissipative strip supported by a dielectric rod, which can rotate and slide relative to the piston. The phase of the reflection from the strip can be varied by sliding the strip, while the magnitude of the net reflection from the short circuit can be varied by rotating[2] the strip. With independent control of these two motions, complete cancellation of reflections can be obtained. On the other hand, with the strip surface perpendicular to the electric field, minimum losses occur in the strip and almost perfect reflection is obtained. It is possible to adjust the termination to any intermediate condition, then to slide the entire assembly, to obtain any reflection coefficient desirable.

---

[2]An attenuator employing a resistive strip rotating in circular waveguide was described by Southworth (1950).

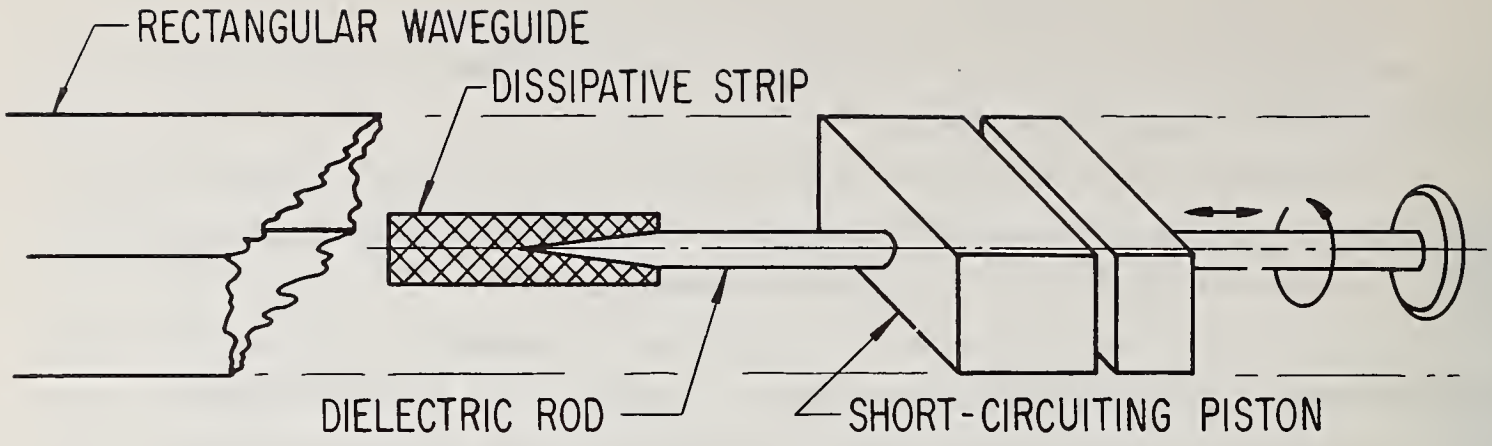

Figure 5-1. Essential features of termination.

c. Theory

Apparently, the analysis of the fields inside a rectangular waveguide containing an arbitrarily positioned dissipative strip has not been published. Lacking this basic information, a rigorous analysis of the action of this termination has not been attempted. An approximate study based upon microwave circuit theory is given below.

As shown in figure 5-2, the termination can be regarded as an attenuator terminated in a short-circuited line of variable length. In terms of the scattering coefficients S_{11}, S_{12}, and S_{22} of the attenuator, the input voltage reflection coefficient is[3]

$$\Gamma_1 = S_{11} - \frac{S_{12}^2}{S_{22} + e^{j2\beta\ell}}, \tag{5.1}$$

where $\beta = 2\pi/\lambda_G$, and λ_G equals the wavelength in the waveguide. The condition for cancellation of reflections ($\Gamma_1 = 0$) is

$$S_{12}^2 = S_{11}e^{j2\beta\ell}(1 + S_{22}e^{-j2\beta\ell}). \tag{5.2}$$

This condition can be readily realized, as will be shown. Normally, $|S_{11}|$ and $|S_{22}|$

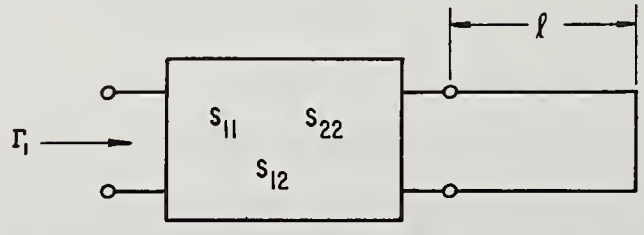

Figure 5-2. Approximate equivalent circuit representation.

[3]See for example, eq. (3.10).

are much less than unity, and the approximate condition for cancellation of reflections is

$$S_{12}^{\ 2} \simeq S_{11} e^{j2\beta\ell}. \tag{5.3}$$

Rotation of the strip will, in general, change both $|S_{12}^{\ 2}|$ and $|S_{11}|$. A typical variation of these quantities with θ (the angle between the electric field direction and the normal to the surface of the strip) is shown in figure 5-3(a). At the angle θc, the magnitudes of $S_{12}^{\ 2}$ and S_{11} are equal, and it is possible to obtain cancellation of reflections by sliding the strip, varying ℓ. If the strip is too short, $|S_{12}^{\ 2}|$ will not decrease to equal $|S_{11}|$, as shown in figure 5-3(b). However, it is possible to increase $|S_{11}|$ by adding a reflecting object at the end of the strip, so that cancellation of reflections can again be obtained as in figure 5-3(c).

Although this discussion of the cancellation of reflections is based upon the approximate condition of eq. (5.3), it should be noted that exact cancellation according to eq. (5.2) is possible under almost the identical conditions.

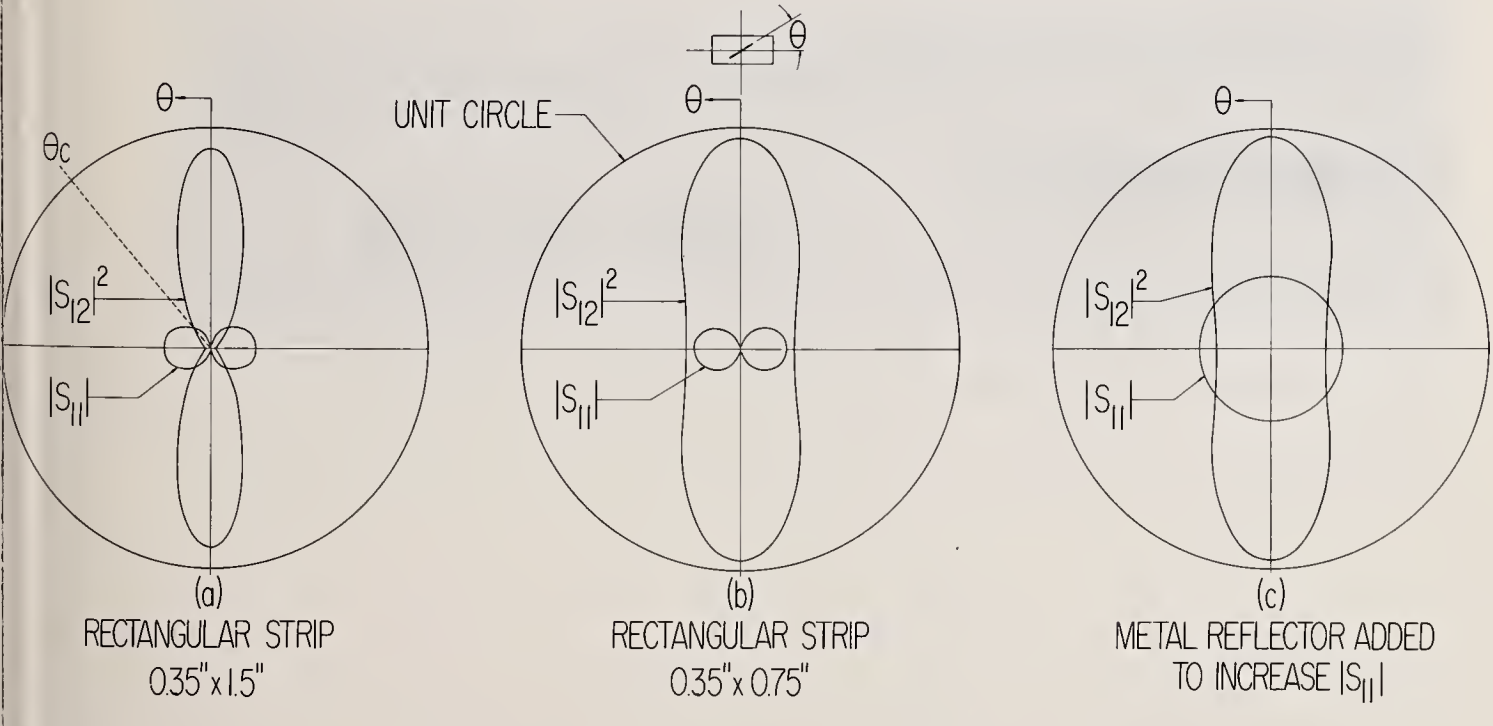

Figure 5-3. Dependence of $|S_{11}|$ and $|S_{12}^{\ 2}|$ upon rotation of thin rectangular strip; (a) rectangular strip 0.35 inch × 1.5 inches, (b) rectangular strip 0.35 inch × 0.75 inch, and (c) metal reflector added to increase $|S_{11}|$.

d. Design

A number of considerations can influence the design (Beatty, 1960) of the termination. If the primary need is for a reflection-free termination, with no need for a wide range of VSWR, it seems advisable to use a thicker strip of dissipative material such as Synthane. The extra thickness can give added strength to a long, tapered strip, which will require less rotation to achieve cancellation of reflection, and give a smoother adjustment which is less frequency sensitive than with shorter strips. Examples of A.S.T.'s for different sizes of waveguide are shown in figure 5-4, and a diagram of typical variation of $|S_{12}{}^2|$ and $|S_{11}|$ is shown in figure 5-5.

If a wide range of adjustment of VSWR is desired, a thin strip is required. IRC resistance strip may be used to obtain fairly high ranges, but a dissipative film on

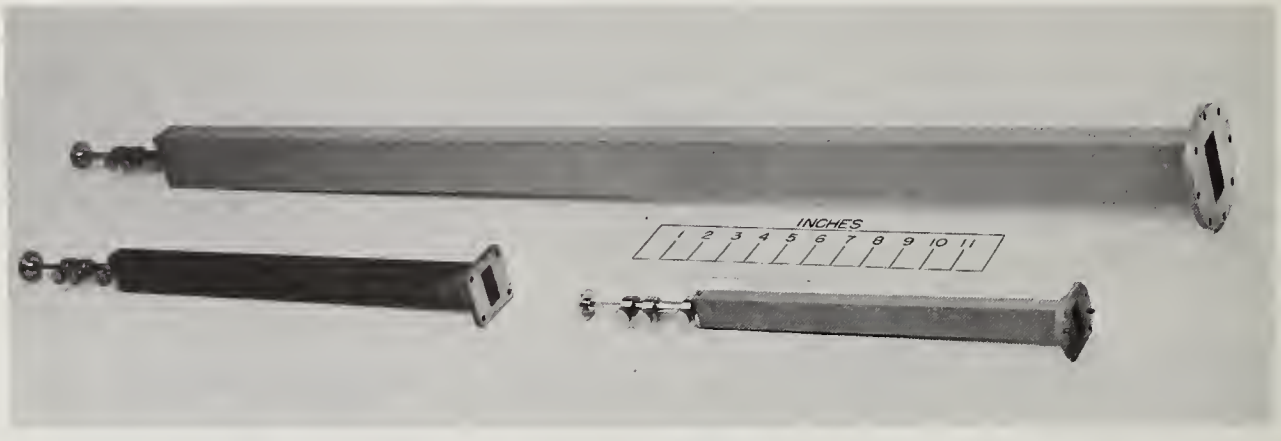

Figure 5-4. Adjustable sliding loads for different waveguide sizes.

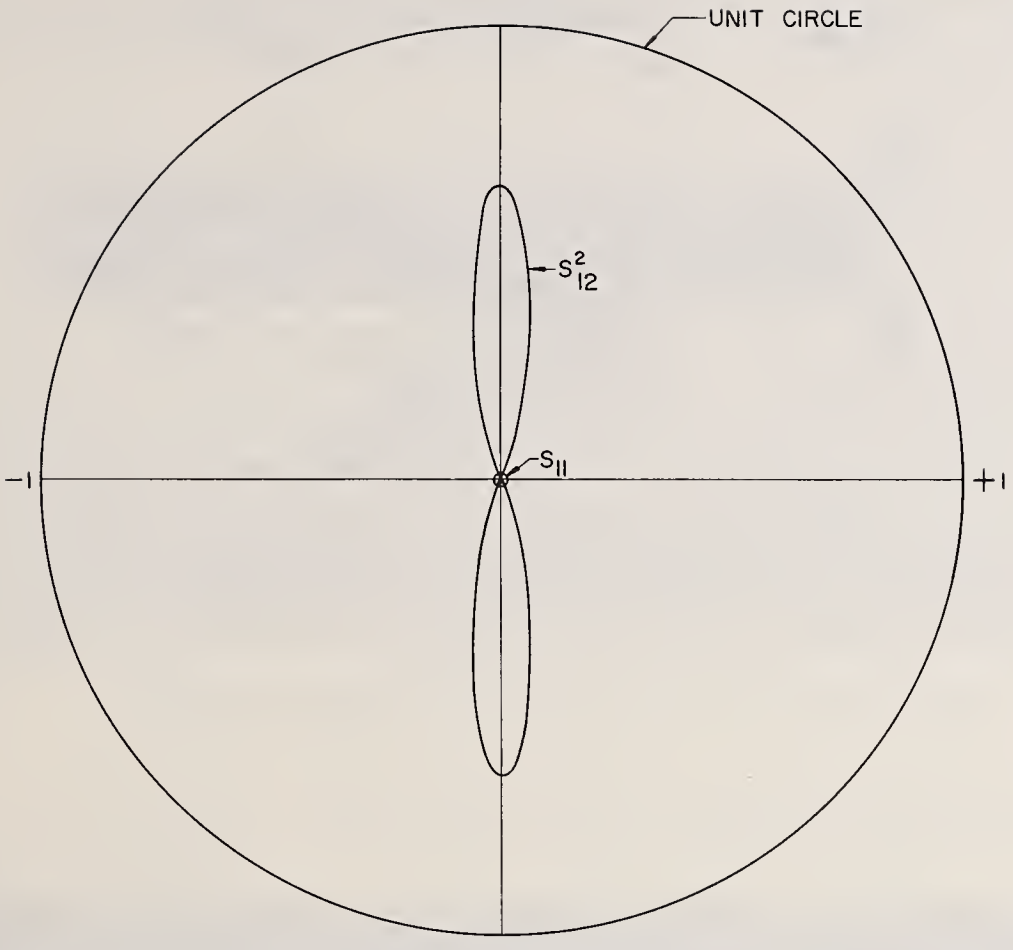

Figure 5-5. Variation of $|S_{11}|$ and $|S_{12}^2|$ with rotation of thick tapered strip.

a thin mica strip is capable of greater range. A thin film has little strength and it may be desirable to add a reflecting disk or rod as shown in figure 5-6. The disk or rod permits a shorter strip to be used, while retaining the ability to cancel reflections.

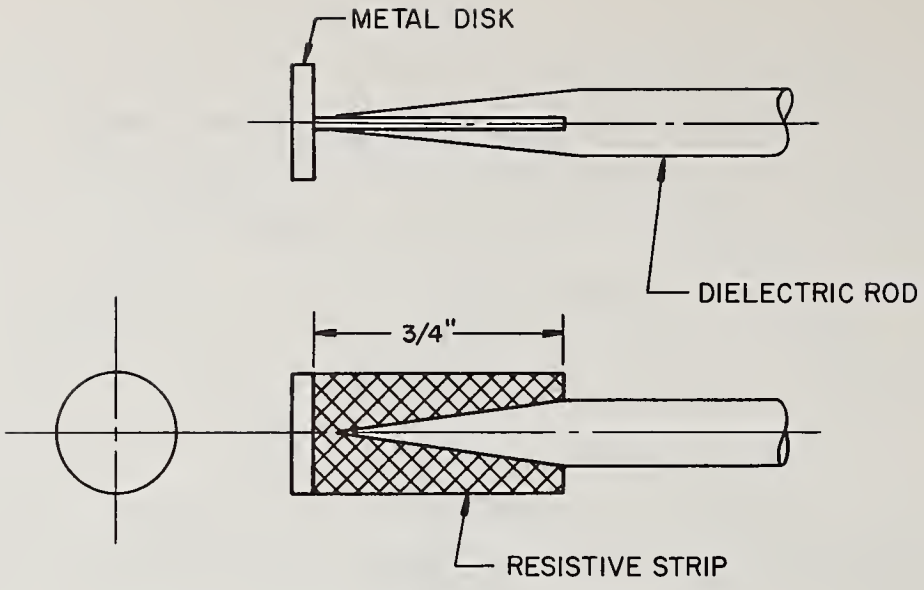

Figure 5-6. Short strip and reflecting disk.

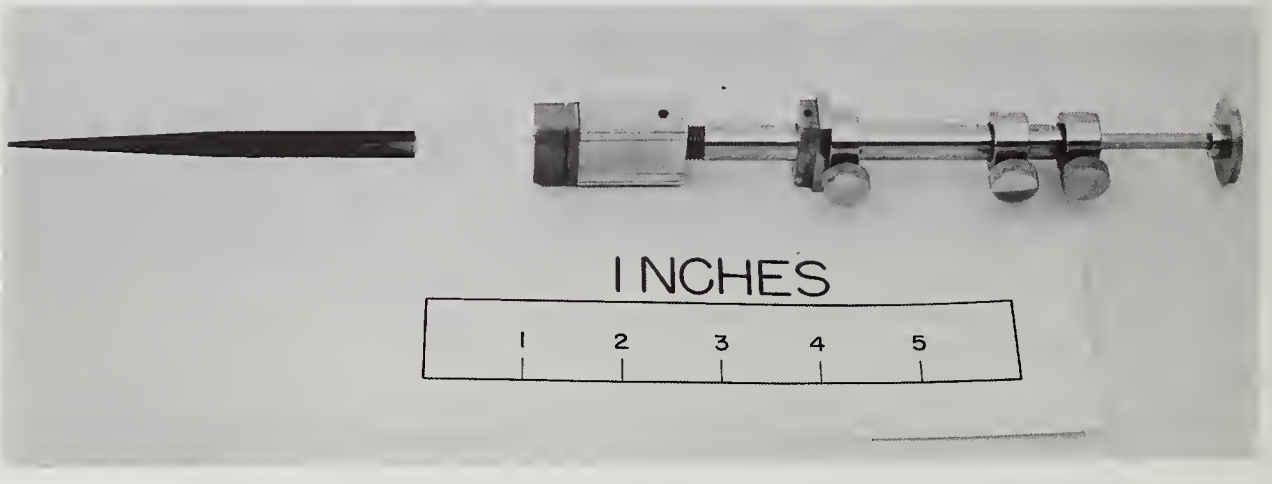

Figure 5-7. Mechanical controls permitting independent adjustment of rotation and sliding, with control locking.

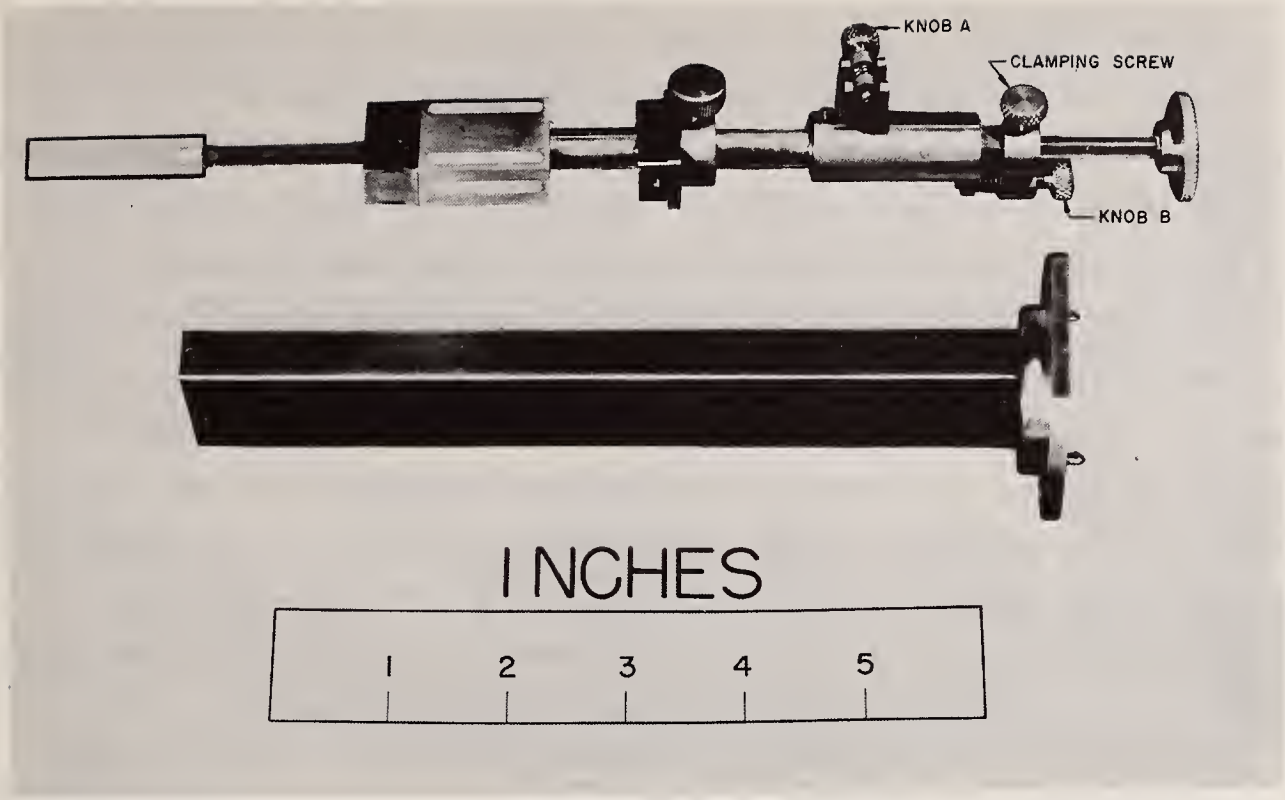

Figure 5-8. Mechanical controls permitting coarse manual adjustment and locking, followed by fine independent adjustments of rotation and sliding.

Control of the mechanical motion required may be achieved by the arrangements shown in figures 5-7 and 5-8.

Independent control of the sliding and rotation of the strip is achieved in both arrangements, but in figure 5-8, the strip may be rotated and slid by hand until the clamping screw is used, which clamps the dielectric rod supporting the strip so that it can only be moved by the limited fine adjustments A and B. One adjustment of sliding (knob A) and an independent adjustment of rotation (knob B) are provided.

An adjustable load having satisfactory performance over the recommended frequency range of WR-90 (X-band) waveguide was constructed, using a rectangular IRC resistance strip 200 ohms per square, 0.35 inch x 1.50 inches. The strip was not tapered, but mounted on a dielectric rod as was shown in figure 5-1.

5.3. Quarter-Wavelength Short-Circuit

a. Introduction

The purpose here is to derive equations and to present a graph (fig. 5-15) for the determination of the return losses of microwave impedance standards. It applies to impedance standards consisting of quarter-wavelength short-circuited sections of

rectangular waveguide or coaxial line (Beatty, 1967a) for which the conductivity is 10^7 mho/m (closely corresponding to platinum). The curves for 50-ohm coaxial line are each labeled with the appropriate inner diameter of outer conductor. The curves for rectangular waveguide are each labeled with the appropriate WR (USA) number except for two WG (British) numbers and two IEC-R (International) numbers for which there are no WR equivalents. All of the IEC standard sizes of rectangular waveguide are covered. See Brady (1967) for cross-referenced waveguide designations. The return loss L_S corresponding to a given conductivity σ may easily be calculated by dividing the return loss read from the graph by the square root of the given conductivity normalized to 10^7 mho/m. For example, if one reads L_S = 0.020 dB, and the normalized conductivity is 4(4×10^7 mho/m, closely corresponding to gold), the return loss for an impedance standard made of gold (or gold-plated) is $0.020 \div \sqrt{4} = 0.010$ dB.

The bases for figure 5-15 are the following formulas. By definition, the return loss is

$$L_S = 20 \log_{10} \frac{1}{|\Gamma_S|} \text{ dB} \tag{5.4}$$

where $|\Gamma_S|$ is the magnitude of the reflection coefficient of the impedance standard. For a lossless quarter-wavelength short-circuit, $|\Gamma_S|$ is ideally unity.

b. Coaxial Line

For a short-circuited quarter-wavelength section of air-dielectric coaxial line[4] operating in the TEM mode, it can be shown[5] as follows that

$$|\Gamma_S| \cong 1 - \frac{2R_{EP}}{Z_0}\left[1 + \frac{60\lambda}{4bZ_0}\left(1 + \frac{b}{a}\right)\right], \tag{5.5}$$

where

$R_{EP} = \frac{Z_0}{120\pi\sigma\delta}$ = resistance of end plate,[6]

$Z_0 = 60 \ln \frac{b}{a}$ = characteristic impedance,

a = outer diameter of inner conductor,

b = inner diameter of outer conductor,

σ = conductivity of metal,

[4]It is assumed that the same metal is used for inner and outer conductors and for the short-circuiting end plate.

[5]Equation (5.5) is equivalent to eq. (2) of Beatty and Yates (1969). (Note that b and a refer to diameters, not radii).

[6]See, for example, p. 70 of Jackson (1951).

δ = skin depth in metal = $\frac{1}{\sqrt{\pi f \mu \sigma}}$, and

μ = permeability of metal ($4\pi \times 10^{-7}$ H/m if relative permeability μ_r is unity).

Consider first the relationship between the magnitude of the reflection coefficient $|\Gamma|$ and the incident, reflected, and dissipated powers P_I, P_R, and P_D, respectively. The incident and reflected wave amplitudes a and b are indicated in figure 5-9.

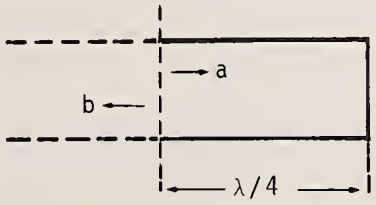

Figure 5-9. Schematic diagram of quarter-wavelength section of short-circuited waveguide.

By definition,

$$|\Gamma_S|^2 = \left|\frac{b}{a}\right|^2 = \frac{P_R}{P_I} = \frac{P_I - P_D}{P_I} = 1 - \frac{P_D}{P_I}, \tag{5.6}$$

where

P_R = reflected power,

P_I = incident power, and

P_D = dissipated power.

It follows that

$$|\Gamma_S| = \sqrt{1 - \frac{P_D}{P_I}} \cong 1 - \frac{P_D}{2P_I}. \tag{5.7}$$

The ratio of dissipated to incident power is calculated as follows. For a single propagating mode in lossless waveguide of usual cross sections, the wall current distribution is well-known. The resistance of the metal walls to the current flow may be calculated corresponding to a given value of the skin depth δ. One then calculates the dissipative loss by integrating the I^2R losses. The expressions for P_D and P_I will both contain an I_M (maximum current) term which cancels out in the ratio. It is of course assumed that the losses are small enough so that the perturbation of the lossless current distribution can be neglected.

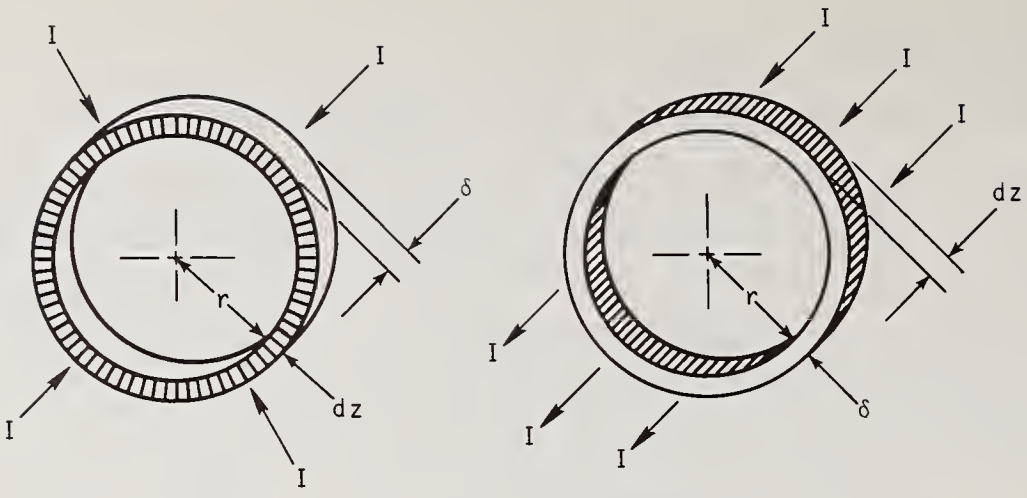

Figure 5-10. (a) Radial and (b) annular current flow in circular rings.

At high frequencies, current flows in the "skin" of a metal. The resistance R of a strip of metal is[7]

$$R = \frac{\ell}{\sigma A}, \tag{5.8}$$

where ℓ is the length in the direction of current flow, σ is the conductivity of the metal, and A is the area of the cross section through which the current flows. The case of figure 5-10(a) corresponds to the short-circuiting end plate of a coaxial line. The resistance between the inner and outer conductors is

$$R_{EP} = \frac{1}{\sigma}\int_a^b \frac{dr}{2\pi r\delta} = \frac{1}{2\pi\sigma\delta}\,\ell n\,\frac{b}{a}. \tag{5.9}$$

The loss in the metal can now be calculated, assuming the current is distributed in the known manner for the TEM-mode as shown in figure 5-11.

[7]See, for example, Michels (1961), p. 982.

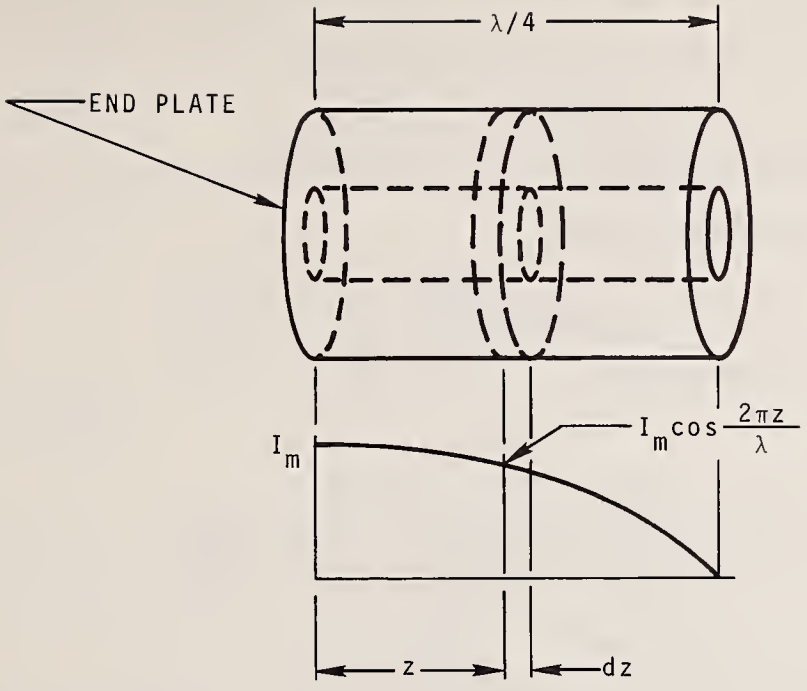

Figure 5-11. Assumed current distribution in quarter wavelength short-circuited section of coaxial line.

The I^2R loss P_{EP} in the end plate is

$$P_{EP} = I_M^2 R_{EP} = \frac{I_M^2}{2\pi\sigma\delta} \ln \frac{b}{a}. \tag{5.10}$$

The I^2R loss P_{OC} in the outer conductor is calculated using the element of figure 5-10(b).

$$P_{OC} = \int_0^{\lambda/4} \left(I_M \cos \frac{2\pi Z}{\lambda}\right)^2 \left(\frac{dz}{\pi b \sigma \delta}\right) = \frac{I_M^2}{2\pi b \sigma \delta} \cdot \frac{\lambda}{4}. \tag{5.11}$$

In a similar way, the loss P_{IC} in the inner conductor is

$$P_{IC} = \int_0^{\lambda/4} \left(I_M \cos \frac{2\pi Z}{\lambda}\right)^2 \left(\frac{dz}{\pi a \sigma \delta}\right) = \frac{b}{a} P_{OC}. \tag{5.12}$$

The total dissipated power is

$$P_D = P_{EP} + P_{OC} + P_{IC} = \frac{I_M^2}{2\pi\sigma\delta} \left\{ \ln \frac{b}{a} + \frac{\lambda}{4} \left(\frac{1}{a} + \frac{1}{b}\right) \right\}. \tag{5.13}$$

The incident current I is one-half I_M. It follows that the incident power is

$$P_I = \frac{I_M^2 Z_0}{4}. \tag{5.14}$$

The magnitude of the reflection coefficient $|\Gamma_S|$ of the short-circuited quarter wavelength section is obtained from eqs. (5.7), (5.13), and (5.14). It is

$$|\Gamma_S| \cong 1 - \frac{1}{\pi\sigma\delta Z_0}\left(\ell n\,\frac{b}{a} + \frac{\lambda}{4}\left(\frac{1}{a} + \frac{1}{b}\right)\right). \tag{5.15}$$

The above equation may also be written

$$|\Gamma_S| \cong 1 - \frac{1}{60\pi\sigma\delta\sqrt{\frac{\mu_r}{\varepsilon_r}}}\left(1 + \frac{60}{Z_0}\sqrt{\frac{\mu_r}{\varepsilon_r}}\cdot\frac{\lambda}{4b}\left(1 + \frac{b}{a}\right)\right), \tag{5.16}$$

or

$$|\Gamma_S| \cong 1 - 2\,\frac{R_{EP}}{Z_0}\sqrt{\frac{\varepsilon_r}{\mu_r}}\left(1 + \frac{60}{Z_0}\sqrt{\frac{\mu_r}{\varepsilon_r}}\cdot\frac{\lambda}{4b}\left(1 + \frac{b}{a}\right)\right). \tag{5.17}$$

This reduces to eq. (5.5) if $\mu_r = \varepsilon_r = 1$.

In the following example the components of power loss are individually calculated. Suppose that $f = 4 \times 10^9$ Hz, $\sigma = 10^7$ mho/m, $\mu_r = \varepsilon_r = 1$, $\mu = 4\pi \times 10^{-7}$ H/m, $Z_0 = 50\ \Omega$, $a = 0.304$ cm, $b = 0.70$ cm, and $I_M = 1$A. We calculate the skin depth $\delta = 2.52 \times 10^{-4}$ cm, $R_{EP} = 0.00527\ \Omega$, $P_{EP} = 5.27$ mW, $P_{OC} = 16.9$ mW, $P_{IC} = 38.9$ mW, $P_D = 61.1$ mW, and $P_I = 12.5$ W. From eq. (5.7),

$$|\Gamma_S| \cong 1 - \frac{61.2}{25.0}\cdot 10^{-3} = 0.99755,$$

and from eq. (5.4), $L_S = 0.0213$ dB. These results agree with Beatty and Yates (1969), and show in addition the distribution of losses in end plate, inner and outer conductors.

In the event that the attenuation constant α of the line is more easily determined than the conductivity σ, the reflection coefficient is determined as follows.

The total loss in the inner and outer conductors may be written in terms of the attenuation constant α of the coaxial line. First consider that the end plate is lossless, and we can write

$$\Gamma = e^{-2\gamma\ell}, \tag{5.18}$$

or

$$|\Gamma_S| = e^{-2\alpha\ell} \cong 1 - 2\alpha\ell. \tag{5.19}$$

Similarly

$$|\Gamma_S|^2 \cong 1 - 4\alpha\ell. \tag{5.20}$$

Comparison with eq. (5.7) shows that

$$\frac{P_{OC} + P_{IC}}{P_I} = 4\alpha\left(\frac{\lambda}{4}\right) = \alpha\lambda. \tag{5.21}$$

We can regard the losses in the end plate P_{EP} as corresponding to an equivalent length of line ℓ_E such that

$$\frac{P_{EP}}{P_I} = 4\alpha\ell_E. \tag{5.22}$$

It then follows that

$$|\Gamma_S| \cong 1 - 2\alpha\left(\frac{\lambda}{4} + \ell_E\right). \tag{5.23}$$

We can determine ℓ_E from eqs. (5.22), (5.21), (5.10), (5.11), and (5.12). It is

$$\ell_E = \frac{Z_0}{60}\sqrt{\frac{\epsilon_r}{\mu_r}} \cdot \frac{b}{1 + b/a}. \tag{5.24}$$

In the previous example, it equals 0.177 cm, and $\alpha = 0.596 \times 10^{-3}$ Neper/cm = 15.8 dB per 100 feet.

c. Rectangular Waveguide

For a quarter guide wavelength, short-circuited section of rectangular waveguide operating in the dominant $TE_{1,0}$ mode, it can be shown as follows that the magnitude of the reflection coefficient is (Beatty and Yates, 1969),

$$|\Gamma_S| \cong 1 - 2\alpha\left(\frac{\lambda_G}{4} + \ell_{EP}\right), \tag{5.25}$$

where

α = attenuation constant (Np/cm),

λ_G = guide wavelength (cm),

ℓ_{EP} = length of waveguide having same loss as short-circuiting plate (cm), and

$$\ell_{EP} = b \cdot \frac{\left(\frac{\lambda}{\lambda_G}\right)^2}{1 + \frac{2b}{a}\left(\frac{\lambda}{\lambda_C}\right)^2}. \tag{5.26}$$

One proceeds in the same way used previously for coaxial line, calculating the ratio of dissipative to incident power and substituting into eq. (5.7) to obtain eq. (5.25).

The distribution of electric and magnetic fields in the $TE_{1,0}$ mode for a wave incident upon a quarter guide wavelength short-circuited section of rectangular waveguide is shown in figure 5-12 and the corresponding wall current distribution is shown in figure 5-13.

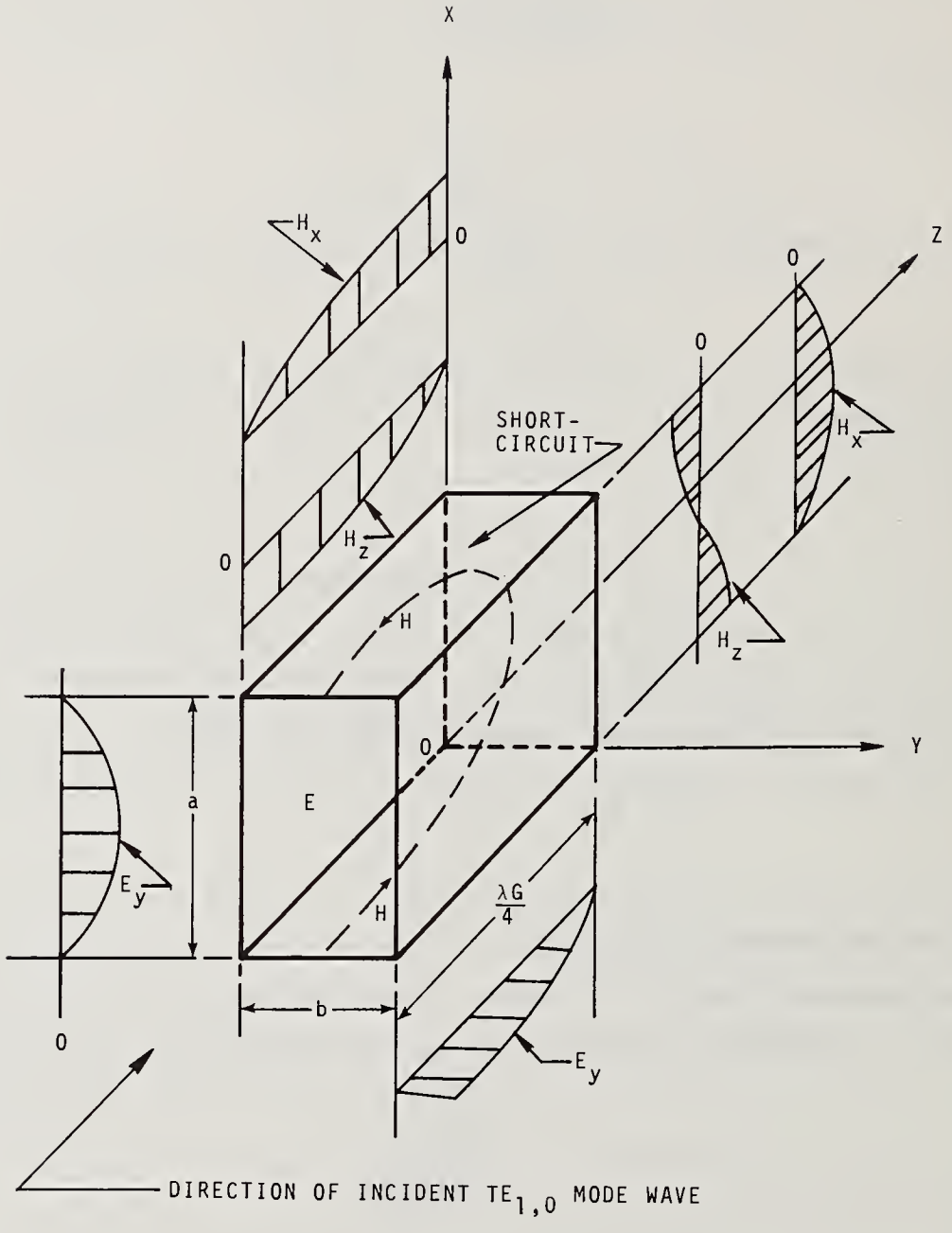

Figure 5-12. Electric and magnetic fields in quarter wavelength section of rectangular waveguide propagating $TE_{1,0}$ mode in +Z direction and short-circuited at Z = 0.

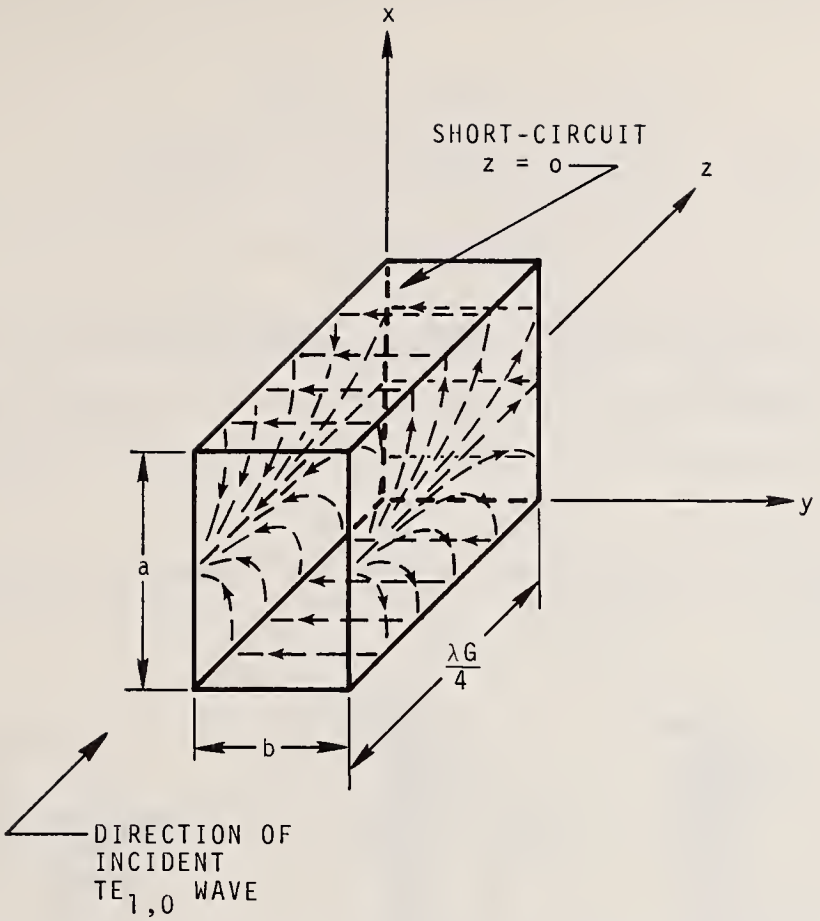

Figure 5-13. Wall currents in short-circuited quarter wavelength section of rectangular waveguide with incident $TE_{1,0}$ mode wave.

For a $TE_{1,0}$ mode, incident wave in +z direction, it can be shown that

$$\begin{cases} H_z = A\left[\cos\left(\frac{\pi x}{a}\right)\right](1 + \Gamma_z e^{j2\beta z})e^{-j\beta z} \\ H_x = j\frac{\beta}{K_c} A\left[\sin\left(\frac{\pi x}{a}\right)\right](1 - \Gamma_z e^{j2\beta z})e^{-j\beta z} \\ E_y = -j\frac{\beta}{K_c} Z_h A\left[\sin\left(\frac{\pi x}{a}\right)\right](1 + \Gamma_z e^{j2\beta z})e^{-j\beta z} \end{cases} \tag{5.27}$$

where

$$\beta = \frac{2\pi}{\lambda_G},\ K_c = \frac{\pi}{a},\ Z_h = -\frac{E_y}{H_x} = \frac{\omega\mu}{\beta},$$

and Γ_z = voltage reflection coefficient at z = 0 (-1 for short-circuit).

It is implicit in eq. (5.27) that sinusoidal time variation with angular frequency ω exists, and that μ is the permeability of the medium (usually air) within the waveguide. The factor A indicates the level of the excitation and for convenience

the rms value of the field strengths are denoted by E and H. The incident power P_I (at z = 0) is

$$P_I = \mathrm{Re} \int [E \times H^*] \cdot \vec{e}_z \, dx \, dy, \tag{5.28}$$

where $\vec{e}_z$ is the unit vector in the +z direction. Upon integration,

$$P_I = \left(\frac{\beta}{K_C}\right)^2 Z_h A^2 \frac{ab}{2}. \tag{5.29}$$

The waveguide walls are assumed to have high conductivity σ and small skin depth δ resulting in small losses which do not appreciably perturb the $TE_{1,0}$ mode fields. One may then calculate the small wall losses by integrating the I^2R losses in the metal.

In order to calculate the resistance to a current element, one uses the elements shown in figure 5-14.

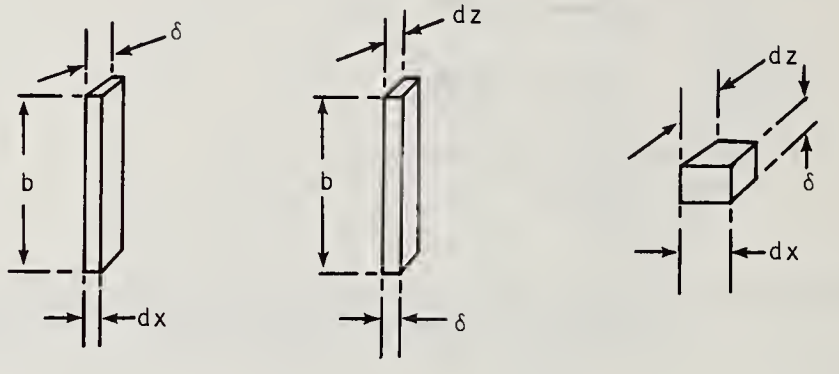

(a) $R = \frac{b}{\sigma \delta dx}$ (b) $R = \frac{b}{\sigma \delta dz}$ (c) $\begin{cases} R_x = \frac{dx}{\sigma \delta dz} \\ R_z = \frac{dz}{\sigma \delta dx} \end{cases}$

Figure 5-14. Elements used to calculate I^2R losses in (a) shorting plate, (b) narrow walls, and (c) broad walls.

It is convenient to write eq. (5.27) in the form

$$\begin{cases} H_Z = -2jA\left[\cos\left(\frac{\pi x}{a}\right)\right] \sin \beta z \\ H_x = 2j\left(\frac{\beta}{K_C}\right) A\left[\sin\left(\frac{\pi x}{a}\right)\right] \cos \beta z \\ E_y = -2\left(\frac{\beta}{K_C}\right) Z_h A\left[\sin\left(\frac{\pi x}{a}\right)\right] \sin \beta z. \end{cases} \tag{5.30}$$

One can now calculate the dissipated power as follows. The magnitude of the current density in the short-circuiting plate is

$$|J_{SP}| = |H_x| = 2\left(\frac{\beta}{K_C}\right) A\left(\sin\left(\frac{\pi x}{a}\right)\right). \tag{5.31}$$

The power P_{SP} dissipated in the short-circuiting plate is

$$P_{SP} = \int_o^a (|J_{SP}|dx)^2 \frac{b}{\sigma\delta dx} = 2\left(\frac{\beta}{K_C}\right)^2 A^2 \frac{ab}{\sigma\delta}. \tag{5.32}$$

The ratio of P_{SP} to P_I is

$$\frac{P_{SP}}{P_I} = \frac{1}{2\sigma\delta Z_h} = \frac{\pi}{\omega\mu\sigma\delta\lambda_G}. \tag{5.33}$$

The magnitude of the current density in the narrow walls is

$$|J_{NW}| = |H_Z| = 2A \sin \beta z. \tag{5.34}$$

The power P_{NW} dissipated in the side walls is

$$P_{NW} = 2\int_o^{\lambda_G/4} (|J_{NW}|dz)^2 \frac{b}{\sigma\delta dz} = A^2 \frac{b\lambda_G}{\sigma\delta}. \tag{5.35}$$

The ratio of P_{NW} to $2P_I$ is

$$\frac{P_{NW}}{2P_I} = \frac{\lambda_G}{4\left(\frac{\beta}{K_C}\right)^2 aZ_h\sigma\delta} = \frac{\pi\lambda_G^2}{2a^3\omega\mu\sigma\delta}. \tag{5.36}$$

The magnitudes of the x and z components of the current densities in the broad walls are

$$|J_x| = |H_z| = 2A\left(\cos\left(\frac{\pi x}{a}\right)\right) \sin \beta z$$

$$|J_z| = |H_x| = 2\left(\frac{\beta}{K_C}\right) A\left(\sin\left(\frac{\pi x}{a}\right)\right) \cos \beta z. \tag{5.37}$$

The power dissipated in the broad walls is

$$P_{BW} = 2\int_o^{x=a}\int_o^{Z=\lambda_G/4} \left((|J_x|dz)^2 \frac{dx}{\sigma\delta dz} + (|J_z|^2 dx) \frac{dz}{\sigma\delta dx}\right) = \frac{a\lambda_G A^2}{2\sigma\delta}. \tag{5.38}$$

The ratio of P_{BW} to $2P_I$ is

$$\frac{P_{BW}}{2P_I} = \frac{\lambda_G}{2bZ_h\sigma\delta}\left(1 + \left(\frac{K_C}{\beta}\right)^2\right). \tag{5.39}$$

The total power dissipated is

$$P_D = P_{SP} + P_{NW} + P_{BW}, \tag{5.40}$$

and the magnitude of the reflection coefficient of the short-circuit is

$$|\Gamma_S| = 1 - \frac{P_D}{P_I} \cong 1 - \frac{P_D}{2P_I}. \tag{5.7}$$

In the event that the attenuation constant α of the waveguide is known, it is convenient to use eqs. (5.25) and (5.26) which are derived as follows, assuming that (1) the short-circuiting plate and the waveguide walls are one continuous piece of metal having no lossy joints, and (2) the waveguide section is filled with a medium such as air whose electrical properties are not significantly different from those of a vacuum.

If we assume for the moment that there are no losses in the short-circuiting plate,

$$|\Gamma_W| = e^{2\alpha\left(\frac{\lambda_G}{4}\right)} \cong 1 - \alpha\frac{\lambda_G}{2} \cong 1 - \frac{P_{NW} + P_{BW}}{2P_I}. \tag{5.41}$$

Thus

$$\alpha \cong \frac{2}{\lambda_G} \cdot \frac{P_{NW} + P_{BW}}{2P_I}, \tag{5.42}$$

or from eqs. (5.36) and (5.39) it follows that

$$\alpha = \frac{4\pi}{\omega\mu\sigma\delta a\lambda_G}\left[\left(\frac{\lambda_G}{2a}\right)^2\left(1 + \frac{a}{2b}\right) + \frac{a}{2b}\right], \tag{5.43}$$

or

$$\alpha = \frac{1}{120\pi b\sigma\delta} \cdot \frac{1 + \frac{2b}{a}\left(\frac{f_c}{f}\right)^2}{\sqrt{1 - \left(\frac{f_c}{f}\right)^2}}, \tag{5.44}$$

where f and f_c are respectively the operating frequency and the cutoff frequency of the waveguide.

It is convenient to account for the losses in the short-circuiting plate by adding an equivalent length ℓ_{EP} of waveguide such that the reflection coefficient $|\Gamma|$ is given by eq. (5.25). One derives eq. (5.26) to calculate ℓ_{EP} as follows. Since

$$|\Gamma_S| \cong 1 - 2\alpha\left(\frac{\lambda_G}{4} + \ell_{EP}\right) \cong 1 - \frac{P_{NW} + P_{BW}}{2P_I} - \frac{P_{SP}}{2P_I},$$

it follows that

$$\ell_{EP} = \frac{1}{2\alpha} \cdot \frac{P_{SP}}{2P_I} = \frac{\lambda_G}{4} \cdot \frac{P_{SP}}{P_{NW} + P_{BW}}. \tag{5.45}$$

Substitution of eqs. (5.32), (5.35), and (5.38) into eq. (5.45) yields eq. (5.26).

It is interesting that the expression for ℓ_{EP} does not involve the conductivity of the metal.

An example of the calculation of $|\Gamma|$ for rectangular waveguide follows. Given $f = 9.4$ GHz, $b = 1.016$ cm, $a = 2.286$ cm (WR-90, or X-band waveguide), $\sigma = 4.0 \times 10^7$ mho/m, we calculate $\lambda = 3.189$ cm, $\lambda_G = 4.451$ cm, $\lambda_C = 4.572$ cm, and $\ell_{EP} = 0.364$ cm, $\alpha = 1.59 \times 10^{-4}$ Np/cm, $|\Gamma_S| = 0.99953$, and $L_R = 0.00408$ dB. If we have 10.64 W incident power, then $P_D = 10$ mW, $P_{SP} = 2.46$ mW, $P_{NW} = 2.20$ mW, and $P_{BW} = 5.34$ mW. The distribution of losses was calculated from the following formulas:

$$\frac{P_{SP}}{P_D} = \frac{1}{1 + \dfrac{\lambda_G/4}{\ell_{EP}}}, \tag{5.46}$$

$$\frac{P_{NW} + P_{BW}}{P_D} = \frac{1}{1 + \dfrac{\ell_{EP}}{\lambda_G/4}}, \tag{5.47}$$

and

$$\frac{P_{BW}}{P_D} = \frac{1}{1 + \dfrac{\ell_{EP}}{\lambda_G/4}} \cdot \frac{1}{1 + \dfrac{2b}{a}\left(\dfrac{\lambda_G}{\lambda_C}\right)^2 \left(\dfrac{\lambda}{\lambda_C}\right)^2}. \tag{5.48}$$

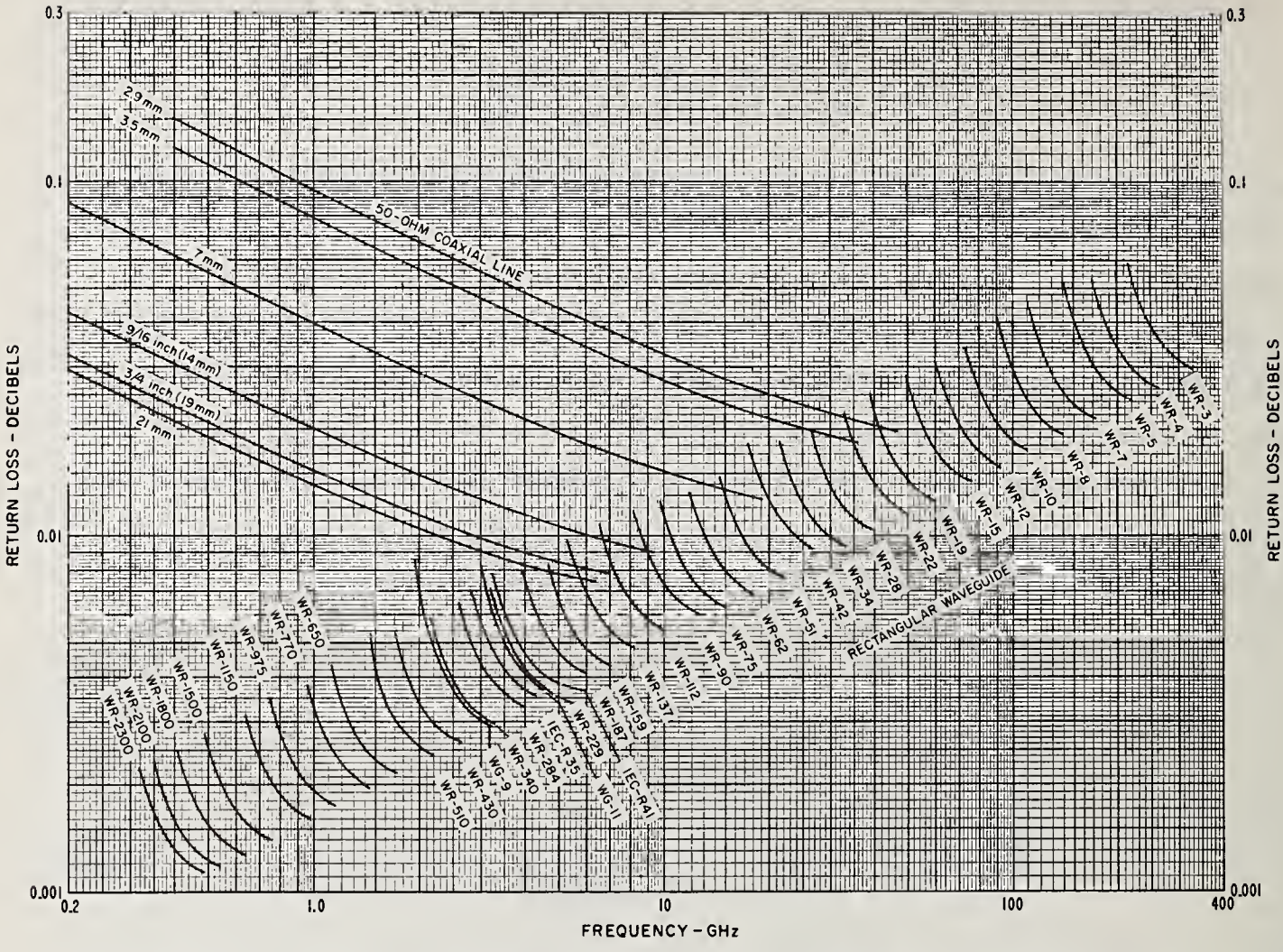

Figure 5-15. Calculated return loss of quarter wavelength short-circuit impedance standards. Basis of normalization: $\sigma = 10^7$ mho/m. Curves for coaxial line are marked with the appropriate inner diameter of outer conductor. Those for rectangular waveguide are marked with appropriate standard waveguide designators.

d. Errors and Design Information

It is estimated that the errors due to approximations in the formulas will be less than the errors in reading the graph of figure 5-15 over the range of values shown. Thus, one can expect the error in L_S determined from the graph to be within ± 2 percent. To this must be added errors from other sources, such as the error in determining conductivity, etc.

Table 5-1 gives bulk conductivities normalized to 10^7 mho/m for a number of metals which might be used to construct quarter-wavelength short-circuits. In the absence of measured conductivities at the frequencies of interest, the values in this table may be used with probably only a few percent error in L_S in most cases.

Table 5-1. Bulk conductivity normalized to 10^7 mho/m of various metals at 20°C.

SILVER	6.29
COPPER (ANNEALED)	5.80
GOLD	4.10
ALUMINUM	3.54
MAGNESIUM	2.17
BRASS	1.19-1.56
NICKEL	1.28
PHOSPHOR BRONZE	1.28
PLATINUM	1.00
STAINLESS STEEL	~0.110

*HANDBOOK OF CHEMISTRY AND PHYSICS. 41st ed. CLEVELAND, OHIO: CHEMICAL RUBBER PUBL. CO., 1959-1960. p. 2588.

5.4. Squared VSWR and Magnified Responses

a. Introduction

The following discussion of research on unusual responses obtained from various kinds of waveguide junctions preceded and is related to the research on tuned reflectometers described later in section 5.5. The discussion is a revised version of Beatty (1959).

In most microwave impedance measuring instruments, such as the slotted line, the resonance line, and rotary standing-wave indicators, the ratio of the maximum to the minimum response (magnitude of voltage output to detector) is ideally equal to the voltage standing-wave ratio (VSWR) of the termination under test or calibration.

Other radically different types of responses are obtainable from various kinds of waveguide junctions. The responses to be discussed here have been called magnified and squared VSWR responses for reasons to become apparent.

A simplified explanation will be given first, followed by a more complicated mathematical description.

The differences among responses are shown in figure 5-16, three response curves calculated for the same termination.

b. Simplified Explanations

(1) Squared VSWR Response

A simplified explanation can be given for one system yielding squared VSWR response. Other systems which have been devised apparently do not permit simplified explanations and have not been thoroughly analyzed. Enough theory will be given however, to permit their use for measurement purposes.

The system shown in figure 5-17(a) consists of a straight section of uniform lossless waveguide (which may be either coaxial line or rectangular waveguide, for example) with oppositely located coupling probes for generator and detector. A short circuit which may be adjusted in position terminates one end of the uniform waveguide section while the other end is terminated in the sliding load to be measured. In this system it is necessary to vary the phase of the load by sliding it inside the waveguide, but in other systems to be described, this is not always required.

Referring to the simplified model of figure 5-17(b),

$$E = e\,\frac{Z_P}{Z_G + Z_P} \simeq i_G Z_P = i_G\,\frac{1}{\frac{1}{Z_S'} + \frac{1}{Z_L'}}. \tag{5.49}$$

If the short circuit is located $\lambda_G/4$ from the probes, $Z_S' = \infty$, and

$$E = i_G Z_L' = i_G\,\frac{1 + \Gamma_L e^{-j2\beta\ell}}{1 - \Gamma_L e^{-j2\beta\ell}}. \tag{5.50}$$

As ℓ varies, $|E|$ goes through maxima and minima. The ratio ρ_A of the maxima to the minima is

$$\rho_A = \left(\frac{1 + |\Gamma_L|}{1 - |\Gamma_L|}\right)^2 = \rho_L^2, \tag{5.51}$$

where ρ_L is the VSWR of the load. The meaning of other symbols used above should become clear upon reference to figure 5-17(b).

(2) Magnified Response

A system yielding magnified response is shown in figure 5-18.

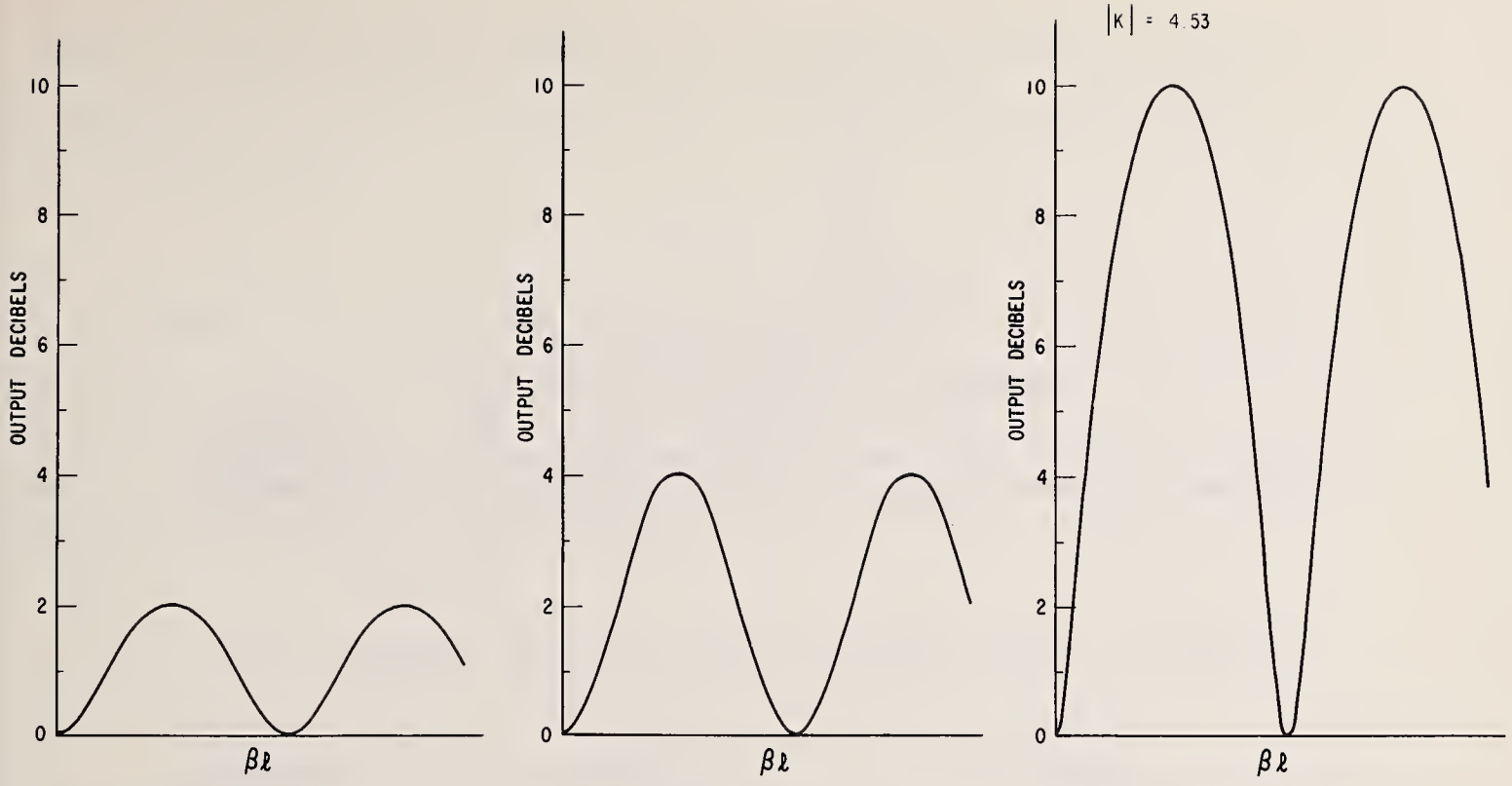

Figure 5-16. Response curve of three measurement systems with termination having a VSWR of 1.26.

(a) idealized slotted line,

$$d = c[1 + K\Gamma_{1e}{}^{-j2\beta l}]$$

(b) squared VSWR response,

$$d = c' \left[\frac{1 + \Gamma_{Le}{}^{-j2\beta l}}{1 - \Gamma_{Le}{}^{-j2\beta l}}\right],$$

(c) magnified response,

$$d = c''[1 + K\Gamma_{Le}{}^{-j2\beta l}].$$

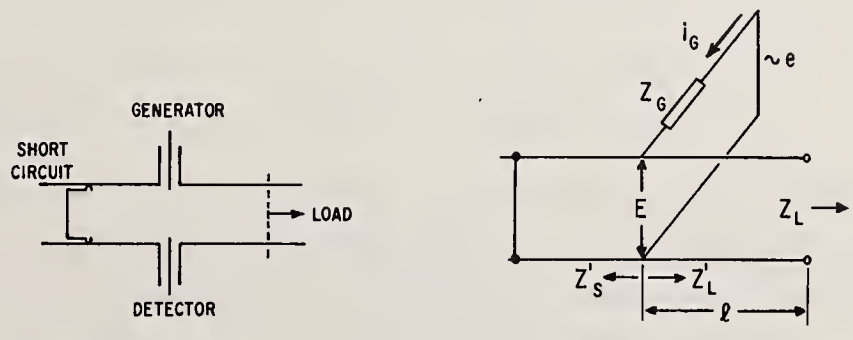

Figure 5-17. Diagram and simplified model of one system yielding squared VSWR response; (a) diagram of system, (b) simplified model.

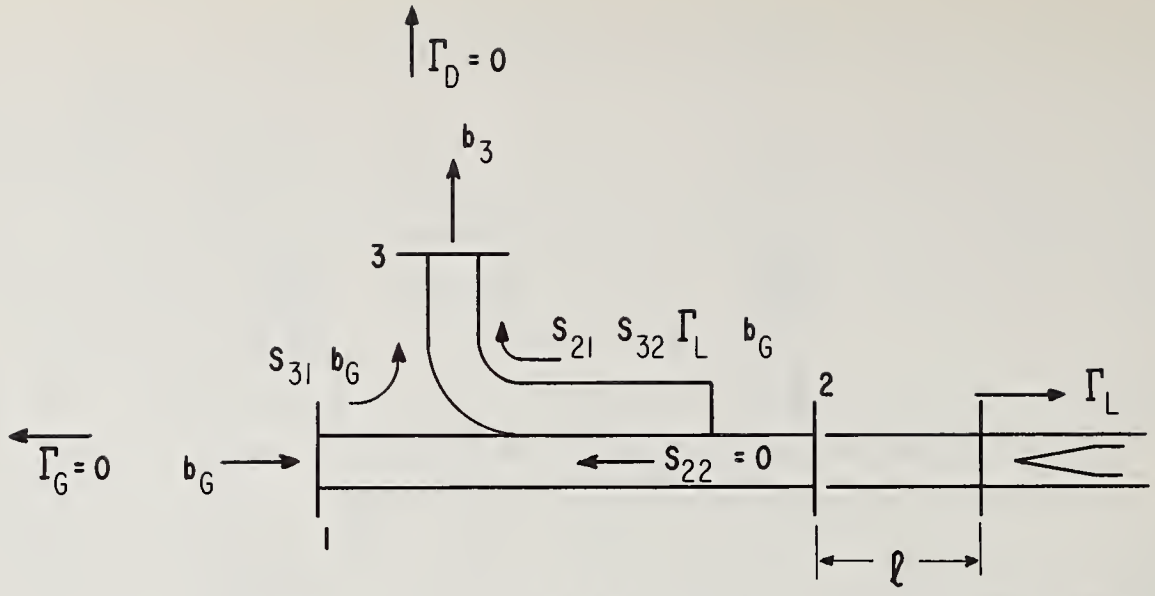

Figure 5-18. Diagram of simplified system to illustrate magnified response.

A directional coupler is connected to respond mainly to the wave reflected from a phasable or sliding termination whose VSWR is to be measured. For simplicity, it is assumed that the generator and detector do not produce reflections ($\Gamma_G = \Gamma_D = 0$), and that no reflections are produced in arm 2 by the directional coupler ($S_{22} = 0$).

The signal coupled to the detector has two components. One is fixed and exists because the directivity is not infinite. The other is from the load reflection and varies in phase as the load is slid inside the waveguide. As the relative phase of the two components vary, the magnitude of the resultant varies. If the components are of approximately equal magnitudes, the range of variation of the resultant may be large even though the reflection from the termination may be small.

Inspection of the diagram of figure 5-18 leads to the following equations describing the response.[8]

$$b_3 \simeq b_G(S_{31} + S_{21}S_{32}\Gamma_L e^{-j2\beta\ell}) = b_G S_{31}(1 + K\Gamma_L e^{-j2\beta\ell}). \qquad (5.52)$$

The response is of the same form as that of the idealized slotted line (see fig. 5-19) excepting that Γ_L is multiplied by the factor K. Since $|K|$ may be very large (it approximately equals the directivity ratio of the directional coupler), one may consider Γ_L to be magnified by the factor $|K|$, leading to the term magnified

[8] In this equation, b represents a wave amplitude, S a scattering coefficient of the directional coupler, and Γ_L the voltage reflection coefficient of the load.

response. It should be noted however that the response variation will increase as one increases $|K|$ up to the point where $|K\Gamma_L| = 1$, and then will decrease with further increase in $|K|$.

c. Analysis

Both magnified and squared VSWR responses may be analyzed by considering the generalized treatment of MacPherson and Kerns (1956) of a 3-arm junction measurement system for phasable loads. Such a junction is shown in figure 5-19, where it has been assumed for convenience that the necessary variation in phase is obtained by changing the length ℓ of uniform, lossless waveguide.

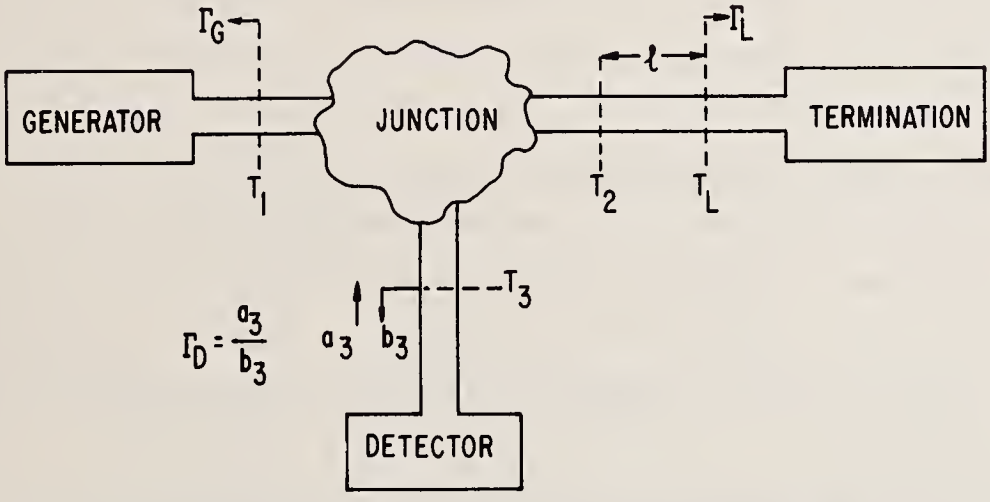

Figure 5-19. Three-arm junction with phasable load.

Instead of using the gathering coefficients employed by MacPherson and Kerns, the solution for b_3 is obtained in terms of the more familiar scattering coefficients (Schafer and Beatty, 1958) and may be expressed as follows:

$$b_3 = C \frac{1 + K\Gamma_L e^{-j2\beta\ell}}{1 - \Gamma_{2i}\Gamma_L e^{-j2\beta\ell}} = CK\Gamma_L e^{-j2\beta\ell} \frac{1 + \frac{1}{K\Gamma_L} e^{j2\beta\ell}}{1 - \Gamma_{2i}\Gamma_L e^{-j2\beta\ell}}, \tag{5.53}$$

where

$$C = \frac{b_G S_{31}}{\begin{vmatrix} (1-S_{11}\Gamma_G) & S_{13}\Gamma_D \\ S_{31}\Gamma_G & (1-S_{33}\Gamma_D) \end{vmatrix}},$$

$$K = \frac{S_{21}S_{32}}{S_{31}} - S_{22},$$

and

$$\Gamma_{2i} = \frac{\begin{vmatrix} (1-S_{11}\Gamma_G) & S_{12} & -S_{13}\Gamma_D \\ -S_{21}\Gamma_G & S_{22} & -S_{23}\Gamma_D \\ -S_{31}\Gamma_G & S_{32} & (1-S_{33}\Gamma_D) \end{vmatrix}}{\begin{vmatrix} (1-S_{11}\Gamma_G) & S_{13}\Gamma_D \\ S_{31}\Gamma_G & (1-S_{33}\Gamma_D) \end{vmatrix}}.$$

In the above expressions, the component of the emergent wave amplitude supplied by the generator is $b_G = a_1 - b_1\Gamma_G$, where a_1 represents the amplitude of the wave incident on the junction in arm 1. Symbols of the form $S_{m,n}$ are the scattering coefficients of the junction, and Γ_G, Γ_D, and Γ_L are the voltage reflection coefficients of the generator, detector, and load, respectively, as indicated in figure 5-19.

The reflection coefficient Γ_{2i} is that which would be obtained "looking into" arm 2 if the generator was turned off and its impedance (as observed at T_1) was unchanged in so doing.

The variation in $|b_3|$ as we vary the phase (ψ_L) of Γ_L is defined to be the response of the systems represented by figure 5-19, and is determined by eq. (5.53).

The properties of eq. (5.53) will be examined in an effort to classify types of responses obtainable. It is evident that the parameter C affects only the level of the response, while the form of the response curve ($|b_3|$ vs ψ_L) is affected by the parameters K and Γ_{2i}.

We may consider the response for the conditions $\Gamma_{2i} = 0$, $|K| = 1$, the usual or normal type of response, since it leads to the form obtained in the case of an idealized slotted line.

The response form previously referred to as magnified response is obtained when $\Gamma_{2i} = 0$, and $|K|$ is unrestricted. However values of $|K|$ may range from zero to infinity, and it is possible to have a magnification factor $|K|$ greater or less than unity. The case where $|K|$ is less than one is of dubious interest, but the possibility of $|K|$ greater than unity appears especially attractive for the measurement of small reflections.

If Γ_{2i} differs from zero, it will cause distortion in the response curve, which is considered undesirable. However, a distinctly different type of response may be obtained if $|\Gamma_{2i}| \simeq 1$, and if the phases of $|K|$ and $|\Gamma_{2i}|$ are equal. This leads to squared VSWR response if $|K| \simeq 1$. This type of response is not only curious, but may prove useful in some measurement applications.

Actually $|\Gamma_{2i}|$ is less than unity in actual (not lossless) systems, so that the ideal squared VSWR response may be closely approached with an actual system, but never quite reached.

A fourth type of response is obtained if the phases of K and Γ_{2i} are the same, $|\Gamma_{2i}| \simeq 1$, and $|K|$ is unrestricted. The ratio of maximum to minimum detector signal level corresponding to eq. (5.51) is

$$\rho_A = \frac{1 + |K\Gamma_L|}{1 - |K\Gamma_L|} \rho_L. \tag{5.54}$$

It seems appropriate to call this a magnified squared VSWR response, and it may have applications in the measurement of large VSWR.

This completes the classification of responses, since conditions other than those mentioned may be regarded as causing distortions of the types described above.

d. Means of Obtaining Various Responses

Examples have already been given (figs. 5-17 and 5-18) of junctions permitting magnified and squared VSWR responses. However other types of arrangements are possible and offer a variety of measurement systems, each with its possible advantages and disadvantages.

In order to closely approach squared VSWR response ($|\Gamma_{2i}| \simeq 1$, $|K| \simeq 1$) it becomes evident that the 3-arm junction should have low loss and low coupling to the load. (This may be shown from a consideration of the conditions imposed upon the scattering coefficients by losslessness.) These conditions are not sufficient however, as one may conclude after trying junctions which satisfy only these conditions. It is necessary for K and Γ_{2i} to have the same phase, and this is obtained by some tuning device, such as the adjustable short-circuit in figure 5-17. There may be some difficulty in obtaining the desired response in some cases, because it is not always possible to obtain correct phase relationship, but the junction forms represented in figure 5-20(a-d) have all ben found experimentally to permit a close approach to squared VSWR response by proper adjustment of the tuner. The arrangement of figure 5-20(e) should also permit squared VSWR response, but has not been constructed or tested.

Magnified Response occurs upon making $|K|$ greater than unity while $\Gamma_{2i} = 0$. It evidently cannot be obtained with a lossless junction, for then $|K| = 1$. If it is assumed that we can always make $\Gamma_G = 0$, then Γ_{2i} would equal S_{22}, and this would vanish, so that $K = S_{21}S_{32}/S_{31}$. The directional coupler connected as shown in figure 5-18 evidently permits magnified response since $|S_{32}/S_{31}|$ is the directivity

ratio and may be quite large while $|S_{21}|$ is usually between 0.7 and 1.0. The use of auxiliary tuners with a directional coupler permits greater versatility since one may adjust the directivity ratio upwards or downwards with one tuner, then adjust the other tuner to make $\Gamma_{2i} = 0$. These adjustments are independent only if made in the order described. Referring to figure 5-21, the tuner in arm 2 is adjusted first in order to obtain the desired value of $|K|$, then the tuner in arm 1 is adjusted to make $\Gamma_{2i} = 0$.

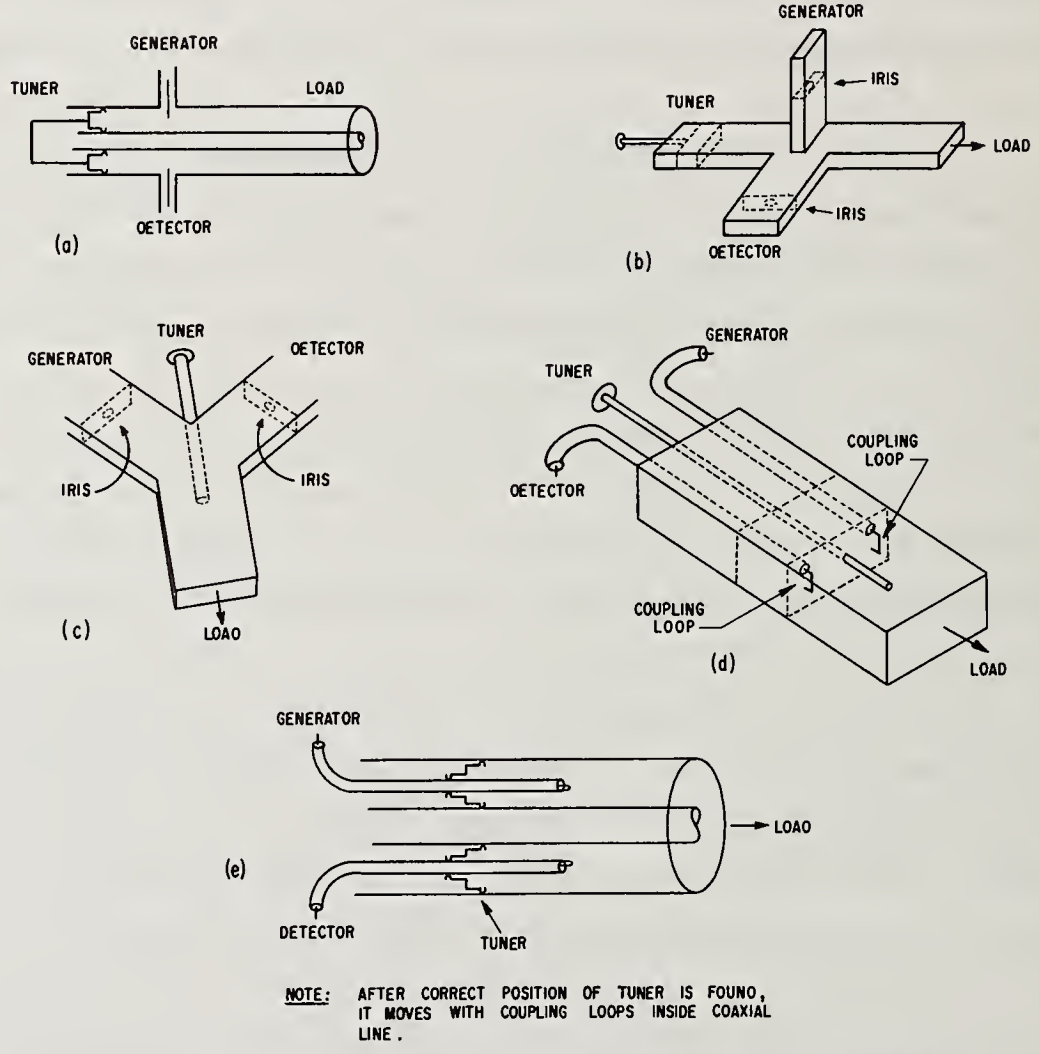

Figure 5-20. Schematic drawings of junctions permitting squared VSWR response: (a), (b), (c), (d), (e).

e. Measurements Using Squared VSWR Response

Any of the junctions of figure 5-20 or their equivalents may be used if the unknown is phasable. This requirement is satisfied if the unknown termination slides inside the waveguide. In principle, a phase shifter or line stretcher may also be used to provide the phase variation, but in practice, they are less than perfect, leading to additional errors in measurement. If the unknown termination does not slide within the waveguide, the arrangements of figures 5-20(d and e) may be used. Either flexible cables must be used to couple the generator and detector to the moving junction, or the generator and detector may be arranged to move with the junction. If the termination is not too large, it and the waveguide section could be moved, keeping everything else fixed. The arrangement shown for rectangular waveguide is not readily adaptable to operation with coaxial line. However the arrangement of figure 5-20(e) should be satisfactory for operation with coaxial line.

The correct adjustment of the tuner is made with $\Gamma_L = 0$ and corresponds to maximum detector output for figures 5-17 and 5-20(a) and to minimum detector output for the others shown. When the correct adjustment has been made, the response curves will be symmetrical about the maxima and minima.

A correction may be made for deviations from the ideal conditions $|K| \simeq 1$, $|\Gamma_{2i}| \simeq 1$, using the methods indicated by MacPherson and Kerns (1956). Instead of analyzing the response curve to obtain the parameter y required for the correction, a shorter method is as follows. Only the real part (g) of y is needed to obtain an intermediate VSWR ρ_I from the apparent VSWR ρ_A. It can be shown that to a good approximation (to the first order in g and b),

$$\rho_I = \frac{1 + |K\Gamma_L|}{1 - |K\Gamma_L|} = \sqrt{\rho_A} + \frac{1}{2}(g + 1)(\rho_A - 1), \tag{5.55}$$

where

$$(g + 1) \simeq \frac{|b_3|(\Gamma_L = 0)}{|b_3|_{max}(|\Gamma_L| = 1)}.$$

It is still necessary to determine $|K|$ in order to obtain $|\Gamma_L|$ or ρ_L. This may be done by measuring ρ_I when a termination of known $|\Gamma_L|$ is connected.

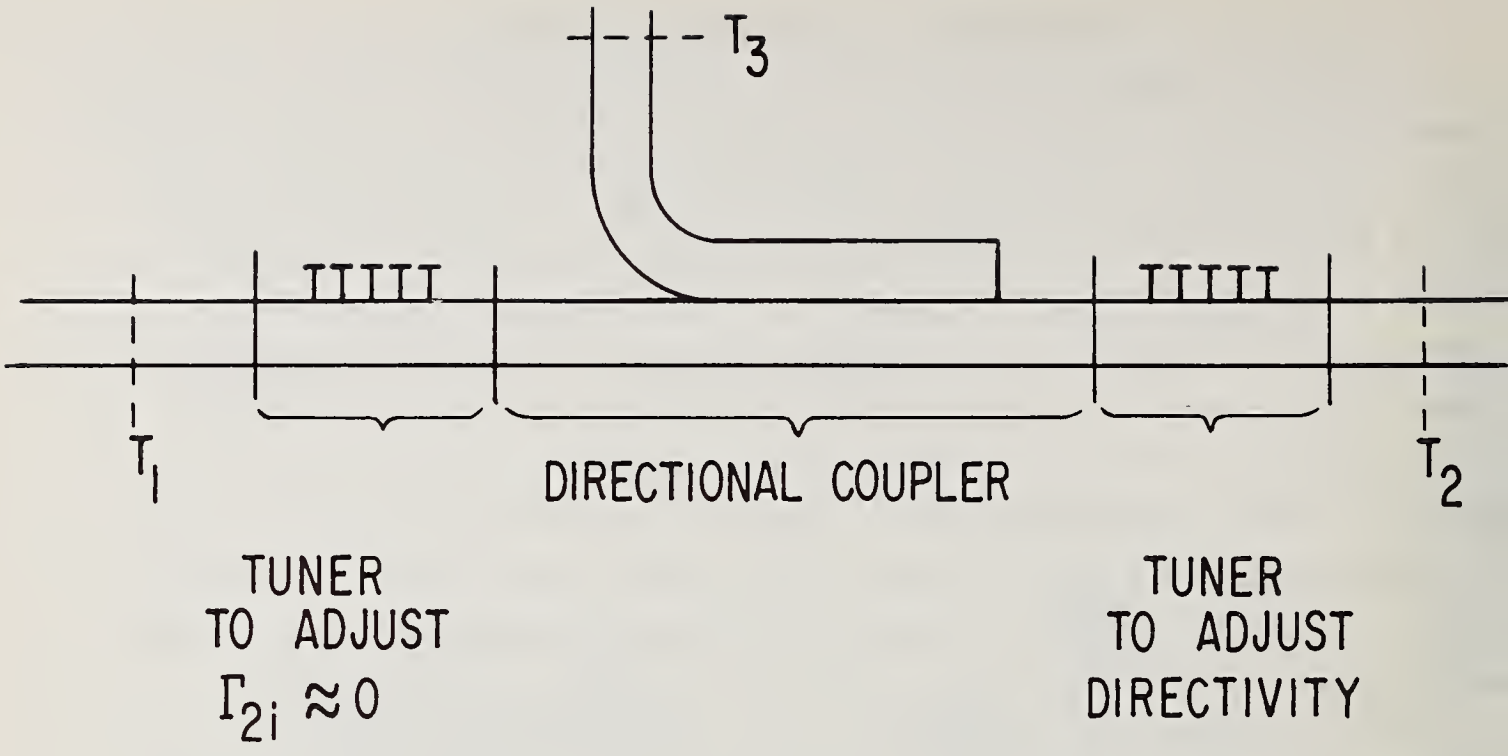

Figure 5-21. Directional coupler with auxiliary tuners.

f. Measurements Using Magnified Response

The arrangement of figure 5-21 may be used to measure the voltage reflection coefficient Γ_U of an unknown termination. Two basic methods will be outlined.

In the first method, the auxiliary tuners are adjusted for the conditions $\Gamma_{2i} = 0$ and $K = \infty$. Inspection of eq. (5.53) shows that $|b_3|$, the magnitude of the detector arm wave amplitude will then be proportional to $|\Gamma_L|$. One then measures the ratio r of the $|b_3|$ values obtained when the load is first unknown (Γ_U), then a standard of known reflection coefficient magnitude $|\Gamma_S|$. Then

$$|\Gamma_U| = r|\Gamma_S|. \tag{5.56}$$

The adjustments of the tuners preceding the measurement is as follows. One adjusts the tuner in arm 2 until no variation is observed in $|b_3|$ as one slides a termination of low reflection inside the output waveguide. Then the tuner in arm 1 is adjusted until no variation in $|b_3|$ is observed as one slides a termination of high reflection inside the output waveguide. If necessary, the above operations are repeated in sequence until no variation in $|b_3|$ is observed as either termination is slid.

In the second method, the tuner in arm 2 is adjusted (with the unknown connected to arm 2) until the detector output is zero. Then $K\Gamma_U = -1$. The tuner in arm 1 is then adjusted until $\Gamma_{2i} = 0$. A reflection standard of known $|\Gamma_S|$ is then connected to arm 2, and the phase of Γ_S is varied. Substitution of the above conditions into eq. (5.53) leads to

$$\rho_A = \frac{|b_3|_{max}}{|b_3|_{min}} = \frac{|\Gamma_U| + |\Gamma_S|}{||\Gamma_U| - |\Gamma_S||}. \tag{5.57}$$

In the event that $|\Gamma_S| \simeq 1$, (approximately true for a sliding short-circuit) then $\rho_A = \rho_U$.

Note that it is unnecessary to vary the phase of Γ_U, the reflection coefficient of the unknown termination in either method. In the second method one needs to vary the phase of Γ_S, but this is easily done if a sliding short-circuit is used.

Alternatively a fixed reflection standard may be used if a suitable line stretcher is incorporated into arm 2 of the measuring instrument.

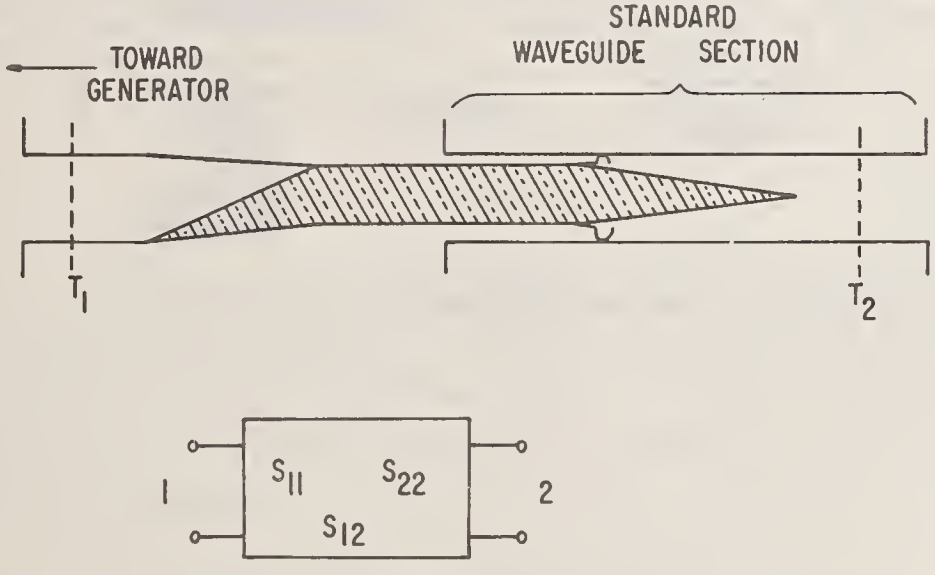

Figure 5-22. Line stretcher and scattering coefficient representation.

Because of the special condition $\Gamma_{2i} = 0$, the line stretcher need not be of the constant impedance type, since reflections that it may introduce may be cancelled by reflection from the tuner in arm 1. Also, the reference plane for arm 2 may be located in the uniform waveguide section of the line stretcher between the source of its reflections and the load. As shown in figure 5-22, the reference plane T_2 remains fixed although the output waveguide and load move. The line stretcher must be stable however, so that the parameters S_{11}, S_{12}, and S_{22} with respect to the reference planes T_1 and T_2 do not vary as it operates.

With the addition of the line stretcher, the second method described above may be called a magnified difference method, since the smaller the difference between $|\Gamma_S|$ and $|\Gamma_U|$, the greater the variation in $|b_3|$ as the phase is changed according to eq. (5.57). The arrangement of apparatus employing a waveguide line stretcher is shown in figure 5-23. Results of measurements of the VSWR of two calculable standards (Booth, 1961) by the above techniques are shown in table 5-2.

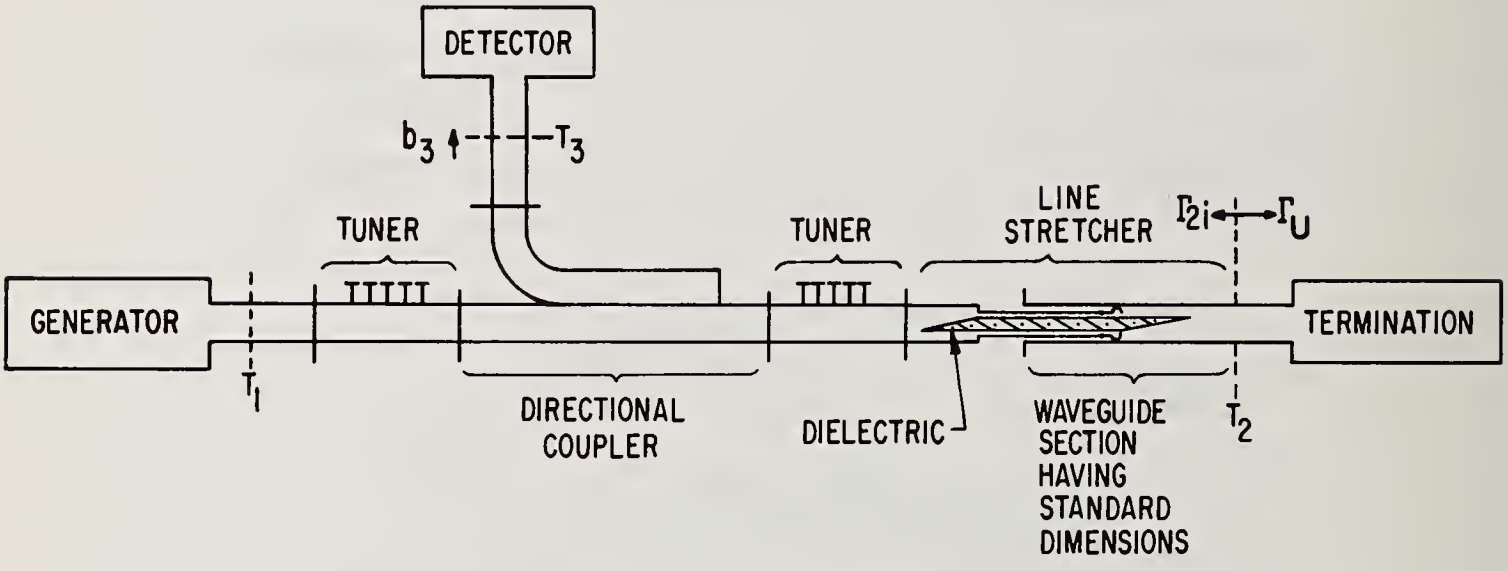

Figure 5-23. Arrangement of apparatus for magnified difference method.

Table 5-2. Comparison of calculated and measured VSWR of half-round obstacle impedance standards of rectangular waveguide using a magnified response measurement technique.

RADIUS (r)	0.1000"	0.1400"
POSITION (ℓ)	1.000"	1.500"
CALCULATED VSWR ASSUMING NO LOSSES	1.226145	1.455465
CALCULATED VSWR CORRECTED FOR ATTENUATION	1.2253	1.4543
MEASURED VSWR	1.2247	1.4538
DEVIATION	0.05 %	0.03 %

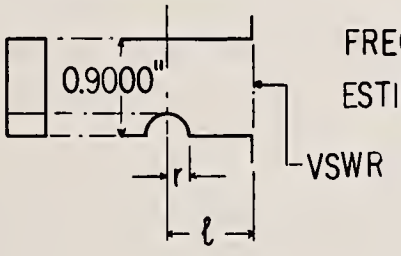

FREQUENCY = 9.3946 Km c/s ±0.015%
ESTIMATED ATTENUATION = 0.070 db per foot

g. Results

The techniques employing magnified response give promise of increased accuracy in the measurement of low and intermediate VSWR. Accuracies of approximately 0.1 percent in VSWR up to 2.0 have been achieved, and perhaps an order of magnitude better than that is possible.

5.5. The Tuned Reflectometer

a. Three-Arm Waveguide Junctions

In the following, some methods for the accurate determination of reflection coefficient magnitude and VSWR will be discussed.

A number of measuring systems can be represented by a three-arm junction with arms connected to a generator, detector, and the unknown.

The variation in detector signal (square root of detector power) as one changes the relative phase of the reflection coefficient of the unknown is called the response of the system. One can obtain different types of response by choosing junctions having certain properties to be discussed. A careful analysis[9] of this type of measuring system reveals that the amplitude b_3 of the output of the third arm (connected to the detector) may be expressed in a form similar to eq. (3.158)

$$b_3 = b_G \frac{\begin{vmatrix} S_{21} & S_{22} \\ S_{31} & S_{32} \end{vmatrix} \Gamma_L + S_{31}}{\begin{vmatrix} (1-S_{11}\Gamma_G) & S_{13}\Gamma_D \\ S_{31}\Gamma_G & (1-S_{33}\Gamma_D) \end{vmatrix} (1-\Gamma_{2i}\Gamma_L)}, \tag{5.58}$$

or similar to eq. (3.162),

$$b_3 = b_G \frac{S_{31}}{\begin{vmatrix} (1-S_{11}\Gamma_G) & S_{13}\Gamma_D \\ S_{31}\Gamma_G & (1-S_{33}\Gamma_D) \end{vmatrix}} \cdot \frac{1 + K\Gamma_L}{1 - \Gamma_{2i}\Gamma_L}, \tag{5.59}$$

where terms of the form $S_{m,n}$ are the scattering coefficients of the junction, and the voltage reflection coefficients of the generator, detector, and load are represented by Γ_G, Γ_D, and Γ_L respectively. The term Γ_{2i} denotes the reflection coefficient corresponding to the internal impedance of the equivalent generator connected directly to the load.

In impedance measuring systems such as the slotted line, it is approximately true that $|K| = 1$ and $\Gamma_{2i} = 0$. For these systems,

$$|b_3| = C\left|1 + |\Gamma_L|\, e^{j(\psi_K+\psi_L)}\right|, \tag{5.60}$$

and as the phase ψ_L of Γ_L varies,

$$\frac{|b_3|_{max}}{|b_3|_{min}} = \frac{1 + |\Gamma_L|}{1 - |\Gamma_L|} = \rho_L, \text{ the VSWR.} \tag{5.61}$$

b. Tuning for Squared VSWR Response

It is possible to construct a "lossless" junction for which $|K| \simeq 1$ and $|\Gamma_{2i}| \simeq 1$. This can yield a squared VSWR response; for as the phase of Γ_L varies,

$$\frac{|b_3|_{max}}{|b_3|_{min}} \simeq \left(\frac{1 + |\Gamma_L|}{1 - |\Gamma_L|}\right)^2 = \rho_L^2. \tag{5.62}$$

[9]For background material, see Macpherson and Kerns (1956) and section 3.15i.

It is necessary to tune the junction in order to obtain the correct phase relationship between K and Γ_{2i}. This response is not only a curiosity, but may find applications in measuring techniques.

c. Tuning for Magnified Response

Of more promise is the class of junctions for which $|K| >> 1$, $\Gamma_{2i} \simeq 0$. Inspection of eqs. (5.58) and (5.59) reveals that $|K|$ may be approximated closely by $|S_{32}/S_{31}|$, the directivity ratio of a directional coupler.

It is well known (Barnett, 1953) that the effective directivity of a given directional coupler may be increased (or decreased) by adjustment of a tuner connected to the coupler output. By this means, one can adjust $|K|$ to any desired value. Then another tuner connected to the coupler input may be adjusted to make $\Gamma_{2i} = 0$. This yields a response similar to that of eq. (5.61) except that Γ_L is multiplied by K. Since $|K|$ may be greater than unity, this can be called a magnified response.

One technique for impedance measurement consists of connecting the unknown ($\Gamma_L = \Gamma_U$), tuning for $b_3 = 0$, ($K\Gamma_U = -1$), then tuning for $\Gamma_{2i} = 0$. If the unknown is removed and a standard ($\Gamma_L = \Gamma_S$) is connected, the response is

$$|b_3| = C\left|1 - \frac{\Gamma_S}{\Gamma_U}\right|. \tag{5.63}$$

If a variable standard were available, one could adjust it until $b_3 = 0$, then $\Gamma_U = \Gamma_S$. If only fixed standards are available, the following procedure may be used to obtain the magnitude of Γ_U.

$$\Gamma_{2i} = \frac{\begin{vmatrix} (1-S_{11}\Gamma_G) & S_{12} & S_{13}\Gamma_D \\ S_{21}\Gamma_G & S_{22} & S_{23}\Gamma_D \\ S_{31}\Gamma_G & S_{32} & (1-S_{33}\Gamma_D) \end{vmatrix}}{\begin{vmatrix} (1-S_{11}\Gamma_G) & S_{13}\Gamma_D \\ S_{31}\Gamma_G & (1-S_{33}\Gamma_D) \end{vmatrix}}. \tag{3.160}$$

If one varies the phase of Γ_S (a line stretcher, not necessarily of the constant impedance type, may be used), the ratio of maximum to minimum response is

$$\left|\frac{b_{3\ max}}{b_{3\ min}}\right| = \left|\frac{|\Gamma_U| + |\Gamma_S|}{|\Gamma_U| - |\Gamma_S|}\right|. \tag{5.64}$$

This type of response is very sensitive to small differences in $|\Gamma_U|$ and $|\Gamma_S|$. One can choose a suitable half-round inductive obstacle impedance standard so that $|\Gamma_S|$ is close to $|\Gamma_U|$. (It is interesting to note that the attenuation of a short section

of waveguide connected to an impedance standard could be determined by this technique.) If a short circuit is used as the standard $|\Gamma_S| \simeq 1$, the ratio very nearly equals the VSWR of the unknown. Variations of these techniques based upon eq. (5.64) are possible.

d. Tuning for Infinite Directivity

It is especially interesting to consider the response when the tuners are adjusted for conditions $\Gamma_{2i} = 0$, and $|K| = \infty$ (or $S_{31} = 0$). Equation (5.58) becomes

$$b_3 = \frac{b_G S_{21} S_{32} \Gamma_L}{(1 - S_{11}\Gamma_G)(1 - S_{33}\Gamma_D)}, \tag{5.65}$$

or

$$|b_3| = C'|\Gamma_L|.$$

With this type of response it is not necessary to vary the phase of Γ_L, but merely to observe $|b_3|$ when one alternately connects the unknown and the standard to the output. In this case

$$\frac{|b_3|_U}{|b_3|_S} = \frac{|\Gamma_U|}{|\Gamma_S|} = r, \text{ or } |\Gamma_U| = r|\Gamma_S|. \tag{5.66}$$

Any standard of known reflection coefficient $|\Gamma_S|$, such as the ones previously mentioned (except $\Gamma_S = 0$), may be used. If a short circuit is used, the measuring system can easily be arranged so that return loss

$$\left(20 \log_{10} \frac{1}{|\Gamma_U|}\right) \tag{5.67}$$

is measured directly.

e. Analysis of Errors

The basic form of the reflectometer is shown in figure 5-24.

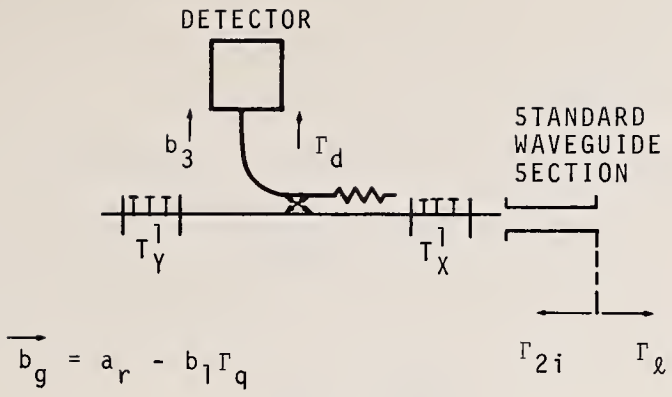

Figure 5-24. Basic form of the reflectometer.

A mathematical treatment shows (assuming linearity) that the response will in general be of the form:

$$|b_3| = \left|\frac{A\Gamma_\ell + B}{C\Gamma_\ell + D}\right|. \tag{5.68}$$

It is evident that the desired response will be realized if B = C = 0. Then

$$|b_3| = \left|\frac{A}{D}\,\Gamma_\ell\right|. \tag{5.69}$$

The sources of error, in determining $|\Gamma_U|$ by the methods to be discussed in this section include: a) incorrect measurement of r, and uncertainty in value of $|\Gamma_S|$, and b) improper adjustment of the tuners, such that B and C do not vanish.

The error due to a) may be determined by inspection. If the equation for $|\Gamma_U|$ is written in the form:

$$|\Gamma_U| = |\Gamma_S|\,\frac{|b_3|_U}{|b_3|_S} = |\Gamma_S|r, \tag{5.70}$$

it is evident that the fractional error in $|\Gamma_U|$ will equal the sum of the fractional errors in $|\Gamma_S|$ and r if the latter are small.

With regard to the second item b) it is assumed that B and C have been reduced to the point where the variations in the expression

$$|b_3| = \frac{|A\Gamma_\ell + B|}{|C\Gamma_\ell + D|} \tag{5.71}$$

are due mainly to variations either in the numerator or the denominator as the loads of small $|\Gamma_\ell|$ and large VSWR are employed respectively.

A first order correction to eq. (5.70) may be written as follows:

$$|\Gamma_U| = |\Gamma_S| \left| \frac{|b_3|_U}{|b_3|_S} \right| 1 + \frac{B}{A} \frac{\Gamma_S - \Gamma_U}{\Gamma_S \Gamma_U} + \frac{C}{D} (\Gamma_S - \Gamma_U) + \ldots \Bigg| . \tag{5.72}$$

The ratios $|B/A|$ and $|C/D|$ may be determined from the expressions:

$$K_1 = 20 \log \left(1 + 2 \left| \frac{B}{A\Gamma_\ell} \right| \right) \tag{5.73}$$

and

$$K_2 = 20 \log \left(1 + 2 \left| \frac{C}{D} \right| \right) \tag{5.74}$$

where K_1 and K_2 are the ratios in decibels of the maximum to minimum outputs with the sliding loads of small $|\Gamma_\ell|$ and large VSWR respectively, $|\Gamma_\ell|$ is the reflection coefficient of the load of small VSWR, and a reflection coefficient of unity has been assumed for the load of large VSWR.

Except for the presence of the factor Γ_ℓ, these equations for K_1 and K_2 are of the same form, and values for $|B/A|$ and $|C/D|$ may be obtained from figure 5-25 where the value of $|C/D|$ is taken from the line $|\Gamma_\ell| = 1$. It will be noted that the evaluation of the right hand side of eq. (5.72) presupposes a knowledge of Γ_U but for the present purpose of assigning a limit of error, an estimated (approximate) value is adequate.

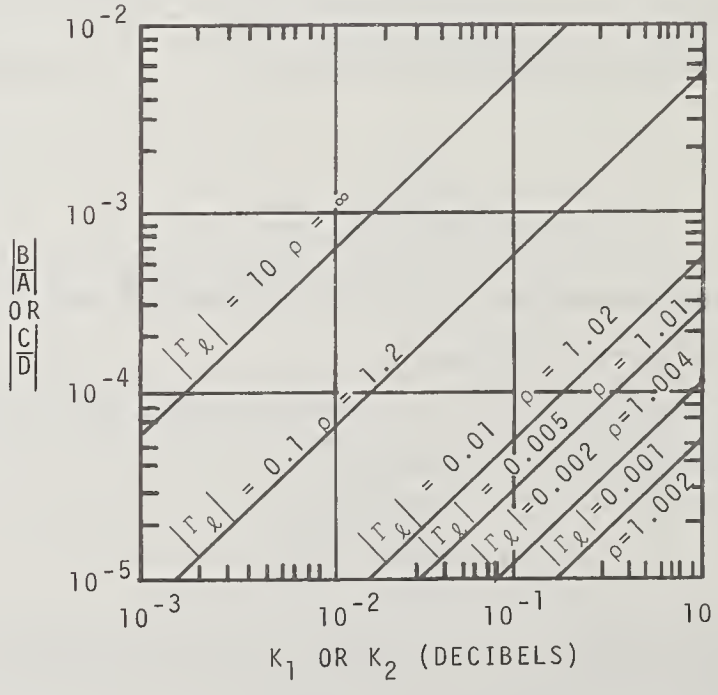

Figure 5-25. Graph for the determination of $|B/A|$ and $|C/D|$.

As an example, if a sliding load of VSWR = 1.005 is employed in the first tuning operation, and the variation in output is reduced to 1 dB, $|B/A|$ will have a value of approximately 1.6×10^{-4}. If the variation in the second step with the sliding short is reduced to 0.02 dB, the value for $|C/D|$ will be approximately 1.2×10^{-3}. Assuming that the unknown load has a value $|\Gamma_U| \simeq 0.2$, ($\rho \simeq 1.5$), $|\Gamma_S| = 1.000$ (corresponding to a short-circuit) and assuming the terms in the right hand factor of eq. (5.72) combine in the worst phase, values of 6 and 1.2 are obtained for

$$\left| \frac{\Gamma_S - \Gamma_U}{\Gamma_S \Gamma_U} \right|$$

and for $|\Gamma_S - \Gamma_U|$ respectively, for a total error of
$\pm (1.6 \times 10^{-4} \times 6 + 1.2 \times 10^{-3} \times 1.2) \simeq \pm 2.4 \times 10^{-3}$, or $\pm$ 0.24 percent.

5.6. Hybrid Reflectometer

a. Introduction

The development and analysis of tuned reflectometers as previously mentioned led to improved accuracy in the measurement of VSWR and magnitude of reflection coefficient. In the following discussion, which is a revised version of Beatty and Anson (1962), two additional developments are described.

First, it is shown in figure 5-26 how one can measure both phase and magnitude of reflection coefficient with a tuned reflectometer. Second, the hybrid reflectometer principle is introduced and illustrated. A hybrid tuned reflectometer is one in which the source, detector, tuners, isolators, and directional coupler are components of a convenient (say rectangular) waveguide system, but the output waveguide, sliding loads, and unknown are components of a different (say coaxial or stripline) waveguide system.

Such an arrangement has obvious advantages which are illustrated by the following description of a rectangular-coaxial waveguide hybrid tuned reflectometer arrangement which was tested at 4 GHz.

In applications to rectangular waveguide systems an accuracy of 0.1% in VSWR was obtained in measuring moderate and small reflection coefficients. It is difficult to obtain corresponding accuracy in coaxial systems, especially those in which the diameters are small.

In the work to be described an accuracy of 1.5% in $|\Gamma_U|$ for $|\Gamma_U| \geq 0.2$ is obtained for the small-diameter coaxial line (internal diameter of outer conductor, 0.276 in; external diameter of inner conductor, 0.120 in) normally associated with the type-N connector.

In order to take advantage of the general superiority of rectangular-waveguide components over coaxial components, a novel hybrid arrangement was employed. Modifications of the measurement techniques are described which overcome difficulties inherent in the coaxial structure.

b. Basic Theory

The necessary theory has already been given in this monograph. It is well to recall that the output of a correctly tuned reflectometer is ideally

$$b_3 = C\Gamma_L \tag{5.65}$$

where b_3 is the amplitude of the wave incident upon the detector, C is a constant and Γ_L is the reflection coefficient of the load.

One normally makes a measurement by alternately connecting standard and unknown loads having reflection coefficients Γ_S and Γ_U, respectively, to the reflectometer and (by means of standard phase-shifters and attenuators) measuring the corresponding change in b_3. This is often obtained by noting the attenuation and phase-shift changes required to maintain b_3 constant. Often phase information is not required and one needs to measure only the attenuation Δa required to return the detector output to the reference level. One can then obtain $|\Gamma_U|$ from the relationship

$$\Delta a = 20 \log_{10} \left| \frac{\Gamma_S}{\Gamma_U} \right| . \tag{5.75}$$

It is also well to recall that one adjusts the auxiliary tuners so that cyclical variations in the detector output $|b_3|$ (which occur when sliding the loads in the measurement arm of the reflectometer) are minimized. In adjusting the tuner on the load arm of the directional coupler, one slides a load having a small VSWR, say 1.05, and in adjusting the other tuner, one slides a short-circuiting piston. The accuracy of the measurement to be made depends in part on how well these adjustments are made.

c. Experimental Equipment

(1) General

In general, the arrangement of equipment is as shown in figure 5-26. The standard phase-shifter and the reflectometer may be of the same form, and the tuning

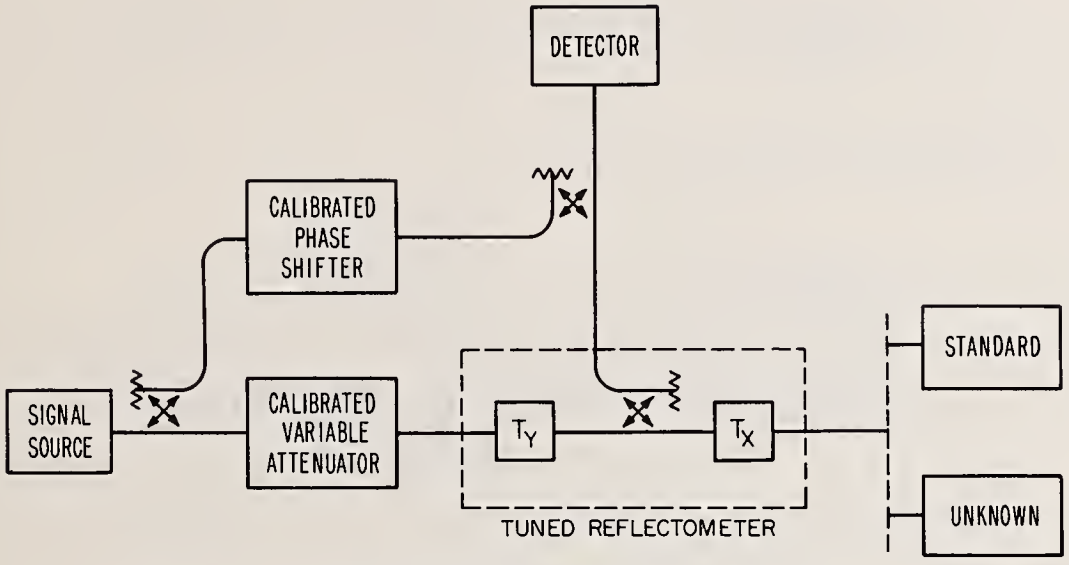

Figure 5-26. Simplified arrangement of apparatus.

procedure for each would then be the same. The arrangement shown permits measurements to be made of phase as well as magnitude of the voltage reflection coefficient. However, in order to illustrate the hybrid system, the phase-shifter was omitted and only VSWR data were obtained.

A hybrid arrangement was used in which all the equipment consisted of rectangular waveguide components with the exception of the measurement arm of the reflectometer and the loads, which were in small-diameter coaxial line. This was done in order to take advantage of the greater availability of excellent components in rectangular waveguide. It was also found that the mechanical stability and freedom from leakage were greater than with coaxial systems. This arrangement permits changes in the diameter of the coaxial line, as desired, merely by changing the waveguide/coaxial adaptor.

The discontinuity in going from rectangular waveguide to coaxial line caused no difficulty since its reflection is tuned out in the normal adjustment of the tuners.

Commercially available WR187 (3.95-5.85 GHz) rectangular-waveguide components were used except for the tuners, which were specially designed and constructed. In addition to the usual stubs located in the center of the broad top wall, the tuners had stubs for fine adjustment located in the center of the narrow side wall.

The coaxial line was made from special phosphor-bronze tubing with tolerances of ± 0.0005 inch on the diameters.

Rods, clamps, and an H-beam were used to increase mechanical rigidity, and ferrite isolators were used to minimize undesirable effects of impedance changes.

(2) Terminating Arrangements

Errors caused by connector discontinuities and losses were minimized by modifying the terminating arrangements as shown in figure 5-27. A joint in the center conductor at the plane of connection was eliminated by special design of the output terminal, the adaptors for connecting the unknown load, and the working standard of reflection, shown in figures 5-27(a), (b) and (c) respectively. Another adaptor, not shown, permitted connection of loads having male type-N connectors.

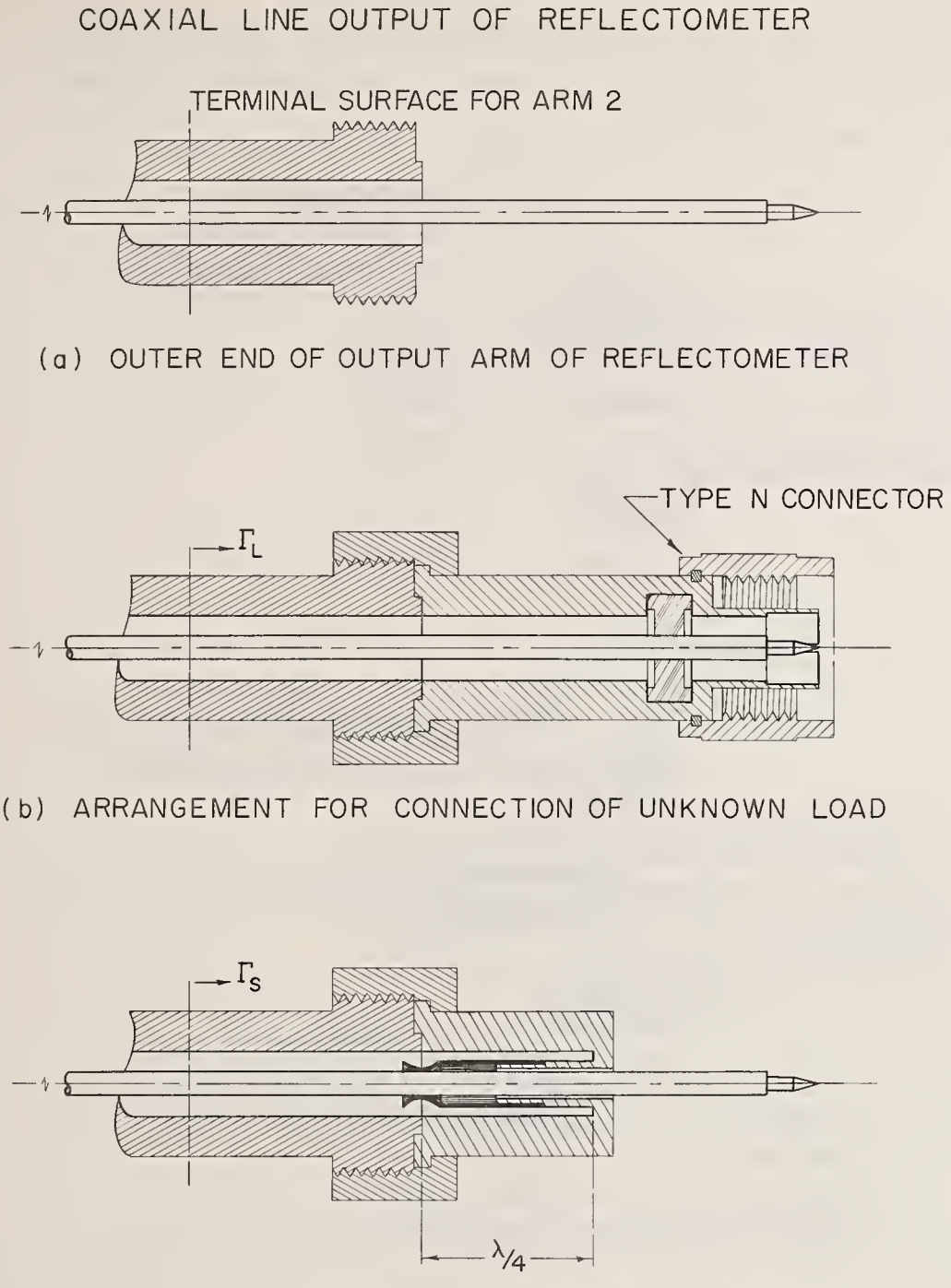

Figure 5-27. Terminating arrangements for coaxial-line output of reflectometer.

The working standard of reflection consisted of a $\lambda/4$ short-circuit having fingers only on the inner conductor. The current flow at its contacts with the line terminal surfaces was thereby minimized. This working standard was calibrated against a similar but more refined standard described later.

(3) Standard Reflections for (Air-Dielectric) Coaxial Line

Although it was not convenient to use as a reference in the measurement of unknown reflection coefficients, the one-piece λ/4 short-circuit as shown in figure 5-28 was used to calibrate the working standard.

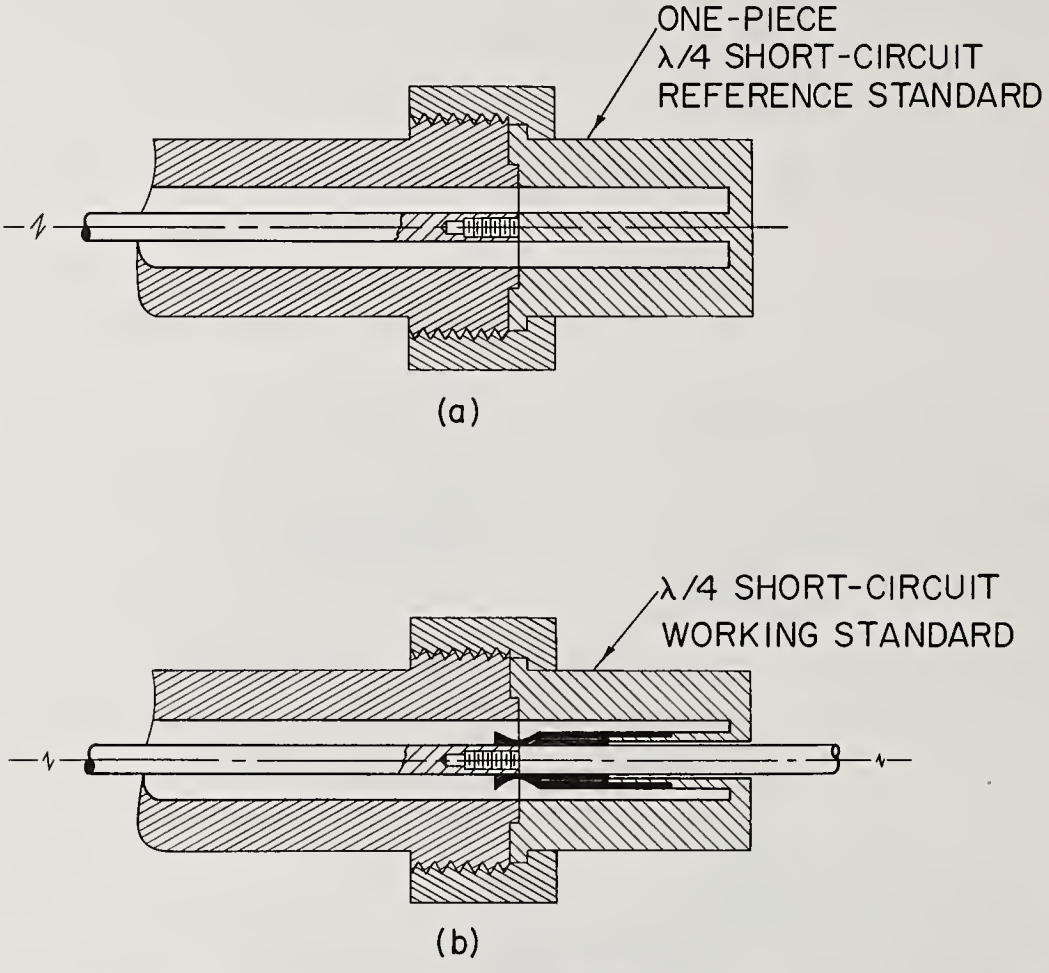

Figure 5-28. Arrangement for comparison of λ/4 short-circuited sections of coaxial line.

(a) One-piece λ/4 short-circuit reference standard.
(b) λ/4 short-circuit working standard.

The reflection coefficient $|\Gamma_S|$ of such a short-circuit can be determined to high accuracy from

$$|\Gamma_S| = 1 - \frac{2R_{EP}}{Z_0}\left[1 + \frac{60\lambda}{8bZ_0}\left(1 + \frac{b}{a}\right)\right], \qquad (5.5)$$

or with moderate accuracy from the graph of figure 5-15. For greatest accuracy the conductivity is obtained from an attenuation measurement on a coaxial-line section made of the same material used in the one-piece λ/4 short-circuit.

(4) Sliding Loads

Unless suitable sliding loads are employed, one cannot proceed far enough in the adjustment of the auxiliary tuners, so that eq. (5.65) applies. Hence the accuracy of measurement depends largely upon the suitability of these components. Their reflection coefficients should not vary appreciably as they are slid or rotated in the coaxial line. Some variation is tolerable provided that one can still recognize when the tuners have received adequate adjustments.

Designs for suitable sliding-short-circuits are shown in figure 5-29 and for sliding absorbing terminations in figure 5-30.

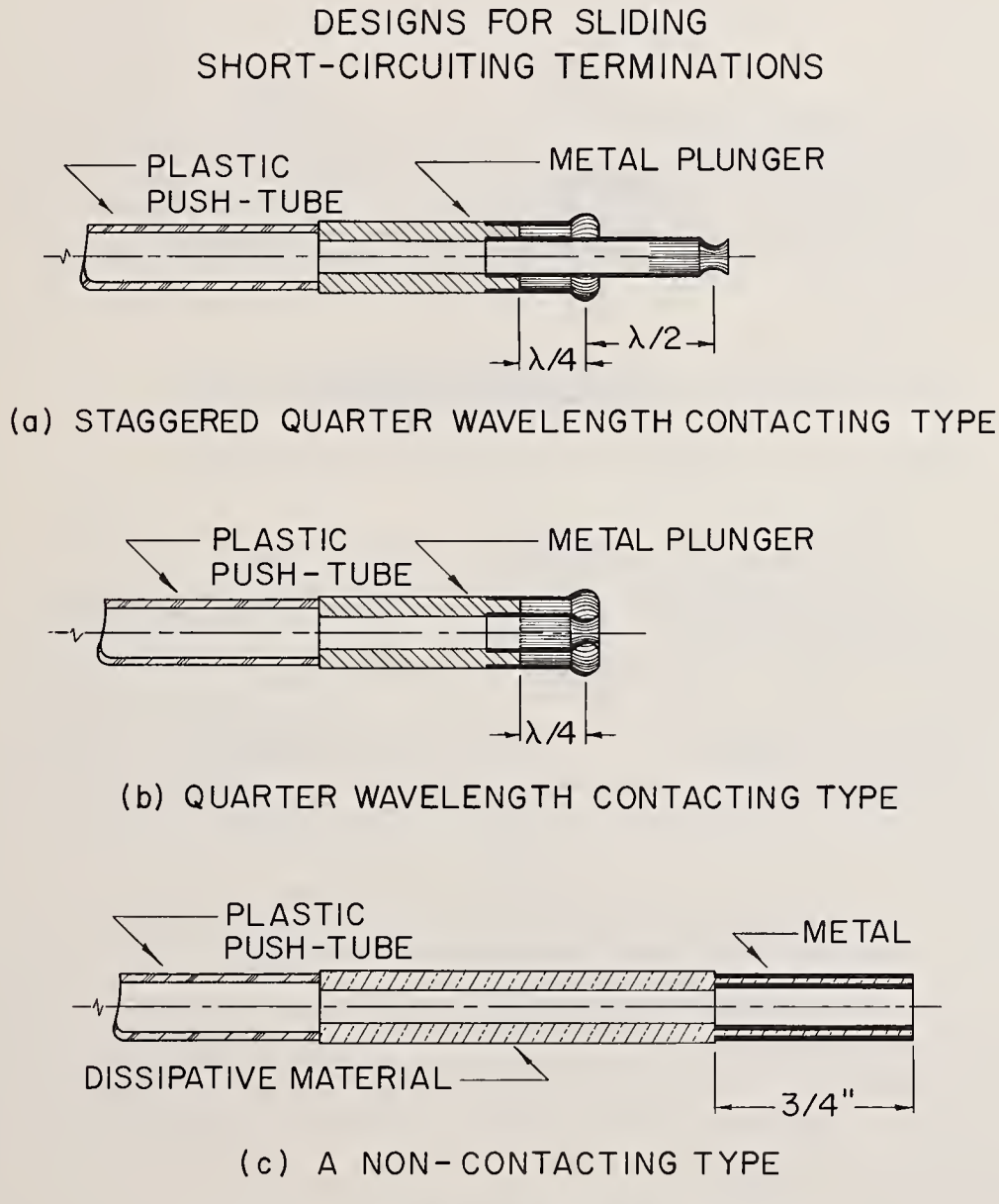

Figure 5-29. Designs for sliding short-circuits.

DESIGNS FOR SLIDING, TAPERED, ABSORBING TERMINATIONS

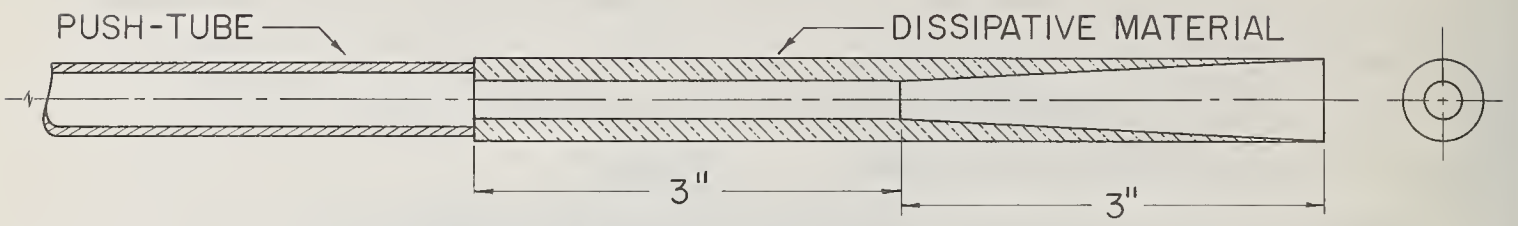

(a) TAPERED SLIDING TERMINATION

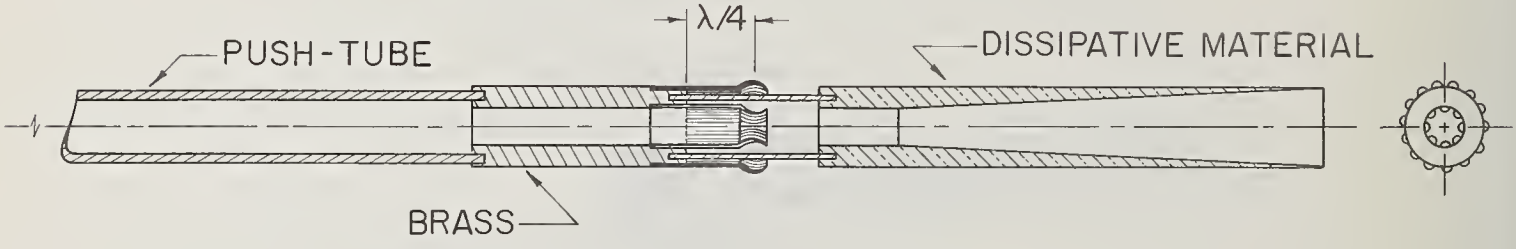

(b) SHORTENED ABSORBING TERMINATION

Figure 5-30. Designs for low-reflection terminations.

d. System Performance and Applications

Various tests were made at 4 GHz to evaluate both overall performance and that of individual components. The results were as follows.

The magnitude $|S_{11}|$ of the reflection coefficient from a joint in the outer conductor was determined to be approximately 0.0025, using a reflectometer technique (Beatty et al., 1960). If no correction is made for this reflection, it can contribute 1.25% to the error in measuring a reflection coefficient of $|\Gamma_U| = 0.2$.

The performance of the sliding loads was obtained as shown in figure 5-31.

The conductivity of the leaded copper used in making the one-piece λ/4 short-circuit was determined to be 4.0×10^7 mho/m, from which the calculated reflection coefficient was 0.9988. Comparison of the working standard of reflection with this one gave its value as $|\Gamma_S| = 0.9931$.

The attenuation of the uniform section of coaxial line was determined as 0.17 dB/ft. The reflection from a joint in the centre conductor alone (its effect was avoided in the method used) corresponded to $|S_{11}| = 0.01$.

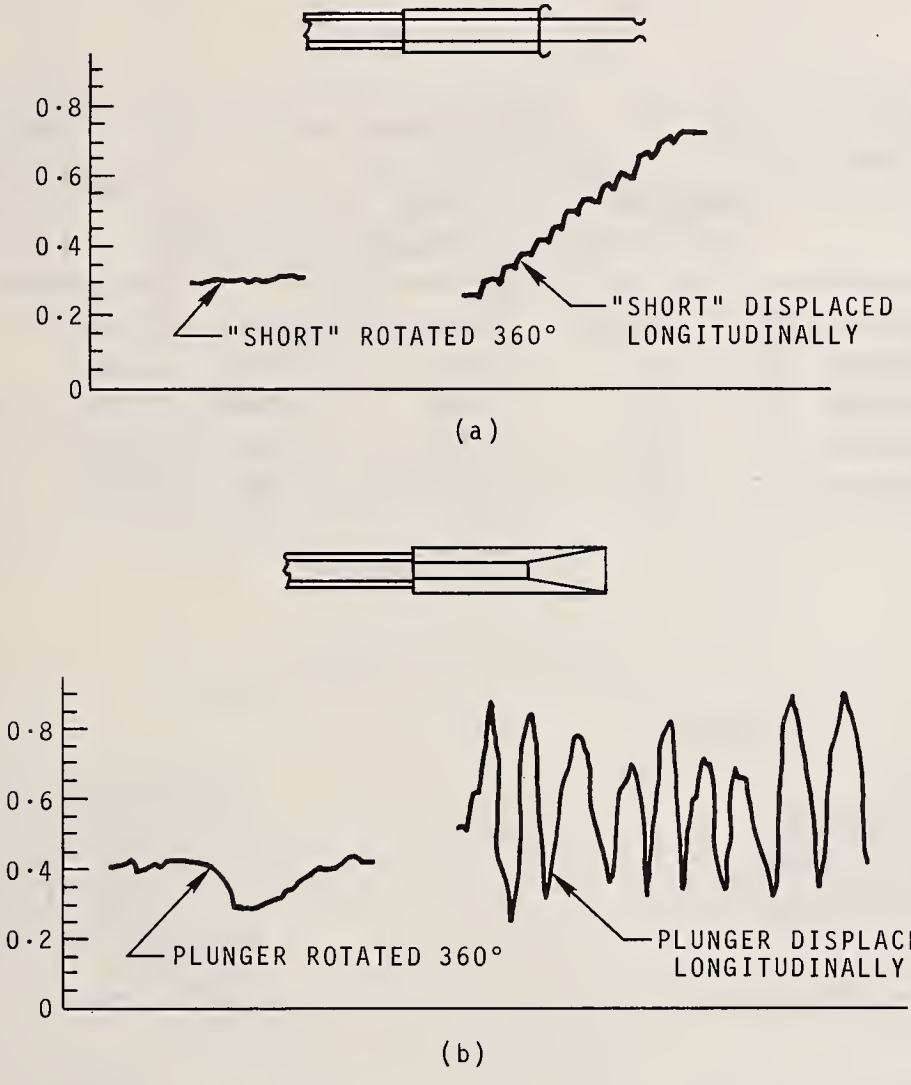

Figure 5-31. Performance of sliding loads.

(a) short-circuit.
(b) absorbing plunger.

e. Results and Discussion of Errors

The VSWR's of a number of commercially available coaxial terminations were measured in order to demonstrate the overall performance. The results are shown in figure 5-32 and are generally within expected limits.

TERMINAL END OF REFLECTOMETER	TERMINATION MANUFACTURED BY:	RETURN LOSS IN DECIBELS AVERAGE OF 10 MEASUREMENTS	MAXIMUM DEVIATION FROM AVERAGE	MAGNITUDE OF REFLECTION COEFFICIENT	VSWR	MANUFACTURERS SPECIFICATION VSWR AT 4 GHz
(a)	COMPANY "A"	28.2 db	0.00 db	0.0389	1.078	< 1.05
(b)	COMPANY "A"	42.1	0.35	0.0079	1.016	< 1.05
(b)	COMPANY "B"	9.22	0.02	0.346	2.058	NOMINAL 2.0
(a)	COMPANY "C"	20.1	0.15	0.0989	1.220	< 1.20 at 3 GHz
(a)	COMPANY "D"	17.2	0.05	0.1380	1.320	< 1.20 from 7-10 GHz

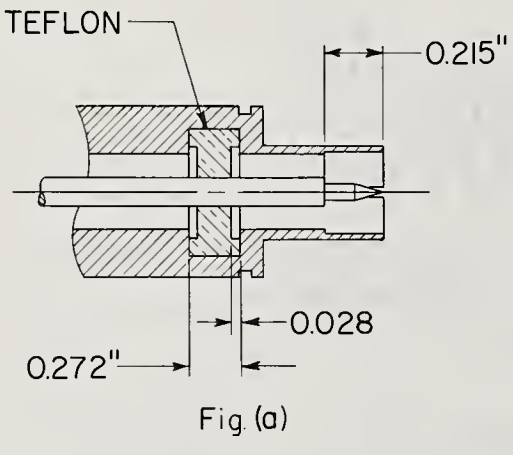

Fig. (a)

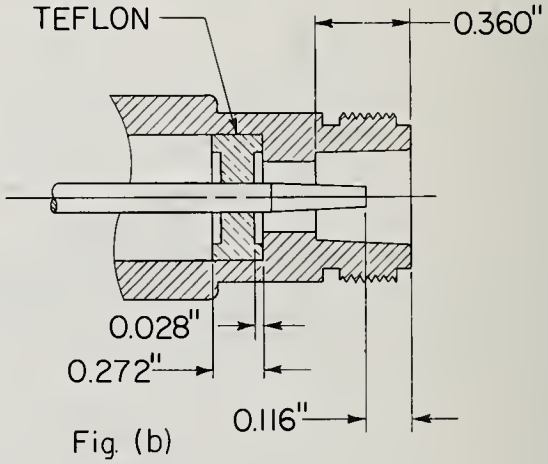

Fig. (b)

Figure 5-32. Results of measurements.

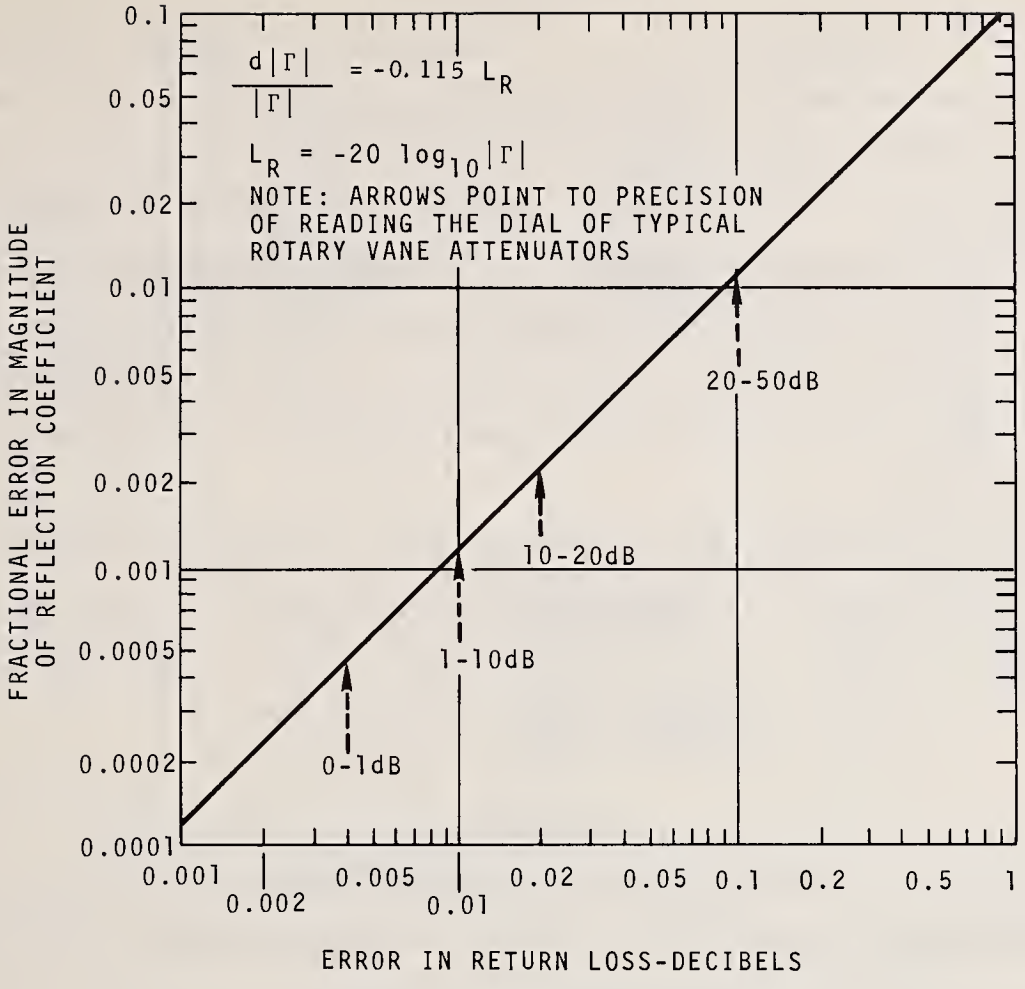

Figure 5-33. Attenuation error.

The principle sources of error which have an appreciable effect, together with their maximum contribution to the overall error in measuring $|\Gamma_U| \simeq 0.2$, are as follows:

(a) Uncorrected reflection coefficient of the joint in the outer conductors: 1.25%.

(b) Error in determining $|\Gamma_S|$: 0.1% or less.

(c) Error in measuring Δa: 0.3% or less, provided that Δa is less than 20 dB (see fig. 5-33).

(d) Error in adjusting the auxiliary tuners: 0.5% or less, provided that $|\Gamma_U|$ is less than 0.2.

The overall r.m.s. error is calculated as 1.4%. Thus an estimate of 1.5% is conservative for $|\Gamma_U| \simeq 0.2$. For $|\Gamma_U|$ less than 0.2, the error would be higher.

f. Conclusions

The results of this investigation of the application of improved reflectometer techniques to the measurement of VSWR in coaxial systems indicates that an accuracy of 1.5% or better is immediately possible. This accuracy can be obtained over a limited but useful range of $|\Gamma_U|$. It is felt that techniques can readily be devised to extend the range without serious loss of accuracy. For example, one needs to reduce the reflection from the joint in the outer conductor, and to make a correction for its effect. Increased accuracy can be expected with the refinement of components such as the sliding loads. Also one would expect less difficulty in working with coaxial line of larger diameters.

The hybrid principle works well in this example, and would be expected to work well with other combinations of different waveguide components.

5.7. Connector Reflections and Losses

a. Introduction

A knowledge of the reflections and losses of waveguide joints or connectors is important in evaluating certain errors occurring in nearly all types of microwave measurements. In some cases, these errors are the limiting ones, and further improvement in the state of the art depends upon improvements in joints or connectors. Sensitive and accurate techniques to measure the characteristics of joints and connectors are vital to such an improvement.

The improvement and refinement of microwave reflectometer techniques has led to sensitive means for determining the small losses and reflections normally associated with good waveguide joints and connectors.

In the following, based upon Beatty, et al. (1960), we describe and discuss tuned reflectometer techniques which provide a powerful tool for the investigation of the properties of waveguide joints or connectors.

b. Preliminary Considerations

As shown in figure 5-34, a waveguide joint or connector may be represented by a 2-arm waveguide junction characterized by four scattering coefficients, S_{11}, S_{12}, S_{21}, and S_{22}. One seldom needs to know all four in order to predict the behavior of the junction. For example, if nonreciprocal behavior is excluded and $\gamma_1 = \gamma_2$,

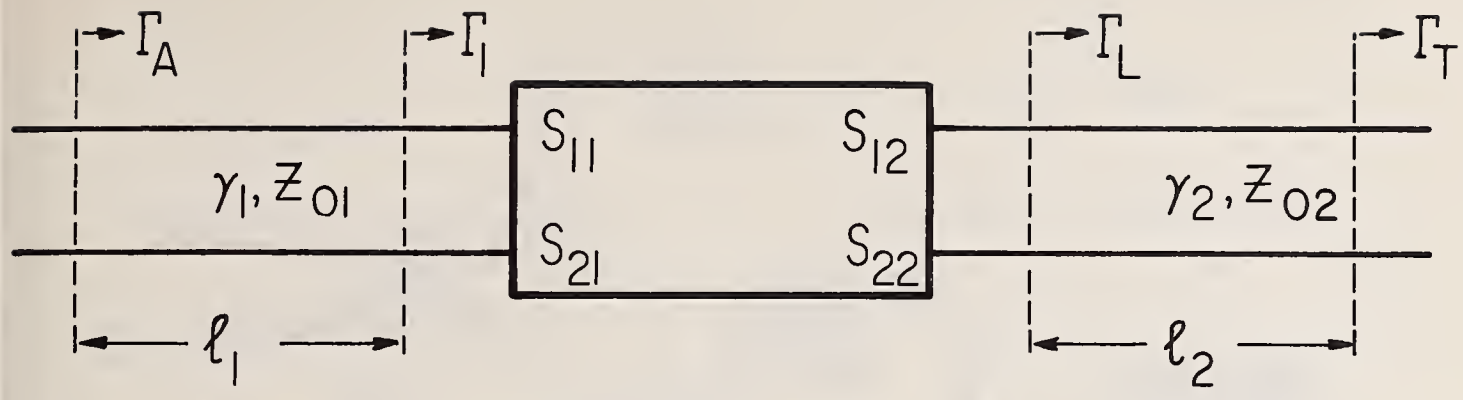

$$\Gamma_A = \Gamma_1 e^{-2\gamma_1 \ell_1}, \quad \Gamma_1 = S_{11} + \frac{S_{12} S_{21}}{\frac{1}{\Gamma_L} - S_{22}}, \quad \Gamma_L = \Gamma_T e^{-2\gamma_2 \ell_2}$$

Figure 5-34. 2-arm waveguide junction representation of waveguide joint.

$Z_{01} = Z_{02}$, then $S_{12} = S_{21}$, and only three are needed. If, in addition, the junction is symmetrical, $S_{11} = S_{22}$, and only two coefficients are required. If the junction is lossless or nearly so, then for practical purposes $|S_{12}| = |S_{21}|$ and $|S_{11}| = |S_{22}|$. It is sufficient for many purposes to determine only the VSWR corresponding to $|S_{11}|$ or $|S_{22}|$ and/or the efficiency η (for energy flowing into arm 1 and out at arm 2,

$$\eta_{21} = \frac{|S_{21}|^2}{1 - |S_{11}|^2}, \tag{5.76}$$

and for the reverse direction,

$$\eta_{12} = \frac{|S_{12}|^2}{1 - |S_{22}|^2}), \tag{5.77}$$

of a 2-arm junction terminated in a nonreflecting load. In practice, the direction of energy flow will make little difference in the efficiency of a low-loss connector (even if it is not physically symmetrical), for the reasons mentioned above. Similarly, the VSWR will be essentially independent of the direction of energy flow.

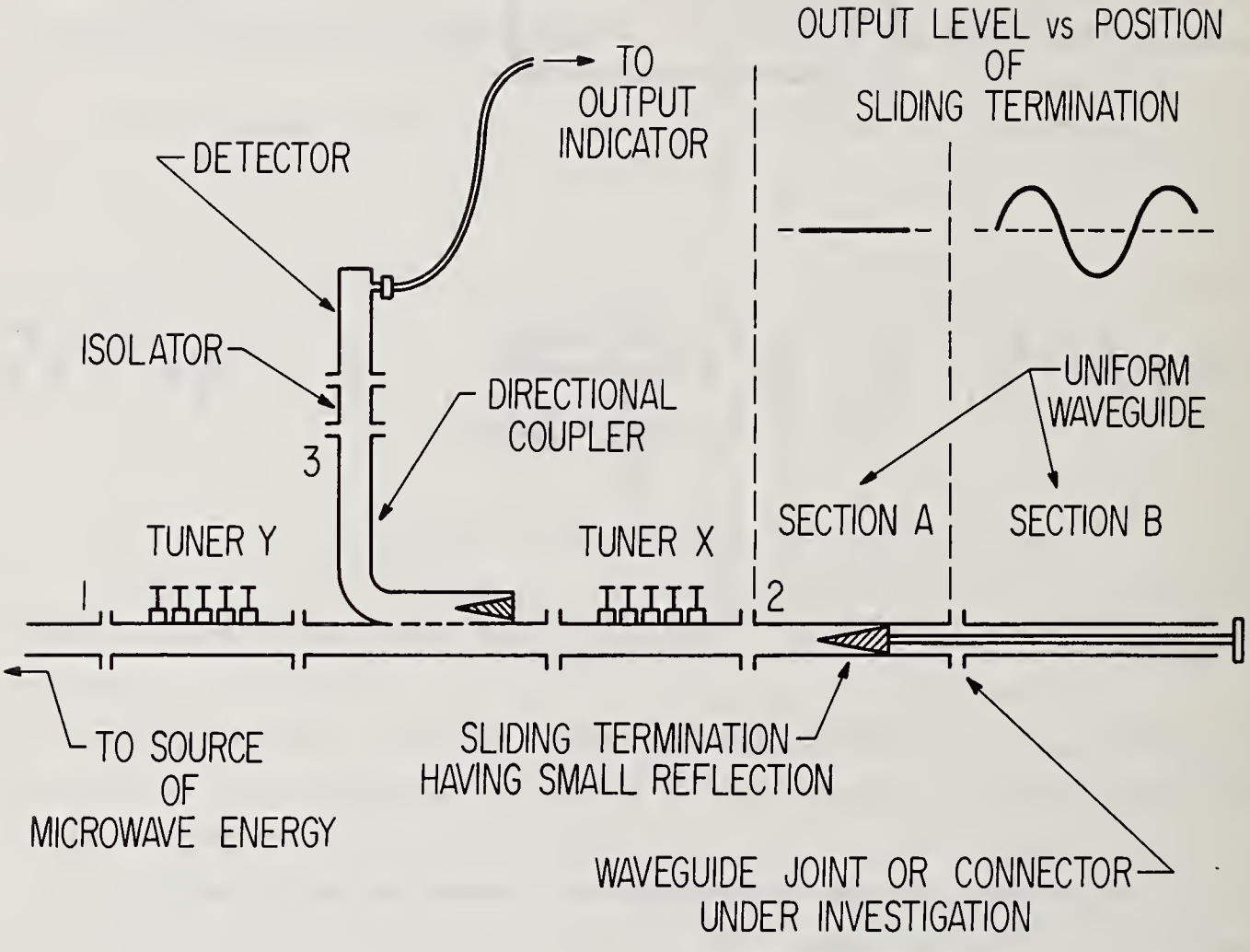

Figure 5-35. Reflectometer arrangement for measuring VSWR of waveguide joint.

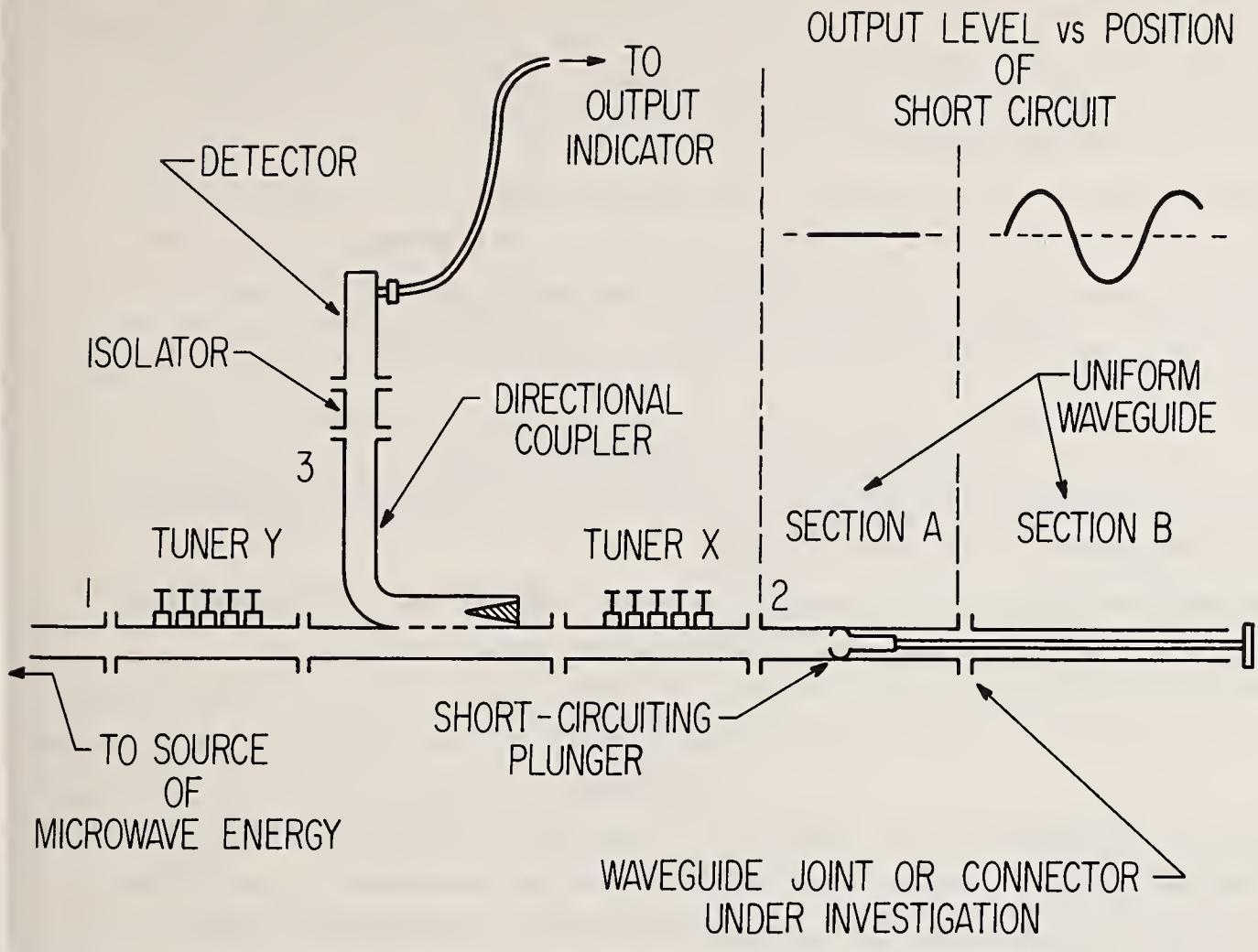

Figure 5-36. Reflectometer arrangement for measuring efficiency of waveguide joint.

c. Brief Description of Method

The measurement techniques used to obtain the VSWR and efficiency are illustrated in figures 5-35 and 5-36, respectively. In both cases, one uses a single directional coupler reflectometer employing two auxiliary tuners, X and Y, which are adjusted in turn in the following way. Tuner X is first adjusted so that the cyclical variations in the sidearm (arm 3) output as one slides a low-reflection termination in waveguide section A (fig. 5-35) are essentially eliminated. Then tuner Y is adjusted to achieve the same condition, as one slides a highly reflecting termination in waveguide section A (fig. 5-36).

The joint or connector under investigation is between the identical waveguide sections A and B. It is intuitively evident that if the joint or connector were perfect ($S_{11} = S_{22} = 0$, and $|S_{12}| = |S_{21}| = 1$), there would be no cyclical variations

in the sidearm output as one slid either termination from waveguide section A into section B. However, if the joint or connector were not perfect, it seems reasonable to expect that the adjustments made with termination sliding in section A would not hold when these terminations were transferred to section B.

This is actually the case, and the VSWR and efficiency of the joint can be obtained from the observed data in such an experiment. The presence of very small reflections is sensitively determined by the arrangement of figure 5-35 and the presence of very small losses by the arrangement of figure 5-36.

d. Review of Reflectometer Techniques

In order to interpret the above experiments and obtain quantitative results, we briefly review some reflectometer theory.

The amplitude b_3 of the wave emerging from the sidearm (arm 3 in figures 5-35 and 5-36) is related to the reflection coefficient Γ_A by eq. (3.162), or

$$b_3 = kb_G \frac{\frac{1}{K} + \Gamma_A}{1 - \Gamma_{2i}\Gamma_A}, \tag{5.78}$$

where b_G is the component of the incident wave amplitude furnished by the generator, K is a function of the scattering coefficients of the reflectometer, Γ_{2i} and k are also functions of these scattering coefficients and the reflection coefficients of the generator and detector, and finally Γ_A is the reflection coefficient terminating arm 2 of the reflectometer. The terminal plane of arm 2 is located in waveguide section A and may have any arbitrary position sufficiently removed from the joints so as to avoid higher modes. The term Γ_{2i} is the reflection coefficient of the equivalent generator at this reference plane, while K is practically equal to the directivity ratio of the reflectometer.

It is possible to adjust tuners X and Y to make both 1/K and Γ_{2i} vanish. Under these conditions eq. (5.78) becomes

$$b_3 = c\Gamma_A, \tag{5.79}$$

where $c = kb_G$. This factor will remain constant if the generator is stable and well isolated, the detector impedance terminating arm 3 is constant, and the tuner adjustments are stable. The detector output power P_D is proportional to $|b_3|^2$ or

$$P_D = p|\Gamma_A|^2. \tag{5.80}$$

The constant of proportionality can be determined if a reflection standard, such as a quarter wavelength short circuit, is connected to a waveguide section A. However, it can be eliminated from consideration by measuring only power ratios in which it cancels out.

e. VSWR Determination

The cyclical variations obtained as one slides the low-reflection termination in waveguide section B (fig. 5-35) occur as the reflection from the termination goes in and out of phase with the reflection from the joint. Assuming that the reflectometer has been adjusted so that eq. (5.79) applies, the behavior of Γ_A is of interest. As indicated in figure 5-34, it may be written in the form of eq. (3.10),

$$\Gamma_A = S_{11} + \frac{S_{12}S_{21}\Gamma_L}{1 - S_{22}\Gamma_L}, \tag{5.81}$$

where the $S_{m,n}$ are the scattering coefficients of the 2-arm junction representing the waveguide joint and short sections of waveguide on either side of the joint. Equation (5.81) may in practice be simplified to

$$\Gamma_A \simeq S_{11} + \Gamma_T e^{-2\gamma_2 \ell_2}, \tag{5.82}$$

since one uses a termination with small $|\Gamma_T|$ ($|\Gamma_T| < 0.005$) and the loss and reflection of the joint are small. Excluding nonreciprocal behavior of the joint, these considerations lead to the conditions $|S_{22}\Gamma_L| \ll 1$, and $|S_{12}S_{21}| \simeq 1$, which are necessary for the above simplification of eq. (5.81).

An illustration of eq. (5.82), neglecting attenuation of the waveguide, is given by the diagram of figure 5-37. The upper diagrams show the circular loci of Γ_A as Γ_T varies in phase, while the lower graphs show the corresponding variations in the output level of the sidearm. In each case, it is seen that

$$|b_3|_{max} = |c|(|S_{11}| + |\Gamma_T|), \tag{5.83}$$

where c is the same as in eq. (5.79).

The determination of $|S_{11}|$ proceeds as follows. Let $|b_3|_{sc} \simeq |c|$ represent the output level of arm 3, when a low-loss circuit terminates waveguide section A, and let $|b_3|_T \simeq |c\Gamma_T|$ represent the corresponding output level, when the short-circuit is removed and the sliding termination inserted in waveguide section A. First $|\Gamma_T|$ may be determined by measuring the ratio of $|b_3|_T$ to $|b_3|_{sc}$ with a calibrated variable attenuator, maintaining the detector output as a fixed reference level so as to make unnecessary any knowledge of the detector law. Second, the quantity $|S_{11}| + |\Gamma_T|$

is similarly determined from the ratio of $|b_3|_{max}$ to $|b_3|_{sc}$. Finally, $|S_{11}|$ is determined by subtraction. There are many refinements and variations of this basic technique, some of which are discussed later.

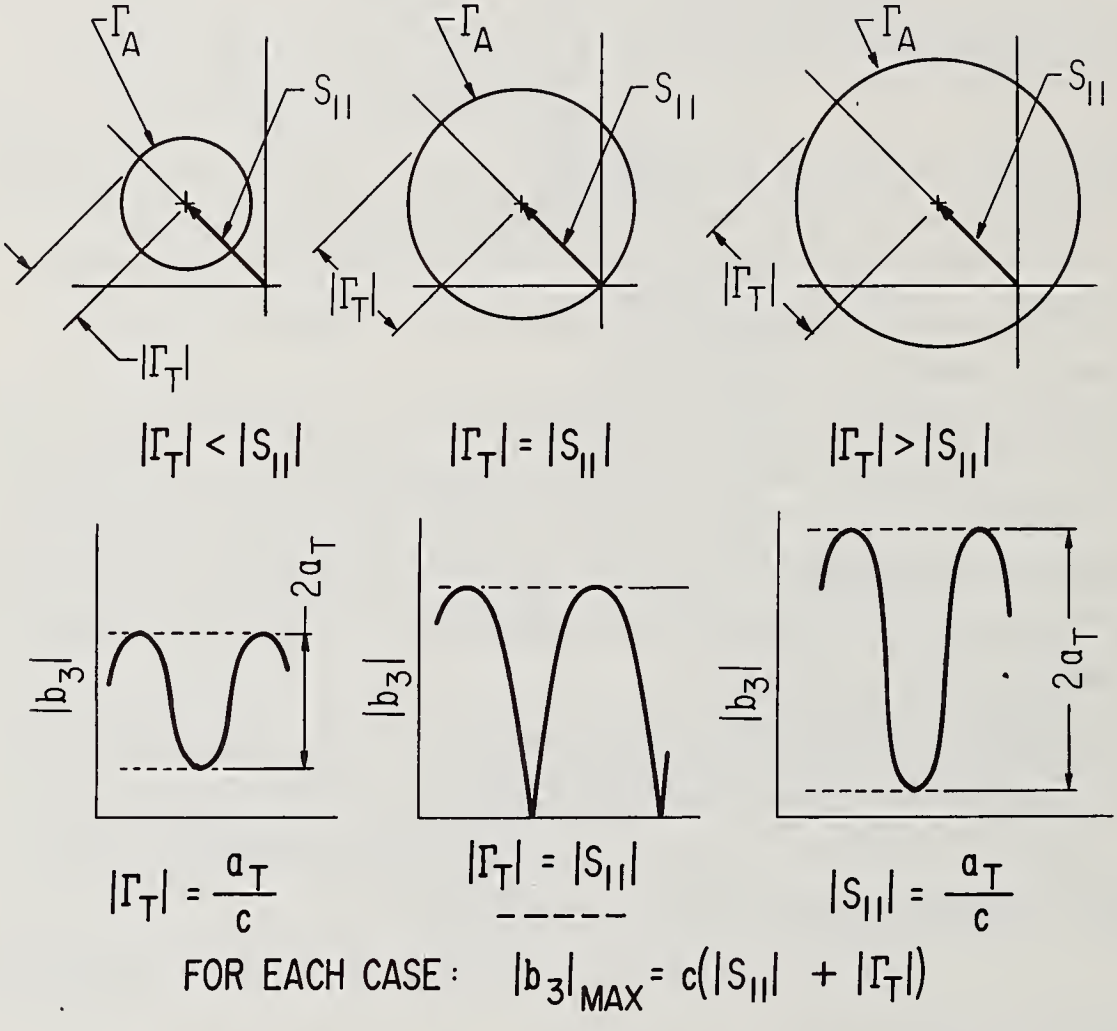

Figure 5-37. Reflection coefficient diagrams and detector response curves arising from eq (5. 82).

f. Efficiency Determination

In the 2-arm junction representation of a waveguide joint or connector, it is necessary to select terminal surfaces on either side of the joint to avoid appreciable higher modes at these surfaces. The length ℓ_T of waveguide between the two terminal surfaces will introduce some wall loss or attenuation in addition to the loss in the joint. The measured efficiency may be written

$$\eta = \eta_A \eta_J, \tag{5.84}$$

where $\eta_A = e^{-2\alpha\ell_T}$, the efficiency of a section of waveguide of length ℓ_T having an attenuation constant α, and η_J is the efficiency of the joint alone. (This separation of the effect of losses is not rigorous, but should hold closely in practice.)

The determination of η follows from previous work[10] in which one measures the radius of the circular locus of the input reflection coefficient as one slides a short circuit in the output waveguide. The situation may be represented by figure 5.34, in which Γ_T now denotes the reflection coefficient of the sliding short circuit. In a uniform waveguide section having finite attenuation, the locus of Γ_L is a logarithmic spiral converging toward the origin. However, this is transformed by the 2-arm junction, and the corresponding locus of Γ_1 is, in general, a distorted logarithmic spiral converging toward S_{11}. It is distorted because the spiral $1/\Gamma_L$ is displaced or translated an amount S_{22} before being inverted. The output level $|b_3|$ of the sidearm of the reflectometer in this general case exhibits variations as shown in figure 5.38. Analysis of the data in this case is not covered here. However, recent papers by Almassy (1971) and Engen (1972) are pertinent.

Fortunately, in many cases the reflection coefficient S_{22} is small and has negligible effect in distorting the spiral locus of Γ_A. In this event, one obtains data similar to that shown in figure 5-39. On each side of the transition length ℓ_T, it is appropriate to consider the waveguide lossless and apply the theory developed under this assumption. This theory is briefly as follows.

[10] See section 6.7, Cullen (1949) and Beatty (1950).

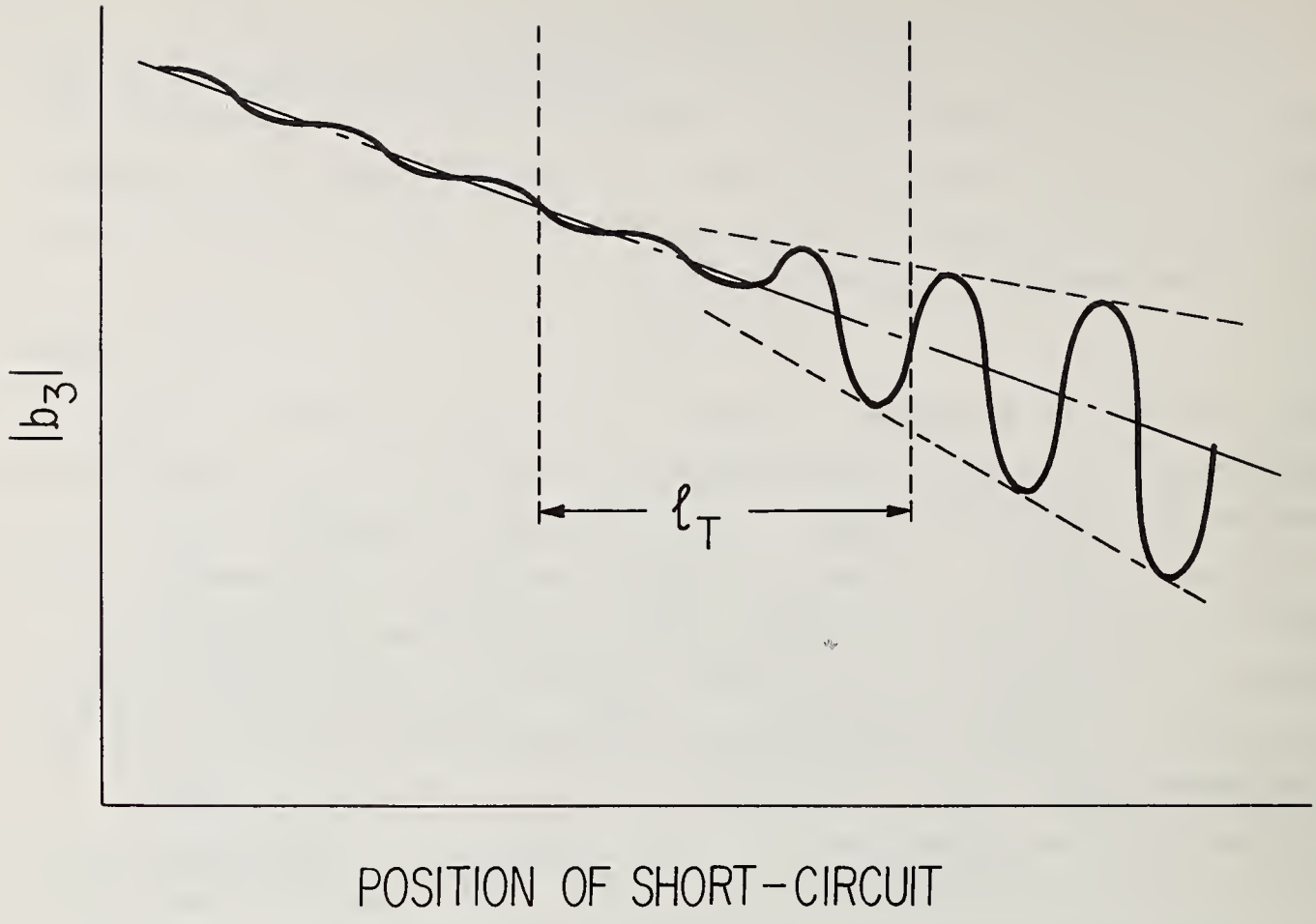

Figure 5-38. Detector output vs position of sliding short when reflection from joint is moderately large.

It was shown in section 3.13b, eq. (3.107), that the radius of the Γ_A-circle as the phase of Γ_T varies is

$$R_{21} = \frac{|S_{12}S_{21}\Gamma_T|}{1 - |S_{22}\Gamma_T|^2}. \tag{5.85}$$

The efficiency of a 2-arm junction with energy flowing into arm 2 and with arm 1 terminated in a nonreflecting load is

$$\eta_{12} = \frac{|S_{12}|^2}{1 - |S_{22}|^2}. \tag{5.77}$$

It is evident that to the extent that $1 - |S_{22}|^2$ equals $1 - |S_{22}\Gamma_T|^2$, and $|S_{12}S_{21}| = |S_{12}|^2$, then $R_{21} \simeq \eta_{12}|\Gamma_T|$. This approximation will be quite good if a low-loss short circuit is used. If the connector has low loss, it will very nearly be true that $|S_{12}| = |S_{21}|$, even if nonreciprocal behavior were permitted.

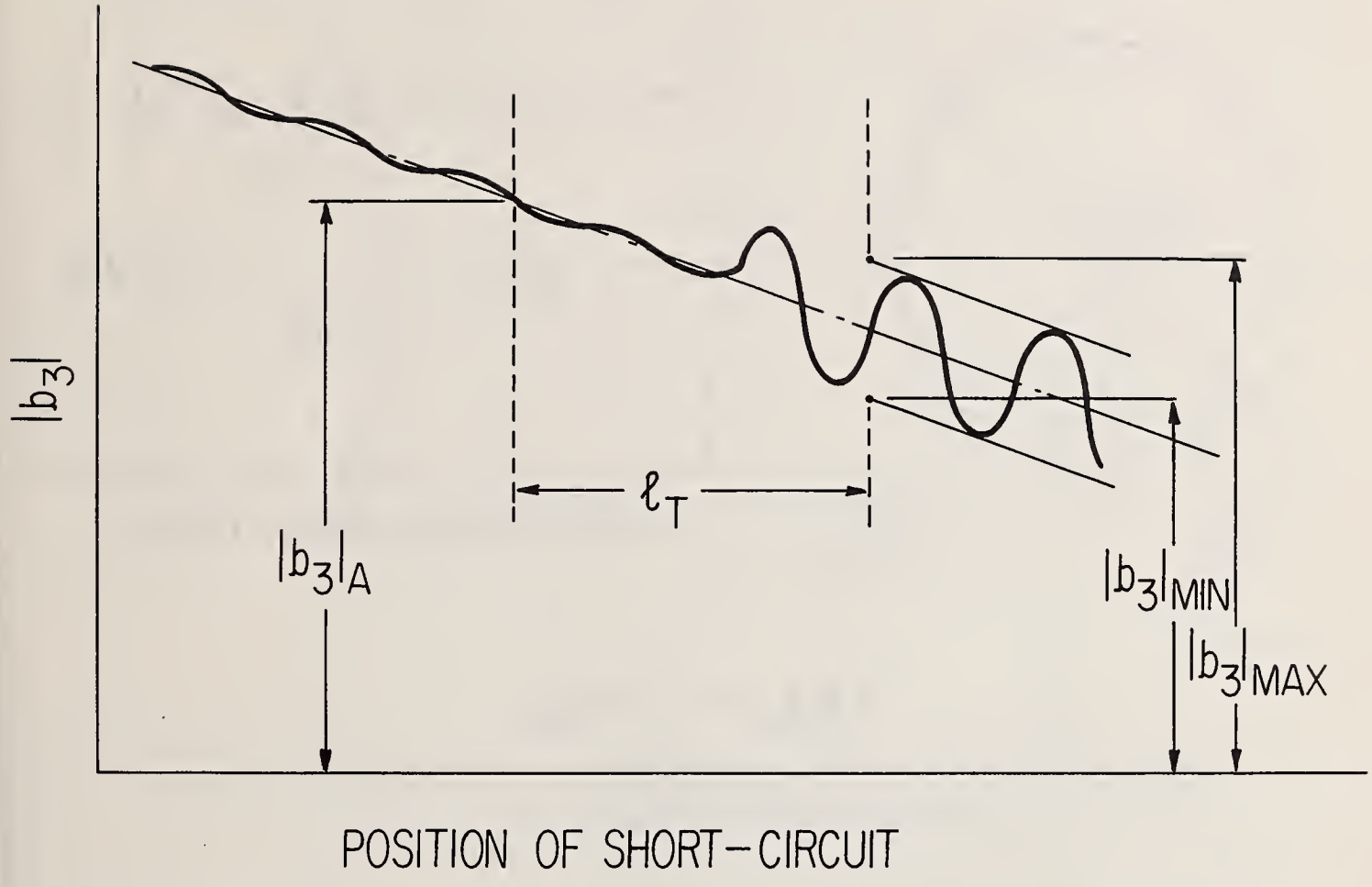

Figure 5-39. Detector output vs position of sliding short when reflection from joint is small.

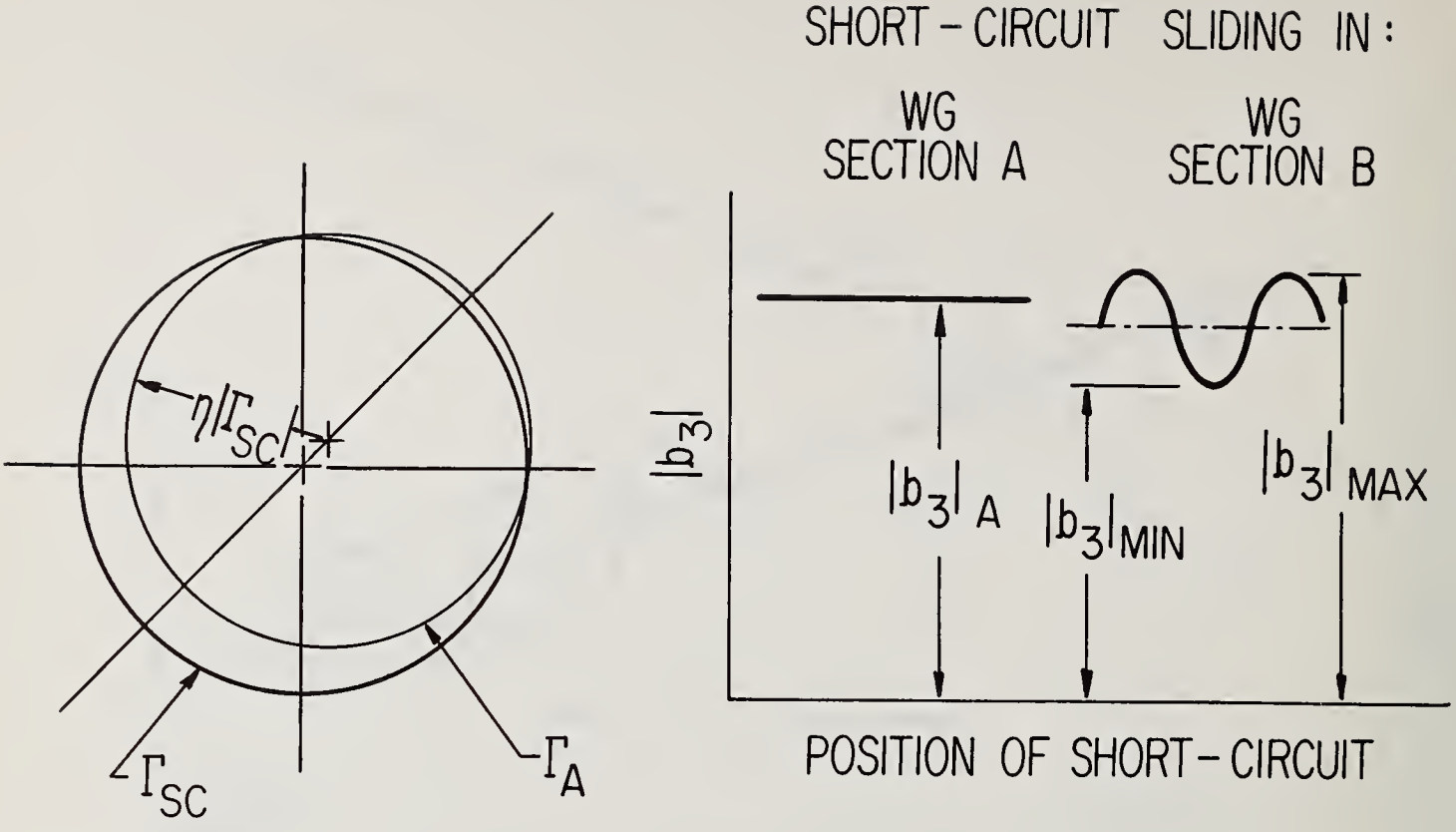

$$|b_3|_A = |c\,\Gamma_{SC}|$$

Figure 5-40. Reflection coefficient diagrams and detector response curves for a sliding short in lossless waveguide.

Referring to figure 5-40, it is apparent that

$$\frac{1}{2}\,\frac{|b_3|_{max} + |b_3|_{min}}{|b_3|_A} = \frac{\eta|\Gamma_{sc}|}{|\Gamma_{sc}|} = \eta, \tag{5.86}$$

since $\eta|\Gamma_{sc}|$ is the radius of the Γ_A-circle and the constant $|c|$ cancels. It is noted that $|\Gamma_T|$ has been replaced by $|\Gamma_{sc}|$.

It is convenient to use instrumentation developed to measure power differences directly, when observing the changes in the sidearm output as one slides the short-circuit. In order to obtain data as shown in figure 5-39, it would be necessary to plot the square root of the observed relative power. However, it is somewhat easier to analyze the data as obtained and take square roots of only the three points needed in the calculation of efficiency.

The attenuation of the waveguide sections is obtained from the slope of the square of the curve to the left of ℓ_T in figure 5-39. If P_1 and P_2 are the side arm powers corresponding to two positions of the short circuit spaced a distance ℓ, the attenuation constant α may be calculated from the expression

$$e^{-4\alpha\ell} = \frac{P_2}{P_1}, \tag{5.87}$$

where P_2 is smaller than P_1.

g. Supplemental Techniques in VSWR Determination

In the technique described for measuring the VSWR corresponding to $|S_{11}|$ of the 2-arm junction representing the waveguide joint or connector, it was assumed that $|1/K|$ was much smaller than $|S_{11}|$. When dealing with very small reflections, the reduction of $|1/K|$ to even smaller values may become difficult, and a number of supplemental techniques have been developed for the solution to this problem.

The behavior of the detector output as one slides a termination having a small reflection ($|\Gamma_T| << 1$) in waveguide section B may be described by

$$b_3 \simeq kb_G\left(\frac{1}{K} + S_{11} + |\Gamma_T|\, e^{j\psi}\right). \tag{5.88}$$

In general, the previous technique for obtaining $|S_{11}|$ will yield $|(1/K) + S_{11}|$ instead. If $|1/K| << |S_{11}|$, there is no difficulty, but if this is not true, we cannot determine $|S_{11}|$ even if we knew $|1/K|$, because the phase difference between the two terms is unknown. It then becomes important either to reduce $|1/K|$ until it is much less than $|S_{11}|$ and to know when this is the case, or to employ a technique in which the relative phase of $1/K$ and S_{11} can be varied so as to separate their magnitudes.

In adjusting tuner X to reduce $|1/K|$ to a small value, it is necessary to avoid the possible false adjustment which could result in approximately constant output if $|1/K| >> |\Gamma_T|$. One way to do this is to begin the adjustment of tuner X with all stubs out of the waveguide, and then adjust for a detector null with the sliding termination in an arbitrary fixed position in waveguide section A. Under this condition, $1/K = -\Gamma_T$, and if the termination is then displaced for maximum detector output, the level will be $|b_3| = 2|c\Gamma_T|$. The adjustment of tuner X is then continued until an essentially constant output level is obtained as one slides the termination, for which the detector level should be approximately half the above level, or 6 dB down.

One should know when to stop trying to improve the adjustment of tuner X so as to avoid needless tedium. This may be done with the aid of figure 5-41, as illustrated in the following example. Suppose that $|S_{11}|$ approximately equals 0.00025 and that it is considered sufficient to reduce $|1/K|$ to one tenth of this value or 0.000025. (The corresponding error in determining $|S_{11}|$ by the previously described technique would then be less than 10 percent.) If the sliding termination has a VSWR of 1.003, the graph shows that the adjustment of tuner X can cease when the total variation of the detector output is within 0.3 dB. This example is representative of what can be done with commercially available components.

The supplemental techniques to be described are included as alternate ways to reduce $|1/K|$ or to prevent error in measuring $|S_{11}|$ because of finite $|1/K|$.

1) The method which is potentially the most powerful in reducing $|1/K|$ is similar to that described above, except that in place of a sliding termination of constant $|\Gamma_T|$, an adjustable sliding termination (Beatty, 1957) is used. One alternately adjusts both tuner X and the termination, so that the sidearm output is reduced to a lower and lower constant value as the termination is slid. By doing this, both $|1/K|$ and $|\Gamma_T|$ are reduced together. It is often found that the adjustment is limited, not by the sensitivity of the detector to respond to the small reflected signal, but by the ultimate failure of $|\Gamma_T|$ to remain constant as the termination is slid. However, a return loss of 100 dB has been obtained with suitable adjustable sliding terminations. This corresponds to $|1/K|$ certainly less than 0.00001. It could be considerably less, depending upon the observed variations in detector output.

Apart from the reduction of $|1/K|$, an adjustable sliding termination may be used in the measurement of $|S_{11}|$ as follows. Referring to figure 5-37, it is apparent that the detector output will vanish if $\Gamma_T = -S_{11}$. This condition can be easily achieved and recognized if an adjustable sliding termination is used. Subsequently, without changing the adjustment, the termination is slid until the detector output is a maximum and proportional to the sum of $|S_{11}|$ and $|\Gamma_T|$ or $2|S_{11}|$. Comparing this output level to that obtained when the termination is removed and replaced by a short circuit will eliminate the constant of proportionality and permit determination of $|S_{11}|$.

2) An auxiliary waveguide channel[11] arranged as in figure 5-42 permits introduction of a signal to the detector of such a phase and magnitude so as to cancel the

[11]The circuit is quite similar to one used in the determination of barretter mount efficiencies by an impedance technique.

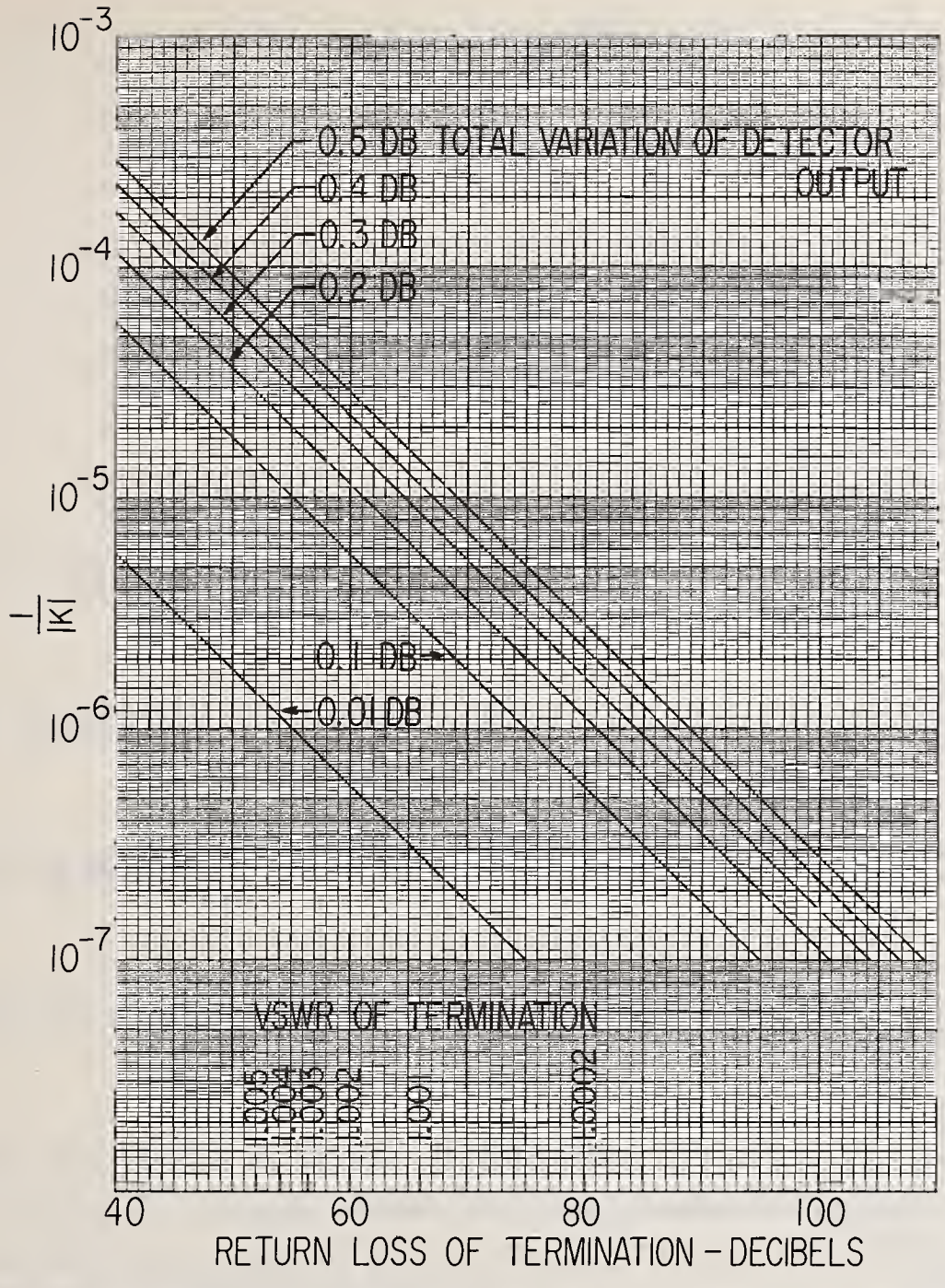

Figure 5-41. Graph for determining $|1/K|$ from variation in detector output as a low-reflection termination is slid in the waveguide section A.

signal component due to finite 1/K. As is indicated by the vector diagrams, the procedure begins with the adjustment of tuner X for a detector null, whereupon $1/K = -\Gamma_T$. The sliding termination is then moved to a position where the detector output is maximum, changing the phase of Γ_T by 180°, so that the signal components from Γ_T and 1/K add. The switch in the auxiliary arm is now opened, introducing a signal component "A" to the detector. The amplitude and phase of this component are adjusted using the

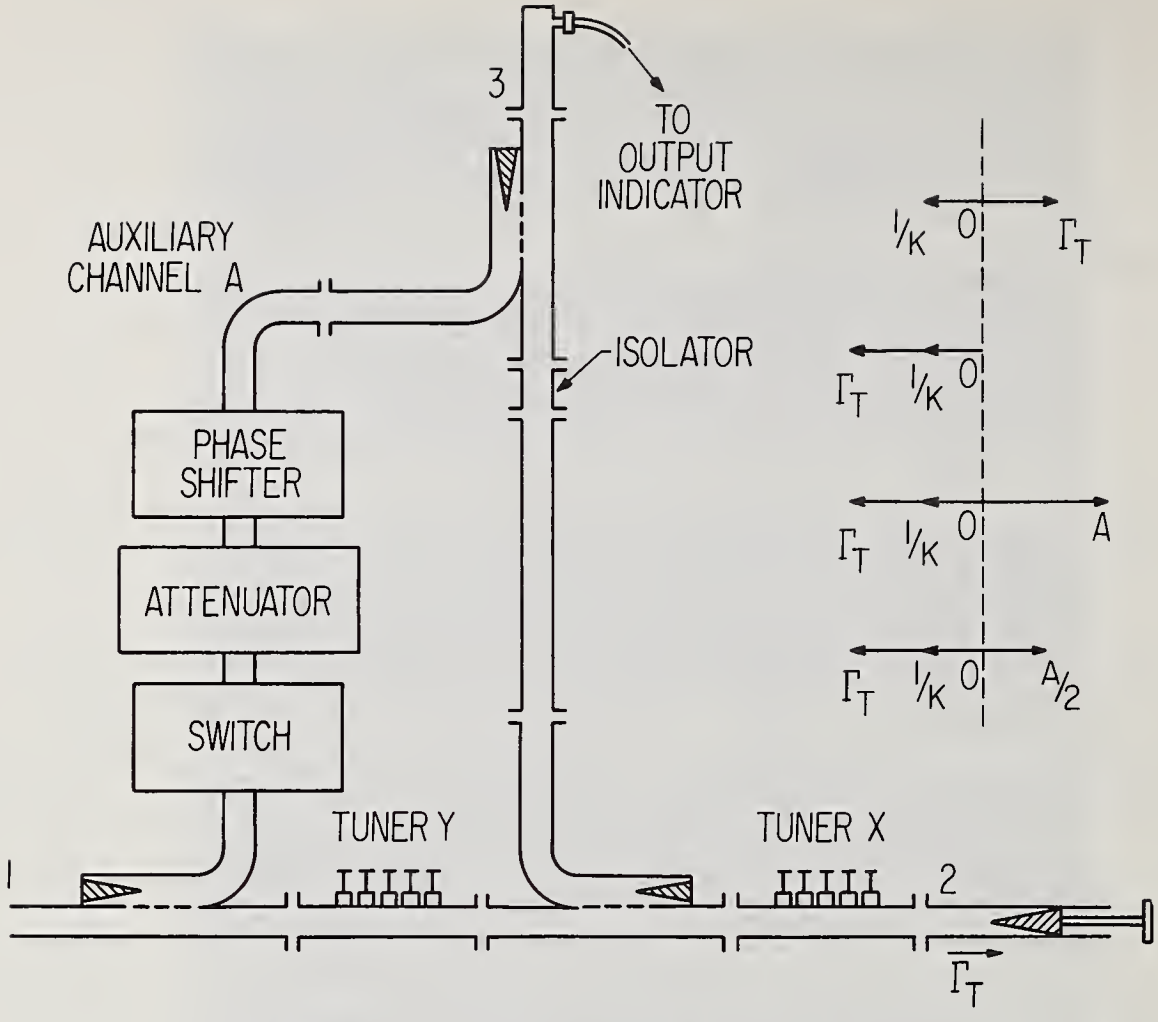

Figure 5-42. Auxiliary channel technique.

phase shifter and variable attenuator to null the detector output. It is apparent from the diagram that "A" is in phase opposition to the 1/K signal component and will cancel it if reduced in amplitude by one half without changing its phase. This is done by adding 6.02-dB attenuation in the auxiliary arm. The measurement of $|S_{11}|$ can now proceed in the manner discussed previously.

Additional tuning (not shown) could be employed to prevent possible interaction between the two channels; however, the isolator shown in the figure should prove adequate for this purpose. The resulting adjustment can be checked by means of the procedure associated with figure 5-41, and it is possible that $|1/K|$ will not be small enough. This could easily be the case if the attenuator did not accurately produce the 6.02-dB change required, or produced some phase shift. Further adjustment of either tuner X or the phase shifter and attenuator would then be necessary

to reduce |1/K| to the desired value. In case of difficulties in obtaining fine adjustments of the tuner, the latter procedure is quite convenient and can provide good resolution.

3) An extension of the previous technique in which a second auxiliary channel is employed permits cancellation of the 1/K signal component without the use of a calibrated attenuator. The arrangement is similar to that of figure 5-42, except for the addition of another similar channel. Vectors representing detector signal components from 1/K, Γ_T and channels A and B are shown in figure 5-43, corresponding to

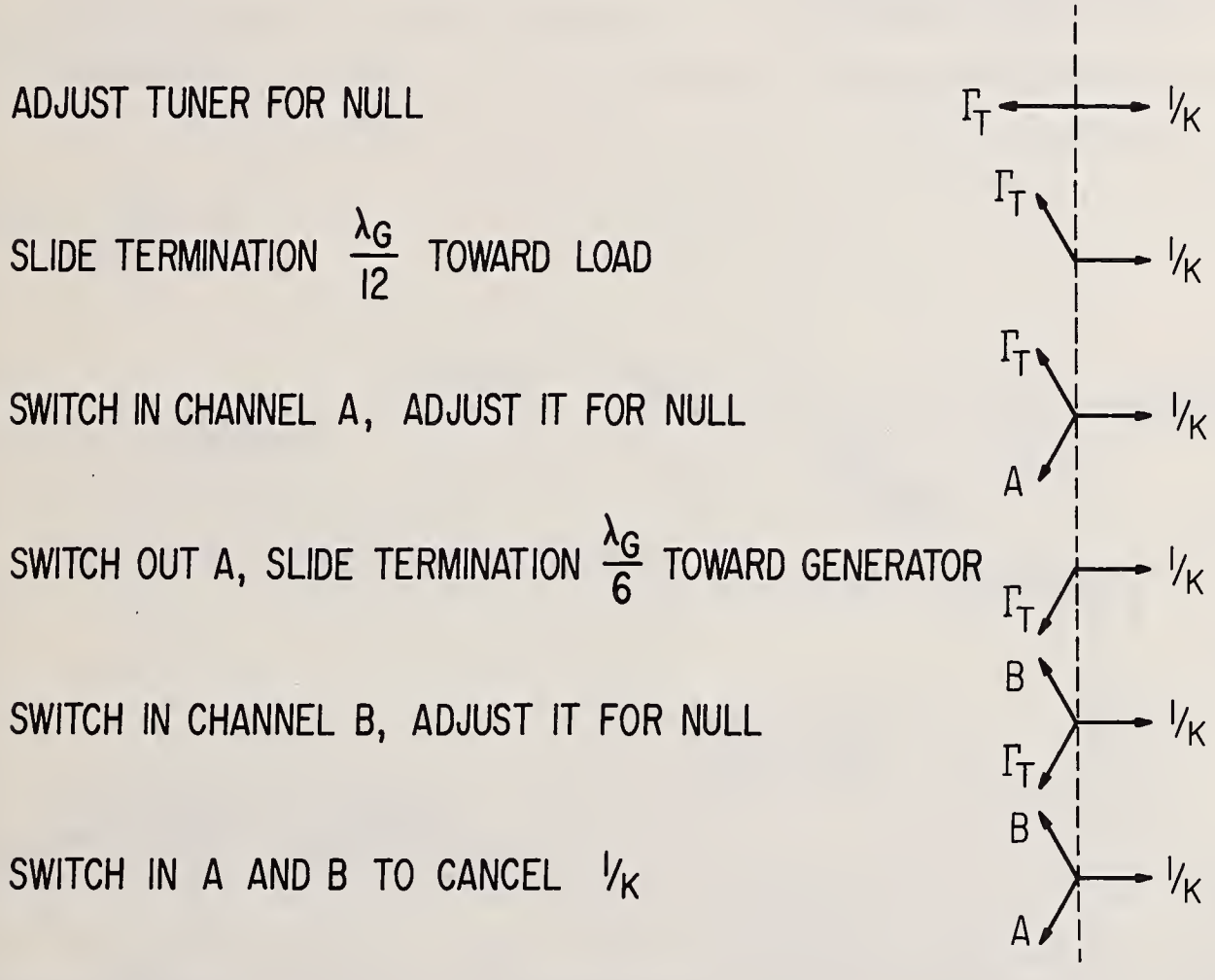

Figure 5-43. Steps in a technique employing two auxiliary channels.

the steps in the procedure mentioned in the figure. Although a calibrated attenuator is not required, it is necessary to vary the phase of Γ_T by prescribed amounts, so that a micrometer drive for the sliding termination is convenient.

4) The relative phase of 1/K and S_{11} may be varied by means of the line stretcher arrangement shown in figure 5-44. Alternate manipulation of the line

stretcher and the sliding termination to obtain maximum detector output results in alignment of the vectors representing 1/K, S_{11}, and Γ_T, as shown in figure 5-45. The remaining steps in the procedure and the corresponding vector diagrams and pertinent equations are shown in the figure. It is apparent that the ratio of $|S_{11}|$ to $|\Gamma_T|$ equals the ratio of $|b_3|_{min}$ to $|b_3|_{max}$. If $|\Gamma_T|$ is known or determined independently, then $|S_{11}|$ may be calculated. In order to deal with conveniently measured ratios, one should use a termination having a $|\Gamma_T|$ not greatly different from $|S_{11}|$.

5) Another technique employing the same arrangement as in figure 5-44 is as follows. Tuner X is adjusted for minimum variations in detector output as a low-reflection termination slides in the waveguide section in which terminal surface 2 is located. This reduces |1/K| to a small value; then, the three vectors 1/K, S_{11}, and Γ_T are lined up as described in the previous technique. One adjusts tuner Y

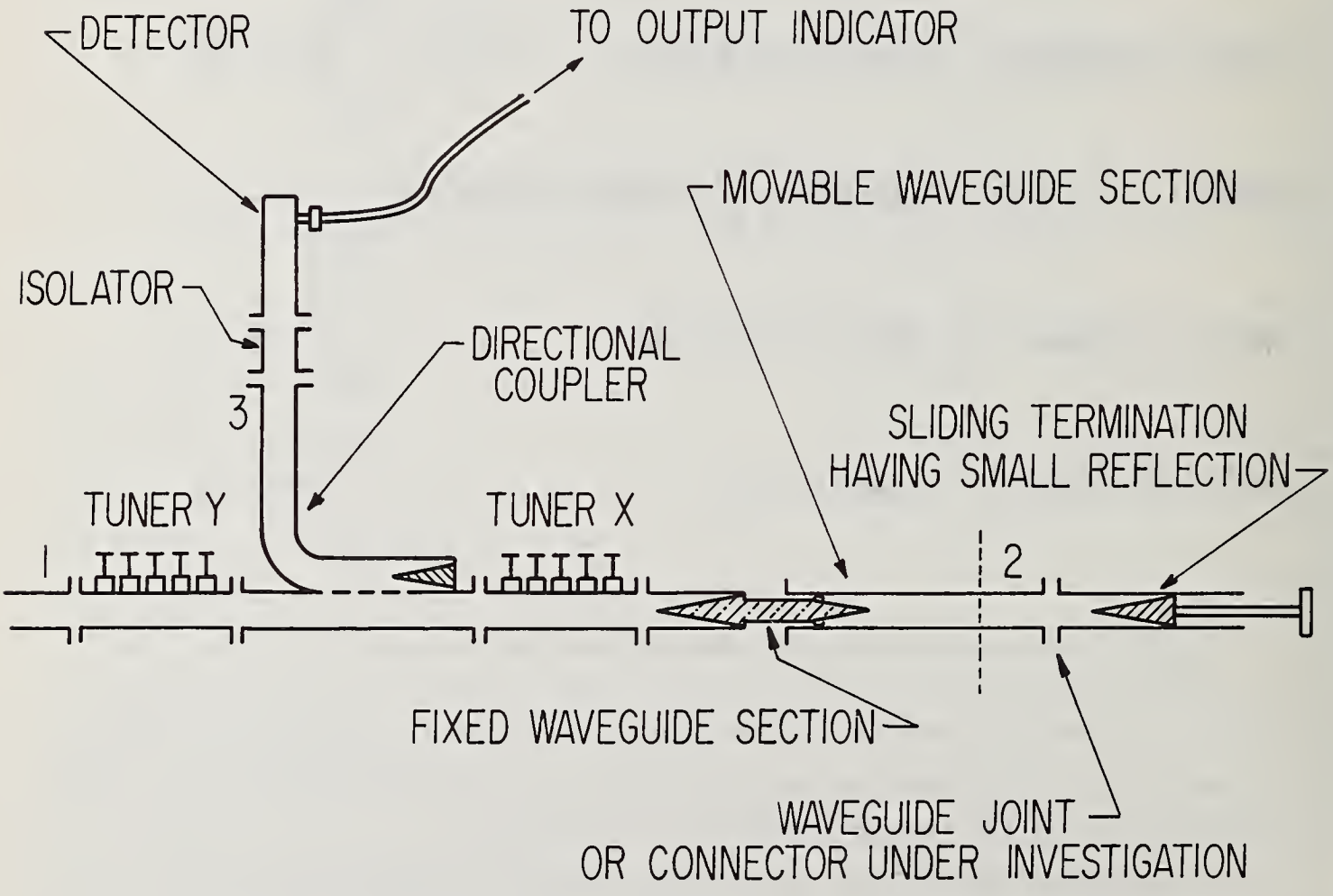

Figure 5-44. Arrangement for varying relative phase of 1/K, S_{11}, and Γ_T.

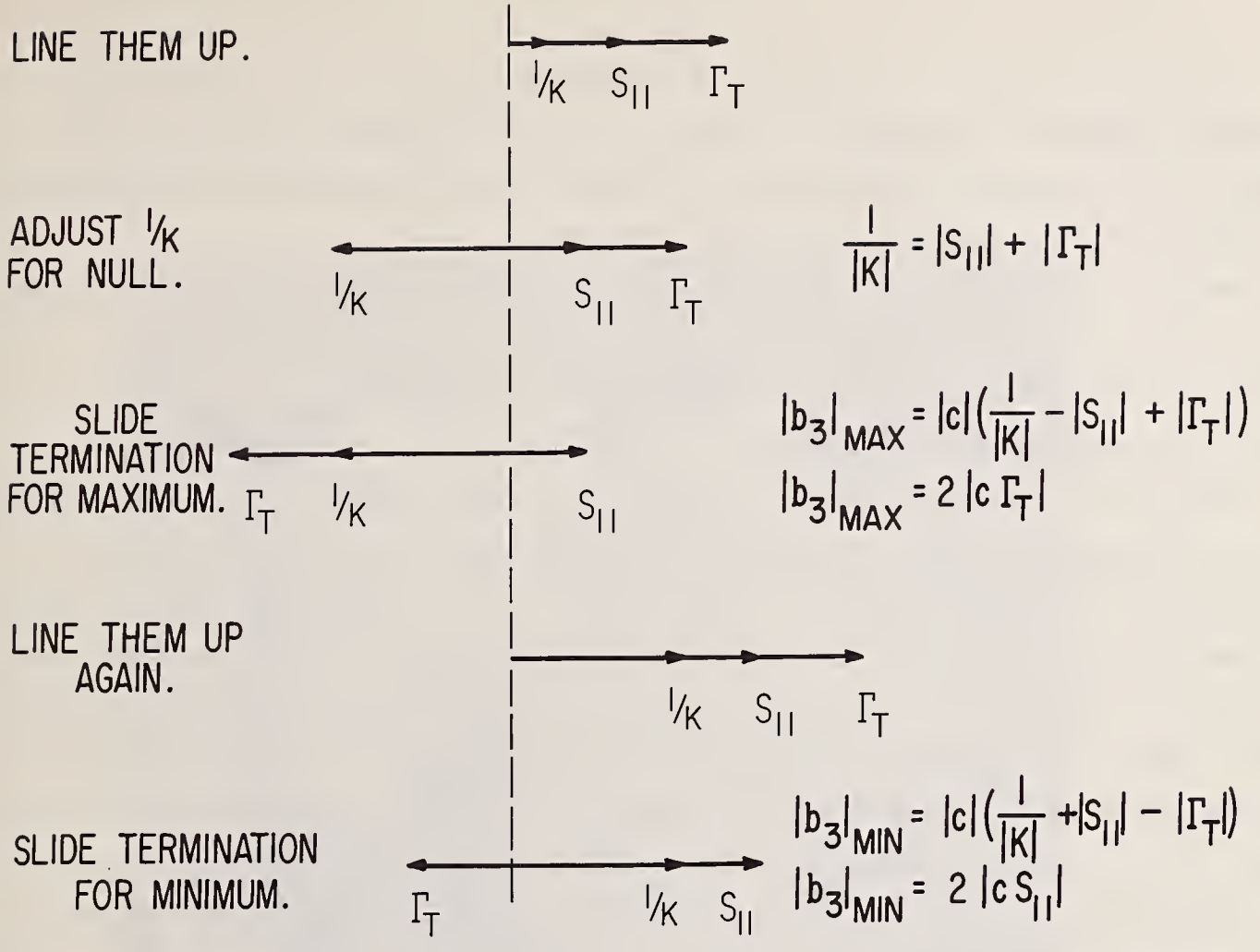

Figure 5-45. Steps in a technique for determining $|S_{11}|$ in terms of $|\Gamma_T|$.

until the detector output variations are minimized as a short circuit is slid in the waveguide section. The detector output level $|b_3|$ will now be proportional to the sum of $|1/K|$, $|S_{11}|$, and $|\Gamma_T|$. The constant of proportionality may be eliminated, in the usual way, by taking the ratio of this output to that obtained when the waveguide section is terminated in a high-quality short circuit. One then determines $|\Gamma_T|$ and $|1/K|$ independently by methods previously described and finally calculates $|S_{11}|$.

h. Results

The techniques described above are applicable in principle to waveguide systems employing waveguide of rectangular, coaxial, or any kind of cross section. However, experimental results have been obtained in a WR90 (X-band) rectangular waveguide system operating at a frequency of approximately 9.39 GHz.

The effects of lateral displacement upon the reflection and efficiency of a plane butt joint in rectangular waveguide were investigated; a few measurements were performed on other types of joints, and the attenuation constants of some short sections of waveguide were determined.

Figure 5-46 is a photograph of the arrangement used to obtain prescribed repeatable lateral displacements of the waveguide at a simple butt joint. Clamps were used for alignment and to insure repeatability, and strips of shim stock of various thicknesses were used to obtain the prescribed displacements. The heavy brass flanges shown were originally one piece. It was soldered in the center of a section of uniform waveguide and the edges were machined flat and square; then it was cut so as to separate into two sections of waveguide, each with its own flange. The mating surfaces were then ground so as to be flat and square.

The initial alignment was checked by visual inspection. A flashlight was used to illuminate the interior of the waveguide, and reflections of light from any visible edges at the joint proved to be a sensitive indication of misalignment or mechanical imperfections, such as burred edges. In spite of care taken to obtain good alignment, the reflection coefficient of the joint was never below 0.00015, and in the results shown, was approximately 0.00071.

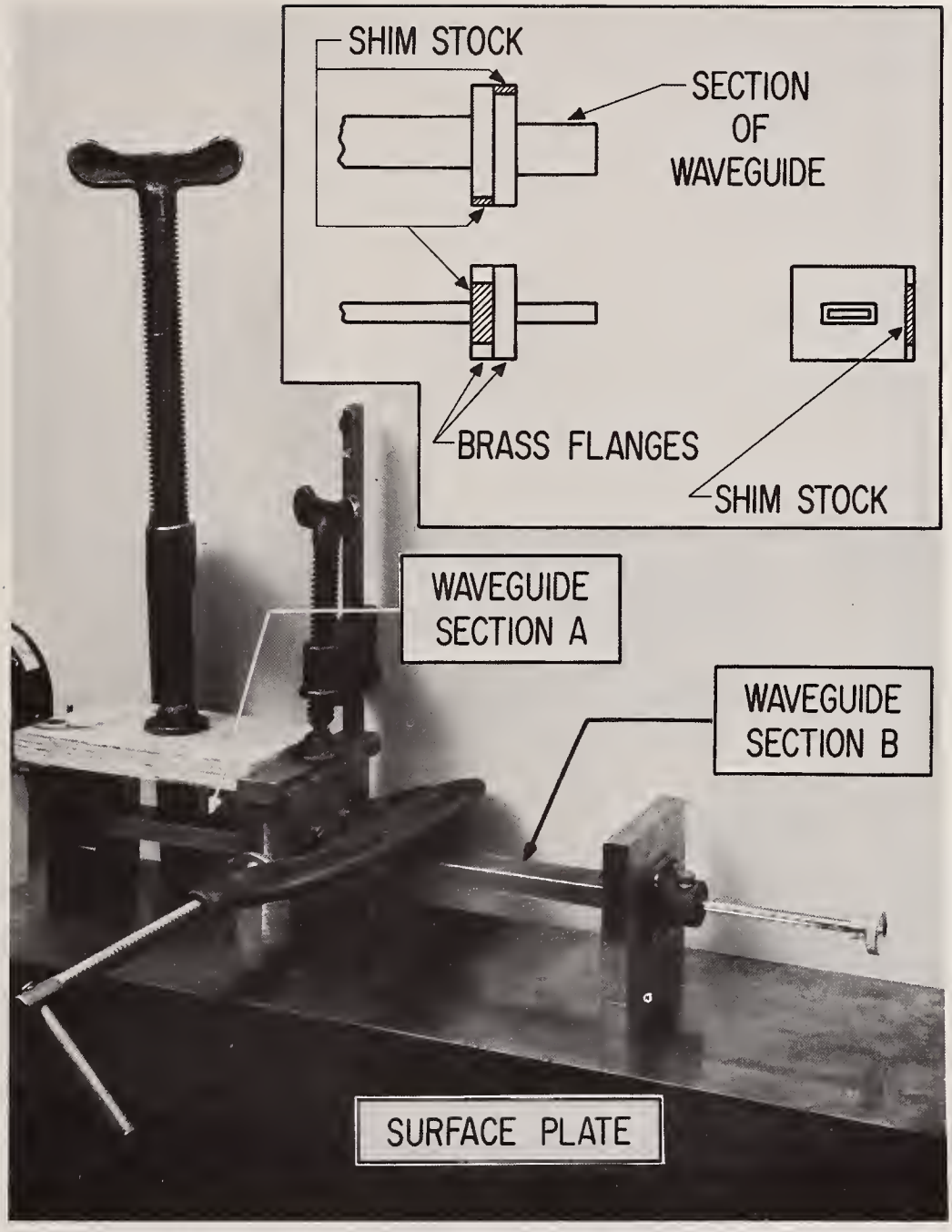

Figure 5-46. Photograph of alignment and clamping apparatus for waveguide joint.

A comparison of experimental and calculated results is shown in figure 5-47. The calculated curve is based upon the equation shown, which differs from that given by Kienlin and Kürzl (1958) by a factor of two, but agrees (when corrected for the different ratio of f to f_c) with the appropriate curve given in their figure 5. The agreement is quite good over a limited range, but it is apparent that the residual reflection that one obtains at zero displacement prevents agreement at the low end. It is probable that the approximations made in deriving the equation contribute to the disagreement at the other end.

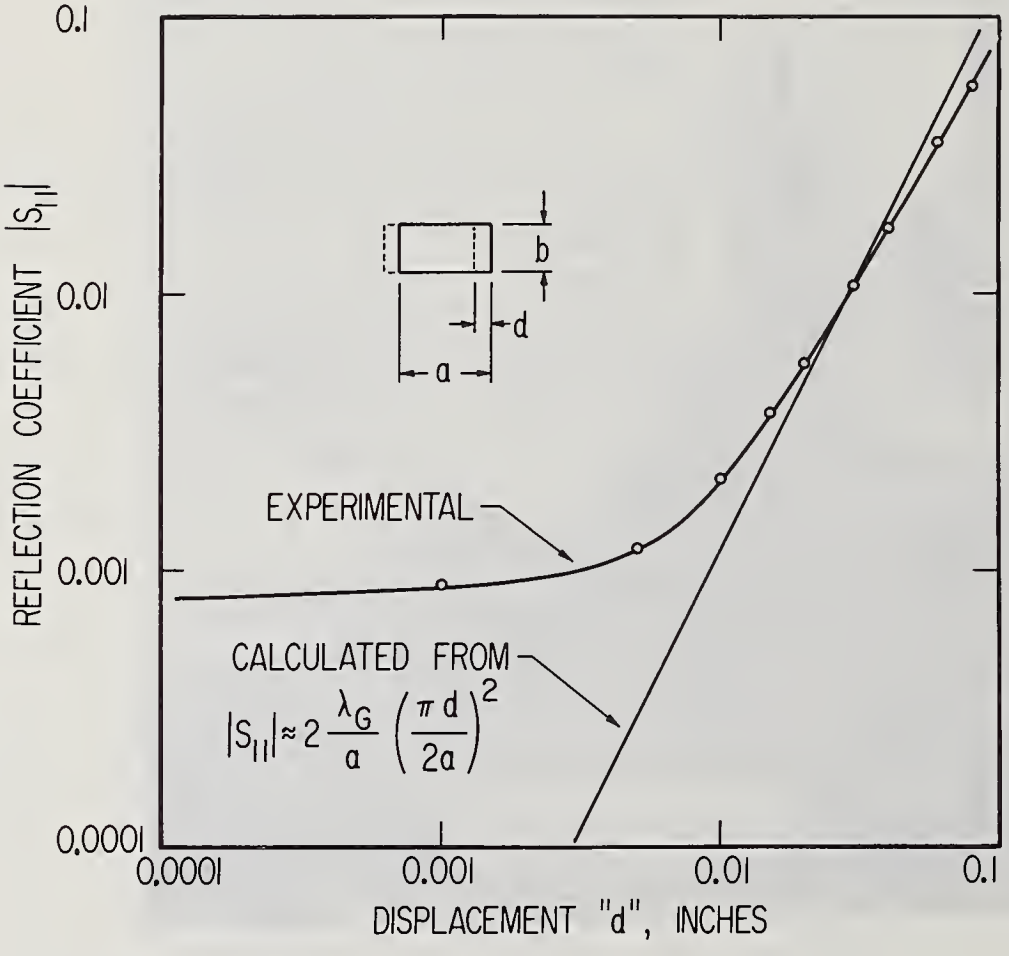

Figure 5-47. Measured and calculated reflections from junction of displaced waveguide sections.

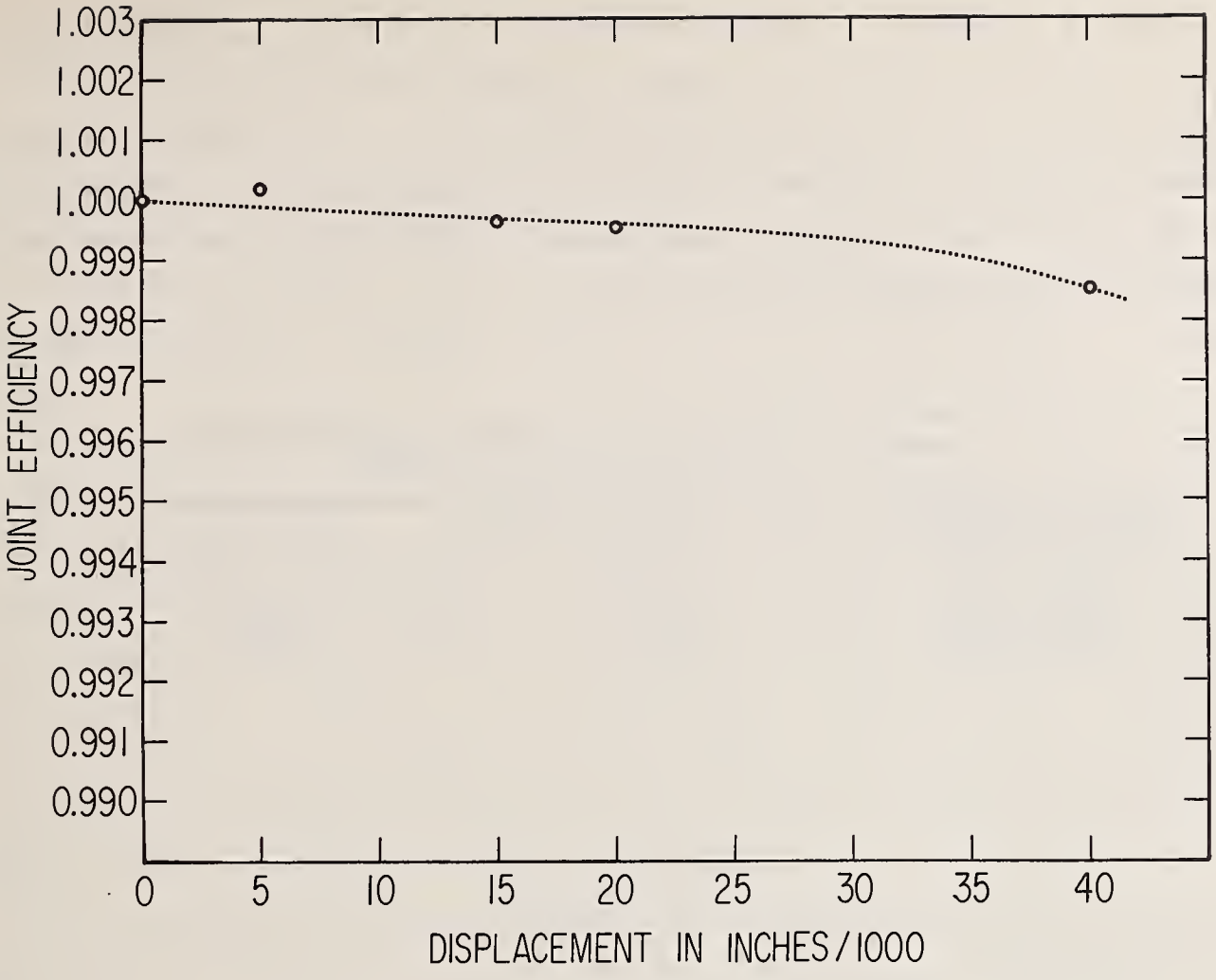

Figure 5-48. Measured efficiency of junction of displaced waveguide sections.

A plot of observed data obtained in an efficiency measurement is shown in figure 5-39. The attenuation constant of the brass waveguide as determined from the slope of the squared curve is 0.056 dB per foot. Measurements were made of the efficiency of the same butt joint described above for the same lateral displacements and the results are shown in figure 5-48. It is not known whether or not the results are representative of this type of joint, since the loss would be expected to depend on the surface finish and cleanliness of the metal at the contacting surfaces, as well as other factors.

The results of additional measurements on commonly used types of joints are given in table 5-3. Again the results may or may not be representative, but were obtained with careful alignment of the waveguides and cleaning of the joint surfaces. It should be noted that the waveguide sections united by a joint were originally a single section of waveguide which was sawed in half. Thus, there is very little, if any, change in the waveguide cross section at any of the joints.

Table 5-3. Reflections and losses of some joints, in WR-90 (X-band) rectangular waveguide measured at 9.39 GHz.

TYPE OF FLANGES USED WITH BUTT JOINT	REFLECTION COEFFICIENT $\lvert S_{11} \rvert$	EFFICIENCY
CHOKE-COVER	0.00064	0.9996
CHOKE-COVER	0.0015	0.9993

6. Attenuation

6.1. Introduction

In attempting to set up National standards of attenuation in the U.S.A. and to compare these with the standards of other countries, the first concern is for a precise definition of what is to be measured and for tight specifications of the measurement conditions. A quantity cannot be accurately measured unless it is sharply defined.

Unfortunately, the term "attenuation" has been defined by many people in many ways so that there is not perfect agreement on what the term really means. Also, the conditions under which it is to be measured have not been carefully specified.

In 6.2, the general meaning of the term is examined, as well as various specialized meanings that have been used. Although the term "attenuation" has been used in various fields and scientific disciplines, its use in electrical and electronics engineering is of main concern in this monograph. Various definitions, such as those published by the American Institute of Electrical Engineers (AIEE), the Institute of Radio Engineers (IRE), and other are discussed and compared.

Using a simple 2-port network representation of a two-port device, equations are given based on the various definitions. By means of the equations, quantitative differences in various attenuation concepts are clearly shown. Examples are given for typical cases.

It is concluded that existing definitions are in some cases contradictory, and in all cases imprecise. Therefore they are inadequate to form a basis for accurate attenuation measurements. A set of definitions is proposed which is based upon specific measurement procedures and precisely specifies the conditions under which the measurements are to be made. Errors in making attenuation measurements due to not perfectly satisfying the specified conditions are discussed. The use of models representing the attenuator or 2-port device and the measurement system is discussed and more complicated models are proposed. Finally, the concept of representing the behaviour of 2-port devices with terminal-invariant parameters is discussed.

Following the discussion of attenuation definitions, specific research is described in developing methods of attenuation measurement and in analyzing errors. For example, in 6.3, the representation of a 2-port device by an idealized linear

2-port network having uniform lossless waveguide leads is used to analyze the cascading of attenuators, and equations are derived for the error one can make in adding individual attenuations to obtain the total attenuation of a cascaded pair or group.

Similarly, in 6.4, the mismatch errors one can make in the calibration and use of fixed and variable attenuators are analyzed. The limits of uncertainty due to mismatch are usually determined by assuming that the phases of the interacting reflections can have any value. However, it is known that the realizability conditions on linear, passive 2-ports restrict the range over which the phases can vary in particular cases. In 6.5, the effect of applying the realizability conditions to the estimation of mismatch error limits is analyzed and discussed.

In most cases where particularly high accuracy in attenuation measurement is not required, the representation of an actual 2-port device by an idealized linear 2-port network having uniform lossless waveguide leads is satisfactory. However, if the accuracy is to be improved in the future, more complicated models, such as that in 6.6, will be needed.

The development of a method for measuring attenuation by measuring the radius of a reflection coefficient circle is described in 6.7. The achievement in 1960 of unprecedented accuracies in attenuation measurement by the use of a very stable power measurement system is described in 6.8.

A method for measuring very small attenuations of low-loss components, such as short sections of waveguide and waveguide joints, was developed using a 2-channel RF nulling technique. The method is described in 6.9 and it is shown how to avoid errors due to losses in waveguide joints and due to changes in losses in variable phase shifters.

Finally, in 6.10, the development of an attenuation divider circuit is described. This circuit makes possible the production of very small accurately known attenuations, such as 0.0001 decibel.

6.2. Definition of Attenuation

a. Introduction

The accuracy with which attenuation can be measured depends upon the limitations of the measuring equipment and methods, the stability and other characteristics of the devices to be measured, and ultimately upon how sharply the quantity to be measured and the conditions of measurement have been defined and specified.

The latter point is discussed in some detail in the following sections. A number of existing definitions, particularly those published by the two institutes which merged to form the IEEE (Institute of Electrical and Electronics Engineers) are examined and compared. A quantitative comparison is made possible by deriving equations based upon a simple 2-port waveguide junction model.

The terminology used in writing and talking about the attenuations of attenuators is discussed, and some concurrence is noted to exist in a confused situation. However, it is recognized that the actual definitions are more important to the achievement of higher accuracy than the terminology. Rather than suggest changes in terminology, improved definitions are proposed, which sharply define the quantity to be measured and the measurement conditions.

Finally, possible future trends, such as the use of more complicated models for analysis, or the use of terminal-invariant parameter definitions are discussed.

b. Broad General Meaning

The word "attenuation" comes from the Latin "attenuatio" which is built from the simpler words "ad" meaning "to," and "tennuis," which means "thin." It generally refers to a decrease of something, especially a gradual weakening or drawing out. It had been used in this sense for a long time before man's use of electricity for signaling and his invention of radio. In Webster (1806), attenuation was defined as the act of making thin or slender. It is still used in the same sense today, to denote a decrease, weakening, emaciation, or rarification (Crowell, 1962).

For example, the following definitions illustrate the wide use of the word.

Biological Sciences: Used specifically of the gradual reduction in virulence of a microorganism (Gray, 1967).

Textiles: The process of making a roving or sliver progressively smaller by doubling and drafting (Fairchild, 1967).

Medicine: The process of preparing homeopathic medicines by repeated dilutions (Funk and Wagnall, 1965).

Distilling and Brewing: The clarification and thinning of saccharine worts incident to the conversion of sugar into alcohol and carbon dioxide by fermentation (Funk and Wagnall, 1965).

It is seen that in each field, a restricted meaning exists which is in agreement with the broad meaning. In the field of electrical and electronic engineering, there are many definitions involving the words "attenuation," and "loss" which are in agreement with the broad general meaning, but are very specialized in application. The bases for these restricted meanings are discussed next.

c. Restricted Meanings

As used in electrical and electronic engineering, the term "attenuation" is used in the most general sense to denote a decrease of the amplitude or magnitude of coherent or incoherent electromagnetic waves or electrical impulses without specifying (1) what quantity shall be used to measure the decrease, (2) whether the decrease is space-dependent, time dependent,[1] or both, (3) the cause of the decrease, or (4) the conditions under which the decrease is to be measured.

However, in various restricted meanings of the term, each of the above has been specified, sometimes in contradictory ways. For example, in the case of an electromagnetic wave radiated by an antenna and traveling over the earth (ground wave), the wave amplitude decreases as one goes farther from the antenna due to (1) spreading out of the radiation -- the inverse distance effect, (2) dissipation or conversion of some energy to heat in the earth, and (3) scattering by irregularities or by objects in the transmission path. In general, "attenuation" denotes the decrease of wave amplitude due to any and all of the above causes, but some definitions exclude the decrease due to spreading.

For example in Michels (1961) on p. 113, one finds the following: "In the most common usage, attenuation does not include the inverse-square decrease of intensity of radiation with distance from the source." However, in the IRE Dictionary of Electronics terms and symbols" (1961), one finds on pp. 8-9 the following: "Note: In a diverging wave, attenuation includes the effect of divergence."

According to the cause of the attenuation or reduction, one finds different terms. In Tweney and Hughes (1961), pp. 3, 373, there is the following: Absorption (Radio) Reduction in the intensity of an electromagnetic wave, due to eddy currents and dielectric losses in the earth. Also called attenuation. Geometrical Attenuation (Radio) The reduction in field strength of an electromagnetic wave as it progresses from the source on account of spreading out.

---

[1] A time-dependent decrease might be caused by a variable attenuator and observed by a detector at a fixed point in space. A space-dependent decrease might be caused by a lossy transmission path and observed by two detectors located at different points along the path.

The American Institute of Electrical Engineers (AIEE, 1942) published the following definition: "Attenuation of a Wave" -- The attenuation of a periodic wave is the decrease in amplitude with distance in the direction of wave propagation when the amplitude at any given place is constant in time, or the decrease in amplitude with time at a given place."

This definition is somewhat restrictive because: 1) It mentions only periodic waves. However, it is possible to decrease the energy of a transient or aperiodic wave, or even electrical noise, by placing some dissipative, reflective, or scattering objects in its path. 2) It ignores the possibility that a wave might simultaneously be decreasing in amplitude with time as it decreases with distance in the direction of propagation.

Consider the following three cases: 1) A detector is placed at a certain position in a transmission path or circuit and observes a decrease with time of the wave amplitude, 2) two detectors are placed at different points along a transmission path or in a circuit and the wave amplitudes are observed simultaneously, giving information about the decrease of wave amplitude with distance along the propagation path, 3) a detector is moved continuously along a wave transmission path, and detects a decrease in wave amplitude in going away from the source. Such a decrease could be both time and space dependent, although quite often, the source is amplitude-stabilized to remove any time-dependence, or the amplitude is monitored at some fixed point and corrections are made to eliminate any time-dependent component.)

It should be clear from the above examples that it is important when using restricted definitions of attenuation that the basis for the restrictions is clearly understood.

d. IRE Definitions

The definitions of attenuation published by the Institute of Radio Engineers (IRE) in 1961, also appear in the IEEE Standard Dictionary of Electrical and Electronics Terms (1972). For this reason, they deserve special study. It appears in IRE (1961) on p. 8 and states: "Attenuation. General transmission term used to denote a decrease of Signal magnitude."

There are two apparent restrictions. First, the phrase "Signal magnitude" would seem to exclude waves[2] which were not "signals." And second, the phrase "transmission term" implies that the decrease takes place as a result of transmission, and thus is space-dependent but perhaps not time-dependent.

In practice, the use of the term "signal" has been expanded to include any electromagnetic wave or electrical impulse whether or not it contains any message to communicate information. Also the phrase "transmission term" does not really rule out time-dependent attenuation. Thus the apparent restrictions have largely been ignored or circumvented.

One notes that the IRE definitions of terms which include the word "attenuation" refer to space-dependent attenuations with one exception. Thus, "Current Attenuation," "Voltage Attenuation," "Power Attenuation," "Attenuation (of Radio Waves)," and "Attenuation (in a Waveguide)" are restricted to space dependent attenuation. However, "Direct-Coupled Attenuation" (TR, Pre-TR, and Attenuator Tubes). The Insertion Loss measured with the resonant Gaps, or their functional equivalents, short-circuited" is a time-dependent attenuation.

On the other hand, the IRE definitions which include the word "loss" consistently employ power as the observed quantity although they are divided among space-dependent and time-dependent attenuations. For example, time-dependent losses include Bridging Loss, Insertion Loss, Transition Loss, Reflection Loss, Return Loss, and Transformer Loss. Among the space-dependent losses are Absorption Loss, Divergence Loss, Heat Loss, Power Loss, Radiation Loss, Refraction Loss, and Transmission Loss.

One can conclude that the IRE recognized both space-dependent and time-dependent attenuations and considered "Loss" concepts as special kinds of attenuation involving power as the observed quantity.

It is noted in some of the definitions (but not all) that attenuation or loss can be expressed either as the amount of the decrease of a quantity (such as power), or the ratio of the large to the small value of the quantity which is decreased. In case the ratio is used, it is often expressed in Decibels or Nepers. On p. 38 of IRE

---

[2]On p. 132 of IRE (1961), we find "Signal. 1) the physical embodiment of a Message. 2) a) A visible, audible, or other indication used to convey information. b) The intelligence, message, or effect to be conveyed over a communication system. c) A Signal wave." On p. 90, we find "Message. 1) An ordered selection from an agreed set of symbols, intended to communicate information. 2) The original modulating wave in a communication system. Note: Definition 1) is the sense in which the term is used in communication theory; definition 2) is the sense in which the term is often used in engineering practice."

(1961) one is cautioned against confusion which may result if ratios of currents or of voltages are expressed in Decibels. The point may be illustrated by the following example. Consider two points in a linear circuit excited by steady-state, sinusoidal, single-frequency electromagnetic waves. If the impedances at the two points are Z_1 and Z_2, and the corresponding powers, voltages, and currents are respectively P_1, V_1, and I_1, and P_2, V_2, and I_2, the decibel relationships for the power, voltage, and current ratios are the following:

$$R_P = 10 \log_{10} \frac{P_1}{P_2}, \text{ where } P = |I|^2 \, ReZ = \frac{|V|^2}{|Z|^2} ReZ, \tag{6.1}$$

$$R_V = 10 \log_{10} \left|\frac{V_1}{V_2}\right|^2 = 10 \log_{10} \left(\left|\frac{Z_1}{Z_2}\right|^2 \cdot \frac{ReZ_2}{ReZ_1} \cdot \frac{P_1}{P_2} \right), \text{ and} \tag{6.2}$$

$$R_I = 10 \log_{10} \left|\frac{I_1}{I_2}\right|^2 = 10 \log_{10} \left(\frac{ReZ_2}{ReZ_1} \cdot \frac{P_1}{P_2} \right). \tag{6.3}$$

Note that if the impedances are equal ($Z_1 = Z_2$), all three ratios expressed in decibels are equal. In the special case where only the real parts of the impedances are equal ($ReZ_1 = ReZ_2$), then the power and current ratios expressed in decibels are equal and the voltage ratio gives a different number of decibels (except for $ImZ_1 = -ImZ_2$). In general, if the impedances are not equal, then the three ratios above expressed in decibels can be different numbers.

The above example applies to the comparison of IRE definitions of Voltage Attenuation, Current Attenuation, and Power Attenuation of Transducers, where the input impedance of the transducer may in general be different from the impedance of the load connected to its output port.

e. Comparisons of Definitions

In this section, comparisons will be made of various IRE definitions of attenuation (including "loss") and of a few definitions derived from those given by the IRE. Practically all of the IRE attenuation definitions pertain to a "transducer" which can be represented by an ideal linear passive 2-port having uniform, lossless waveguide leads. Equations may then be derived for the different attenuations and quantitative comparisons are then possible. In the following, the equations are given without derivation. The derivation follows from the principles given in section 3.8 and the equations use the same notation and conventions.

First, simple equations are given which define the attenuations in terms of the ratios of the appropriate quantities. Then, the corresponding equations are given in terms of the scattering coefficients S_{11}, S_{12}, S_{21}, and S_{22} of the two-port model of figure 6-1 assumed to represent the transducer, the characteristic impedances Z_{01} and Z_{02} of the principal modes in the waveguide leads, and the reflection coefficients Γ_G and Γ_L of the equivalent generator and load "seen by" the transducer. Finally, simplified equations are given for the case of $Z_{01} = Z_{02}$ and $\Gamma_G = \Gamma_L = 0$, or simply $\Gamma_L = 0$.

Consider first space-dependent attenuations which can be defined in terms of the terminal variables v_1, i_1, a_1, b_1, v_2, i_2, a_2, and b_2 which are indicated on figure 6-1. Note that for generality, the generator system is a Z_{01} system and the load system is a Z_{02} system.

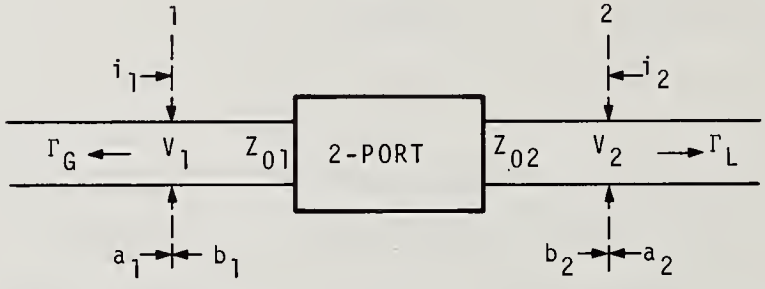

Figure 6-1. Model assumed to represent a two-port device.

$$\text{Voltage Attenuation } A_V = 20 \text{ Log}_{10} \left| \frac{v_1}{v_2} \right|. \tag{6.4}$$

$$\text{Current Attenuation } A_C = 20 \log_{10} \left| \frac{i_1}{i_2} \right|. \tag{6.5}$$

$$\text{Power Attenuation or Transmission Loss } A_P = 10 \text{ Log}_{10} \left(\frac{P_1}{P_2} \right) = 10 \text{ Log}_{10} \frac{1}{\eta}, \tag{6.6}$$

where

$$P_1 = \frac{1}{Z_{01}} (|a_1|^2 - |b_1|^2),$$

$$P_2 = \frac{1}{Z_{02}} (|b_2|^2 - |a_2|^2),$$

and η is the efficiency. Note that P_1 and P_2 are net (transmitted or delivered) powers.

$$\text{Intrinsic Attenuation}^3 \quad A_I = 10 \text{ Log}_{10} \frac{1}{\eta_{max}}. \tag{6.7}$$

(See section 3.9.)

$$\text{Voltage Wave Amplitude Attenuation}^4 \quad A_{VWA} = 20 \text{ Log}_{10} \left| \frac{a_1}{b_2} \right| = 10 \text{ Log}_{10} \left(\frac{P_{I1}}{P_{E2}} \cdot \frac{Z_{01}}{Z_{02}} \right), \tag{6.8}$$

where P_1 denotes incident power and P_E denotes emergent power.

$$\text{Available Power Attenuation}^5 \quad A_A = 10 \text{ Log}_{10} \left(\frac{P_{A1}}{P_{A2}} \right), \tag{6.9}$$

where P_A = Available Power.

The following relationships between the available powers and the terminal variables shown on the above figure 6-1 can be derived from inspection of section 3.6.

$$P_{A1} = P_1 \frac{|1 - \Gamma_G \Gamma_1|^2}{(1 - |\Gamma_G|^2)(1 - |\Gamma_L|^2)} \quad \text{where } \Gamma_L = \frac{b_1}{a_1}, \tag{6.10}$$

and

$$P_{A2} = P_2 \frac{|1 - \Gamma_{2i} \Gamma_L|^2}{(1 - |\Gamma_{2i}|^2)(1 - |\Gamma_L|^2)}, \text{ where } \Gamma_{2i} = S_{22} + \frac{S_{12} S_{21} \Gamma_G}{1 - S_{11} \Gamma_G}, \tag{6.11}$$

and

$$\Gamma_L = \frac{a_2}{b_2}.$$

The above eqs. (6.4) through (6.9) all define an attenuation associated with the ratio of a quantity at port 1 to the corresponding quantity at port 2. It would also be possible to form a ratio of a quantity at port 1 to a different quantity at port 2, but this would not be in agreement with the general definition of attenuation.

---

[3] This is an extension of Power Attenuation to the case in which the 2-port is terminated in a load impedance for which it has maximum efficiency η_{max}.

[4] This is not given in the IRE Dictionary, but follows from application to waveguide circuits of the IRE definition: Attenuation (in a Waveguide). Of a quantity associated with a traveling waveguide wave, the decrease with distance in the direction of propagation (53 IRE 2.S1).

[5] This is the inverse of the IRE definition of the "Available Power Gain" (of a linear transducer). (51 IRE 20.S2.)

The ratio of a power at port 1 to a different kind of power at port 2 is used in some attenuation definitions, for example in the definition of "transducer loss." However, this is not regarded as a space-dependent attenuation unless the two different kinds of powers can be simultaneously observed. In the case of "transducer loss," the available power might be measured at port 1 by removing the 2-port and connecting to the source a detector whose impedance is adjusted to conjugately match that of the source. Once P_{A1} has been measured, the 2-port is reconnected to the source and P_2 (the power delivered to a specified load) is measured.

For the purpose of making comparisons, equations for the above space-dependent attenuations are given as follows (the equation for A_I is not given because it is rather large, and does not reduce to a simple form when $Z_{01} = Z_{02}$ and $\Gamma_G = \Gamma_L = 0$).

$$A_V = 20 \text{ Log}_{10}\left|\frac{(1+S_{11})(1-S_{22}\Gamma_L) - S_{12}S_{21}\Gamma_L}{S_{21}(1+\Gamma_L)}\right| \rightarrow 20 \text{ Log}_{10}\left|\frac{1+S_{11}}{S_{21}}\right|, \tag{6.12}$$

for $\Gamma_L = 0$;

$$A_C = 20 \text{ Log}_{10}\left\{\frac{Z_{02}}{Z_{01}} \cdot \left|\frac{(1-S_{11})(1-S_{22}\Gamma_L) - S_{12}S_{21}\Gamma_L}{S_{21}(1-\Gamma_L)}\right|\right\} \rightarrow 20 \text{ Log}_{10}\left|\frac{1-S_{11}}{S_{21}}\right|, \tag{6.13}$$

for $\Gamma_L = 0$ and $Z_{01} = Z_{02}$;

$$A_P = 10 \text{ Log}_{10}\left\{\frac{Z_{02}}{Z_{01}} \cdot \frac{|1-S_{22}\Gamma_L|^2 - |(S_{12}S_{21}-S_{11}S_{22})\Gamma_L + S_{11}|^2}{|S_{21}|^2(1-|\Gamma_L|^2)}\right\} \rightarrow 10 \text{ Log}_{10} \frac{1 - |S_{11}|^2}{|S_{21}|^2}, \tag{6.14}$$

for $\Gamma_L = 0$ and $Z_{01} = Z_{02}$;

$$A_{VWA} = 20 \text{ Log}_{10}\left|\frac{1-S_{22}\Gamma_L}{S_{21}}\right| \rightarrow 20 \text{ Log}_{10} \frac{1}{|S_{21}|}, \tag{6.15}$$

when $\Gamma_L = 0$; and

$$A_A = 10 \text{ Log}_{10}\left\{\frac{Z_{02}}{Z_{01}} \cdot \frac{|1-S_{11}\Gamma_G|^2 - |(S_{12}S_{21}-S_{11}S_{22})\Gamma_G + S_{22}|^2}{|S_{21}|^2(1-|\Gamma_G|^2)}\right\} \rightarrow 10 \text{ Log}_{10} \frac{1 - |S_{22}|^2}{|S_{21}|^2}, \tag{6.16}$$

for $\Gamma_G = 0$ and $Z_{01} = Z_{02}$.

It is significant that the above equations do not become equal when the conditions $\Gamma_G = \Gamma_L = 0$ and $Z_{01} = Z_{02}$ are imposed. However, if, in addition, the transducer is non-reflecting ($S_{11} = S_{22} = 0$), then they are all equal.

The differences are due to reflection interactions, and if the reflections are small, the differences will be small. However, in the case of highly accurate measurements, even small differences may be important.

For example, if the input and output VSWR's of the 2-port[6] are 1.05, corresponding to $|S_{11}| = |S_{22}| = 0.0244$, and we assume that $\Gamma_G = \Gamma_L = 0$ and $Z_{01} = Z_{02}$, then the attenuations A_P and A_A will be about 0.026 decibel lower than A_{VWA}, and A_C and A_V can be about 0.4 decibel higher or lower than A_{VWA}, depending upon the phases of S_{11} and S_{22}.

These differences are significant and illustrate the importance of clearly defining the quantity to be measured.[7]

Consider next the time dependent attenuations "insertion loss" (L_I), "transducer loss" (L_T), and "substitution loss" (L_S). The first two can be defined in terms of the third, as will be demonstrated. In figure 6–2, the substitution of a final 2-port for an initial 2-port is shown.

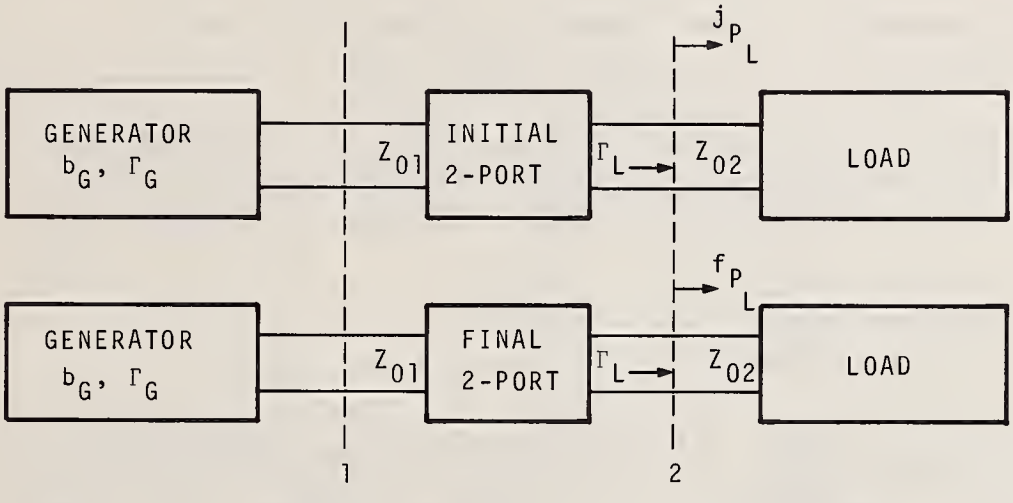

Figure 6-2. Model representing substitution of final 2-port for initial 2-port in a simple system.

The defining equation for all of the three losses is:

$$L = 10 \, \mathrm{Log}_{10} \left(\frac{i_{P_L}}{f_{P_L}} \right), \qquad (6.17)$$

where P_L is the power absorbed by the load, and the front superscripts i and f refer to initial and final conditions, respectively.

[6]VSWR's higher than 1.05 are commonly encountered, even in high-quality components. Thus, the example given is conservative.

[7]These differences also verify the advisability of avoiding the use of current and voltage attenuation concepts in situations where the impedance varies along the transmission path.

In the case of "substitution loss," there are no restrictions on the properties of the initial 2-port. If the initial 2-port is a perfect connector pair having no dissipative loss or leakage, no reflection, and no phase shift, then the substitution loss equals L_I, the insertion loss. (The case where the initial connector pair is not perfect is discussed later in section 6.6.) The insertion loss under non-reflecting conditions ($\Gamma_G = \Gamma_L = 0$) is characteristic of the 2-port and is called the insertion loss of the 2-port, the word "characteristic" being understood.

If the initial 2-port is a perfect transducer having no dissipative loss or leakage and provides a conjugate match to the generator, then ${}^{i}P_L$ is the available power, and the substitution loss equals L_T, the transducer loss.

Note that the definitions of "insertion loss" and "transducer loss" are equivalent to those given in the IRE Dictionary on pages 75 and 152, respectively.

In the equations to follow, it is assumed that the initial and final characteristics of the generator and load are unchanged by substitution of the 2-ports. However, in making an analysis of the errors due to these assumptions failing to hold, the front superscripts i and f would be retained on Γ_G and Γ_L.

From eqs. (3.51), (3.53), and (3.52), respectively, we have the following:

$$L_S = 20 \operatorname{Log}_{10}\left|\frac{{}^{i}S_{21}[(1 - {}^{f}S_{11}\Gamma_G)(1 - {}^{f}S_{22}\Gamma_L) - {}^{f}S_{12}\,{}^{f}S_{21}\Gamma_G\Gamma_L]}{{}^{f}S_{21}[(1 - {}^{i}S_{11}\Gamma_G)(1 - {}^{i}S_{22}\Gamma_L) - {}^{i}S_{12}\,{}^{i}S_{21}\Gamma_G\Gamma_L]}\right|,$$

$$= 20 \operatorname{Log}_{10}\left|\frac{{}^{i}S_{21}}{{}^{f}S_{21}}\right|, \text{ if } \Gamma_G = \Gamma_L = 0. \tag{6.18}$$

$$L_I = 10 \operatorname{Log}_{10}\left\{\frac{Z_{02}}{Z_{01}} \cdot \frac{|(1 - S_{11}\Gamma_G)(1 - S_{22}\Gamma_L) - S_{12}S_{21}\Gamma_G\Gamma_L|^2}{|S_{21}(1 - \Gamma_G\Gamma_L)|^2}\right\},$$

$$= 20 \operatorname{Log}_{10}\left|\frac{1}{S_{21}}\right|, \text{ if } \Gamma_G = \Gamma_L = 0, \text{ and } Z_{01} = Z_{02}. \tag{6.19}$$

$$L_T = 10 \operatorname{Log}_{10}\left\{\frac{Z_{02}}{Z_{01}} \cdot \frac{|(1 - S_{11}\Gamma_G)(1 - S_{22}\Gamma_L) - S_{12}S_{21}\Gamma_G\Gamma_L|^2}{|S_{21}|^2(1 - |\Gamma_G|^2)(1 - |\Gamma_L|^2)}\right\},$$

$$= 20 \operatorname{Log}_{10}\left|\frac{1}{S_{21}}\right|, \text{ if } \Gamma_G = \Gamma_L = 0, \text{ and } Z_{01} = Z_{02}. \tag{6.20}$$

It is seen that when the system is non-reflecting ($\Gamma_G = \Gamma_L = 0$) and $Z_{01} = Z_{02}$, the transducer loss, insertion loss, and the voltage wave amplitude attenuation (a space-dependent attenuation) are identical. It is also noteworthy that if the

condition $\Gamma_L = 0$ is removed, the insertion loss and A_{VWA} according to eq. (6.15) continue to be identical for any value of Γ_L.

Consider now another set of concepts which are defined by the IRE in terms of quantities which can be measured simultaneously. These are the transition loss L_{TN}, the reflection loss L_{RN}, and the return loss L_R. These are defined with reference to figure 6-3. It will be shown that these losses are equivalent to time-dependent attenuations.

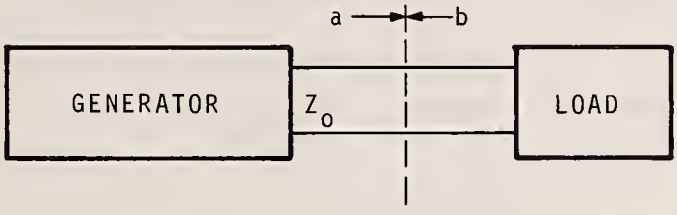

Figure 6-3. Model representing generator connected to load by a uniform, lossless waveguide lead.

$$L_{TN} = 10 \text{ Log}_{10} \frac{P_A}{P_N}, \tag{6.21}$$

where P_A is the available power, and P_N is the net power absorbed by the load.

$$L_{RN} = 10 \text{ Log}_{10} \frac{P_I}{P_N}, \text{ where } P_I = \frac{|a|^2}{Z_0}, \text{ the incident power.} \tag{6.22}$$

$$L_R = 10 \text{ Log}_{10} \frac{P_I}{P_R}, \text{ where } P_R = \frac{|b|^2}{Z_o}, \text{ the reflected power.} \tag{6.23}$$

Additional insight is obtained about the meaning of these losses when they are expressed as time-dependent attenuations as follows. Consider the situation in figure 6-4 where two loads are alternately connected to the same generator.

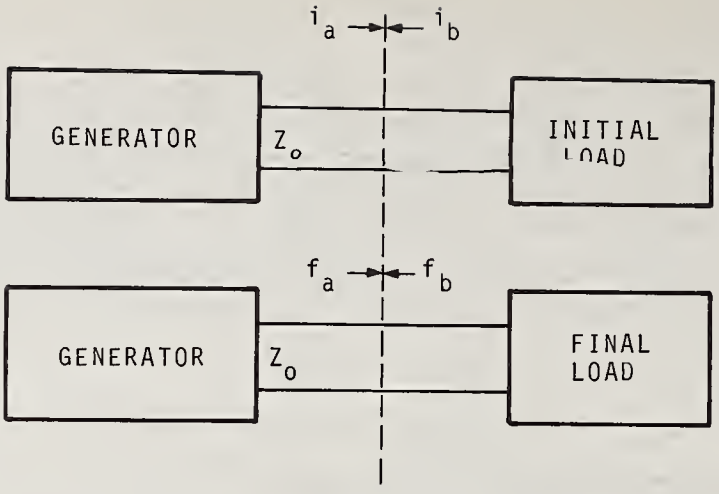

Figure 6-4. Model representing two loads alternately connected to the same generator.

The attenuation of the reflected wave is:

$$A_R = 20 \text{ Log}_{10}\left|\frac{i_b}{f_b}\right| = 10 \text{ Log}_{10}\left|\frac{i_{P_R}}{f_{P_R}}\right|. \tag{6.24}$$

This can be shown to be equal to the return loss L_R when two conditions are imposed 1) non-reflecting generator, and 2) perfectly reflecting initial load. Considering section 3.6, the above equation can be written as follows:

$$A_R = 20 \text{ Log}_{10}\left|\frac{1 - \Gamma_G {}^{f}\Gamma_L}{1 - \Gamma_G {}^{i}\Gamma_L} \cdot \frac{{}^{i}\Gamma_L}{{}^{f}\Gamma_L}\right| = 20 \text{ Log}_{10}\left|\frac{1}{{}^{f}\Gamma_L}\right|, \tag{6.25}$$

when $\Gamma_G = 0$ and $|{}^{i}\Gamma_L| = 1$.

Initially, the incident wave is totally reflected and returned to the generator, where it is absorbed. When a different load is finally connected, the reflected wave is reduced or attenuated. The return loss L_R is thus equal to the attenuation of the wave returned to a non-reflecting generator when a perfectly reflecting load is replaced by a different load.

From the defining equation for return loss given above,

$$L_R = 10 \text{ Log}_{10}\frac{P_I}{P_R} = 10 \text{ Log}_{10}\left|\frac{b}{a}\right|^2 = 20 \text{ Log}_{10}\frac{1}{|\Gamma_L|}. \tag{6.26}$$

Thus the return loss is equal to A_R for the two assumed conditions.

Next, the transition loss can be seen by inspection of its definition to be equal to the attenuation of the net power delivered by a generator when a conjugately matched load is replaced by a different load. This follows because a conjugately matched load absorbs maximum power and a different load then must absorb less power.

Finally, the reflection loss can be shown to be equal to the attenuation of the net power delivered by a non-reflecting generator when a non-reflecting load is replaced by a different load. This follows because a non-reflecting load absorbs maximum power from a non-reflecting generator and a different load must then absorb less power.

In addition to the IRE definitions of attenuation, many others have been proposed and used. However, it is not considered necessary or useful to discuss them in this monograph.

f. Terminology

There has been a long-standing lack of agreement about which names are most suitable for which attenuation concepts as well as which concepts are most useful to characterize a device for measurement purposes. Although a complete discussion of this situation would be interesting, it is only briefly summarized in order to relate the terminology used in this monograph to what is in common use today. Particular attention will be given to the terminology of attenuation concepts used to characterize attenuators.

Attenuating devices may be classified as either 2-ports or multiports. In the case of multiports, two of the ports may be selected as available for connecting to a transmission system and the remaining are not connected to the system, but to loads or independent circuits. The system may generally be a complicated one involving many paths between the source and the detector. However, for the purpose of defining attenuations, it is usually tacitly assumed that there is only one path from the source to the detector. One deals only with the attenuation in a single path. Thus, attenuation measurements are basically concerned with 2-ports, which may be either fixed or variable. The attenuation which characterizes a variable device is different than that which characterizes a fixed device.

In the case of non-variable devices such as attenuator pads, space-dependent attenuations such as A_P and A_{VWA}, as well as time-dependent attenuations such as L_S, L_I, and L_T which involve power ratios might be used to characterize the device.

It has been noted that in the case of a non-reflecting system, A_{VWA}, L_I, and L_T give the same simple equation in terms of the scattering coefficient S_{21}, assuming the 2-port model has ideal waveguide leads. Thus, differences between these three would be very small and would depend upon how much the actual situation differed from the ideal model.

It has been common practice to measure the insertion loss L_I in a non-reflecting system and to call this either 1) the insertion loss of the device, or 2) the attenuation of the device. It is understood that the word "characteristic" should precede the word "of," but for brevity, it is usually omitted. The use of either 1) or 2) is optional and has been a matter of individual preference.

In discussing mismatch errors in attenuation measurements (see 6.4b) one defines the error as the difference between what is actually measured (insertion loss or substitution loss) and the desired quantity (attenuation or characteristic insertion loss). In this usage, the word "attenuation" is understood to imply a non-reflecting system at the insertion point.

When the device is an attenuator, it is natural to speak of "its attenuation." However, since L_I is usually measured, there is some preference for the term "its insertion loss." It would be equally valid to measure A_{VWA}, which is not an insertion loss. The term "attenuation of a 2-port device" is a more general term than "insertion loss," and includes both A_{VWA} and L_I.

There is a class of two-port devices which cannot be simply inserted into a system, but must be substituted for something already in the system. For example, an attenuator pad having female connectos on both ends can be substituted for a female-to-female adapter which is originally in the system. In this case, the substitution loss in a non-reflecting system may be used to characterize the attenuator, providing that the characteristics of te adapter initially in the system are completely specified. Other items in his category are devices such as waveguide-to-coaxial adapters and connector pair themselves.

Although the term "insertion lossof a connector pair" has been used, what is usually measured is a substitution los. For example, a section of cable having the connector pair under test in its centr is substituted for an identical section of cable which has no connector pair in.ts center. Since a connector pair cannot be simply inserted into a system and reoved again, the term "insertion loss" is not so applicable as "substitution loss of connector pair" or the "attenuation of a connector pair." Other alternatives a available such as the relative efficiency of a connector pair. In addition to te efficiency, one would also require the VSWR or

return loss. The phase shift might also be important. This topic is considered further in section 6.6.

In the case of a variable 2-port device such as a variable attenuator, two terms are commonly used to denote its attenuation. They are 1) "its insertion loss" and 2) "its attenuation." The first term refers to the initial attenuation when the variable attenuator is set to "zero" or is switched to the state of minimum attenuation. It could be either space-dependent or time-dependent, according to how it would be defined and measured. Usually, the time-dependent attenuation is measured and called the insertion loss." The second term is used to denote the time-dependent attenuation due to its adjustment or its switching from one position to another. Usually the reference point is the "zero" setting or the minimum attenuation switching state, but any reference may be used. For example, in a step attenuator, one may allude to the attenuation between the 25 dB step and the 30 dB step. In all cases, it is assumed that the system has been adjusted for the non-reflecting condition prior to the measurement.

The variable attenuator may then be characterized by its insertion loss and its attenuation versus dial setting or step position data. If the variable attenuator has only two states, then its insertion loss and its attenuation are all that is required to characterize it.

If one considers a fixed pad as a special case of a variable attenuator having only one state, then by extension, it would be characterized by its insertion loss and its attenuation would be zero. This is one argument for the use of the term "insertion loss" rather than "attenuation" to characterize a pad. As previously mentioned, there are valid arguments for the opposite preference. It really makes no difference which is used, as long as the concept is clearly defined.

In other words, for precision measurement applications, the terminology is not as important as the tightness of the definition of the concept. In the next section, an attempt is made to tighten up the definitions of insertion loss and attenuation.

g. Precise Definitions

In the following section, precise definitions of attenuation will be presented. All of the things which were mentioned in the general definition of attenuation in section 6.2c as not being specified will be specified here. The definition will be based upon the basic measurement method and will tightly specify the conditions of measurement. It will be independent, as far as possible, of any idealized model, although strangely enough, it has been found difficult to completely avoid any idealized conditions in definitions.

In all of the definitions, it will be assumed that the source of electrical energy supplies a sinusoidal wave of single frequency and that we are considering only a single mode propagating in each waveguide of the system. It is assumed that the net power to the detector excludes any leakage (energy coming by a path other than directly through the device in question). If the detector responds to leakage power and it cannot be separated from the direct path energy, this represents a source of error.

The scope of the definitions will be limited to those which involve net power or delivered power. Only time-dependent attenuations will be defined, and only attenuations due to dissipation or to reflection of energy will be considered.

The general definition of attenuation given in the first paragraph of section 6.2c is considered to be an improvement on the AIEE and IRE definitions in that it is less restrictive. It is used as a reference in formulating the specific, restrictive definitions to follow.

The "insertion loss (characteristic) of an insertable, fixed 2-port device" is defined to be in decibels, 10 times the logarithm to the base 10 of the ratio of the initial to final net powers delivered to a non-reflecting detector by a non-reflecting source initially connected directly to the detector and finally connected so as to feed energy only through the two-port device to the detector. (In order for a device to be insertable, the connectors at its two ports must be of the same type as the system connectors which mate at the insertion point, and be either sexless, or of the opposite sex.)

The conditions under which the detector powers are measured are as follows:

1) The source is initially connected to the detector by means of a connector pair constructed so as to tightly adhere to standard specifications for such connector types as are used. Each connector of the pair is attached to a uniform section of waveguide constructed so as to adhere as closely as possible to standard dimensions and of sufficient length to effectively eliminate any higher modes which may have been excited by the connector pair.

2) The system is adjusted so that ideally there are no reflections looking towards the source or towards the detector in the waveguide sections belonging to the system. (Actually the adjustment is usually made in practice so that no reflections are observed in an auxiliary waveguide which is part of the reflection measuring instrument. Thus the system will then have reflections equal to those caused by a connector pair plus any residual reflection of the measurement instrument. This will represent a source of error.)

An improved technique to adjust for no system reflections is illustated in figure 6-5. Only the case of adjustment for no reflections looking towards the detector is shown. One can easily deduce how to use this technique to obtain no reflections on the generator side of the system.

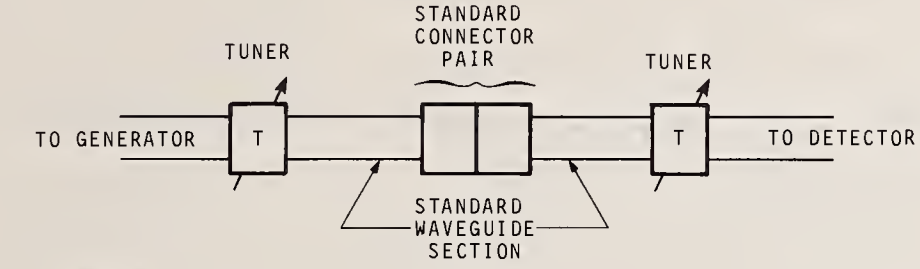

a) INSERTION POINT

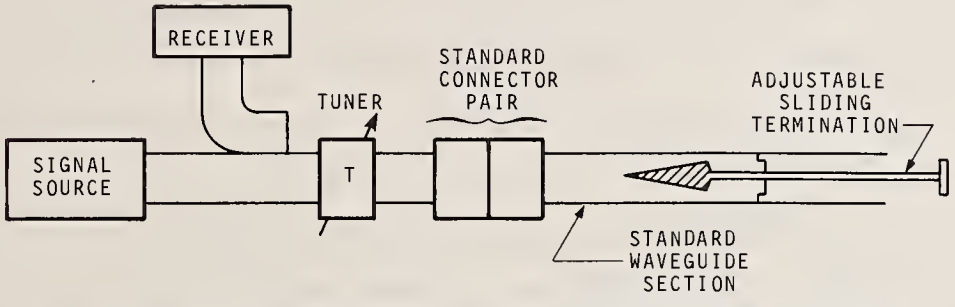

b) ARRANGEMENT TO ADJUST REFLECTOMETER TO INDICATE NON-REFLECTING CONDITION ON SYSTEM DETECTOR SIDE OF CONNECTOR PAIR. TUNER AND ADJUSTABLE SLIDING TERMINATION ARE ALTERNATELY ADJUSTED TO REDUCE AND MAINTAIN OUTPUT TO RECEIVER BELOW NOISE LEVEL AS TERMINATION SLIDES AT LEAST HALF WAVELENGTH.

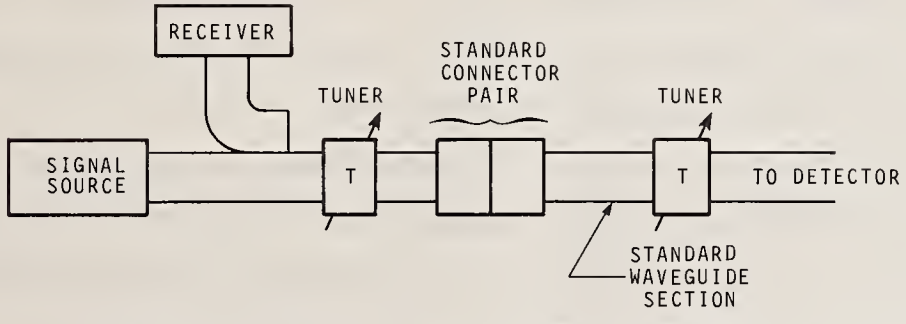

c) ARRANGEMENT TO ADJUST SYSTEM DETECTOR SIDE OF CONNECTOR PAIR FOR NON-REFLECTING CONDITION. AFTER ADJUSTING TUNER ON SIGNAL SOURCE SIDE OF DETECTOR AS ABOVE, ADJUST TUNER NEAR DETECTOR FOR RECEIVER NULL.

Figure 6-5. Improved technique to adjust for no system reflections.

3) The generator wave amplitude b_G and internal reflection coefficient Γ_G, and the detector sensitivity or gain and reflection coefficient Γ_L, are initially the same as when the final relative net power is observed.

4) It is assumed that the power level is either low enough to avoid appreciable non-linear effects, or is set at a specified level before insertion of the device.

The "attenuation (characteristic) of an insertable, fixed 2-port device" is synonymous with the above definition of the insertion loss. However, one could also define a "voltage wave amplitude attenuation (characteristic) of a fixed 2-port device," an "intrinsic attenuation of a fixed 2-port device," or any attenuation regarded to be characteristic of the device. Such definitions are not presently required for precise measurement purposes, and will be left for future research.

In the case of a fixed 2-port device which is not insertable, the following definition may be useful. The "substitution loss of a fixed 2-port device" is in decibels, 10 times the logarithm to the base 10 of the ratio of the initial to final net powers delivered to a non-reflecting detector by a non-reflecting source, connected initially to feed energy only through a removable fixed value 2-port device (having specified properties) and finally the fixed 2-port device under consideration. The conditions of measurement are the same as those listed for "the insertion loss of an insertable fixed 2-port device," with the exceptions indicated above.

The "attenuation (corresponding to a particular adjustment or change of state) of a variable 2-port device" is in decibels, 10 times the logarithm to the base 10 of the ratio of the higher to the lower net powers delivered to a non-reflecting detector by a non-reflecting source connected so as to feed energy only through the device, which is adjusted or switched from an initial setting or state to a final setting or state. The conditions of measurement are the same as those specified above with exceptions which are evident upon inspection.

The foregoing definitions are understood to apply also to any pair of ports of a multiport device, whose other ports which are not involved in the definition, being connected in some specified way, such as, but not necessarily, all connected to non-reflecting loads.

h. Future Trends

One can predict future trends on the basis of certain assumptions. The probability that they will actually occur depends in part upon the validity of the assumptions. It seems reasonable to assume that higher accuracy will be required in the future in attenuation measurements. This may lead to improvements in waveguides, connectors, and in attenuators themselves. If these improvements are substantial enough, then errors will be reduced. The more that errors are reduced in this way, the less need there will be for improved analytical techniques to evaluate

errors, as discussed in section 6.6. Also there will be less need to consider replacing conventional insertion loss and attenuation concepts by a "terminal invariant parameter" (Engen, 1969) such as intrinsic attenuation.

If, however, improvements in waveguides, connectors, and attenuators do not keep pace with accuracy requirements, these analytical techniques and special concepts should prove more useful.

It is also conceivable that new methods will be developed to make more accurate attenuation measurements, and that they might make popular the measurement of some attenuation other than insertion loss. For example, the voltage wave amplitude attenuation appears promising as an attenuation to characterize a 2-port device.

The increased use of computer-controlled automatic measurement systems will make feasible new measurement techniques that would have formerly been impractical because of tedious adjustments or calculations that are required. These techniques are likely to place a higher demand on connector repeatability and make greater use of substitution, as opposed to insertion techniques.

6.3. Cascade-Connected Attenuators

a. Introduction

It is well known that if one connects two fixed attenuators, say exactly 5 dB each, together and measures without error the attenuation of the combination, the result may not exactly equal the sum of the attenuations (say 10 dB). A difference can occur due to reflection interactions in the waveguides or transmission lines both where the attenuators are connected together and where they are connected to the measurement system. Depending upon the relative phases of the reflections, the difference in attenuation may be positive, negative, or (in relatively rare cases) zero.

This effect becomes important when one is testing the accuracy and repeatability of a measurement system by measuring attenuators individually, then in combination; and comparing the results (Beatty, 1971). Such a test will give useful information about the accuracy of the measuring system only if the uncertainty due to attenuator reflections is considerably less than the uncertainty or inaccuracy of the measuring system under investigation. The above effect is also important when attenuators

are used as "gage blocks" to extend ranges of power meters, or when fixed and variable attenuators are cascade-connected in order to extend the range. In turret-type attenuators, this effect may limit the useful frequency range because reflections usually increase with frequency.

An early analysis of this effect has been published (Beatty, 1950). The analysis was performed before the use of scattering coefficients had been widely accepted and wave matrices were employed. The results are still valid and the nomogram giving limits of error in terms of VSWR's is still useful.

An extension of this analysis was made by Hashimoto (1968), in which the connector pairs joining the pads were represented by cascaded 2-ports in a manner similar to Beatty (1964b), and the 2-port representing the contacting portion of the joint was represented by a single series impedance in a manner similar to Harris (1965).

The analysis was extended to the case of cascade-connected variable attenuators by Schafer and Rumfelt (1959).

In the present discussion, the results of the original analysis are presented in a more convenient and slightly more general form. Scattering coefficients are employed and non-reciprocal elements are not excluded.

b. Analysis

In the following analysis, UHF or microwave attenuators are considered. It is assumed that the individual attenuators have been calibrated in a transmission-line system having the same characteristic impedance (Z_0) and critical dimensions as the system in which the attenuators are to be used. A further requirement is that the attenuators are passive linear 2-port devices having connectors or waveguide flanges that permit connection to the waveguide or transmission-line system without discontinuity. Although attenuators can usually be considered as reciprocal devices, there is little need to assume reciprocity in the analysis, and it is not assumed.

First the case of two attenuators is considered. Then the cases of 3 or more cascaded 2-ports are analyzed.

(1) Two Attenuators

The analysis of cascade two-ports have already been described in section 3.11 and 3.12. The results of those sections are directly applicable. First, the attenuation of a single 2-port for energy entering port 1, is

$$A = 10 \text{ Log}_{10} \frac{1}{|S_{21}|^2}. \tag{3.55}$$

For the case of two attenuators designated as M and N connected in cascade as in figure 3-15, the scattering coefficient S_{21} of the composite 2-port is written in terms of the scattering coefficients m_{21}, m_{22}, n_{21}, and n_{11} of the individual attenuators as follows.

$$S_{21} = \frac{m_{21}n_{21}}{1 - n_{11}m_{22}}. \tag{3.98}$$

The attenuation of the combination is

$$A_C = 20 \text{ Log}_{10} \frac{1}{|m_{21}|} + 20 \text{ Log}_{10} \frac{1}{|n_{21}|} + 20 \text{ Log}_{10}|1 - n_{11}m_{22}|. \tag{6.27}$$

or $A_C = A_M + A_N + \varepsilon_2$.

The last term represents the error ε_2 that must be added to the sum of the attenuations of the individual attenuators to obtain the correct attenuation of the combination.

If we have (as is often the case) knowledge of the VSWR's ${}^{n}\rho_{11}$ and ${}^{m}\rho_{22}$ corresponding to n_{11} and m_{22}, but no knowledge of the phases, then we can calculate the following limits between which ε_2 must lie

$$20 \text{ Log}_{10}\left\{1 + \frac{{}^{m}\rho_{22} - 1}{{}^{m}\rho_{22} + 1} \cdot \frac{{}^{n}\rho_{11} - 1}{{}^{n}\rho_{11} + 1}\right\} \geq \varepsilon_2 \geq 20 \text{ Log}_{10}\left\{1 - \frac{{}^{m}\rho_{22} - 1}{{}^{m}\rho_{22} + 1} \cdot \frac{{}^{n}\rho_{11} - 1}{{}^{n}\rho_{11} + 1}\right\}. \tag{6.28}$$

These limits are shown in the nomogram of figure 6-6.

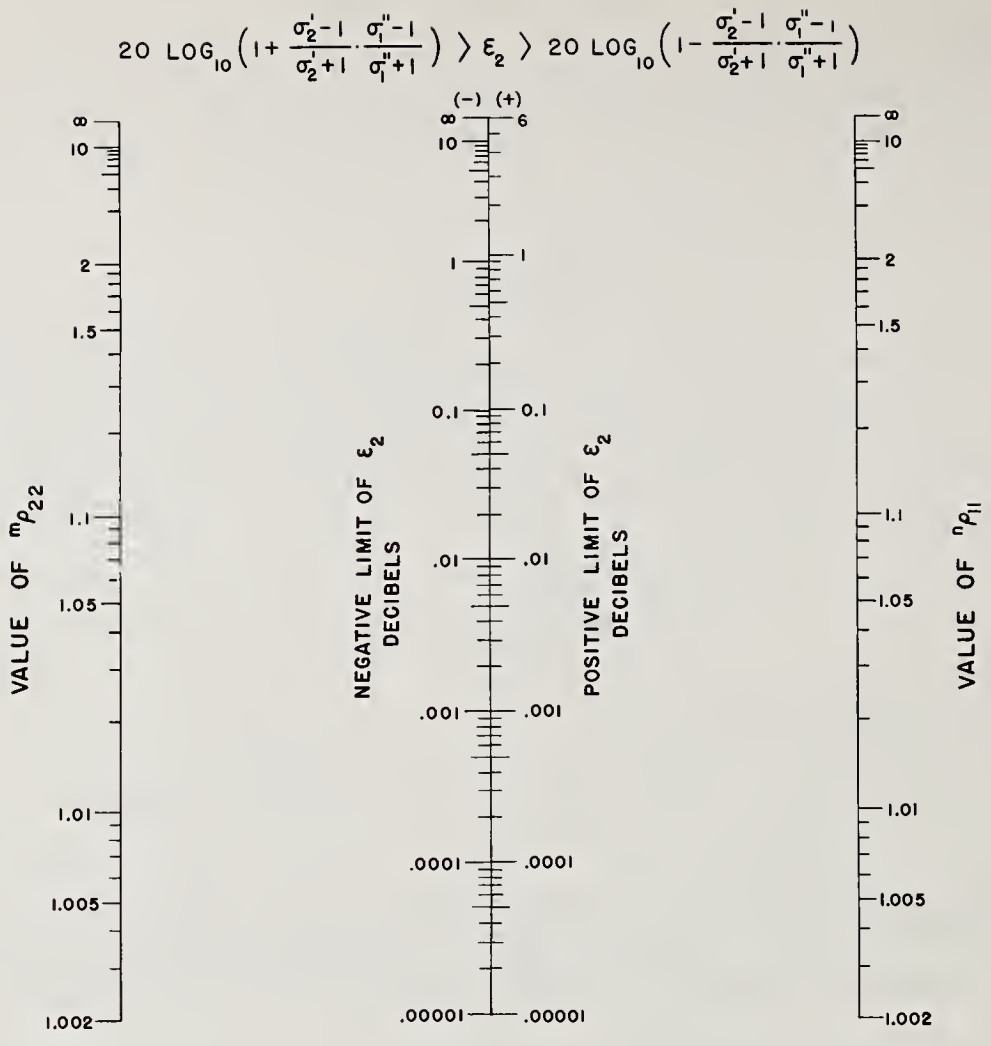

Figure 6-6. Limits of error according to eq (6.28).

(2) Three Attenuators

The analysis of 3 cascaded attenuators can be based upon that for 2 attenuators as follows. Suppose we designate the 3 attenuators as L, M, and N connected as shown in figure 6-7, and their scattering coefficients by the lower case letters, ℓ, m, and n with the appropriate subscripts. We can consider that attenuator L is cascaded with one other attenuator (which is formed by combining M and N). Thus the 3 attenuator case is a simple extension of that for 2 attenuators.

It can be shown (Kerns and Beatty, 1967) that for the cascade connection of 3 attenuators,

$$S_{21} = \frac{\ell_{21} m_{21} n_{21}}{[(1 - \ell_{22} m_{11})(1 - m_{22} n_{11}) - \ell_{22} m_{12} m_{21} n_{11}]}. \tag{6.29}$$

The attenuation of the combination is

$$A_C = A_L + A_M + A_N + 20 \text{ Log}_{10} |(1-\ell_{22} m_{11})(1-m_{22} n_{11}) - \ell_{22} m_{12} m_{21} n_{11}|, \tag{6.30}$$

where the last term is ε_3, the error that one would make in assuming that the attenuation of the combination equals the sum of the attenuations of the individual attenuators.

Note that the error term may be written

$$\varepsilon_3 = 20 \text{ Log}_{10} |[1 - \ell_{22} (mn)_{11}][1 - m_{22} n_{11})|, \tag{6.31}$$

where $(mn)_{11}$ is the scattering coefficient of the combination of M and N and is given by eq. (3.98) if S_{11} there is replaced by $(mn)_{11}$.

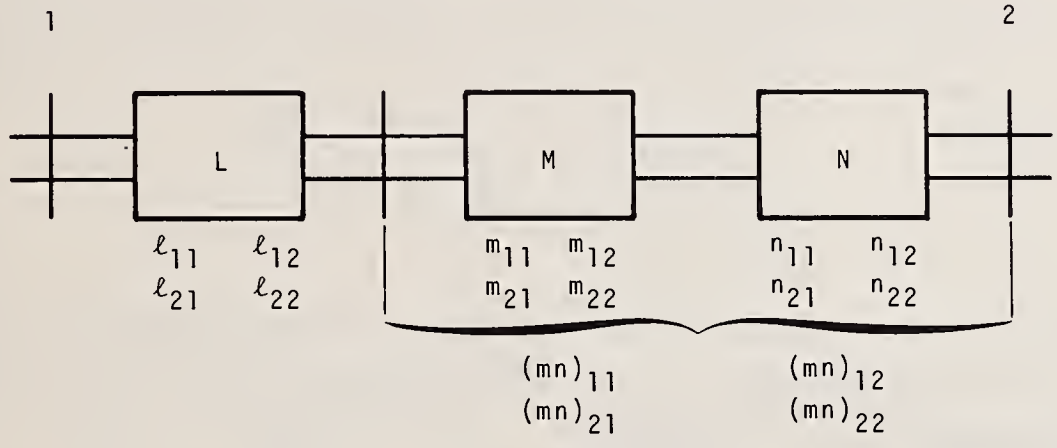

Figure 6-7. Three cascaded 2-ports, L, M, and N.

Assuming that we can obtain the VSWR's corresponding to ℓ_{22}, $(mn)_{11}$, m_{22}, and m_{11}, we can then obtain the limits of ε_3 by referring twice to the nomogram of figure 6-6. In the special case where the term $|\ell_{22} m_{12} m_{21} n_{11}|$ from eq. (6.30) is small, we can obtain the limits of ε_3 by referring to the nomogram twice if we can obtain the VSWR's corresponding to ℓ_{22}, m_{11}, m_{22}, and n_{11}. The limits of ε_3 are obtained by adding the limits obtained for each term, $20 \log_{10}|1 - \ell_{22} m_{11}|$, and $20 \text{ Log}_{10}|1 - m_{22} n_{11}|$.

(3) Any Number n of Attenuators

The attenuation of any number n of cascaded attenuators is

$$A_C = \sum_{K=1}^{n} {}^{K}A + \varepsilon_n, \tag{6.32}$$

where K denotes the position of the attenuator, numbering from the input side.

In evaluating ε_n, one can proceed as in the cases of 2 or 3 attenuators, deriving expressions which are extensions of eq. (6.27) and eq. (6.29). These involve transmission coefficients of the interior located attenuators both in the A_K and the ε_n terms.

One can avoid deriving complicated expressions by the procedure used in the case of 3 attenuators. Consider first two attenuators at one end of the chain, using eq. (6.27) to find the attenuation of the combination. Then one considers these two attenuators as a unit, and determines S_{11} and S_{22} for the combination. These are combined with the next attenuator in the chain and again an equation of the form of eq. (6.27) will give the attenuation of the new combination. One repeats this process until one reaches the end of the chain. It can be deduced that the term ε_n in eq. (6.32) is

$$\varepsilon_n = \sum_{K=2}^{n} 20 \operatorname{Log}_{10} |1 - {}^{K-1}S_{22}\ {}^{K}S_{11}|, \tag{6.33}$$

where ${}^{K-1}S_{22}$ denotes the scattering coefficient of the combined attenuators to the left (direction of decreasing numbers) of the K^{th} attenuator, and ${}^{K}S_{11}$ denotes the scattering coefficient of the K^{th} attenuator.

6.4. Mismatch Errors in Attenuation Measurements

a. Introduction

Presently, the most significant source of error in microwave attenuation measurements is the mismatch error. It is not only significant in calibrating attenuators, but largely determines how much one must degrade the accuracy of measurements subsequently made with a calibrated attenuator in a different system than that in which it was calibrated.

In the following, a simple analysis and evaluation of mismatch errors dating back to 1947 will be reviewed, and subsequent work mainly by the author will then be described. The cases of measurement errors for fixed pads and for variable attenuators will be discussed.

b. Analysis of Case of Fixed Pad

Ernst Weber (1947) analyzed the mismatch error in the measurement of the attenuation of a fixed pad. He assumed that a pad could be represented by a 2-port network which could be inserted into a system in the manner shown in figure 6-8. He expressed the mismatch error ε as

$$\varepsilon = L_I - A, \tag{6.34}$$

where L_I is the insertion loss one actually measures, and A (the attenuation) is the insertion loss that one would measure if the system were matched, or non-reflecting ($\Gamma_G = \Gamma_D = 0$).

We will derive an expression for ε using modern notation that is equivalent to Weber's expression. The insertion loss L_I is

$$L_I = 10 \text{ Log}_{10} \frac{{}^{i}P_D}{{}^{f}P_D}, \tag{6.35}$$

where the front superscripts i and f refer to initial and final conditions, respectively.

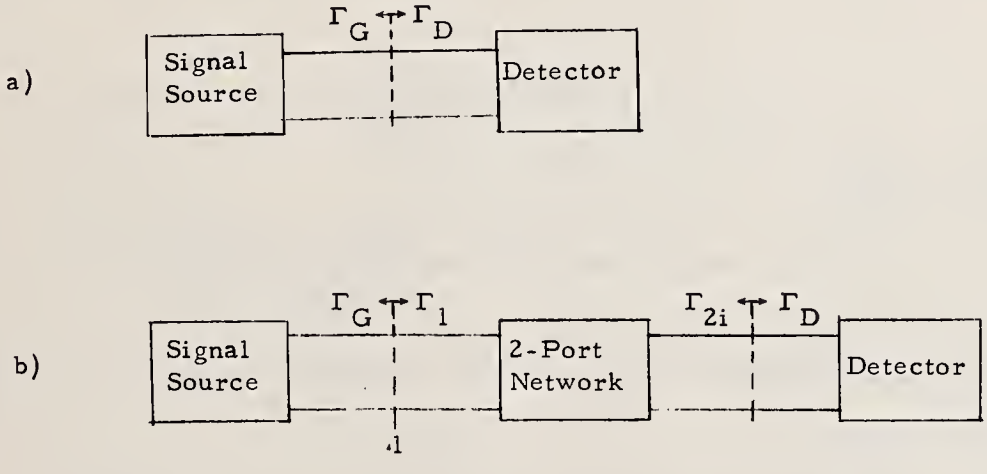

Figure 6-8. Model illustrating a) a measurement system, and (b) insertion of a 2-port network into the measurement system.

Before insertion of the 2-port, the power ${}^{i}P_D$ delivered to the detector is (Kerns and Beatty, 1967)

$${}^{i}P_D = \frac{P_A}{|1 - \Gamma_G\Gamma_D|^2}, \tag{6.36}$$

where P_A is the available power from the generator.

After insertion of the 2-port network, the power $^{f}P_D$ delivered to the detector is

$$^{f}P_D = P_A \cdot \frac{1 - |\Gamma_1|^2}{1 - |\Gamma_D|^2} \cdot \frac{\eta}{|1 - \Gamma_G\Gamma_1|^2}, \tag{6.37}$$

where η is the efficiency of the 2-port network as terminated in figure 6-8(b).

It follows that

$$L_I = 10 \text{ Log}_{10}\left\{\frac{1 - |\Gamma_D|^2}{1 - |\Gamma_1|^2}\left|\frac{1 - \Gamma_G\Gamma_1}{1 - \Gamma_G\Gamma_D}\right|^2 \cdot \frac{1}{\eta}\right\}. \tag{6.38}$$

However,

$$\eta = \left|\frac{S_{21}}{1 - S_{22}\Gamma_L}\right|^2 \frac{1 - |\Gamma_D|^2}{1 - |\Gamma_1|^2}. \tag{6.39}$$

Hence,

$$L_I = 20 \text{ Log}_{10}\left|\frac{(1 - \Gamma_G\Gamma_1)(1 - S_{22}\Gamma_L)}{S_{21}(1 - \Gamma_G\Gamma_D)}\right|. \tag{6.40}$$

If the system is non-reflecting ($\Gamma_G = \Gamma_D = 0$), the insertion loss is the attenuation

$$A = 20 \text{ Log}_{10} \frac{1}{|S_{21}|}. \tag{3.55}$$

The mismatch error ε is

$$\varepsilon = L_I - A = 20 \text{ Log}_{10}\left|\frac{(1 - \Gamma_G\Gamma_1)(1 - S_{22}\Gamma_D)}{1 - \Gamma_G\Gamma_D}\right|. \tag{6.41}$$

This is equivalent to Weber's eq. (24), p. 826 where $R_o' = S_{11}$, $R_o'' = S_{22}$, $R_L = \Gamma_D$, $R' = \Gamma_1$, and $R_G = \Gamma_G$.

c. Evaluation of Error

Weber noted that his eq. (24) could be decomposed into three terms, each of the same form. In a similar way, eq. (6.41) equals

$$\varepsilon = 20 \text{ Log}_{10}|1 - \Gamma_G\Gamma_1| + 20 \text{ Log}_{10}|1 - S_{22}\Gamma_D| - 20 \text{ Log}_{10}|1 - \Gamma_G\Gamma_D|. \tag{6.42}$$

If the complex coefficients belonging to these terms were determined, one could then calculate each term and combine them to obtain ε.

It has been the practice to determine only the magnitudes of these coefficients (not their phases) and calculate the corresponding limits of ε, assuming that the phases might take on any value. Weber presented a graph (fig. 13·18 on his p. 827) which enables one to determine the limits of the components when one is given the VSWR corresponding to the magnitude of the complex coefficient.

Suppose that the VSWR's corresponding to $|\Gamma_G|$, $|\Gamma_1|$, $|S_{22}|$, and $|\Gamma_D|$ equal respectively 2.0, 1.15, 1.1, and 1.4. (These are the numbers in Weber's example.) The limits of the individual terms are:

$$\begin{aligned}
-0.21\ \text{dB} &\leq 20\log_{10}|1 - \Gamma_G\Gamma_1| \leq 0.20\ \text{dB} \\
-0.07 &\leq 20\log_{10}|1 - S_{22}\Gamma_D| \leq 0.07 \\
-0.48 &\leq 20\log_{10}|1 - \Gamma_G\Gamma_D| \leq 0.51 \\
\hline
-0.76\ \text{dB} &\leq \quad \varepsilon \quad \leq 0.78\ \text{dB}
\end{aligned}$$

The mismatch error ε must lie somewhere between the above limits, depending upon the relative phases of the reflection coefficients.

It would seem desirable to determine both phases and magnitudes of the reflection coefficients in order to determine ε and make a correction so as to get closer to the correct value.

It would also seem desirable to reduce Γ_G and Γ_D to extremely low values, because then ε would lie between very small limits and might even be negligible.

In practice, one can adjust Γ_G and Γ_D to have very small magnitudes indeed, but there remains an uncertainty about their residual value. For example, if a slotted line is used to indicate the achievement of $\Gamma_G = 0$, the best one can normally do is to obtain a flat response of the slotted line. The residual VSWR of the slotted line then represents the uncertainty in the assumption that $|\Gamma_G| = 0$. This might be 1.02, for example. If the same slotted line is used to indicate the achievement of $|\Gamma_D| = 0$, the uncertainty would be the same, or 1.02. One seldom has any corresponding phase information. Hence the mismatch error limits would be obtained by the above procedure. Assuming the same VSWR's corresponding to $|\Gamma_1|$ and to $|S_{22}|$, the limits of error would be as follows:

$$\begin{aligned}
-0.0064\ \text{dB} &\leq 20\log_{10}|1 - \Gamma_G\Gamma_1| \leq 0.0064\ \text{dB} \\
-0.0047 &\leq 20\log_{10}|1 - S_{22}\Gamma_D| \leq 0.0047 \\
-0.0008 &\leq 20\log_{10}|1 - \Gamma_G\Gamma_D| \leq 0.0008 \\
\hline
-0.0119\ \text{dB} &\leq \quad \varepsilon \quad \leq 0.0119\ \text{dB}
\end{aligned}$$

The importance of adjusting both generator and detector for low reflection is clearly shown by the large reduction in the limits of ε.

d. Effects of Attenuator Characteristics

The 2-port representing the attenuator is characterized by its scattering coefficients S_{11}, S_{12}, S_{21}, and S_{22}. They can appear explicitly in the equation for ε by substituting from eq. (3.10)

$$\Gamma_1 = \frac{(S_{12}S_{21} - S_{11}S_{22})\Gamma_D + S_{11}}{1 - S_{22}\Gamma_D} \tag{6.43}$$

into eq. (6.41). One obtains

$$\varepsilon = 20 \log_{10} \left| \frac{(1 - S_{11}\Gamma_G)(1 - S_{22}\Gamma_D) - S_{12}S_{21}\Gamma_G\Gamma_D}{1 - \Gamma_G\Gamma_D} \right| . \tag{6.44}$$

This can be used to evaluate the mismatch error when a given attenuator is inserted into a known system. One notes in particular that the magnitude of the term $S_{12}S_{21}\Gamma_G\Gamma_D$ becomes smaller as the attenuation becomes larger. In the practical case, it is negligible for attenuations of 20 dB or larger. If the attenuator is then reciprocal and nearly symmetrical, the simple graph of figure 6-9 (Beatty, 1967b) can be used to rapidly estimate approximate limits of mismatch error.

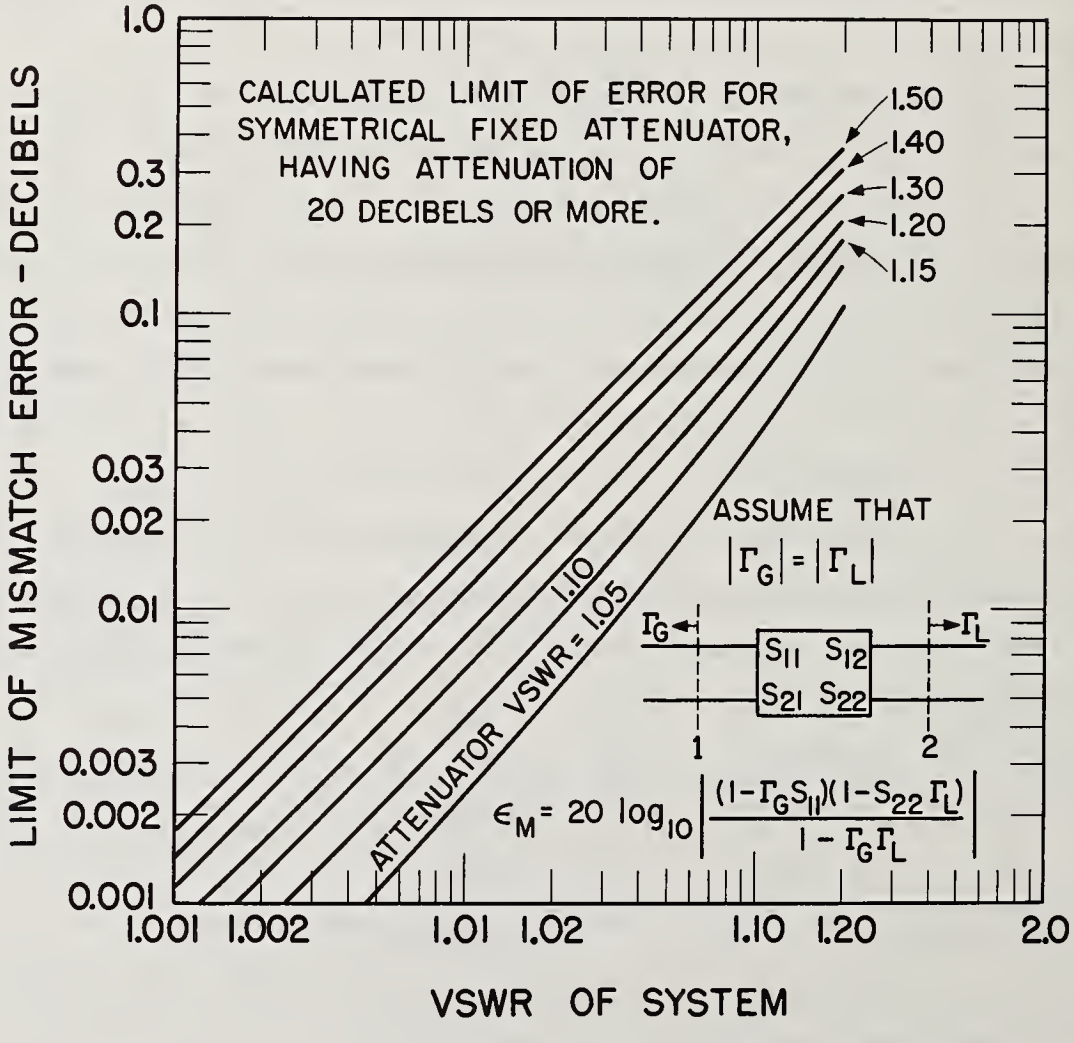

Figure 6-9. Graph for rapid estimates of limits of mismatch error.

As the limits of error become smaller, the magnitudes of the positive and negative limits become nearly equal.

e. Effect of Realizability Conditions

In calculating the limits of mismatch error, it has been assumed that the phases of the complex coefficients involved can have any value. In theory, realizability conditions for 2-ports impose limits on the permissible variations of phase. However, it is shown in section 6.5 that this is not important for most attenuators and only becomes significant when the attenuation is small (say less than 3 dB).

f. Variable Attenuators

The above analysis is extended to variable attenuators as follows. The discussion is a modified version of Beatty (1954).

(1) Introduction

The error in the measurement of changes in attenuation is important in the calibration of variable attenuators and in the calibration of large attenuators, using known pads as gage blocks or fixed attenuation standards.

The calibration of a variable attenuator consists in measuring the change in the insertion loss as the attenuator dial moves from a zero or reference position to another position that is marked or can be read on a scale. The change in the insertion loss equals the change in attenuation if the attenuator is placed in a reflectionless, or matched, system. There is always a degree of uncertainty regarding the match, depending upon the accuracy of the instruments used to indicate or recognize matched conditions and upon the reflections from connectors. For this reason the change in the insertion loss cannot be considered to be exactly equal to the change in attenuation, and the difference is called the mismatch error.

(2) Expression for Mismatch Error

Variable attenuators are of two types; (1) continuously variable, and (2) variable in steps. The mismatch errors may be analyzed in the same way for both types, since a change in a continuously variable attenuator from the reference position to another position is equivalent to removing one attenuator and inserting

another attenuator in the circuit. The insertion loss, in decibels, of the attenuator corresponding to the initial (reference) position of the variable attenuator is given by eq. (3.53) assuming that $Z_{01} = Z_{02}$, and is

$$ {}^{i}L = 20 \log_{10} \left| \frac{(1 - {}^{i}S_{11}\Gamma_G)(1 - {}^{i}S_{22}\Gamma_L) - {}^{i}S_{12}{}^{i}S_{21}\Gamma_G\Gamma_L}{{}^{i}S_{21}(1 - \Gamma_G\Gamma_L)} \right| . \tag{6.45} $$

The voltage-reflection coefficients Γ_G and Γ_L refer to the generator and load, respectively, and are measured at the terminals where the attenuator is inserted. The scattering coefficients S_{11}, S_{12}, S_{21}, and S_{22} refer to the attenuator, corresponding to the reference or zero position of the variable attenuator. The corresponding insertion loss for a different (final) setting of the variable attenuator is

$$ {}^{f}L = 20 \log_{10} \left| \frac{(1 - {}^{f}S_{11}\Gamma_G)(1 - {}^{f}S_{22}\Gamma_L) - {}^{f}S_{12}{}^{f}S_{21}\Gamma_G\Gamma_L}{{}^{f}S_{21}(1 - \Gamma_G\Gamma_L)} \right| . \tag{6.46} $$

The change in the insertion loss is

$$ \Delta L = {}^{f}L - {}^{i}L = 20 \log_{10} \left| \frac{1}{{}^{f}S_{21}} \right| - 20 \log_{10} \left| \frac{1}{{}^{i}S_{21}} \right| $$

$$ + 20 \log_{10} \left| \frac{(1 - {}^{f}S_{11}\Gamma_G)(1 - {}^{f}S_{22}\Gamma_L) - {}^{f}S_{12}{}^{f}S_{21}\Gamma_G\Gamma_L}{(1 - {}^{i}S_{11}\Gamma_G)(1 - {}^{i}S_{22}\Gamma_L) - {}^{i}S_{12}{}^{i}S_{21}\Gamma_G\Gamma_L} \right| , \tag{6.47} $$

or

$$ \Delta L = {}^{f}A - {}^{i}A + \varepsilon , \tag{6.48} $$

where ${}^{f}A$, ${}^{i}A$, and ε in eq. (6.48) correspond to the three terms in eq. (6.47). The error ε must be subtracted from the change in the insertion loss to obtain the change in attenuation, ${}^{f}A - {}^{i}A$.

The error term may also be written

$$ \varepsilon = 20 \log_{10} \left| \frac{(1 - {}^{f}\Gamma_1\Gamma_G)(1 - {}^{f}S_{22}\Gamma_L)}{(1 - {}^{i}\Gamma_1\Gamma_G)(1 - {}^{i}S_{22}\Gamma_L)} \right| , \tag{6.49} $$

where ${}^{i}\Gamma_1$ and ${}^{f}\Gamma_1$ are the input-voltage reflection coefficients of the attenuator terminated in a load having a voltage reflection coefficient Γ_L.

The mismatch error in the measurement of a single attenuator can be obtained as a special case of eq. (6.49). The reference attenuator vanishes in this case,

changing Γ_1 to Γ_L, S_{12} to unity, and S_{11} and S_{22} to zero. Substituting these values for Γ_1 and S_{22} into eq. (6.49) yields

$$\varepsilon = 20 \log_{10} \left| \frac{(1 - {}^{f}\Gamma_1\Gamma_G)(1 - {}^{f}S_{22}\Gamma_L)}{1 - \Gamma_G\Gamma_L} \right|, \tag{6.50}$$

which corresponds to our eq. (6.41) and to eq. (24), page 826 of Weber (1947).

(3) Evaluation of the Mismatch Errors

It is possible in principle to evaluate the mismatch error by measuring the voltage reflection coefficients Γ_G, Γ_L, Γ_1, ${}^{i}\Gamma_1$, S_{22}, and ${}^{i}S_{22}$, and substituting them into eq. (6.49).

In many cases, the magnitudes of the reflection coefficients can be determined, but their phases cannot be conveniently determined because of the limitations of a particular measuring apparatus. Equation (6.49) can then be used to find the limits of the mismatch error, permitting the phases of the reflection coefficients to have all possible values. The limit of error can be expressed in the form

$$\varepsilon_{limit} = 20 \log_{10} \frac{(1 \pm |{}^{f}\Gamma_1\Gamma_G|)(1 \pm |{}^{f}S_{22}\Gamma_L|)}{(1 \mp |{}^{i}\Gamma_1\Gamma_G|)(1 \mp |{}^{i}S_{22}\Gamma_L|)}, \tag{6.51}$$

and the corresponding limit of error for single attenuators is

$$\varepsilon_{limit} = 20 \log_{10} \frac{(1 \pm |\Gamma_1\Gamma_G|)(1 \pm |S_{22}\Gamma_L|)}{1 \mp |\Gamma_G\Gamma_L|}. \tag{6.52}$$

For example, in order to reduce mismatch errors in the calibration of attenuators, the magnitudes of Γ_G and Γ_L are made as small as possible, and their probable amplitude is estimated from the accuracy of the apparatus used to recognize matched conditions and from the known connector characteristics. It is difficult to accurately determine the phases of these small reflection coefficients, and the mismatch error can generally be determined not exactly, but within limits.

An example will illustrate the determination of mismatch error. If the voltage standing-wave ratios ρ_G, ρ_L, ρ_1, ρ_1', ρ_{22}, and ρ_{22}' [$\rho = (1 + |\Gamma|)/(1 - |\Gamma|)$] corresponding to $|\Gamma_G|$, $|\Gamma_L|$, $|\Gamma_1|$, $|\Gamma_1'|$, $|S_{22}|$, and $|S_{22}'|$ are 1.1, 1.1, 1.2, 1.5, 1.2, and 1.5, the limits of error for the initial attenuator calculated from eq. (6.52) are approximately ± 0.095 decibel. The corresponding limits of error for the final attenuator are approximately ± 0.185 decibel. The limits of error for the change in

attenuation calculated from eq. (6.51) are approximately ± 0.242 decibel. It is seen that the mismatch error for the change in attenuation is less than the sum of the mismatch errors in measuring each attenuator individually.

g. Avoidance of Mismatch Error

It has been mentioned that it is possible in principle to measure both amplitudes and phases of reflection coefficients and make a correction to an attenuation measurement. (Although not often done in the past, it may be done more often now when using computer-controlled measurement systems.)

Another method for avoiding mismatch error has been proposed (Rabinovitch, 1962), but its value has been questioned (Leber, 1964).

h. Later Work

Additional analysis of mismatch errors when using rotary-vane type variable attenuators has been published (Engen and Beatty, 1960), (Holm et al., 1967). This type of attenuator causes little change in phase shift and hence the mismatch errors are small.

The effects of reflections and dissipative losses in connectors and adapters are not adequately taken into account in the previous analysis because the attenuator is represented by a single 2-port. Later, in section 6.6, the attenuator and the connector pairs are represented by three cascaded 2-ports (Beatty, 1964b), so as to involve the connector parameters explicitly in the analysis of mismatch error.

6.5. Effects of Realizability Conditions

The purpose here is to discuss the effect of the realizability conditions for 2-ports upon the estimation of limits of mismatch error in high-frequency and microwave attenuation measurements. Only the case of fixed attenuators is considered. It will be shown that the realizability conditions need be considered only for certain ranges of attenuation and VSWR, and that the conventional method of estimating mismatch error limits is satisfactory for most attenuators.

As shown in the previous section 6.4c, the mismatch error is

$$\varepsilon = 20 \log_{10} \left| \frac{(1 - S_{11}\Gamma_G)(1 - S_{22}\Gamma_D) - S_{12}S_{21}\Gamma_G\Gamma_D}{1 - \Gamma_G\Gamma_D} \right| . \qquad (6.44)$$

If only the magnitudes of the individual factors in this expression are known, and it is assumed that the phases can have any values, ε will have limits determined by

$$\varepsilon_{limit} = 20 \log_{10} \frac{(1 \pm |S_{11}\Gamma_G|)(1 \pm |S_{22}\Gamma_D|) \pm |S_{12}S_{21}\Gamma_G\Gamma_D|}{1 \mp |\Gamma_G\Gamma_D|}. \qquad (6.53)$$

The limits of mismatch error in measuring the attenuation of a fixed attenuator are usually determined from eq. (6.53), or its equivalent. This is a valid procedure if the above assumption about the phases is valid. However, within certain ranges of attenuation and VSWR, realizability conditions limit the values which may be reached by both magnitudes and phases of the scattering coefficients. Within these ranges, the limits of error estimated from the above equations may be too conservative. Therefore it is of interest to determine these ranges of attenuation and VSWR.

In order to simplify the analysis and presentation of results, only symmetrical reciprocal attenuators are considered. This is felt to be a useful approach, since most attenuator pads approximate these assumed conditions.

The realizability conditions (Kerns and Beatty, 1967) for a symmetrical reciprocal 2-port network can be written as follows. (From symmetry, the characteristic impedances $Z_{01} = Z_{02}$, and $S_{22} = S_{11} = |S_{11}|e^{j\psi_{11}}$, and also from reciprocity, $S_{12} = S_{21} = |S_{21}|e^{j\psi_{21}}$.)

$$|S_{21}|^2 < 1 - |S_{11}|^2, \qquad (6.54)$$

and

$$|\cos(\psi_{21} - \psi_{11})| < \frac{1 - |S_{11}|^2 - |S_{21}|^2}{2|S_{11}S_{21}|}. \qquad (6.55)$$

The above equations define the ranges of attenuation and VSWR (regions) over which a passive, symmetrical, reciprocal 2-port is 1) not realizable; 2) realizable providing $(\psi_{21} - \psi_{11})$ is limited to certain values, when the right side of eq. (6.55) is less than unity; and 3) realizable with no limits on $(\psi_{21} - \psi_{11})$ when the right side of eq. (6.55) is greater than or equal to unity. These three cases are shown in figure 6.10. When the attenuator characteristics lie in region 3), the conventional method of estimating mismatch error limits is satisfactory. In region 2) the conventional methods would give too-conservative limits, and a different method (Youla and Paterno, 1964) would be required.

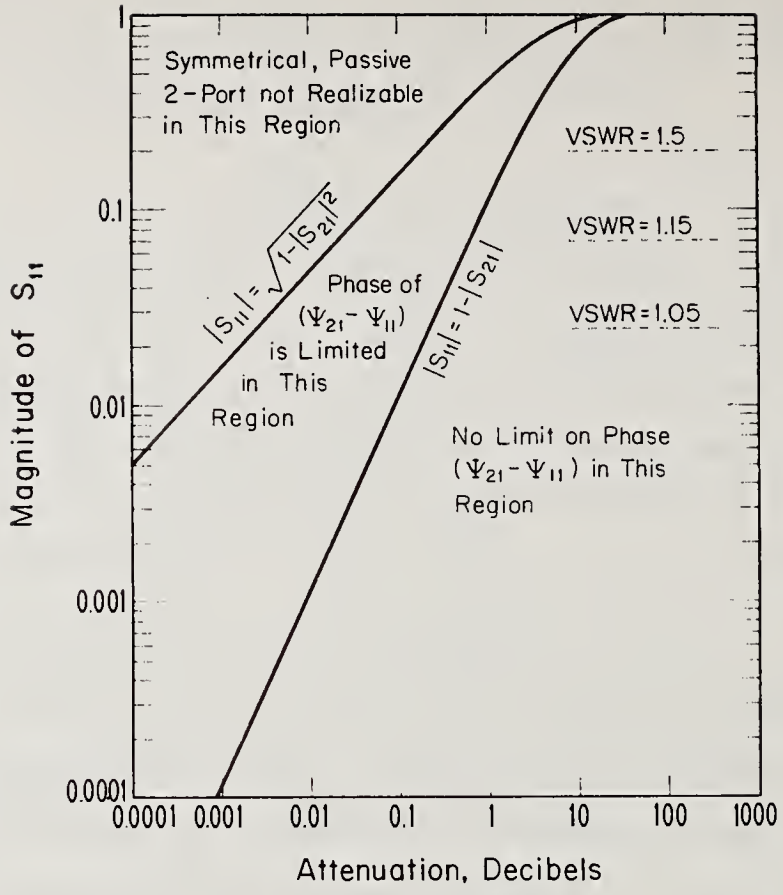

Figure 6-10. Ranges of attenuations and reflection coefficients of symmetrical reciprocal attenuators for which realizability conditions restrict the relative phases of the scattering coefficients.

It can be seen by inspection of figure 6-10 that the conventional method of estimating limits of mismatch error is satisfactory for attenuators having an attenuation greater than 2 dB and a VSWR less than 1.50. Since most fixed attenuators have characteristics which fall within these limits, it is not often necessary to consider the effect of realizability conditions upon mismatch error limits.

6.6. Effects of Connectors and Adapters

a. Introduction

This section is a modified version of Beatty (1964b). Suppose that we wish to answer the following question: (If the attenuation of a stable fixed attenuator is measured at the same operating frequency in two different systems, to what extent is

the difference of results attributable to differences in the waveguide[8] joints or connectors[9] used at the insertion points?[10] (Effects of connector reflections and dissipative losses are taken into account, but leakage is not considered.)

In seeking an answer to this question, the representation ordinarily used for the insertion of an attenuator into a waveguide system, and the concept of insertion loss itself were found to be inadequate, and a new analysis was developed. The essential feature of the new approach is that the waveguide joints or connectors at insertion points are not assumed to be perfect,[9] i.e., having no loss, no reflection, and effectively no characteristic phase shift, but are represented by two-ports having appropriate characteristics. In addition, the attenuator when installed in a circuit is no longer represented by a single two-port, but by three cascaded two-ports, the outer ones representing the connector pairs, and the inner one representing the core or kernel of the attenuator. The quantity of interest is the loss in power delivered to the load when the above three cascaded two-ports (representing the attenuator and its associated connector pairs) are substituted for the single two-port representing the connector pair at the insertion point. This loss in power, expressed in decibels, is called the substitution loss (Beatty, 1964a).

Since the result of an attenuation measurement does depend upon the characteristics of the connectors at the insertion point, one must specify these characteristics if such a measurement is to be precisely defined. This leads to a slightly modified definition of the quantity of interest in the measurement of a quantity characteristic of the attenuator, and it is called the standard attenuation. (In section 6.2g, it is called "characteristic insertion loss" or "characteristic attenuation.")

The analytical methods developed here are applicable to other situations in which a waveguide component is inserted into a waveguide system. They might be applied

---

[8]The term "waveguide" is used here in a broad sense to include, for example, both uniconductor waveguide having a rectangular cross section and two-conductor waveguide having a concentric-circular or coaxial cross section.

[9]The term "connector" is used here in a broad sense to designate the devices designed to join together two sections of waveguide having the same cross section. A "perfect connector pair" is one which would have no leakage, no loss, no reflection, and effectively-zero-characteristic phase shift.

[10]The term "insertion point" is used to designate the place where a waveguide component such as an attenuator is inserted into a waveguide system. It is thus not a geometrical point, but may be the region where a connector pair belonging to the system is disconnected, or where an adapter belonging to the system is removed, in order to insert a waveguide component.

for example to analyze the effects of connectors or adapters[11] on accurate measurements of the characteristic phase shift of phase shifters, or on the frequency of transmission-type cavity wavemeters. However, at present they will be applied only to microwave attenuation measurements.

Previous analytical methods used to obtain equations for insertion loss, attenuation, and mismatch error for the case of a single fixed attenuator have been given in sections 3.8 and 6.4. Corresponding equations will be obtained using different methods and the results will be discussed. The specified question mentioned earlier will be answered and a calculated limit given for the effect. The techniques developed will then be applied to the case of variable attenuators, and to fixed attenuators having nonmating[12] connectors. Some of the cases having immediate interest will be discussed in some detail and calculated examples given to illustrate the use of the error equations. Useful formulas and graphs supplemental to the analysis will be given.

b. Previous Analyses

It has been customary to represent a waveguide component such as an attenuator by a two-arm waveguide junction (two-port), as shown in figure 6-11 where i_P and

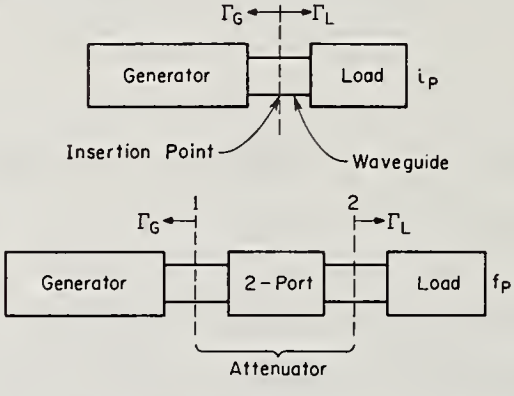

Figure 6-11. Simple representation of an attenuator by a two-port inserted into a waveguide circuit.

[11]The term "adapter" is used to designate a device designed to join together two sections of waveguide which have already been fitted with connectors. A perfect adapter-connector combination would have no leakage, no loss, no reflection, and effectively-zero-characteristic phase shift.

[12]The term "nonmating connectors" as applied to a waveguide components such as an attenuator is meant to imply that the connectors on each end of the components are of such a type or sex that they could not be joined together even if it were possible to move them physically into a favorable position for such joining.

^{f}P designate the powers dissipated in the load under the initial and final conditions, respectively. The reflection coefficients of the generator and the load are designated as Γ_G and Γ_L, respectively. It is usually assumed that they are the same at the times that ^{i}P and ^{f}P are observed. (Since the load in attenuation measuring may also be a detector, one finds Γ_D instead of Γ_L in many previous equations.

It is also apparent from the diagram that the connector pair or adapter at the insertion point is assumed to be perfect.

It has been customary to assume that one actually measures the insertion loss and that it can be written

$$L_I = 10 \log_{10}\frac{i_P}{f_P} = 10 \log_{10} \cdot \left\{\frac{Z_{02}}{Z_{01}}\left|\frac{(1 - S_{11}\Gamma_G)(1 - S_{22}\Gamma_L) - S_{12}S_{21}\Gamma_G\Gamma_L}{S_{21}(1 - \Gamma_G\Gamma_L)}\right|^2\right\}. \qquad (3.53)$$

It has also been assumed that the desired quantity is the attenuation, which may be written

$$A = [L_I]_{\Gamma_G=\Gamma_L=0} = 10 \log_{10}\left\{\frac{Z_{02}}{Z_{01}}\frac{1}{|S_{21}|^2}\right\}. \qquad (3.54)$$

The difference between A and L_I is due mainly to system reflections or mismatch and has been called the mismatch error. It is written

$$\varepsilon_M = L_I - A = 20 \log_{10}\left|\frac{(1 - S_{11}\Gamma_G)(1 - S_{22}\Gamma_L) - S_{12}S_{21}\Gamma_G\Gamma_L}{1 - \Gamma_G\Gamma_L}\right|. \qquad (6.44)$$

It is seen that the connector or adapter used at the insertion point is not shown in the diagram, and its characteristics do not appear in the equations. Hence there is no way to calculate its effect on the measurement.

c. An Improved Representation

A two-port, or two-arm waveguide junction or transducer has associated with it two waveguide leads through which energy may enter and leave. The terminal surfaces of the two-port are cross-sectional surfaces within the waveguide leads. Usually only one propagating mode is associated with each lead and each terminal surface. A waveguide component such as an attenuator evidently cannot itself be represented by a two-port unless the connectors are perfect and all connectors mate at coplanar butt joints. Since this requirement is often not very closely approximated by actual connectors, the representation of figure 6-12 is more realistic. The attenuator installed in the circuit is represented by a composite two-port composed of three cascaded two-ports, A, B, and C.

The central core or kernel of the attenuator is represented by B. The connectors B_G and B_L at each end of the attenuator mate with the connectors D_G and D_L, respectively, of the system to form connector pairs represented by two-ports A and C. When the attenuator is removed, the system may be closed as shown in figure 6-13 by joining connectors D_G and D_L.

The precise manner in which the connectors join and separate is not specified, as this would call for further more complicated analysis of specific discontinuities. Further work has been done in characterizing connectors (Harris, 1965), (Hashimoto, 1968).

The analysis of the situation represented in figure 6-13 proceeds as follows.

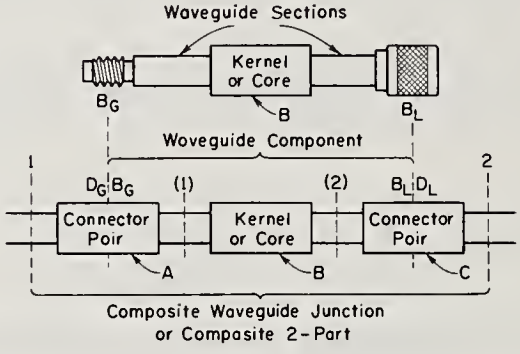

Figure 6-12. Representation of a waveguide component.

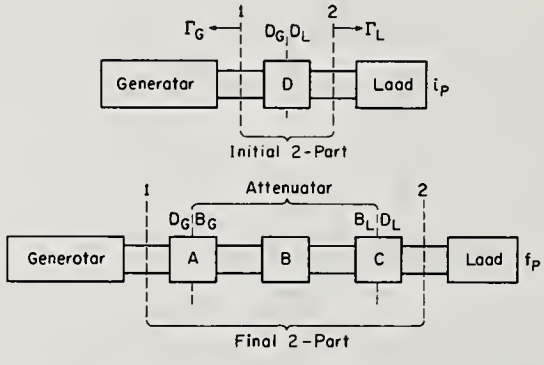

Figure 6-13. Improved representation of attenuator insertion into a waveguide system (Case 1).

d. Substitution Loss

When inserting an attenuator into a measuring system, as shown in figure 6-13, one actually substitutes the attenuator and two sets of connector pairs A and B, for the connector pair D which initially connects the system together. Thus one

measures the substitution loss, or the ratio of ${}^{i}P$ to ${}^{f}P$. It is similar to eq. (3.53), but the characteristics of the connectors are now implicitly involved, as they influence the scattering coefficients of the initial and final two-ports. The substitution loss L_S is written as follows:

$$L_S = 10 \log_{10} \frac{{}^{i}P}{{}^{f}P} = 20 \log_{10}$$

$$\cdot \left| \frac{{}^{i}S_{21}}{{}^{f}S_{21}} \cdot \frac{(1 - {}^{f}S_{11}\Gamma_G)(1 - {}^{f}S_{22}\Gamma_L) - {}^{f}S_{12}{}^{f}S_{21}\Gamma_G\Gamma_L}{(1 - {}^{i}S_{11}\Gamma_G)(1 - {}^{i}S_{22}\Gamma_L) - {}^{i}S_{12}{}^{i}S_{21}\Gamma_G\Gamma_L} \right|, \qquad (3.51)$$

where the front superscripts i and f on the scattering coefficients refer to the initial and final two-ports, respectively.

Additional insight is obtained by writing eq. (3.51) in two additional forms. First, it is written as the difference between the insertion losses of the initial and final two-ports as follows:

$$L_S = {}^{f}L - {}^{i}L = 20 \log_{10} \left| \frac{(1 - {}^{f}S_{11}\Gamma_G)(1 - {}^{f}S_{22}\Gamma_L) - {}^{f}S_{12}{}^{f}S_{21}\Gamma_G\Gamma_L}{{}^{f}S_{21}(1 - \Gamma_G\Gamma_L)} \right|$$

$$- 20 \log_{10} \left| \frac{(1 - {}^{i}S_{11}\Gamma_G)(1 - {}^{i}S_{22}\Gamma_L) - {}^{i}S_{12}{}^{i}S_{21}\Gamma_G\Gamma_L}{{}^{i}S_{21}(1 - \Gamma_G\Gamma_L)} \right|. \qquad (6.56)$$

It is apparent that, analytically, substitution loss is equivalent to a difference between two insertion losses. One could thus avoid the use of the concept of substitution loss, if desired. However the assumptions made in the definition of substitution loss are more easily realized in practice. In addition, it is more convenient to use when analyzing variable attenuators, as will be seen later.

Another form of eq. (3.51) is the following

$$L_S = ({}^{f}A - {}^{i}A) + 20 \log_{10} \left| \frac{(1 - {}^{f}S_{11}\Gamma_G)(1 - {}^{f}S_{22}\Gamma_L) - {}^{f}S_{12}{}^{f}S_{21}\Gamma_G\Gamma_L}{1 - \Gamma_G\Gamma_L} \right|$$

$$- 20 \log_{10} \left| \frac{(1 - {}^{i}S_{11}\Gamma_G)(1 - {}^{i}S_{22}\Gamma_L) - {}^{i}S_{12}{}^{i}S_{21}\Gamma_G\Gamma_L}{1 - \Gamma_G\Gamma_L} \right|. \qquad (6.57)$$

The first two terms above on the right are attenuations as defined in eq. (3.53) and the last two terms are similar in form to eq. (6.44), the mismatch error of the previous analysis.

More complex expressions, containing the scattering coefficients of two-ports, A, B, C, and D could be obtained by making the appropriate substitutions for the scattering coefficients of the composite final two-port (Hashimoto, 1968).

The substitution loss which would occur in a non-reflecting system is of interest and can be deduced from eq. (6.57) when $\Gamma_G = \Gamma_L = 0$. It is

$$(L_S)_{\Gamma_G=\Gamma_L=0} = ({}^{f}A - {}^{i}A) = 20 \log_{10}\left|\frac{{}^{i}S_{21}}{{}^{f}S_{21}}\right|. \tag{6.58}$$

It is simply the difference in the attenuations between the initial and final two-ports.

e. Standard Attenuation

In practice, one is not interested in the attenuation ${}^{f}A$ of the final two-port for two reasons. First, it is difficult to measure since the initial two-port would need to be a perfect connector which cannot be actually realized. And second, it is not characteristic of the attenuator itself but of the attenuator kernel B plus two associated connector pairs A and C. The system connectors D_G and D_L which do not belong to the attenuator are parts of A and C.

The quantity of interest is the standard attenuation which is the above difference in attenuation when the initial two-port represents not a perfect connector pair, but a standard connector pair.[13] An expression for standard attenuation ${}^{S}A$ is obtained as follows: Equation (6.58) is written in terms of the scattering equations of two-ports A, B, C, and D as

$$\begin{aligned}(L_S)_{\Gamma_G=\Gamma_L=0} &= A_A + A_B + A_C - A_D \\ &\quad + 20 \log_{10}\left|\frac{(1 - a_{22}b_{11})(1 - b_{22}c_{11}) - a_{22}b_{12}b_{21}c_{11}}{1 - a_{22}c_{11}}\right| \\ &\quad - 20 \log_{10}|1 - a_{22}c_{11}|\end{aligned}$$

or

$$(L_S)_{\Gamma_G=\Gamma_L=0} = 20 \log_{10}\left|\frac{d_{21}}{a_{21}b_{21}c_{21}}\,[(1 - a_{22}b_{11})(1 - b_{22}c_{11}) - a_{22}b_{12}b_{21}c_{11}]\right|. \tag{6.59}$$

If the two-port D represents a standard connector pair, and d_{21} is replaced by ${}^{S}S_{21}$, the standard attenuation is

$${}^{S}A = 20 \log_{10}\left|\frac{{}^{S}S_{21}}{a_{21}b_{21}c_{21}}\,[(1 - a_{22}b_{11})(1 - b_{22}c_{11}) - a_{22}b_{12}b_{21}c_{11}]\right|. \tag{6.60}$$

[13] A "standard connector" is one which is made precisely to standard specifications for the particular type of connector under consideration. Standard connector pairs usually have low but appreciable dissipative loss, reflection, and leakage.

It is of interest to examine the form of eq. (6.58) when the connector pairs are all identical and nonreflecting. One obtains

$$(L_S)_{\substack{\Gamma_G=\Gamma_L=0 \\ A\equiv C\equiv D}} = A_A + A_B. \tag{6.61}$$

Under this assumption, eq. (6.61) expresses a quantity characteristic of the attenuator itself as represented by the kernel B and connectors B_G and B_L.

To the extent that all connectors are identical and nonreflecting, eq. (6.60) will also express a quantity characteristic of the attenuator itself. The standard attenuation as defined above is thus to a good approximation characteristic of the attenuator itself, and will be considered the desired quantity in an attenuation measurement.

f. Connector and Mismatch Errors

The error ε_S in the measurement of standard attenuation cannot be obtained simply by subtracting eq. (6.60) from eq. (3.51), eq. (6.56), or eq. (6.57). This is evident when we consider figure 6-14 which represents the substitution loss of an attenuator measured in two different systems, M and N. Even though the attenuator is the same in both cases, it is associated with connector pairs A and C in system M and with P and Q in system N. Thus the final two-ports are different in the two systems.

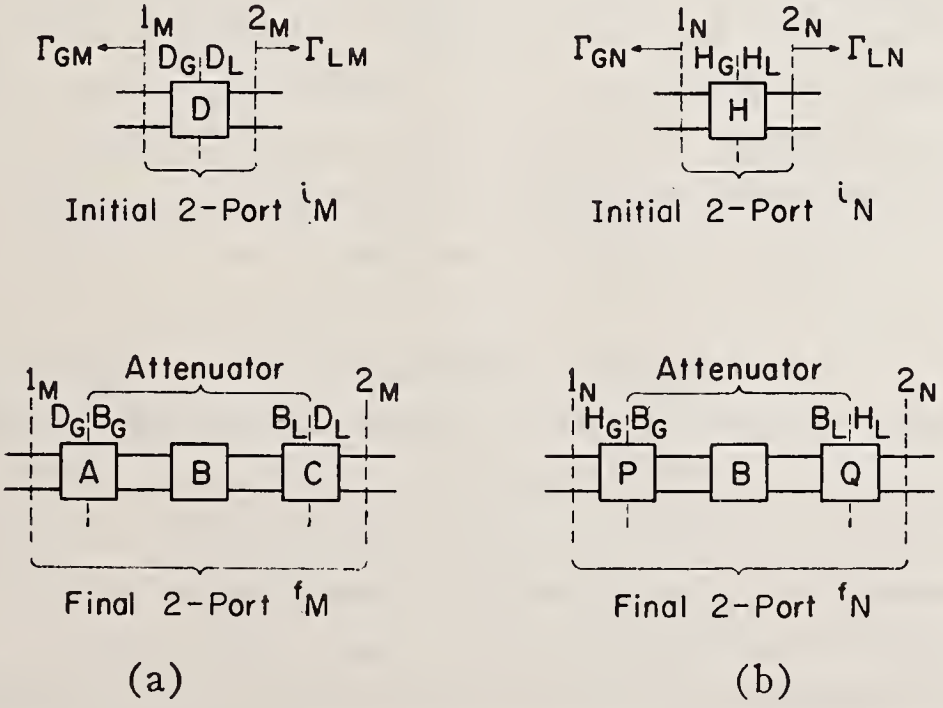

Figure 6-14. Representation of same attenuator installed alternately into two different systems. (a) System "M." (b) System "N."

In order to obtain an expression for ε_S, let system M be nonreflecting and two-port D represent a standard connector pair having an attenuation A_S. Then the error ε_S is the difference between the substitution losses in systems M and N, and is written

$$\varepsilon_S = \varepsilon_I + \varepsilon_{II} + \varepsilon_{III}$$

where

$$\varepsilon_I = (A_S - A_{II}) + (A_P - A_A) + (A_Q - A_C)$$

$$\varepsilon_{II} = 20 \log_{10}\left|\frac{(1 - p_{22}b_{11})(1 - b_{22}q_{11}) - p_{22}b_{12}b_{21}q_{11}}{1 - p_{22}q_{11}}\right|$$

$$- 20 \log_{10}\left|\frac{(1 - a_{22}b_{11})(1 - b_{22}c_{11}) - a_{22}b_{12}b_{21}c_{11}}{1 - a_{22}c_{11}}\right|$$

$$+ 20 \log_{10}\left|\frac{1 - p_{22}q_{11}}{1 - a_{22}c_{11}}\right|$$

and

$$\varepsilon_{III} = 20 \log_{10}\left|\frac{(1 - {}^{fN}S_{11}\Gamma_G)(1 - {}^{fN}S_{22}\Gamma_L) - {}^{fN}S_{12}\,{}^{fN}S_{21}\Gamma_G\Gamma_L}{1 - \Gamma_G\Gamma_L}\right|$$

$$- 20 \log_{10}\left|\frac{(1 - h_{11}\Gamma_G)(1 - h_{22}\Gamma_L) - h_{12}h_{21}\Gamma_G\Gamma_L}{1 - \Gamma_G\Gamma_L}\right|. \qquad (6.62)$$

The error component ε_I will vanish if corresponding connectors at the insertion points are identical, since it is seen from figure 6-14 that the resulting condition will be that D ≡ H, A ≡ P, and C ≡ Q. This is a sufficient, but not a necessary, condition since ε_I will vanish for any condition for which $A_S + A_P + A_Q = A_H + A_A + A_C$. Usually the corresponding connectors at the insertion points will be similar, and it is evidently worthwhile to make them as nearly identical as possible.

The error component ε_{II} will also vanish if corresponding connectors at the insertion points in the two systems are identical, and this is again a sufficient but not a necessary condition. It will also approach zero if the attenuator kernel is nonreflecting and its attenuation becomes arbitrarily large. The individual terms are of the same familiar form as eq. (6.44) for mismatch error in the simpler analysis.

The error component ε_{III} is very similar in form to eq. (6.44) and will vanish if the system reflection coefficients Γ_G and Γ_L vanish. Again this is a sufficient but not a necessary condition, since the relative phases of the reflection coefficients involved might possibly be such as to make the two terms vanish or cancel

each other. It is clear that ε_{III} differs from the other two components in that the condition of identical corresponding connectors at the insertion points does not make it vanish. The limits of terms in ε_{II} and ε_{III} similar to eq. (6.44) may be evaluated by methods previously described in section 6.4, and they are typically each of several tenths of a decibel, or less. Since each such positive term is paired with a similar negative term, it is the differences which are important in these errors.

Since the various terms in eq. (6.62) may not all be of the same sign, some of them may tend to cancel others, and the overall error ε_S may be lower than some of the individual terms. In careful measurements however, one cannot afford to take this for granted, but should either make a thorough investigation, or quote a conservative limit of error, assuming the most unfavorable phase relationships of the coefficients involved.

g. Same Fixed Attenuator in Two Systems

The motivating question asked earlier can now be answered using the representation of figure 6-14 letting two-port D represent a connector pair which is not necessarily a standard one, and letting Γ_{GM} and Γ_{LM} be representative of an actual system, and not an idealized one having no reflections.

Assume that in attempting to measure the standard attenuation of a fixed attenuator in two different systems, we actually measure the substitution loss. We are interested in the difference ΔL_S in substitution loss as measured in two systems. As in the previous situation, a part of this difference is primarily due to differences in connectors D_G and H_G, and D_L and H_L, and the other part of the difference is due primarily to differences in system generator and load reflection coefficients.

Referring to figure 6-14 and eq. (6.57), we can write

$$\Delta L_S = L_{S\dot{N}} - L_{SM} = ({}^{fN}A - {}^{fM}A) + ({}^{iM}A - {}^{iN}A)$$

$$+ 20 \log_{10}\left|\frac{(1 - {}^{fN}S_{11}\Gamma_{GN})(1 - {}^{fN}S_{22}\Gamma_{LN}) - {}^{fN}S_{12}{}^{fN}S_{21}\Gamma_{GN}\Gamma_{LN}}{1 - \Gamma_{GN}\Gamma_{LN}}\right|$$

$$- 20 \log_{10}\left|\frac{(1 - {}^{iN}S_{11}\Gamma_{GN})(1 - {}^{iN}S_{22}\Gamma_{LN}) - {}^{iN}S_{12}{}^{iN}S_{21}\Gamma_{GN}\Gamma_{LN}}{1 - \Gamma_{GN}\Gamma_{LN}}\right|$$

$$- 20 \log_{10}\left|\frac{(1 - {}^{fM}S_{11}\Gamma_{GM})(1 - {}^{fM}S_{22}\Gamma_{LM}) - {}^{fM}S_{12}{}^{fM}S_{21}\Gamma_{GM}\Gamma_{LM}}{1 - \Gamma_{GM}\Gamma_{LM}}\right|$$

$$+ 20 \log_{10}\left|\frac{(1 - {}^{iM}S_{11}\Gamma_{GM})(1 - {}^{iM}S_{22}\Gamma_{LM}) - {}^{iM}S_{12}{}^{iM}S_{21}\Gamma_{GM}\Gamma_{LM}}{1 - \Gamma_{GM}\Gamma_{LM}}\right|. \qquad (6.63)$$

The sufficient conditions under which ΔL_S will vanish are ${}^{i}M = {}^{i}N$, ${}^{f}M = {}^{f}N$, $\Gamma_{GM} = \Gamma_{GN}$, and $\Gamma_{LM} = \Gamma_{LN}$. In practice, one might try to achieve these conditions, but some uncertainty will always exist. In order to evaluate ΔL_S using eq. (6.63), information would be needed on the characteristics of the two-ports ${}^{i}M$, ${}^{f}M$, ${}^{i}N$, and ${}^{f}N$, as well as on the system generator and load reflection coefficients Γ_{GM}, Γ_{LM}, Γ_{GN}, and Γ_{LN} effective at terminal surface 1_M, 2_M, 1_N, and 2_N.

It is possible to reduce the magnitudes of the system reflection coefficients to very low values (say 0.001) by the use of tuners, in which case the last four terms of eq. (6.63) would be negligible, e.g., less than 0.001 dB. Thus the case of ΔL_S for $\Gamma_{GM} = \Gamma_{LM} = \Gamma_{GN} = \Gamma_{LN} = 0$ is of interest and is given by

$$(\Delta L_S)_{\substack{[\Gamma_{GM}=\Gamma_{LM}=0] \\ [\Gamma_{GN}=\Gamma_{LN}=0]}}$$

$$= \Delta A = (A_D - A_H) + (A_P - A_A) + (A_Q - A_C)$$

$$+ 20 \log_{10}\left|\frac{(1 - p_{22}b_{11})(1 - b_{22}q_{11}) - p_{22}b_{12}b_{21}q_{11}}{(1 - a_{22}b_{11})(1 - b_{22}c_{11}) - a_{22}b_{12}b_{21}c_{11}}\right|. \qquad (6.64)$$

The above result equals $\varepsilon_I + \varepsilon_{II}$ of eq. (6.62) if we replace A_D by A_S, and vanishes if connectors $D_G \equiv H_G$ and $D_L \equiv H_L$.

The use of eq. (6.64) in the evaluation of errors due to differences in the system connectors is illustrated by the following calculated examples. Consider the case in which all connector pairs in system M are identical, or A ≡ C ≡ D, but the left-hand connector D_G at the insertion point is modified and becomes H_G, but D_L and H_L remain the same. Under this supposition, connector pairs H and P will be the same, and connector pairs A, C, D, and Q will be alike.

If connector D_G were a male type-N connector, for example, it might be modified by removing the compensating step in the outer conductor and moving the step in the male center conductor outward so as to close the gap or notch normally present. In the following examples certain values are assumed for the reflection coefficients appearing in eq. (6.64) which are thought to be realistic in view of the measured results obtained at NBS for certain type-N connectors shown in figure 6-15. Since large variations among connectors of the same type are possible, these results cannot be regarded as typical of all type-N connectors.

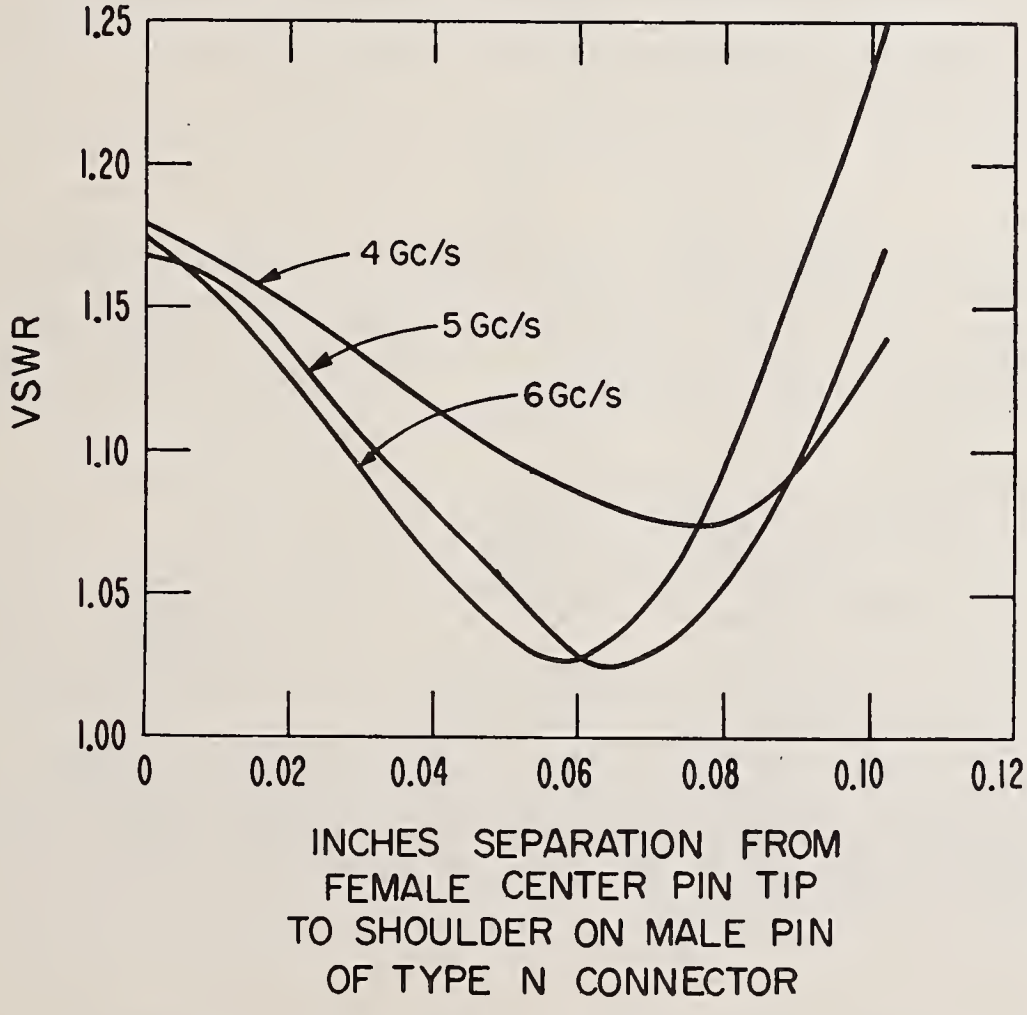

Figure 6-15. Experimental data for VSWR of type-M connector pair.

Example 1

Given a 3 dB fixed attenuator having a kernel VSWR of 1.22, connector pairs A, C, D, and Q having VSWR's of 1.22, and connector pairs H and P having VSWR's of 1.00. Thus $|p_{11}| = |p_{22}| = |h_{11}| = |h_{22}| = 0$, $|b_{11}| = |a_{22}| = |c_{11}| = |q_{11}| = 0.10$, and $|b_{12}b_{21}| = 0.5$.

The attenuation terms in eq. (6.64) have components due to dissipation and reflection, and those due to reflection cancel in the above example. The dissipative components should also nearly cancel, leaving only the final term of eq. (6.64). It can be written to a good approximation as

$$20 \log_{10}|1 + b_{11}(a_{22} - p_{22}) + b_{22}(c_{11} - q_{11}) + b_{12}b_{21}(a_{22}c_{11} - p_{22}q_{11})|, \qquad (6.65)$$

if the connector reflections are small, corresponding to reflection coefficients of magnitude less than 0.11. Limits of ΔA, assuming the worst phase combinations are

$$-0.131 \text{ dB} \leq \Delta A \leq 0.129 \text{ dB}.$$

The limits of error in the above example are significant ones, well above the usual precision of a good attenuation measurement. However, many attenuators which are presently commercially available have better characteristics than were assumed above. Hence, another example follows.

Example 2

Given a 3 dB fixed attenuator having a kernel VSWR of 1.15, connector pairs A, C, D, and Q having VSWR's of 1.15, and connector pairs H and P having VSWR's of 1.00. Thus $|p_{11}| = |p_{22}| = |h_{11}| = |h_{22}| = 0$, $|b_{11}| = |a_{22}| = |c_{11}| = |q_{11}| = 0.07$, and $|b_{12}b_{21}| = 0.5$

Proceeding as in Example 1, the limits of ΔA are

$$-0.064 \text{ dB} \leq \Delta A \leq 0.064 \text{ dB}.$$

The limits of error in this example are smaller, but still significant, since a precision of 0.03 dB is often obtained in a measurement of 3 dB at frequencies of 4 GHz and above.

If the fixed attenuators in Examples 1 and 2 above have attenuations of 20 dB or more (instead of 3 dB), the calculated limits of ΔA will be reduced to approximately $\pm$ 0.09 dB and $\pm$ 0.04 dB, respectively.

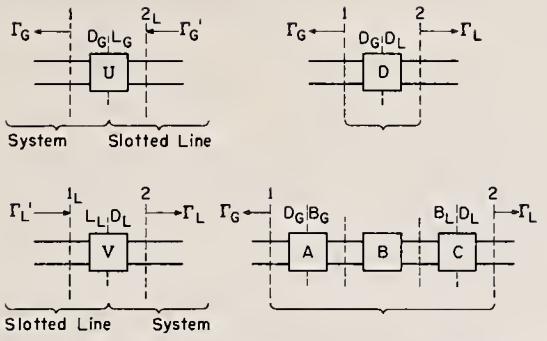

Figure 6-16. Representation of arrangement often used to adjust system reflections prior to attenuation measurement.

h. Adjusting Systems for Zero Reflections

In adjusting an attenuation measurement system in an effort to make $\Gamma_G = \Gamma_L = 0$, the arrangement represented in figure 6-16 is often used. A slotted line is connected in turn to system connectors D_G and D_L, and tuners are adjusted until the reflection coefficients Γ_G' and Γ_L' observed in the slotted section effectively vanish. This does not necessarily make the reflection coefficients Γ_G and Γ_L of the system vanish because, in general, the two-ports U and V may have reflections. The two-ports U and V are composite two-ports representing a connector pair and the taper or transition section at the end of the slotted line.

Alternatively, a tuning stub may be included, and is used to adjust for the condition $u_{22} = v_{22} = 0$ (Mathis, 1955). This condition, together with the condition $\Gamma_G' = \Gamma_L' = 0$, will make the reflection coefficients Γ_G and Γ_L of the measurement system vanish. The measured substitution loss will then equal the standard attenuation, provided that connector pair D is standard. Experimental arrangements are indicated in figure 6-5, section 6.2.

A tuning circuit using directional couplers can be used to achieve source or load Z_0-match (Beatty and Fentress, 1971). It is worthwhile to tune for the condition $u_{22} = v_{11} = 0$ (tuning out of the residual VSWR) because one can then adjust for system VSWR's of 1.01 or less instead of having to "add" to this the residual VSWR of 1.04 to 1.10 that may be present.

If the condition $u_{22} = v_{11} = 0$ is not obtained and Γ_G' and Γ_L' are not made to vanish, the measured substitution loss then is given by eq. (3.51) where

$$\Gamma_G = \frac{\Gamma_G' - u_{22}}{(u_{12}u_{21} - u_{11}u_{22}) + u_{11}\Gamma_G'}$$

$$\Gamma_L = \frac{\Gamma_L' - v_{11}}{(v_{12}v_{21} - v_{11}v_{22}) + v_{22}\Gamma_L'}$$

$$^{i}S_{11} = d_{11},\ ^{i}S_{12} = d_{12},\ ^{i}S_{21} = d_{21},\ ^{i}S_{22} = d_{22}$$

$$^{f}S_{11} = a_{11} + a_{12}a_{21}\frac{b_{11} + (b_{12}b_{21} - b_{11}b_{22})c_{11}}{(1 - a_{22}b_{11})(1 - b_{22}c_{11}) - a_{22}b_{12}b_{21}c_{11}}$$

$$^{f}S_{12} = \frac{a_{12}b_{12}c_{12}}{(1 - a_{22}b_{11})(1 - b_{22}c_{11}) - a_{22}b_{12}b_{21}c_{11}}$$

$$^{f}S_{21} = \frac{a_{21}b_{21}c_{21}}{(1 - a_{22}b_{11})(1 - b_{22}c_{11}) - a_{22}b_{12}b_{21}c_{11}}$$

and

$$^{f}S_{22} = c_{22} + c_{12}c_{21}\frac{b_{22} + (b_{12}b_{21} - b_{11}b_{22})a_{22}}{(1 - a_{22}b_{11})(1 - b_{22}c_{11}) - a_{22}b_{12}b_{21}c_{11}}. \qquad (6.66)$$

i. Same Variable Attenuator in Two Systems

Both continuously variable and step attenuators can be analyzed by the same method, which is an extension of the previous analysis. A continuously variable attenuator can be regarded as though one removed an initial attenuator corresponding to the initial setting, and substituted in its place a final attenuator corresponding to the final setting. This point of view is valid, even though the continuously variable attenuator remains in the circuit at all times.

A representation which applies to the measurement of a given change in a variable attenuator first in one system and then in a different system is shown in figure 6-17. The system connectors D_G and D_L, H_G and H_L are not shown as joined together because in some cases it is not possible to do so. For example, if the step attenuators have female connectors on both ends, the system connectors will all be male and will not mate together.

Although the initial attenuator, represented by J_G - J - J_L and the final attenuator, represented by B_G - B - B_L are the same in two systems, the initial and final composite two-ports are not.

The difference in the substitution loss measured in the two systems M and N is written down directly from inspection of figure 6.17 and a knowledge of eq. (3.51).

$$L_{SN} - L_{SM} = ({}^{f}A_N - {}^{f}A_M) + ({}^{i}A_M - {}^{i}A_N)$$

$$+ 20 \log_{10}\left|\frac{(1 - {}^{i}m_{11}\Gamma_{GM})(1 - {}^{i}m_{22}\Gamma_{LM}) - {}^{i}m_{12}{}^{i}m_{21}\Gamma_{GM}\Gamma_{LM}}{1 - \Gamma_{GM}\Gamma_{LM}}\right|$$

$$- 20 \log_{10}\left|\frac{(1 - {}^{f}m_{11}\Gamma_{GM})(1 - {}^{f}m_{22}\Gamma_{LM}) - {}^{f}m_{12}{}^{f}m_{21}\Gamma_{GM}\Gamma_{LM}}{1 - \Gamma_{GM}\Gamma_{LM}}\right|$$

$$+ 20 \log_{10}\left|\frac{(1 - {}^{f}n_{11}\Gamma_{GN})(1 - {}^{f}n_{22}\Gamma_{LN}) - {}^{f}n_{12}{}^{f}n_{21}\Gamma_{GN}\Gamma_{LN}}{1 - \Gamma_{GN}\Gamma_{LN}}\right|$$

$$- 20 \log_{10}\left|\frac{(1 - {}^{i}n_{11}\Gamma_{GN})(1 - {}^{i}n_{22}\Gamma_{LN}) - {}^{i}n_{12}{}^{i}n_{21}\Gamma_{GN}\Gamma_{LN}}{1 - \Gamma_{GN}\Gamma_{LN}}\right|. \quad (6.67)$$

In order for eq. (6.67) to vanish we not only would need identical connectors at the insertion points ($D_G = H_G$ and $D_L = H_L$) but corresponding system reflection coefficients would need to be equal ($\Gamma_{GM} = \Gamma_{GN}$ and $\Gamma_{LM} = \Gamma_{LN}$). Even if these (sufficient) conditions are not obtained, it is possible for eq. (6.67) to vanish under other less easily described conditions, although it is not very probable. In general, there will be a difference in the substitution losses measured in the two systems.

If both systems are nonreflecting, eq. (6.67) reduces to

$$(L_{SN} - L_{SM})\begin{pmatrix}\Gamma_{GM}=\Gamma_{LM}=0\\ \Gamma_{GN}=\Gamma_{LN}=0\end{pmatrix} = ({}^{f}A_N - {}^{f}A_M) + ({}^{i}A_M - {}^{i}A_N) = 20 \log_{10}\left|\frac{{}^{f}m_{21}}{{}^{i}m_{11}} \cdot \frac{{}^{i}n_{21}}{{}^{f}n_{21}}\right|. \quad (6.68)$$

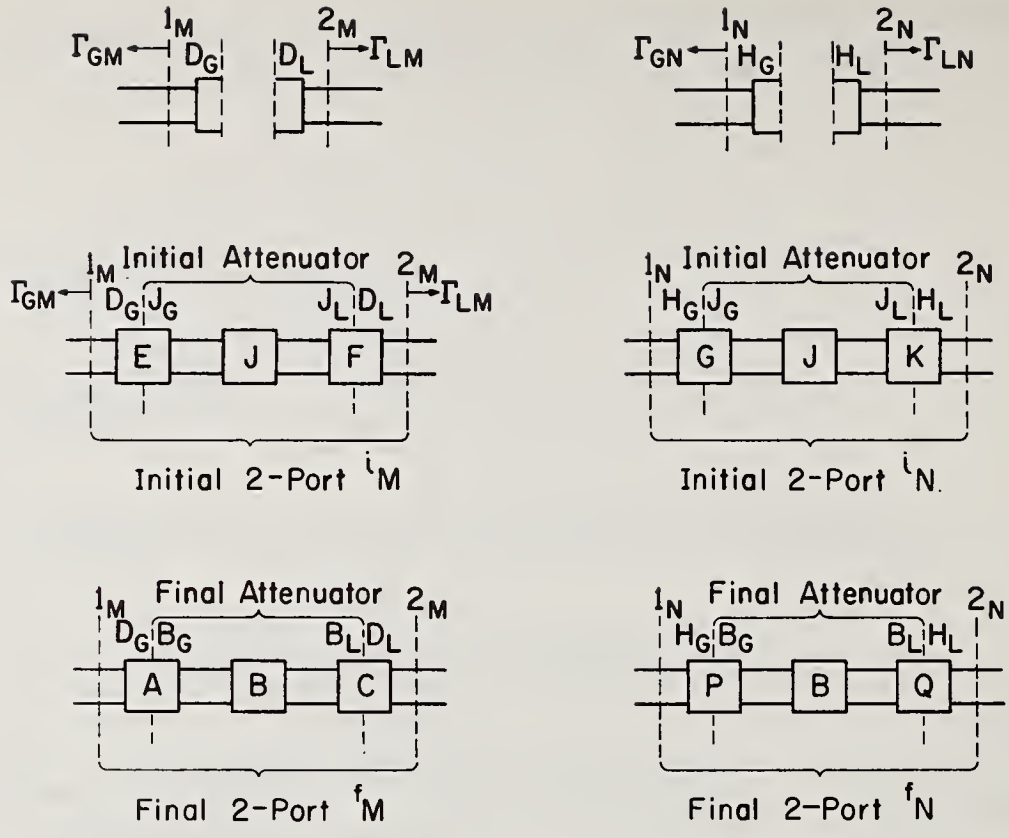

Figure 6-17. Representation of substitution of same final and initial attenuators in two different systems.

The above equation is written in terms of the scattering coefficients of the individual two-ports which make up the initial and final composite two-ports as follows:

$$
\begin{aligned}
&(L_{SN} - L_{SM})\begin{pmatrix}\Gamma_{GM}=\Gamma_{LM}=0\\ \Gamma_{GN}=\Gamma_{LN}=0\end{pmatrix} \\
&= (A_A - A_P) + (A_C - A_Q) - (A_E - A_G) - (A_F - A_K) \\
&\quad + 20\log_{10}\left|\frac{(1 - a_{22}b_{11})(1 - b_{22}c_{11}) - a_{22}b_{12}b_{21}c_{11}}{1 - a_{22}c_{11}}\right| \\
&\quad - 20\log_{10}\left|\frac{(1 - e_{22}j_{11})(1 - j_{22}f_{11}) - e_{22}j_{12}j_{21}f_{11}}{1 - e_{22}f_{11}}\right| \\
&\quad + 20\log_{10}\left|\frac{(1 - g_{22}j_{11})(1 - j_{22}k_{11}) - g_{22}j_{12}j_{21}k_{11}}{1 - g_{22}k_{11}}\right| \\
&\quad - 20\log_{10}\left|\frac{(1 - p_{22}b_{11})(1 - b_{22}q_{11}) - p_{22}b_{12}b_{21}q_{11}}{1 - p_{22}q_{11}}\right| \\
&\quad + 20\log_{10}\left|\frac{(1 - a_{22}c_{11})(1 - g_{22}k_{11})}{(1 - c_{22}f_{11})(1 - p_{22}q_{11})}\right|
\end{aligned}
\tag{6.69}
$$

If corresponding connectors at the insertion points in the two systems are identical ($D_G \equiv H_G$ and $D_L \equiv H_L$), eq. (6.69) will vanish. Even if this condition does not hold, it could vanish if the positive and negative terms canceled each other.

It is interesting to consider the case in which corresponding connectors at the insertion points in the two systems are not identical, but corresponding connectors on the two attenuators are. ($J_G = B_G$ and $J_L = B_L$.) In this case we have $A \equiv E$, $F \equiv C$, $G \equiv P$, and $K \equiv Q$. Many terms cancel and eq. (6.69) reduces to

$$
\begin{aligned}
(L_{SN} - L_{SM}) \Big|_{\substack{\Gamma_{GM}=\Gamma_{LM}=0 \\ \Gamma_{GN}=\Gamma_{LN}=0 \\ J_G=B_G \\ J_L=B_L}} &= 20 \log_{10} \left| \frac{(1 - a_{22}b_{11})(1 - b_{22}c_{11}) - a_{22}b_{12}b_{21}c_{11}}{1 - a_{22}c_{11}} \right| \\
&- 20 \log_{10} \left| \frac{(1 - a_{22}j_{11})(1 - j_{22}c_{11}) - a_{22}j_{12}j_{21}c_{11}}{1 - a_{22}c_{11}} \right| \\
&+ 20 \log_{10} \left| \frac{(1 - g_{22}j_{11})(1 - j_{22}k_{11}) - g_{22}j_{12}j_{21}k_{11}}{1 - g_{22}k_{11}} \right| \\
&- 20 \log_{10} \left| \frac{(1 - g_{22}b_{11})(1 - b_{22}k_{11}) - g_{22}b_{12}b_{21}k_{11}}{1 - g_{22}k_{11}} \right| . \qquad (6.70)
\end{aligned}
$$

The conditions $J_G = B_G$ and $J_L = B_L$ would apply in the case of a continuously variable attenuator that was not physically removed from the circuit. They would also apply to step attenuators provided their connectors were sufficiently identical.

The additional conditions $J_G \equiv J_L \equiv B_G \equiv B_L$, $D_G \equiv D_L$, and $H_G \equiv H_L$ would not reduce the size of eq. (6.70), but would reduce the uncertainty in the measurements of the two systems.

It is clear from the foregoing that in order to insure the same change in loss in two systems from the same change in settings of a variable attenuator, 1) the corresponding system reflection coefficients must be the same and 2) the corresponding system connectors at the insertion points must be the same. Even when these conditions are not realized, some reduction in the difference is obtainable if all other connectors are as nearly alike as possible. It is also clear that reduction of connector reflections and dissipative losses will also reduce the difference. A fortuitous relationship of the phases of the reflection coefficients may also make the difference vanish, although the probability of this happening is low.

j. Standard Incremental Attenuation

The desired quantity in a measurement of a variable attenuator is the change in attenuation or incremental attenuation (Weinschel, 1960) from an initial setting to a final setting. This equals the substitution loss when the system is nonreflecting and is given by eq. (6.58). However it must be recognized that the characteristics of the connectors D_G and D_L at the insertion point are implicitly involved, even if only to small degree. This is evident from inspection of figure 6-17, where it is seen that connectors D_G and D_L are involved in a slightly different way in the initial and final two-ports.

In order to define a precisely-repeatable incremental attenuation, the connectors at the insertion point should always be the same, and should be standardized. With standard connectors at the insertion point, we then can measure "standard incremental attenuation."

This quantity may be expressed by reference to system M in figure 6-17 as

$$\Delta^S A = 20 \log_{10} \left| \frac{i_{m_{21}}}{f_{m_{21}}} \right|$$

or

$$\begin{aligned} \Delta^S A = {} & A_A + A_B + A_C - A_E - A_J - A_F \\ & + 20 \log_{10} |(1 - a_{22}b_{11})(1 - b_{22}c_{11}) - a_{22}b_{12}b_{21}c_{11}| \\ & - 20 \log_{10} |(1 - e_{22}j_{11})(1 - j_{22}f_{11}) - e_{22}j_{12}j_{21}f_{11}| . \end{aligned} \tag{6.71}$$

where it is understood that D_G and D_L, which form parts of two-ports A, E, C, and F, are standard connectors.

The error in measuring standard incremental attenuation (due to system reflections and differences from standard conditions in the actual system) can be evaluated by comparing eq. (6.71) with eq. (6.67), letting M represent the idealized system with standard conditions ($\Gamma_{GM} = \Gamma_{LM} = 0$, D_G and D_L standard connectors) and letting N represent the actual system. The procedure in writing equations and calculating examples follows along lines of the analysis pertaining to fixed attenuators. The error is written

$$\varepsilon_{SI} = L_{SN} - \Delta^S A = 20 \log_{10} \left| \frac{f_{m_{21}}}{i_{m_{21}}} \cdot \frac{i_{n_{21}}}{f_{n_{21}}} \right|$$

$$+ 20 \log_{10} \left| \frac{(1 - f_{n_{11}}\Gamma_{GN})(1 + f_{n_{22}}\Gamma_{LN}) - f_{n_{12}} f_{n_{21}} \Gamma_{GN}\Gamma_{LN}}{(1 - i_{n_{11}}\Gamma_{GN})(1 - i_{n_{22}}\Gamma_{LN}) - i_{n_{12}} i_{n_{21}} \Gamma_{GN}\Gamma_{LN}} \right| \tag{6.72}$$

where the m's and n's are the scattering coefficients of the composite two-ports in figure 6-17 and it is understood that system M represents the idealized, and system N the actual system. The first term in eq. (6.72) vanishes if connectors H_G and H_L are standard, for then $^{i}M \equiv {}^{i}N$, and $^{f}M = {}^{f}N$. The second term vanishes if the reflection coefficients Γ_{GN} and Γ_{LN} of the actual system vanish.

In order to calculate a simple example, let the second term above vanish and assume that only the connector H_G is nonstandard. Then two-ports A, C, E, F, K, and Q are alike and represent standard connector pairs and two-ports G and P are alike and represent nonstandard connector pairs. The first term in eq. (6.72) can be written

$$
\begin{aligned}
&20 \log_{10}\left|\frac{f_{m_{21}}}{i_{m_{21}}} \cdot \frac{i_{n_{21}}}{f_{n_{21}}}\right| \\
&= A_P + A_Q - A_G - A_K + A_E + A_F - A_A - A_C \\
&\quad + 20 \log_{10}\left|\frac{(1 - e_{22}j_{11})(1 - j_{22}f_{11}) - e_{22}j_{12}j_{21}f_{11}}{(1 - a_{22}b_{11})(1 - b_{22}c_{11}) - a_{22}b_{12}b_{21}c_{11}}\right| \\
&\quad + 20 \log_{10}\left|\frac{(1 - p_{22}b_{11})(1 - b_{22}q_{11}) - p_{22}b_{12}b_{21}q_{11}}{(1 - g_{22}j_{11})(1 - j_{22}k_{11}) - g_{22}j_{12}j_{21}k_{11}}\right|. \qquad (6.73)
\end{aligned}
$$

Applying the above assumptions, the right side of eq. (6.73) reduces to just its last two terms. Assuming that reflections are small and neglecting the smaller terms, as in obtaining eq. (6.65), the last two terms of eq. (6.73) become

$$
\begin{aligned}
&20 \log_{10}|1 + j_{11}(g_{22} - c_{22}) + j_{22}(k_{11} - f_{11}) \\
&\qquad + j_{12}j_{21}(g_{22}k_{11} - e_{22}f_{11})| \\
&\qquad + 20 \log_{10}|1 + b_{11}(a_{22} - p_{22}) + b_{22}(c_{11} - q_{11}) \\
&\qquad + b_{12}b_{21}(a_{22}c_{11} - p_{22}q_{11})|. \qquad (6.74)
\end{aligned}
$$

Example 3

Suppose that the initial attenuator is a 3-dB pad having a kernel VSWR = 1.222, the final attenuator is a 10 dB pad having a kernel VSWR of 1.15, the standard connector pair VSWR's are 1.15, and the other connector pair VSWR's are 1.00. Thus $|j_{12}j_{21}| = 0.5$, $|j_{11}| = |j_{22}| = 0.1$, $|b_{12}b_{21}| = 0.1$, $|b_{11}| = |b_{22}| = 0.07$, $|a_{22}| = |c_{11}| = |c_{22}| = |f_{11}| = |k_{11}| = |q_{11}| = 0.07$, and $|g_{22}| = |p_{22}| = 0$.

The resulting error limits are

$$-0.13 \text{ dB} \leq \varepsilon_{SI} \leq 0.13 \text{ dB}.$$

The error limits in this example are appreciable and it is possible to make such an error in actual measurements. However, it is easy to reduce this error by careful control of the connectors used in the measuring systems.

k. Basic Insertion Arrangements

The representation schemes and analyses presented can be extended to other insertion arrangements for waveguide components such as attenuators.

The basic insertion arrangements considered are classified into three groups as follows, depending upon whether the waveguide component has 1) sexless or mating connectors, 2) nonmating connectors of the same type, and 3) nonmating connectors of different types.

An example of the first case was shown in figure 6-12, and examples of the other cases are shown in figures 6-18 to 6-20. In the last two cases, adapters are employed. Adapters for Case 2 are simpler than for Case 3, since a transition between waveguide of different cross sections is not employed.

Case 1 has already been considered, and some of the analysis applying to figure 6-17 will find applications in Cases 2 and 3. Insertion arrangements other than those shown are possible, and may also be of some interest, but will not be specifically considered. For example, the case of two or more cascade-connected variable attenuators is of interest and has been analyzed (Schafer and Rumfelt, 1959) by simpler techniques, but will not be presently considered.

(1) Cases 2A and 3A -- Combining the Component with an Adapter

In the arrangement of figure 6-18, an adapter is connected to the waveguide component having nonmating connectors to form a composite waveguide component having mating connectors. The insertion arrangement for the composite component is then the same as for Case 1, and the previous analysis applies.

However, if we are primarily interested in the attenuation of the waveguide component itself without the adapter attached to it, this insertion arrangement will not give a direct answer.

Neglecting reflections, it is seen that the attenuation of the cascaded two-ports A, B, C, and P would be obtained, provided that D ≡ Q. The attenuation of A and B together would be nearly characteristic of the waveguide component itself, so that the attenuation of C and P together would need to be determined and subtracted. If reflections were taken into account, it would be even more difficult to obtain the desired characteristic loss from the measured substitution loss.

It is concluded that unless the adapter is to be permanently attached to the waveguide component, this insertion arrangement does not directly yield the desired information.

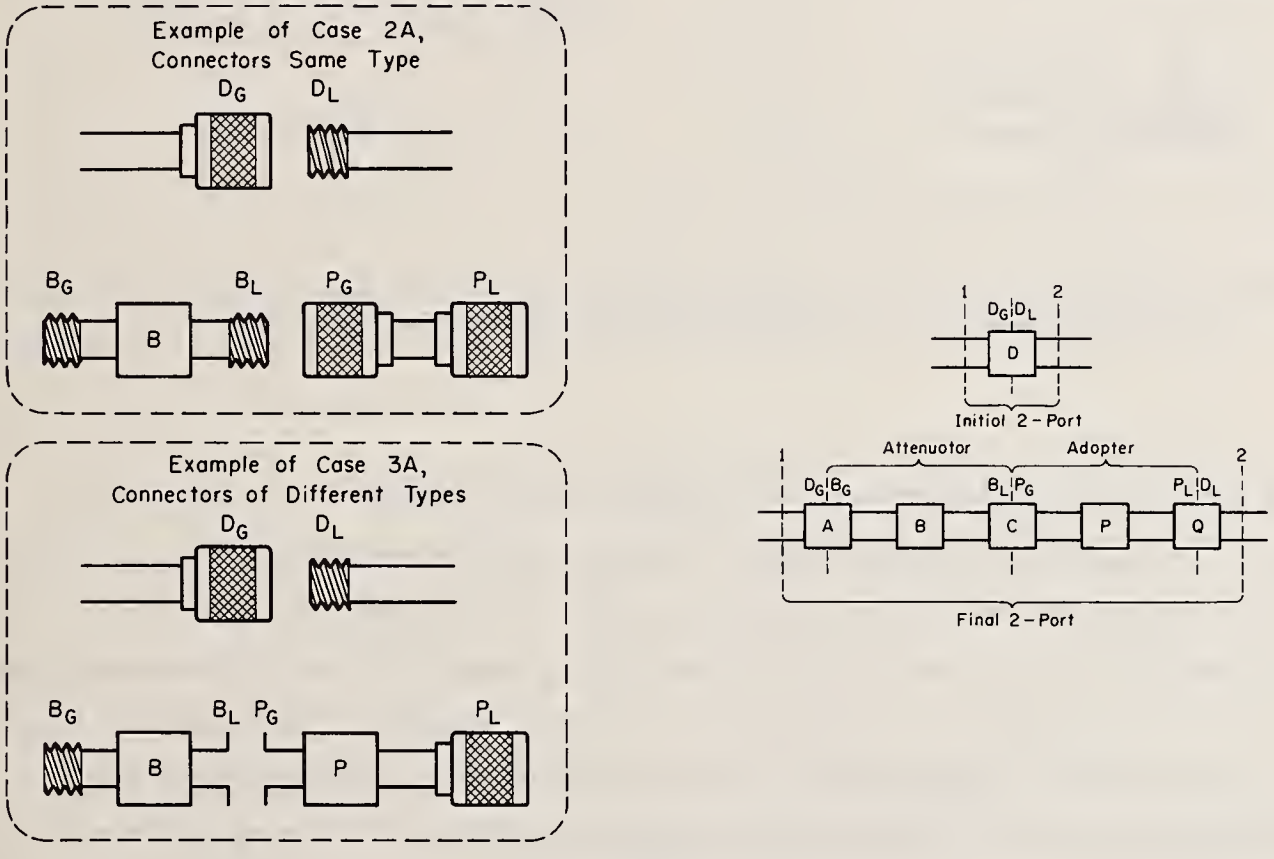

Figure 6-18. Representation of insertion of a waveguide component (such as an attenuator) having nonmating connectors by connecting it to an adapter (Cases 2A and 3A).

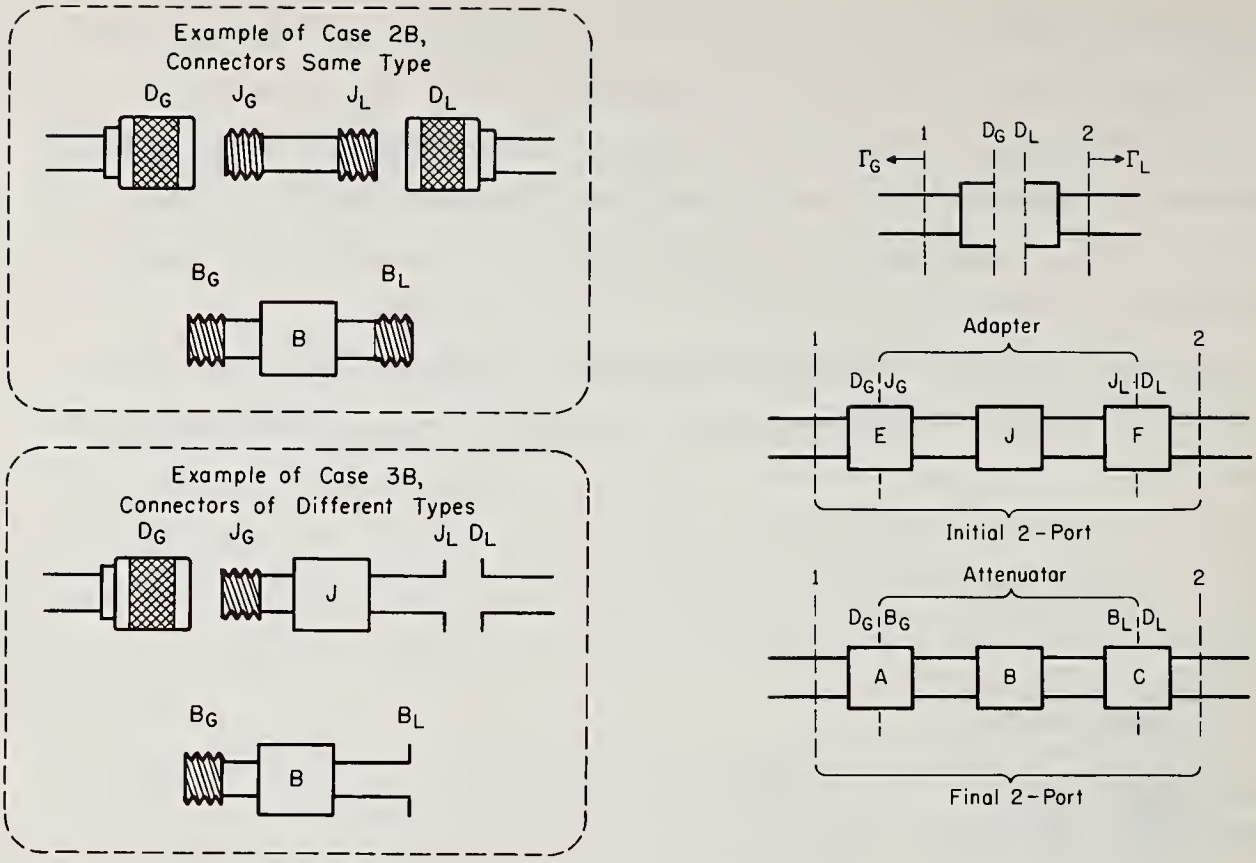

Figure 6-19. Representation of insertion of a waveguide component (such as an attenuator) having nonmating connectors by substituting it for an adapter (Cases 2B and 3B).

(2) Cases 2B and 3B -- Substituting the Component for an Adapter

The same basic representation shown in figure 6-19 applies analytically to either Case 2B or 3B as one can see from the examples given. The example of Case 2B is especially familiar as the drum or turret-type step attenuator. The attenuation steps are usually referred to a "zero dB attenuator" which is an adapter designed to have nominally no loss. This example has already been analyzed in the section on the variable attenuator in two systems as represented by figure 6-17. It is apparent that calibrations of such an attenuator in different systems may not agree if the connectors at the insertion points are different. To avoid such a possibility, it is advisable to make certain that they are identical. This requires standardizing the design of various types of connectors and then adhering to that standard in their construction. (In addition, tolerances of construction should be extremely small.)

If one is interested in the change of attenuation of such an attenuator relative to an adapter, then the design of the adapter should also be standardized and the adapters should be constructed according to this standard design.

If one is interested in the attenuation characteristic of the attenuator itself, this insertion arrangement will not give direct information. Instead, additional calculations would be necessary after having first determined the characteristics of the adapter and connector pairs used. It will be found that Case 2C is a better arrangement for the above purpose.

Case 3B is similar to Case 2B except that the waveguide component such as an attenuator has nonmating connectors of different types, and the adapter for which it is substituted must also have corresponding types of connectors. This case occurs in practice for example if one desires to measure the coupling of a directional coupler by measuring the attenuation between two arms, the other arms terminated. The side arm in some cases may have a different waveguide than the main arm so that the connectors are of different types.

In using the substitution arrangement of figure 6-19, one can determine the attenuation relative to a given adapter, which must be standardized if the measurement is to be repeatable and significant. No direct information is obtained concerning the waveguide component such as the directional coupler itself, and additional calculations would be necessary, given the characteristics of the adapter. It will be found that the arrangement of Case 3C gives better direction information, but still may not be completely satisfactory.

(3) Cases 2C and 3C -- Combining the Component with an Adapter and Substituting for Another Adapter

These cases are of interest because the quantity directly measured is to a good approximation characteristic of the waveguide component alone, and no additional calculations are required to take into account the adapter. This is true at least for Case 2C, if not for 3C, for which additional measurements are required.

In the examples of Case 2C, it is seen that if the kernels J and P of the two adapters are the same, and all of the connector pairs are standard, the measured substitution loss to a good approximation can equal the attenuation of the kernel B plus one connector pair. This is characteristic of the waveguide component which consists of the kernel B plus two connectors. The argument is similar to that following eq. (6.61), and is subject to the additional assumption here that the connector loss splits equally between the male and female connectors. A detailed analysis will not be given, but would follow along lines of those already presented.

In the examples of Case 3C, shown in figure 6-20, it is seen that the measured quantity is not likely to be a good approximation to a characteristic of the waveguide component itself as represented by the kernel B and connectors B_G and B_L. We would have to assume not only that connector pairs E ≡ A and F ≡ Q (which is quite reasonable), but also that adapter kernels J ≡ P, and that the losses in connector pair C equal those in connectors B_G and B_L. The latter two assumptions could be quite unrealistic and not correct to a good approximation.

A combination of Case 3A and Case 3B substitution measurements as shown in figure 6-21 could be used to obtain more or less directly a quantity characteristic of the waveguide component itself. It is evident that waveguide components such as are shown in these examples are troublesome, and require extra effort in their evaluation. In case that the waveguide component under consideration is itself an adapter, this technique is of particular interest and deserves further study. A detailed analysis would follow along the lines already presented.

1. Conclusions

A more rigorous representation and analysis have been presented to enable calculation of the effects of connectors and adapters on accurate attenuation measurements. The measured substitution loss replaces the insertion loss, and the former mismatch error is replaced by an error having three components. One condition under which the error vanishes is that the system is nonreflecting and has standard connectors at the insertion point.

A method of obtaining the nonreflecting condition using a tuning stub and slotted line is discussed.

The need for use of standard connectors is emphasized by some calculated examples in which error limits up to 0.13 decibel are obtained when such a connector is nonstandard. Examples are calculated for both fixed and variable attenuators and are based upon measured data on type N connectors.

Situations in which adapters are used in different insertion arrangements are discussed, and it is concluded that adapters also need to be standardized when used in precision measurement techniques.

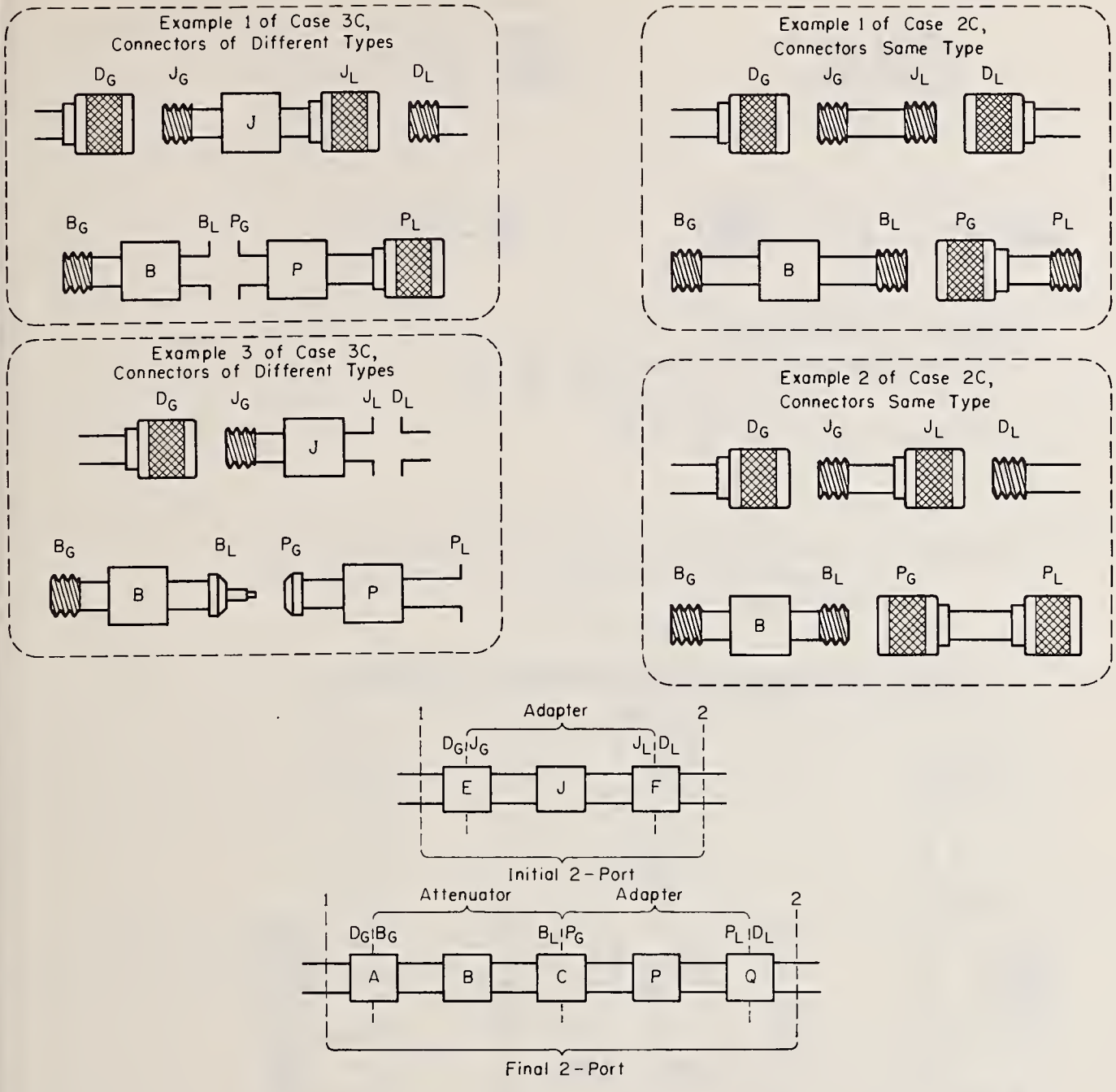

Figure 6-20. Representation of insertion of a waveguide component (such as an attenuator) having nonmating connectors by connecting it to an adapter, and substituting the composite component thus formed for another adapter (Cases 2C and 3C).

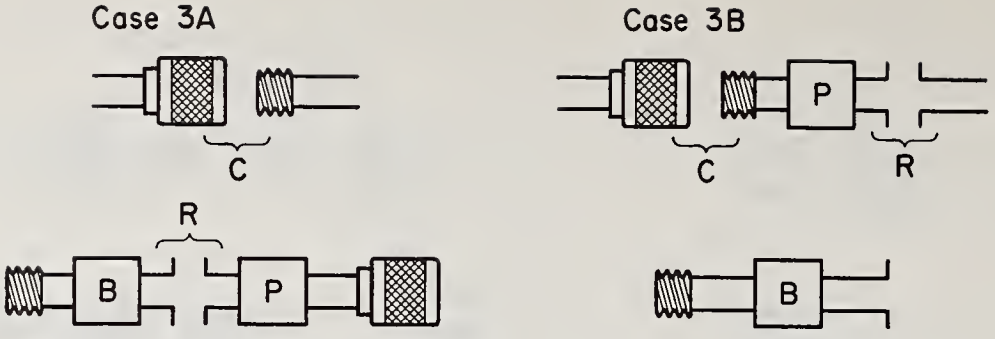

Neglecting Reflections:

$L_{S1} = A_B + A_R + A_P + A_C$, AND $L_{S2} = A_B - A_P$.

$$\tfrac{1}{2}(L_{S1} + L_{S2}) = A_B + \frac{A_R}{2} + \frac{A_C}{2}$$

Figure 6-21. Example of arrangement for measuring attenuation approximately characteristic of waveguide component of Case 3C.

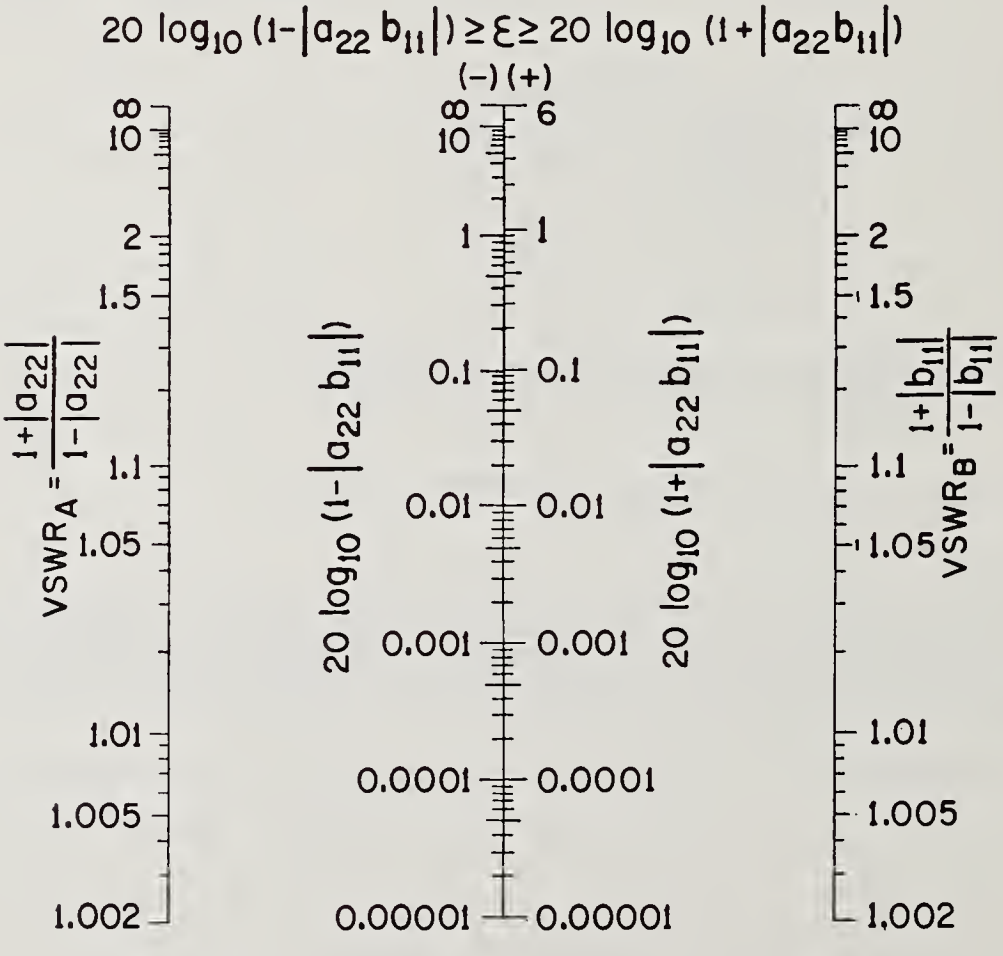

Figure 6-22. Nomogram of "Error Limits."

The form 20 $\text{Log}_{10}(1 - |a_{22}b_{11}|)$ is frequently observed in the error equations. In order to facilitate calculations, the nomogram of figure 6-22 may be used. The nomogram gives only error limits assuming that there is some possibility that the phases of the reflections might combine to produce the greatest effect. In some cases, the error limits given by this procedure are overly conservative because the variation of the phases is limited by realizability conditions (previously mentioned in section 6.5).

Some basic insertion arrangements are described for waveguide components having nonmating connectors. The ones giving a measured loss most nearly characteristic of the waveguide component are singled out for special mention, although a complete analysis is not presented.

6.7. Efficiency and Attenuation of 2-Ports from Reflection Coefficient Measurements

a. Introduction

It was shown in section 3.13c that under certain conditions,[14] the efficiency of a two-port terminated in a nonreflecting load equals the radius R_2 of the Γ_2-circle obtained when short-circuit terminations of various lengths are connected to arm 1. The dissipative component of attenuation equals

$$[A_1]_D = 10 \log_{10} \frac{1}{R_2}. \tag{3.111}$$

An additional measurement of the VSWR ρ_{11} corresponding to $|S_{11}|$ of the attenuator yields the component of attenuation due to reflection

$$[A_1]_R = 10 \log_{10} \frac{(\rho_{11} + 1)^2}{4\rho_{11}} = 10 \log_{10} \frac{1}{1 - |S_{11}|^2}. \tag{6.75}$$

This is similar to eq. (3.66). The total attenuation $[A_1]_T$ is the sum of $[A_1]_D$ and $[A_1]_R$. Some measurements using this method are shown in figure 6-23 and results of some measurements are given in table 6-1.

---

[14] The conditions are (1) short-circuit terminations are lossless, and (2) the reciprocity condition ($Z_{02}S_{12} = Z_{01}S_{21}$) holds for the 2-port.

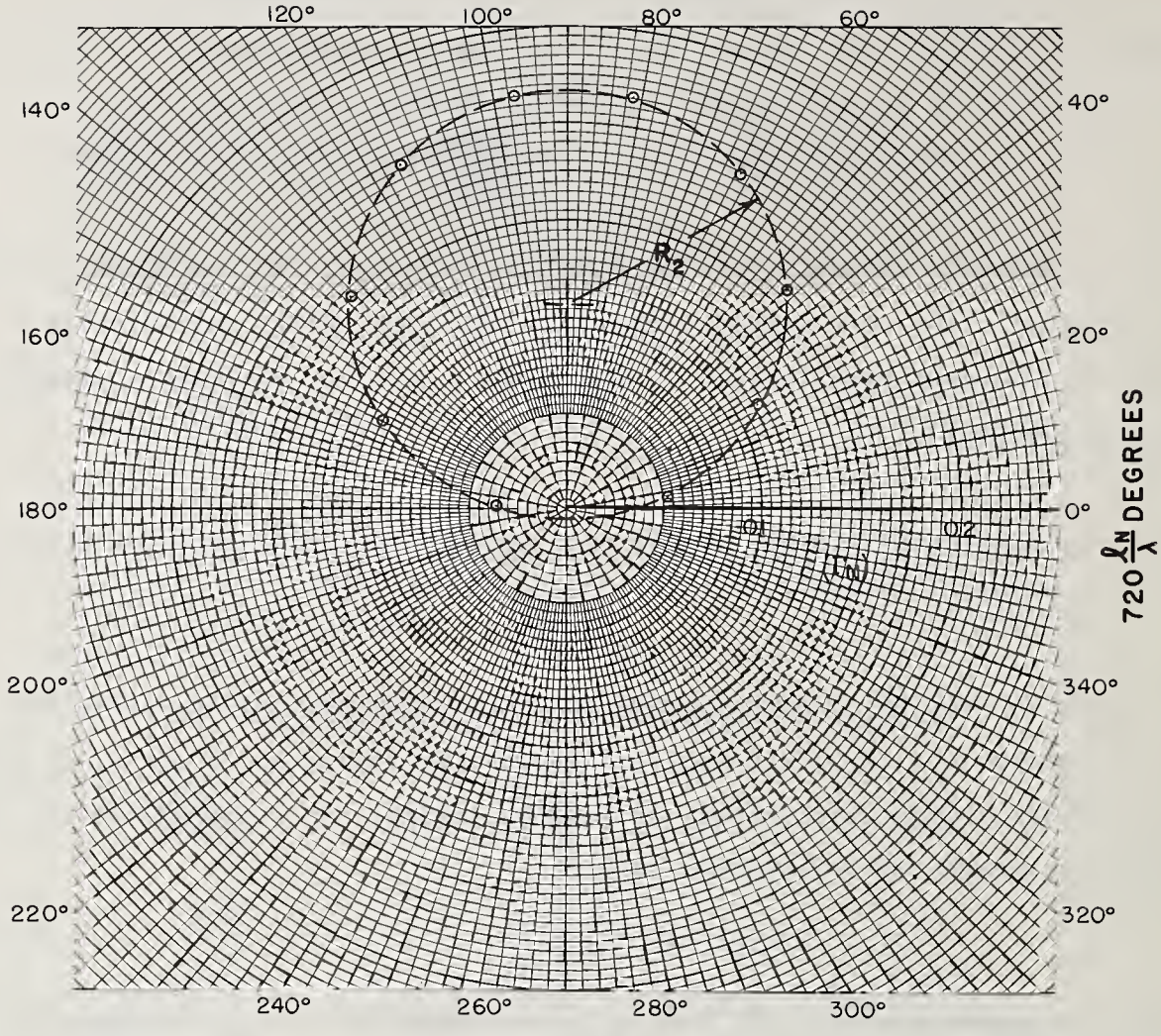

Figure 6-23. Measured reflection coefficients of 20-dB attenuator, A_0 = 9.50 dB, 1,000 GHz, R_2 = 0.112.

Table 6-1. Observed attenuation data.

Nominal Value of Attenuation	MEASURED ATTENUATION					
	Input VSWR	A_R	A_D	A_T	A_T From Power Ratio Method	Difference
3 dB	1.070	.005 dB	2.87 dB	2.88 dB	2.85 dB	.03 dB
6 dB	1.235	.048	5.74	5.79	5.75 dB	.04 dB
10 dB	1.180	.030	9.50	9.53	9.53 dB	.00 dB
20 dB	1.240	.050	19.74	19.79	19.81 dB	.02 dB

In the case of a reciprocal 2-port, the attenuation $[A_2]_T$ for energy incident upon arm 2 equals $[A_1]_T$. However it does not follow that $[A_1]_D = [A_2]_D$ and $[A_1]_R = [A_2]_R$ unless the 2-port is also symmetrical.

The above method for measuring the efficiency of a 2-port terminated in a non-reflecting load has been described (Beatty, 1950). It has also been shown how one can obtain from the same data, the efficiency of a 2-port terminated in any arbitrarily chosen load (Beatty, 1972a). In the following, it will be shown how to extend this method to the case where one measures impedances rather than reflection coefficients, and the 2-port may consist of lumped circuit elements and have terminal pairs rather than waveguide (or transmission line) leads.

b. 2-Port having Terminal Pairs

Consider such a 2-port as shown in figure 6-24.

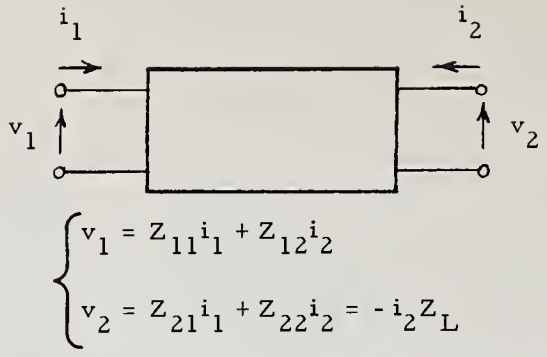

Figure 6-24. Diagram of 2-port having 2 sets of terminal pairs.

For energy incident upon port no. 1 and a load of impedance Z_L connected to port no. 2, the efficiency η_1 is

$$\eta_1 = \frac{P_L}{P_1} = \frac{|i_2|^2 \, \mathrm{Re}Z_L}{|i_1|^2 \, \mathrm{Re}Z_1} = \left| \frac{Z_{21}}{Z_{22} + Z_L} \right|^2 \frac{\mathrm{Re}Z_L}{\mathrm{Re}Z_1},$$

or

$$\eta_1 = \left| \frac{Z_{21}}{Z_{22} + Z_L} \right|^2 \frac{|Z_L| \cos \phi_L}{|Z_1| \cos \phi_1}, \tag{6.76}$$

where ϕ_L is the phase of Z_L and ϕ_1 is the phase of Z_1.

Similarly, for energy incident upon port 2 and a load of impedance Z_L connected to port 1,

$$\eta_2 = \left| \frac{Z_{12}}{Z_{11} + Z_L} \right|^2 \frac{|Z_L| \cos \phi_L}{|Z_2| \cos \phi_2}. \tag{6.77}$$

The method of measuring η_2 is described as follows. We connect reactive loads to port 2 having an impedance $|x_2|e^{j\pi/2}$. For each load so connected we measure the corresponding input impedance Z_1 at port 1. We measure at least three values of Z_1, and possibly 5 or 10 values in order to reduce the effect of random errors.

Suppose that we wish to determine the efficiency η_2 when a load of impedance Z_L is connected to port 1. Let

$$\Gamma_1 = \frac{Z_1 - Z_L}{Z_1 + Z_L}, \tag{6.78}$$

where

$$Z_1 = \frac{Z_{11}|x_1|e^{j\pi/2} + Z_{11}Z_{22} - Z_{12}Z_{21}}{|x_1|e^{j\pi/2} + Z_{22}}.$$

We can write eq. (6.78) in the form

$$\Gamma_1 = \frac{a|x_1|e^{j\pi/2} + b}{c|x_1|e^{j\pi/2} + d}, \tag{6.79}$$

where $a = Z_{11} - Z_L$, $b = (Z_{11} - Z_L)Z_{22} - Z_{12}Z_{21}$, $c = Z_{11} + Z_L$, and $d = (Z_{11} + Z_L)Z_{22} - Z_{12}Z_{21}$.

We note that eq. (6.79) is a linear fractional transformation and hence, as $|x_1|$ varies, Γ_1 has a circular locus of radius

$$R_1 = \left|\frac{ad - bc}{c^2}\right| \cdot \frac{1}{2\left|\frac{d}{c}\sin(\delta - \gamma - \pi/2)\right|}, \tag{6.80}$$

where δ is the phase of d, γ is the phase of c, and the derivation of eq. (6.80) is the same as for eq. (3.124) of section 3.14b. We can also write

$$R_1 = \left|\frac{ad - bc}{c^2}\right| \cdot \frac{1}{2\ \mathrm{Re}\left(\frac{d}{c}\right)}. \tag{6.81}$$

It can be shown as follows that η_2 is closely related to R_1. Consider that

$$\begin{cases} ad - bc = 2\ Z_L Z_{12} Z_{21} = 2\ Z_L Z_{12}^2 \ (\text{if } Z_{12} = Z_{21}) \\ \dfrac{d}{c} = Z_{22} - \dfrac{Z_{12}^2}{Z_{11} + Z_L} = Z_2, \\ \text{and} \quad c = Z_{11} + Z_L. \end{cases} \tag{6.82}$$

It follows from eq. (6.77) that

$$\eta_2 = \left|\frac{ad - bc}{c^2}\right| \frac{1}{2\ \mathrm{Re}\left(\frac{d}{c}\right)} \cdot \cos\phi_L, \tag{6.83}$$

or

$$\eta_2 = R_1 \cos\phi_L. \tag{6.84}$$

We note that when Z_L is real, $\eta_2 = R_1$.

In a similar way, it may be shown that

$$\eta_1 = R_2 \cos\phi_L, \tag{6.85}$$

where ϕ_L is the phase of Z_L, the impedance of the load connected to port 1.

c. 2-Port Having Waveguide Leads

If we wish to measure in a similar way the efficiency of a 2-port having waveguide leads, it may be more convenient to measure the reflection coefficients

Γ_1 and Γ_2 at ports 1 and 2, respectively. Suppose that we have measured Γ_2 at port 2 for reactive loads on port 1, and have determined

$$[\eta_1]_{\Gamma_L=0} = \frac{Z_{01}}{Z_{02}} \cdot \frac{|S_{21}|^2}{1 - |S_{11}|^2}. \tag{3.29}$$

we can process the same data to obtain (Beatty, 1972) η_1 for any value of Γ_L (load connected to port 2).

The procedure is to convert each measured value of Γ_2 to a new reflection coefficient Γ_{2N} by means of the transformation

$$\Gamma_{2N} = \frac{\Gamma_2 - \Gamma_L}{1 - \Gamma_2\Gamma_L}. \tag{6.86}$$

We plot Γ_{2N} and observe it has a circular locus. We measure the radius R_{2N}.

Then we calculate

$$\eta_1 = \frac{R_{2N}}{\sqrt{1 + \left\{\frac{2|\Gamma_L \sin \psi_L|}{1 - |\Gamma_L|^2}\right\}^2}}, \tag{6.87}$$

where ψ_L is the phase of Γ_L.

In a similar manner, it follows that

$$\eta_2 = \frac{R_{1N}}{\sqrt{1 + \left\{\frac{2|\Gamma_L \sin \psi_L|}{1 - |\Gamma_L|^2}\right\}^2}}. \tag{6.88}$$

Although it is assumed that the short-circuited waveguide terminations are lossless, one could in principle measure the losses and make a correction taking into account eq. (3.107), for example.

d. Conclusions

The method of determining 2-port efficiencies from the radius of an impedance circle or reflection coefficient circle may be applied to reciprocal 2-port networks having either terminal pairs or waveguide (or transmission line) leads. The method is not recommended for determining attenuation if conventional attenuation measuring equipment is available, but is useful for determining efficiencies. If more than 3 measurements are made to determine a circle, then the accuracy can be better than that for 3-point methods, at the cost of additional measurement time.

6.8. Attenuation from Power Measurements

a. Introduction

In the measurement of microwave attenuation, the stability or resolution of the measuring system places a limit on the accuracy. Reduction of the other sources of error (such as mismatch) will tend to make the error limit approach the system instability limit. In practice, this limit has been typically of the order of ±0.01 dB, for systems in which the generator is not frequency-stabilized.

In the following, the application of amplitude stabilization and accurate power measurement techniques to the problem of attenuation measurement is described. A measurement system having a stability and resolution of the order of ±0.0001 dB was obtained. This system was used to calibrate a rotary vane type of variable microwave attenuator, which has a high degree of resolution for small values of attenuation.

In order to take maximum advantage of the improved stability and resolution, refined techniques were used in the evaluation and reduction of mismatch error. The capability of the system is indicated by the tabulated results of the attenuator calibration, and the estimate of the limits of error is supported by an analytic and experimental treatment. The following discussion is a modified version of Engen and Beatty (1960).

b. The Measurement System

A simplified diagram of the measurement system is shown in figure 6-25. The attenuator under test is placed between an amplitude-stabilized microwave signal source (Engen, 1958) and a bolometer mount-power meter. The power meter consists of a self-balancing d-c bolometer bridge (Engen, 1957) having provisions for measuring and recording the d-c bias power required to maintain the bolometer at its operating resistance of 200 ohms. The two bolometer mounts M_1 and M_2 shown in the temperature stabilized water bath are for power measurement and signal source stabilization, respectively. A reasonable amount of care was exercised in order to obtain good performance from each item of equipment, with a resultant system performance as shown in figures 6-26 and 6-27. Figure 6-26 shows the stability and repeatability with the attenuator alternately set at the 0.00 and 0.01 dB positions. It will be noted that the stability and repeatability are better than 0.0001 dB (10 microbels). A recording of the long term stability is given in figure 6-27 where the maximum variation is of the order of ±10 μB.

The accuracy of measurement of small changes in d-c power at this level is estimated to be of the order of 0.02 μW. This indicates that further improvement could be expected in the results if the system stability were improved, perhaps by the use of a frequency-stabilized signal source.

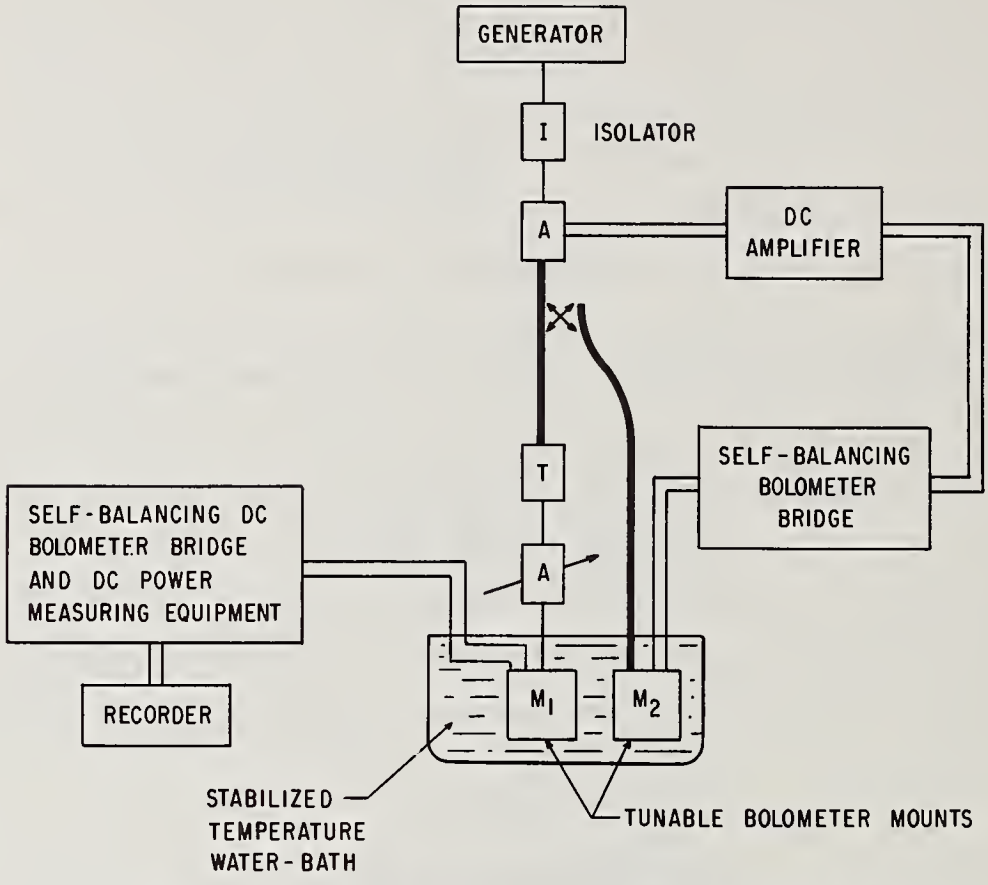

Figure 6-25. Simplified diagram of measurement system.

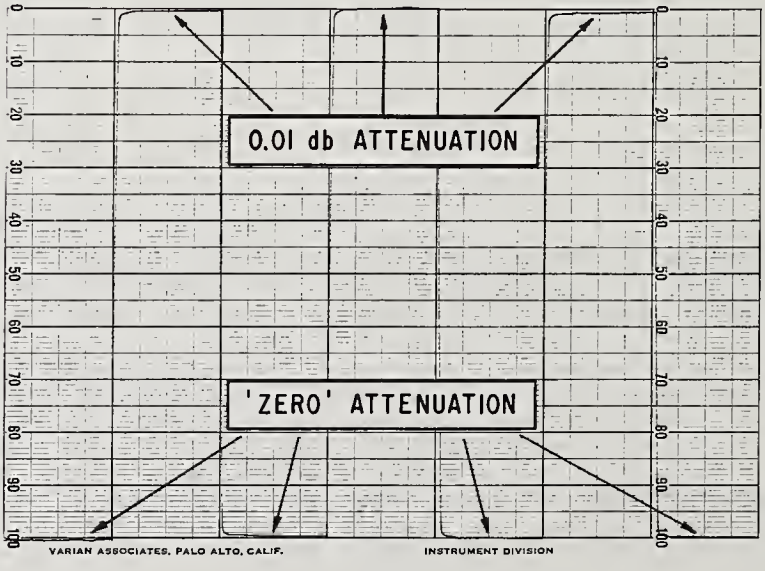

Figure 6-26. System response to a 0.01 dB attenuation.

c. Theory of Measurement

One can make an attenuation measurement by measuring the microwave powers P_1 and P_2 absorbed by the bolometer mount M_1 when the attenuator is set first on zero, then to some other setting. The attenuation is

$$A = 10 \log_{10} \frac{P_1}{P_2}. \tag{6.89}$$

It is of course necessary that the interaction of reflections between the attenuator and the measuring system is negligible.

In making such a measurement, one assumes that the microwave power P absorbed by the bolometer element is proportional[15] to the d-c power required to bias the bolometer at its operating resistance when P = 0. Then,

$$A = 10 \log_{10} \frac{W_0 - W_1}{W_0 - W_2}, \tag{6.90}$$

where W_1 and W_2 are the d-c bias powers corresponding to P_1 and P_2. (For the bolometer used, W_0 = 15 mW and P_1 = 10 mW.)

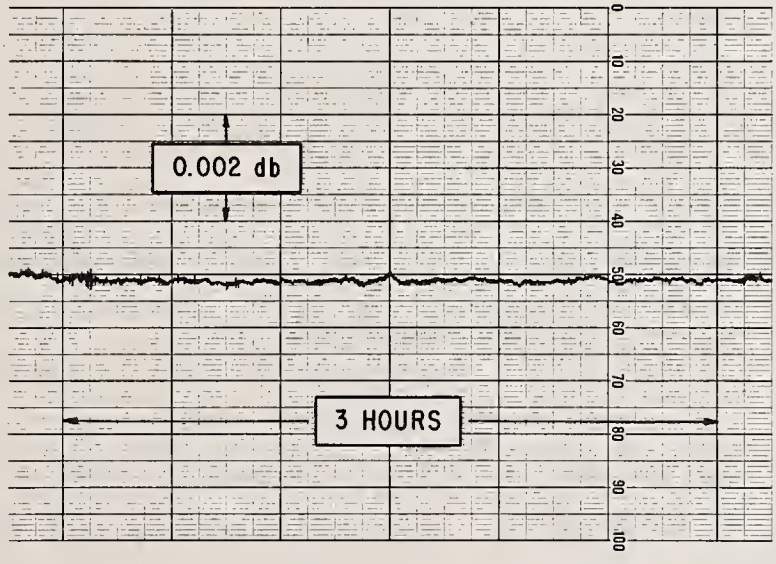

Figure 6-27. Long-term system stability.

The apparatus employed permitted direct measurements of differences in d-c power, a procedure permitting greater accuracy and convenience than calculation of differences from separate measurements. The changes in d-c power level during an attenuation measurement are shown in figure 6-28.

[15]The constant of proportionality is determined by the substitution error of the bolometer which is known from previously obtained experimental data to be independent of power level.

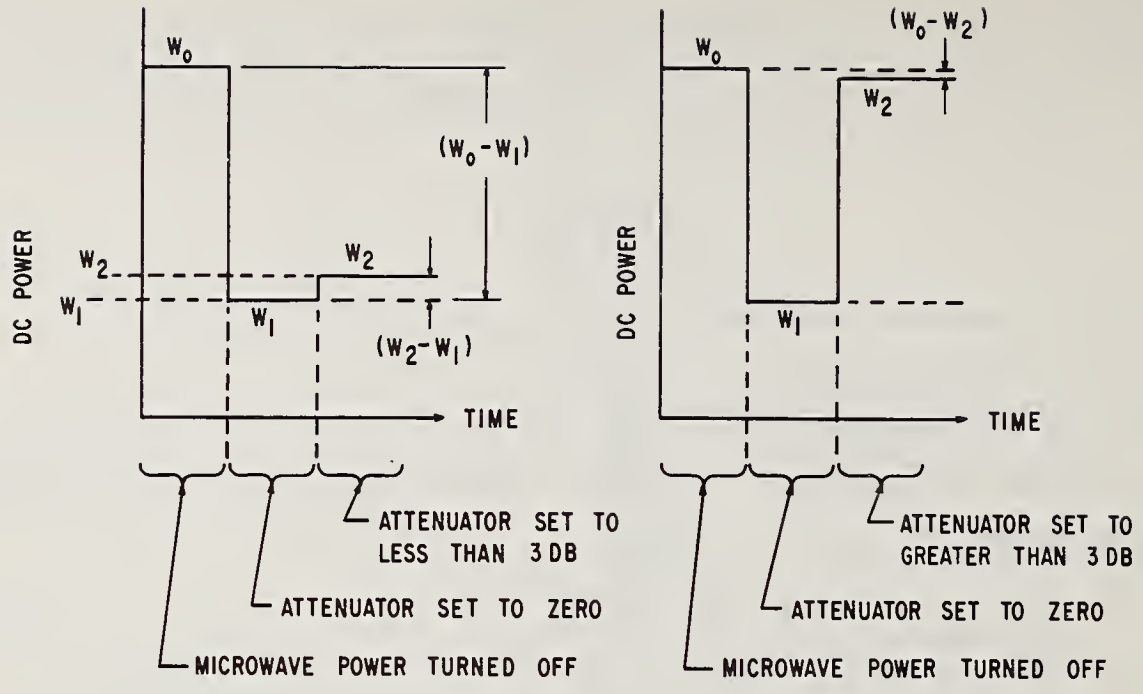

Figure 6-28. Changes in d-c power level during an attenuation measurement.

For attenuations less than approximately 3 dB, the power difference $W_2 - W_1$ was measured directly. If we let $W_{21} = W_2 - W_1$, and $W_{01} = W_0 - W_1$, eq. (6.90) becomes

$$A = 10 \log_{10} \left(\frac{1}{1 - \frac{W_{21}}{W_{01}}} \right). \tag{6.91}$$

For attenuations greater than approximately 3 dB, the power differences $W_{01} = W_0 - W_1$ and $W_{02} = W_0 - W_2$ were measured directly. Then the attenuation according to eq. (6.90) becomes

$$A = 10 \log_{10} \frac{W_{01}}{W_{02}}. \tag{6.92}$$

d. Propagation of Error in Measuring d-c Power Differences

It is estimated that the error in measuring d-c power differences is within 0.1 percent +0.1 μW. When $W_2 - W_2$ is measured, it can be shown that the limit of error in determining the attenuation is

$$\varepsilon = 10 \log_{10}\left[\frac{1}{1 - \frac{1}{1 - \frac{W_{21}}{W_{01}}}\left(\frac{0.1\ \mu W}{W_{01}} + 0.001\ \frac{W_{21}}{W_{01}}\right)}\right], \tag{6.93}$$

and when $W_2 - W_0$ is measured,

$$\varepsilon = 10 \log_{10}\left[\frac{1}{1 - \frac{0.1\ \mu W + 0.001\ W_{02}}{W_{02}}}\right]. \tag{6.94}$$

The calculated limits of error are shown in figure 6.27.

e. Mismatch Errors

The mismatch error (Beatty, 1954) in calibrating a variable attenuator depends upon the reflections from the system in which the attenuator is placed and upon the changes in characteristics of the attenuator as its dial is moved from the reference position. The graph of figure 6-29 shows calculated limits of error for the attenuator used, based upon measurements of the magnitude of the changes in the scattering coefficients S_{11} and S_{22} of the attenuator. It was assumed that there was negligible phase change in S_{21}. The mismatch error is below 0.0001 dB for attenuator settings up to 0.1 dB, and remains below 0.001 dB for higher settings.

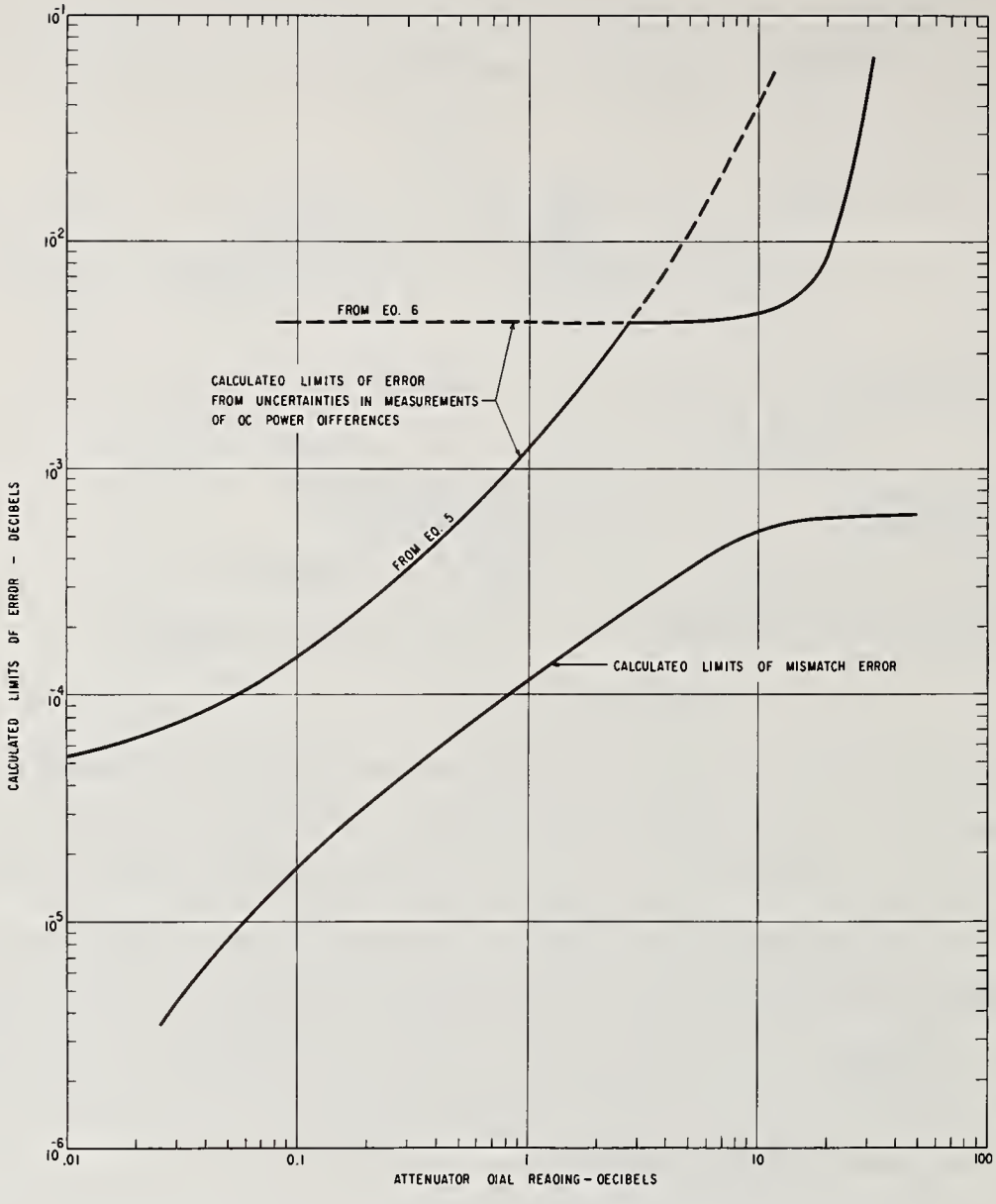

Figure 6-29. Limits of error as a function of attenuation.

f. Results

The calibration data taken at 9.3897 GHz is shown in table 6-2. Three sets of data are shown in order to give an idea of the resettability of the attenuator, and more significant figures are given than one can normally use when interpolating between the marked dial divisions.

Table 6-2. Results of three sets of measurements and calculated limits of error in single measurements.

Attenuator Dial Reading	Measured Attenuations Corresponding to Dial Reading				Maximum Deviation From Average	Calculated Limit of Error in Single Measurement
	1	2	3	Average		
dB	dB	dB	dB	dB	dB	dB
.01	.01077	.01083	.01044	.0107	0.0003	.000055
.02	.02123	.02145	.02145	.0214	0.0002	.000068
.03	.03015	.03035	.03038	.0303	0.0001	.000080
.04	.04043	.04088	.04074	.0407	0.0003	.000091
.05	.05181	.05216	.05226	.0521	0.0003	.00010
.06	.06102	.06067	.06086	.0609	0.0002	.00011
.07	.06992	.07027	.06985	.0700	0.0003	.00013
.08	.07991	.08056	.08017	.0802	0.0004	.00014
.09	.09075	.09104	.09078	.0909	0.0001	.00015
.1	.10226	.10203	.10210	.1021	0.0002	.00016
.12	.11886	.11884	.11951	.1191	0.0004	.00019
.14	.13681	.13760	.13819	.1375	0.0007	.00021
.16	.15737	.15765	.15703	.1573	0.0003	.00024
.18	.17806	.17792	.17888	.1783	0.0006	.00026
.2	.20071	.20089	.20041	.2007	0.0003	.00029
.25	.24702	.24709	.24724	.2471	0.0001	.00035
.5	.49799	.49762	.49795	.4979	0.0003	.00065
1	1.0037	1.0037	1.0037	1.004	0.0000	.0013
2	1.9954	1.9972	1.9948	1.996	0.0010	.0029
3	2.9968	2.9975	2.9993	2.998	0.0015	.0047
5	4.9841	4.9923	4.9927	4.990	0.006	.0048
10	9.9624	9.9671	9.9647	9.965	0.003	.0053
15	14.991	14.988	15.001	14.99	0.000	.0063
20	19.963	19.956	19.945	19.95	0.01	.0093
25	24.999	25.031	24.987	25.01	0.02	.014
30	30.080	30.049	30.074	30.07	0.02	.015
40	40.354	40.281	40.367	40.33	0.05	.02
50	52.338	52.041	52.336	52.24	0.20	.06

The estimated limits of error for the complete range of the attenuator, as determined from figure 6-29, are also shown in table 6-2. Above 20 dB, the calibration was made in two parts: Measurement of the 20 dB step, and measurement of the additional attenuation referred to this step. For these values, the quoted limit of error is the sum of the errors in the individual steps. The accuracy of carefully setting the attenuator dial on the marks is not as good as the accuracy of the measurements.

It is noted that even at the low end where the resolution is approximately 0.0001 dB, the estimated accuracy of the measurement is also better than the repeatability of setting the attenuator on the mark. As a result of this work, it was evident that attenuators needed improvement if full advantage was to be realized of the accuracy available. Such improvements have been recently reported (Little, et al., 1971, Warner, et al., 1972).

g. Analysis and Evaluation of Mismatch Errors

The analysis of mismatch errors in the calibration of variable attenuators (Beatty, 1954), yielded an equation for the error in terms of the scattering coefficients of two fourpoles corresponding to two settings of the attenuator dial, and the reflection coefficients of the system in which the attenuator was placed (see section 6.4e). The measurement of all of these quantities may be tedious or difficult, and to avoid this, an approximate method has been developed. One obtains reasonably close limits within which the error lies from a fairly simple experimental procedure.

The complete expression for the mismatch error is adapted from eq. (6.47) and is

$$\varepsilon = 20 \log_{10} \left| \frac{(1 - S_{11}'\Gamma_G)(1 - S_{22}'\Gamma_L) - (S_{21}')^2\Gamma_G\Gamma_L}{(1 - S_{11}\Gamma_G)(1 - S_{22}\Gamma_L) - (S_{21})^2\Gamma_G\Gamma_L} \right|, \tag{6.95}$$

where scattering coefficients are denoted by S_{11}, S_{12}, S_{21}, and S_{22}; and Γ_G, Γ_L represent, respectively, the reflection coefficients of the system "looking towards" the generator and load. Primes are used to designate a setting of the attenuator other than the zero or reference setting.

For small reflections, the following expression was derived from eq. (6.95)

$$\varepsilon \simeq 20 \log_{10} |1 - (S_{11}'-S_{11})\Gamma_G - (S_{22}'-S_{22})\Gamma_L + [S_{11}'S_{22}'-S_{11}S_{22}-(S_{21}')^2+S_{21}^2]\Gamma_G\Gamma_L|. \tag{6.96}$$

If the attenuator VSWR is not much greater than unity, the products $S_{11}'S_{22}'$ and $S_{11}S_{22}$ may be neglected. Then eq. (6.96) becomes

$$\varepsilon \simeq 20 \log_{10} |1 + (S_{11}-S_{11}')\Gamma_G + (S_{22}-S_{22}')\Gamma_L + [S_{21}^2-(S_{21}')^2]\Gamma_G\Gamma_L|. \tag{6.97}$$

It is convenient to determine the magnitudes of the individual terms but not their phases, so that the limit of error, allowing the phases of S_{11} and S_{22} to take on any values (but the phase of S_{21} is assumed constant) is

$$\varepsilon \simeq 20 \log_{10} [1 + |S_{11}'-S_{11}||\Gamma_G| + |S_{22}'-S_{22}||\Gamma_L| + (|S_{21}|^2-|S_{21}'|^2)|\Gamma_G\Gamma_L|]. \tag{6.98}$$

The quantity $|S_{11} - S'_{11}|$ is determined as follows. With the attenuator under test connected as shown in figure 6-30, and set to its zero or reference position, tuner A is adjusted for a detector null, and tuner B is adjusted until the reflection coefficient Γ_{2i} of the equivalent generator at terminal plane 2 vanishes. (This condition may be recognized by means of an auxiliary reflectometer).

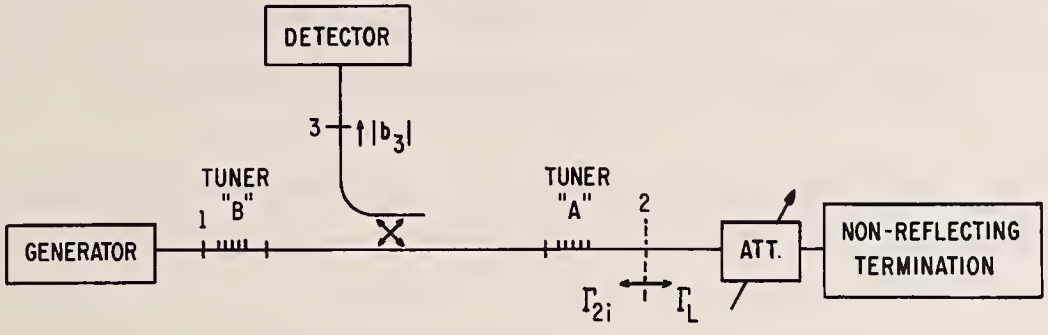

Figure 6-30. Schematic diagram of system for measuring $|S_{11} - S'_{11}|$.

Movement of the attenuator dial to some other setting will then give an observable output. Using the theory of a directional coupler having auxiliary tuners (Beatty and Kerns, 1958) one can obtain $|S_{11} - S'_{11}|$ in the following way.

The magnitude of the wave emerging from the side arm of the directional coupler in figure 6-29 is

$$|b_3| = k\left|\frac{1 + K\Gamma_L}{1 - \Gamma_{2i}\Gamma_L}\right|, \tag{6.99}$$

where k is a constant for a given stable generator operating level.

With the attenuator set first on zero, $\Gamma_L = S_{11}$. Adjusting tuner A for $b_3 = 0$ changes K so that $KS_{11} = -1$. Adjusting tuner B for $\Gamma_{2i} = 0$ makes the dependence of $|b_3|$ on Γ_L simply

$$|b_3| = k\left|1 - \frac{\Gamma_L}{S_{11}}\right|. \tag{6.100}$$

Suppose that the attenuator dial is moved to a new position such that Γ_L now equals S'_{11}; then

$$b_3 = k\left|1 - \frac{S'_{11}}{S_{11}}\right| = \frac{k}{|S_{11}|}|S_{11} - S'_{11}|. \tag{6.101}$$

The factor $k/|S_{11}|$ is obtained by replacing the attenuator with a waveguide section containing a sliding short-circuit. Upon sliding the short, $|b_3|$ goes through small variations so that one may observe $|b_3|_{max}$ and $|b_3|_{min}$. It is easily shown that

$$\frac{k}{|S_{11}|} = \frac{1}{2}(|b_3|_{max} + |b_3|_{min}). \tag{6.102}$$

One can assume that $|b_3|_{max} = |b_3|_{min}$ and employ a fixed short-circuit with negligible error if the VSWR corresponding to $|S_{11}|$ is less than 1.15. It may be that this error is also tolerable for higher VSWR's since it is not important to know $|S_{11} - S'_{11}|$ to great accuracy.

The quantity $|S_{22} - S'_{22}|$ is found in the same way as above with the attenuator turned end for end.

6.9. Two-Channel Nulling Method

We introduce a new technique to measure the attenuation constants of short sections of waveguide and the losses of waveguide joints.[16]

The measurement method is described with reference to figure 6-31 which shows a two-channel system. The test section of waveguide is placed in the lower channel in such a way that the microwave energy traverses it twice, being reflected from a short circuit. The energy then passes through a level-set attenuator and is combined with energy from the upper channel which contains a direct-reading attenuator and phase shifter. Upon adjusting the upper channel to obtain a detector null, the losses in the two channels are equal. It is apparent that one can measure the loss in the test section of waveguide by observing the difference in attenuator settings to obtain nulls with the test section inserted and then removed from the circuit.

The main difference from previous methods (Altschuler, 1963) is that no special items of equipment are needed such as precision-sliding short circuits or special amplifiers. Only stock items of commercially available equipment are used, such as are encountered in most measurement laboratories. The main disadvantage of the method is the necessity for making four to seven measurements at slightly different frequencies each time an attenuation constant is desired. This procedure reduces errors from several troublesome sources, leaving the uncertainty of the reference attenuator as the major source of error. If one uses a good commercially available rotary-vane

[16]This discussion is a modified version of Beatty (1965).

attenuator with 0.01-dB divisions at the low end of the scale, and uses a superheterodyne receiver as a null detector, one can expect a resolution and repeatability of ± 0.001 dB, and an accuracy of perhaps ± 0.002 dB without calibrating the attenuator.

Details of the measurement procedure are as follows:

1) Compute an operating frequency such that the length of the test section of waveguide is an integral number of half-guide-wavelengths. Calculated frequencies for a 10.537" test section of WR-90 (X-band) waveguide are shown in figure 6-32.

2) Set the signal source and the receiver to one of these frequencies, and set the adjustable short circuit to be a quarter-guide-wavelength ($\lambda_G/4$). This is conveniently done by using the direct-reading phase shifter to obtain nulls when first a flat plate, and then the adjustable short circuit, are placed, in turn, at terminal surface "T." The short circuit is adjusted until it requires a change of 180° of the phase shifter to restore the null.

3) With the $\lambda_G/4$ short circuit at terminal surface "T," and the direct-reading attenuator set on zero, adjust the level-set attenuator and the phase shifter to obtain a detector null, or "initial balance."

4) Insert the test section of waveguide as shown and adjust the direct-reading attenuator and phase shifter to restore the detector null or to obtain a "final balance."

Note that if the frequency selected were exactly right, insertion of the test section of waveguide would have introduced no phase shift, and it would have been unnecessary to change the phase shifter in going from initial balance to final balance. The measurement of attenuation constant would then be completed by dividing the reading of the attenuator by two, and then dividing this result by the length of the test section of the waveguide.

In practice, one cannot predict the required frequency exactly, and must approach it by trial and error, in the manner indicated by figure 6-33. The phase shift to restore the null is plotted vs. the frequency. At the crossover frequency, this phase shift is zero and the attenuator reading is then the correct one to use. If the foregoing procedure is not followed, it will usually be found that serious errors are introduced by the change in signal level caused by the change in the phase shifter. The reduction in phase shift in this manner also reduces error due to changes of reflection interactions between the short circuit and the system. These changes

occur when the test section of waveguide is inserted. The use of a quarter-guide-wavelength short circuit and an $N(\lambda_G/2)$ test section of waveguide makes the losses in the waveguide joints negligible, since current flow across the joining planes is reduced to zero. (N is an integer.)

The change of the direct-reading attenuator causes a corresponding change in phase-shift which affects the above results. However, in a typical commercially available rotary-vane type attenuator, such phase shifts are certainly less than one degree and can be safely neglected.

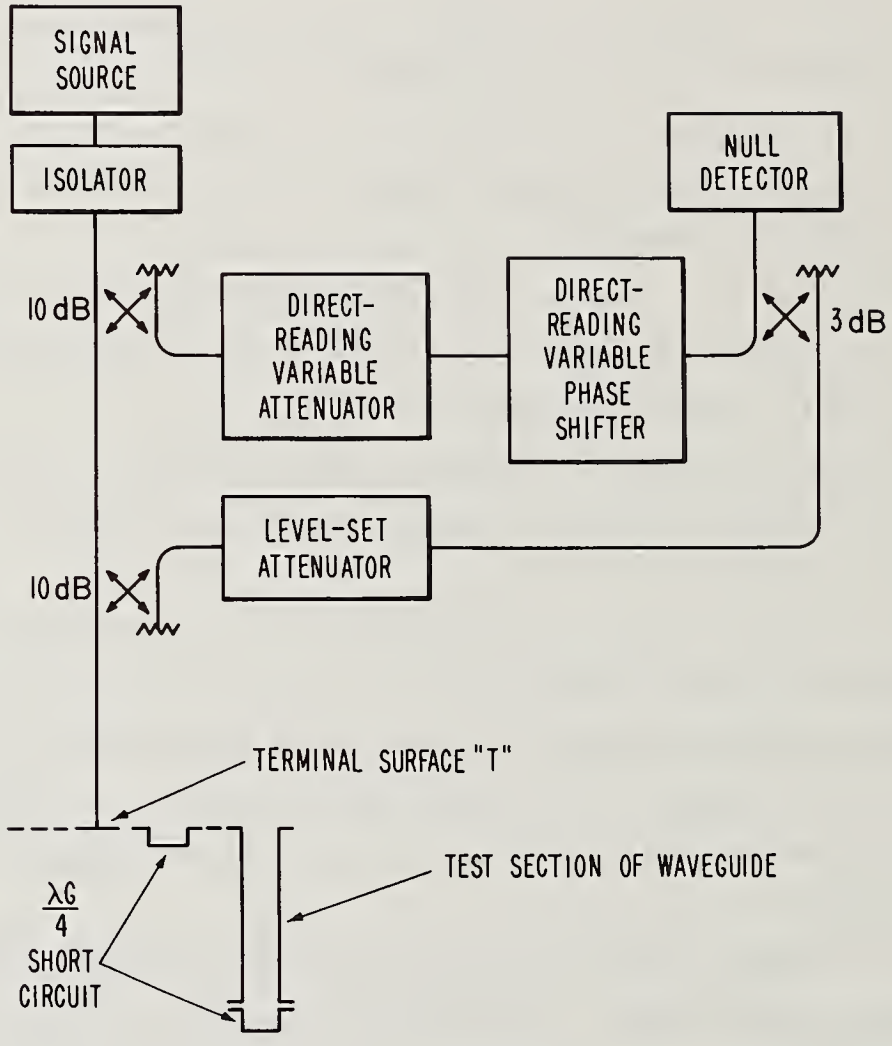

Figure 6-31. Simplified diagram of measurement system.

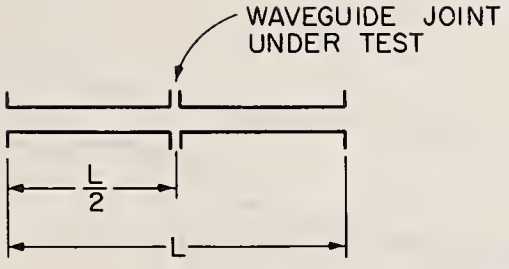

NUMBER OF λ_G IN L	λG (INCHES) FOR L = 10.537"	FREQUENCY GHz
4.5	2.340	8.27
5	2.107	8.62
5.5	1.915	9.00
6	1.756	9.39
6.5	1.621	9.80
7	1.505	10.22
7.5	1.405	10.65
8	1.317	11.10
8.5	1.239	11.56
9	1.171	12.02

Figure 6-32. Arrangement of waveguide joint for measurement of its loss, and calculated crossover frequencies for X-band (WR-90) rectangular waveguide.

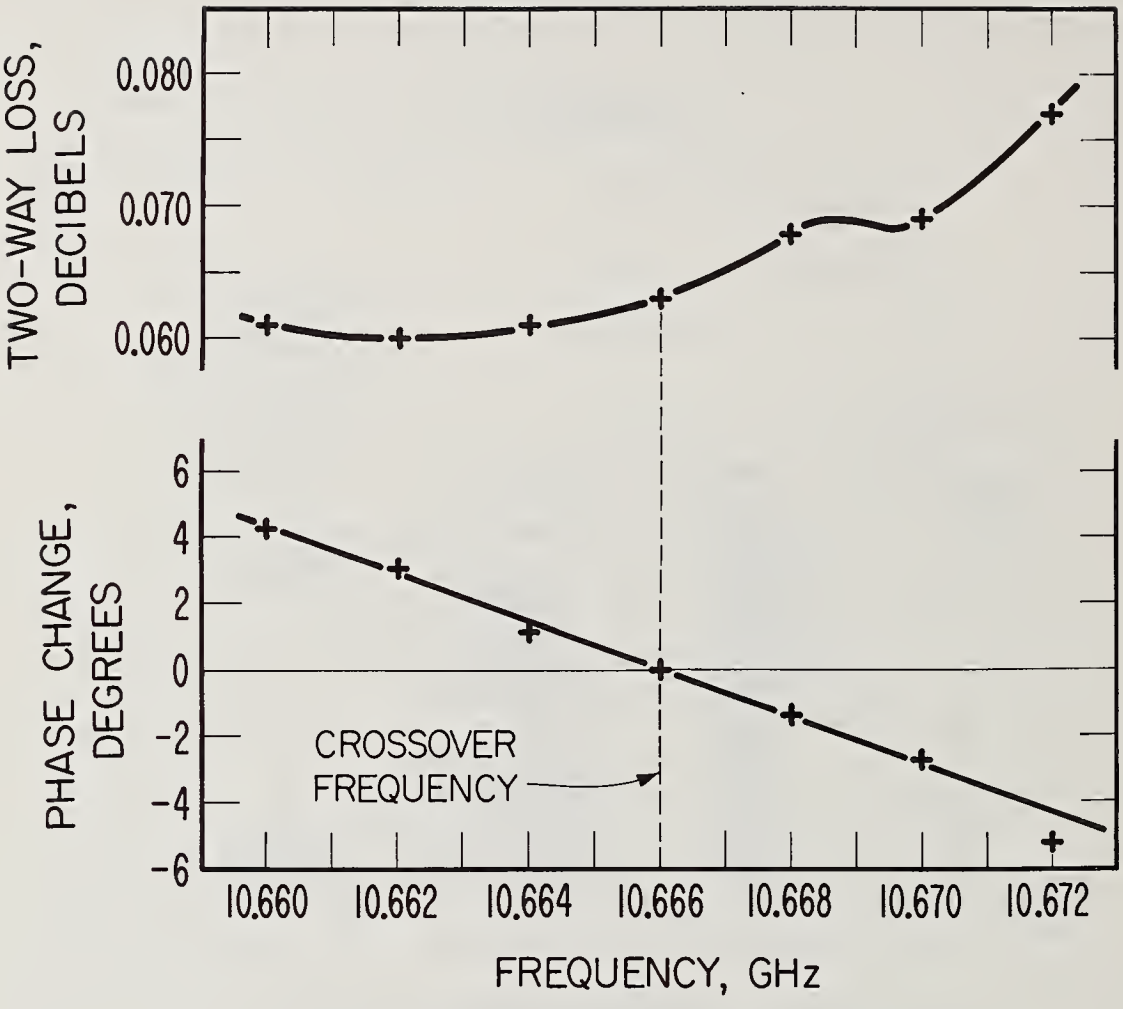

Figure 6-33. Data illustrating trial and error method of obtaining two-way loss at crossover frequency.

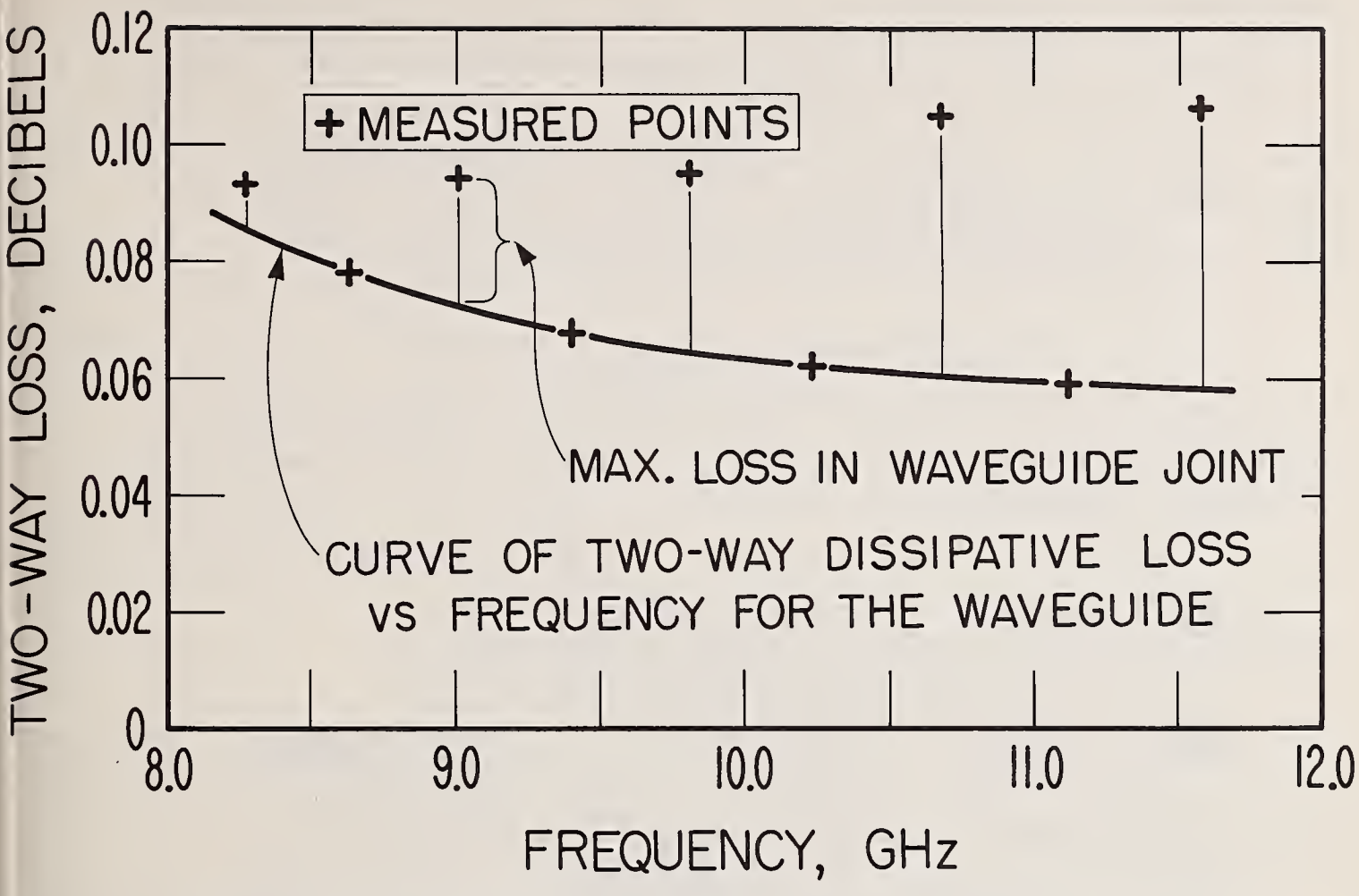

Figure 6-34. Plot of data to obtain maximum loss vs. frequency of waveguide joint.

The loss in the waveguide joint can be measured by the same method. Instead of using a continuous section of waveguide as the test section, one uses two shorter sections which are joined by the waveguide joint under test. The overall length of the resultant waveguide is equal to the length of the single continuous section which it replaces. Assuming that the waveguides have the same attenuation constant, the increase in loss of the joined sections over the continuous section of the same length is caused by the loss in the waveguide joint. Maximum loss occurs when the test joint is an integral number of half-guide-wavelengths from the short-circuiting plate of the short circuit. One divides the maximum loss by four in order to predict the loss of this joint when used in a nonreflecting system.

A number of variations of this technique have been devised. One that is convenient is illustrated in figures 6-32 and 6-34. Note that the test section of waveguide is an integral multiple of half-guide-wavelengths at a number of frequencies, as shown in figure 6-32. At some of these frequencies the

test joint is located an odd number of $\lambda_G/4$ from "T." Thus, its loss is negligible at some frequencies and maximum at others. A plot of the two-way loss through the test section of waveguide at the various crossover frequencies is shown in figure 6-34. The lower points lie on a curve of attenuation vs. frequency for the waveguide. The vertical distance between this curve and each of the upper points is the "maximum" loss in the waveguide joint. One divides these by four to obtain the losses of the waveguide joint when used in a nonreflecting system.

6.10. Attenuation Divider Circuit

A circuit has been investigated (Beatty and Fentress, 1968) which divides by a known ratio small attenuation and phase shift changes of variable attenuators and

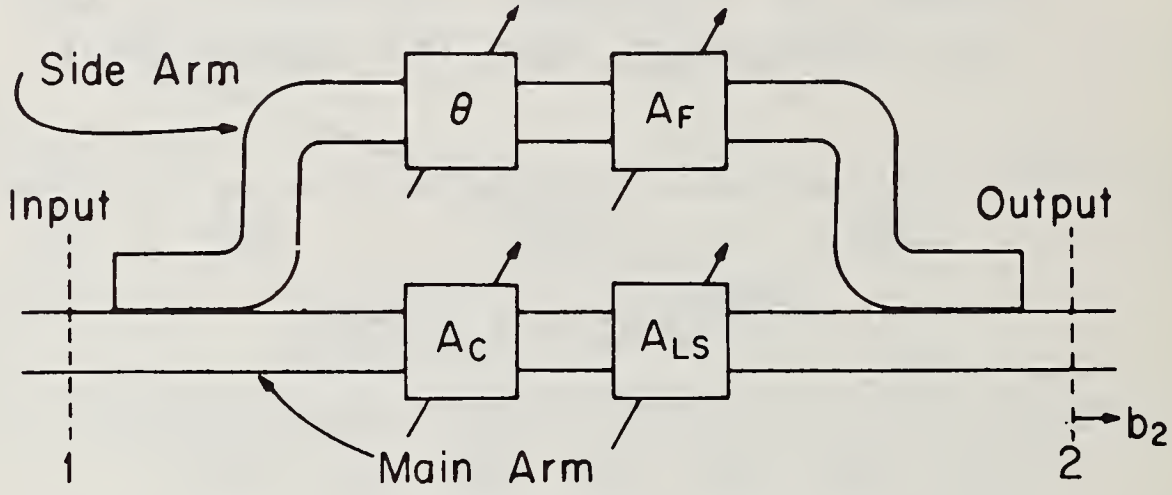

Figure 6-35. Basic attenuation divider circuit.

phase shifters. For example, attenuation changes of 0.01 dB of an attenuator can be made to produce accurate changes of 0.0001 dB in the circuit output. The attenuator application will be described first.

The circuit employs variable attenuators and a phase shifter as shown in figure 6-35. It is assumed that adjustment of the attenuators produces negligible differential phase shift and that adjustment of the phase shifter produces negligible change in attenuation. These requirements are closely met by commercially available attenuators and phase shifters of the rotary vane type. The basic principle is as follows: A fraction of the energy in the main arm is routed around a side arm and recombined in phase with the energy in the main arm. An attenuator A_F in the side

arm then produces a change in signal level which has a reduced effect on the circuit output. A phase shifter is necessary to produce the correct phases for addition of the signals from the two channels. A level-set attenuator A_{LS} is employed to obtain the correct ratio between the signals.

The basic theory is as follows. Consider the wave amplitude components b_M and b_s from main arm and side arm, which combine at terminal surface 2 (the output). Assume that $|b_s| = (1/K)|b_M|$, where K is the ratio of division which results mainly from the decoupling of the side arm from the main arm.[17] Initially, before any change in A_F, the circuit output level is

$$|^i b_2| = |b_M| + |^i b_s|, \tag{6.103}$$

assuming that b_M and $^i b_s$ are in phase. A change of ΔA_F dB in A_F produces a change in $|b_s|$ according to the relationship

$$\Delta A_F = 20 \log_{10} \left| \frac{^i b_s}{^f b_s} \right| = 20 \log_{10}(1 + \delta), \tag{6.104}$$

where the front superscripts denote initial and final conditions, respectively. For small ΔA_F, we can write the following approximate expression:

$$\Delta A_F \cong 8.686\ \delta \text{ dB}. \tag{6.105}$$

The change in decibels of the output circuit level is

$$\Delta A = 20 \log_{10} \left| \frac{^i b_2}{^f b_2} \right| = 20 \log_{10} \frac{|b_M| + |^i b_s|}{|b_M| + |^f b_s|} = 20 \log_{10} \frac{K + 1}{K + \frac{1}{1 + \delta}}. \tag{6.106}$$

This can be written

$$\Delta A = 20 \log_{10} \left(\frac{1}{1 - \frac{\delta}{(k + 1)(1 + \delta)}} \right) = 20 \log_{10} \frac{K + 1}{K + 10^{-\Delta A_F/20}}. \tag{6.107}$$

When ΔA_F is small, δ is small, and the following approximatation gives accurate results:

$$\Delta A \cong 20 \log_{10} \left(1 + \frac{\delta}{K + 1} \right) \cong 8.686 \frac{\delta}{K + 1} \cong \frac{\Delta A_F}{K + 1}. \tag{6.108}$$

---

[17] The ratio K depends upon both the coupling ratios of the two directional couplers and the difference in loss between the main arm and the side arm. The latter is strongly influenced by the amount of level-set attenuation remaining after adjustment. It is desirable to keep the loss in the main arm, and hence the transmission loss through the circuit, low by 1) choosing the coupling ratio to give nearly the desired ratio A, as recommended, or 2) using say 3-dB couplers and installing attenuators in both arms, increasing the one in the side arm, in order to obtain the desired ratio.

The percent error in calculating ΔA from eq. (6.108) rather than from eq. (6.107) is shown in figure 6-36. It is seen that the change in ΔA_F is divided by the factor $K + 1$, which can be controlled as follows.

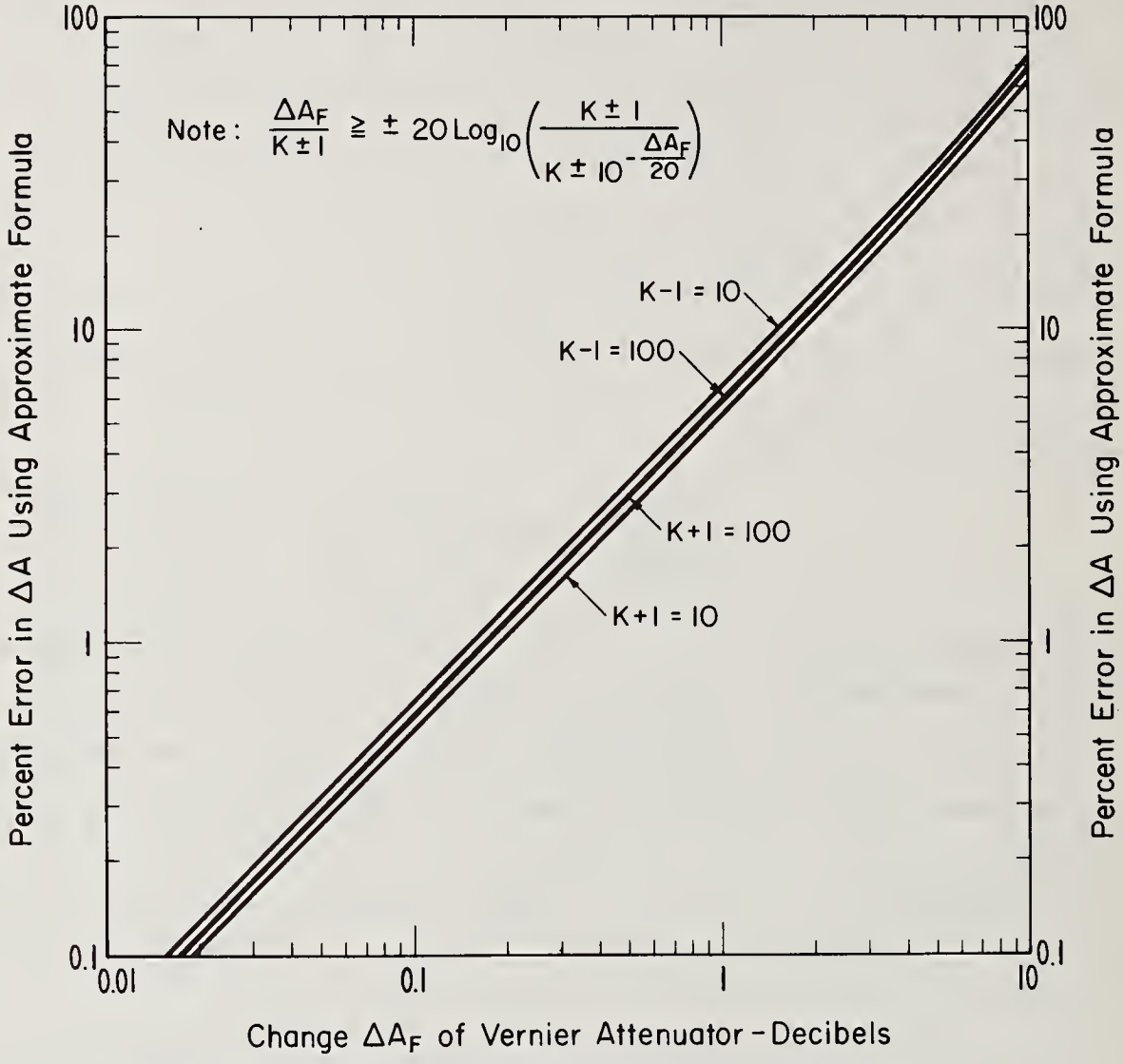

Figure 6-36. Percent error in calculating desired attenuation ΔA using approximate formula $\Delta A \cong \Delta A_F/(K \pm 1)$.

Suppose that we wish to make $K + 1 = 100$. This requires the side arm contribution $|b_s|$ to be $\frac{1}{99}$ of $|b_M|$, or 39.91 dB down. We choose two 20-dB couplers[17] to connect the side arm to the main arm and get a bit more decoupling than we need. The exact ratio of $|b_s|$ to $|b_M|$ is obtained with the level-set attenuator by the following steps: 1) Adjust A_{LS} and the phase shifter to obtain a null output. Then $b_M = - {}^N b_s$. 2) Change the phase shift[18] by 180. Then $b_M = {}^N b_s$, 3) Reduce A_{LS} by 39.91 dB, reducing $|{}^N b_s|$ to $|{}^i b_s| = |b_M|/99$. The circuit is now adjusted to give the required division ratio.

[18]The circuit will operate a bit more accurately without this step, but eq. (6.108) then becomes $\Delta A \cong -\Delta A_F(K - 1)$. An increase in A, then causes a decrease in the circuit output, which is awkward in some applications.

This circuit has been found useful for producing and measuring small attenuation changes when available attenuators do not have sufficiently low ranges. (Many variable attenuators have a minimum dial marking of 0.05 dB or 0.01 dB.) The circuit gives fine control which is often important in adjusting null circuits. The circuit can function as an attenuation vernier. (One can set A_c to an exact dial division much more accurately than one can estimate between divisions of A_c.) The circuit can also function as a step attenuator by switching off the side channel after adjustment. The attenuation change is $20 \log_{10}(1 + 1/K)$. This procedure may be used to check the circuit adjustment. Another check consists of balancing a change of A_F against a corresponding opposite change of A_c.

In order to obtain good accuracy, rotary vane attenuators are recommended because they produce little or no change in phase shift. When adjusting the phase shift[18] 180°, any change in signal level which it produces will cause error in setting the desired ratio. This is normally small for rotary phase changers and can be reduced by determining the change and readjusting A_{LS} accordingly. Typically, changes in signal level will be less than $\pm$ 0.2 dB, corresponding to changes of less than 2.4 percent in the dividing factor. It is good practice to employ isolators having low VSWR on each side of the attenuators and the phase shifter. With calibrated attenuators, the accuracy of this attenuation divider circuit can be very good.

The application to division of small changes of phase shift is similar. The circuit adjustment is the same, and the desired differential phase shift ϕ is obtained in terms of the change θ in the vernier phase shifter by the following expression:

$$\phi = \tan^{-1}\left(\frac{\sin \theta}{K \pm \cos \theta}\right), \tag{6.109}$$

where one uses the + or - sign according to whether the signals from the two channels are in or out of phase, respectively. For small changes in phase, one can use the approximate formula

$$\phi \cong \frac{\theta}{K \pm 1}. \tag{6.110}$$

The error in using the approximate formula is shown in figure 6-37.

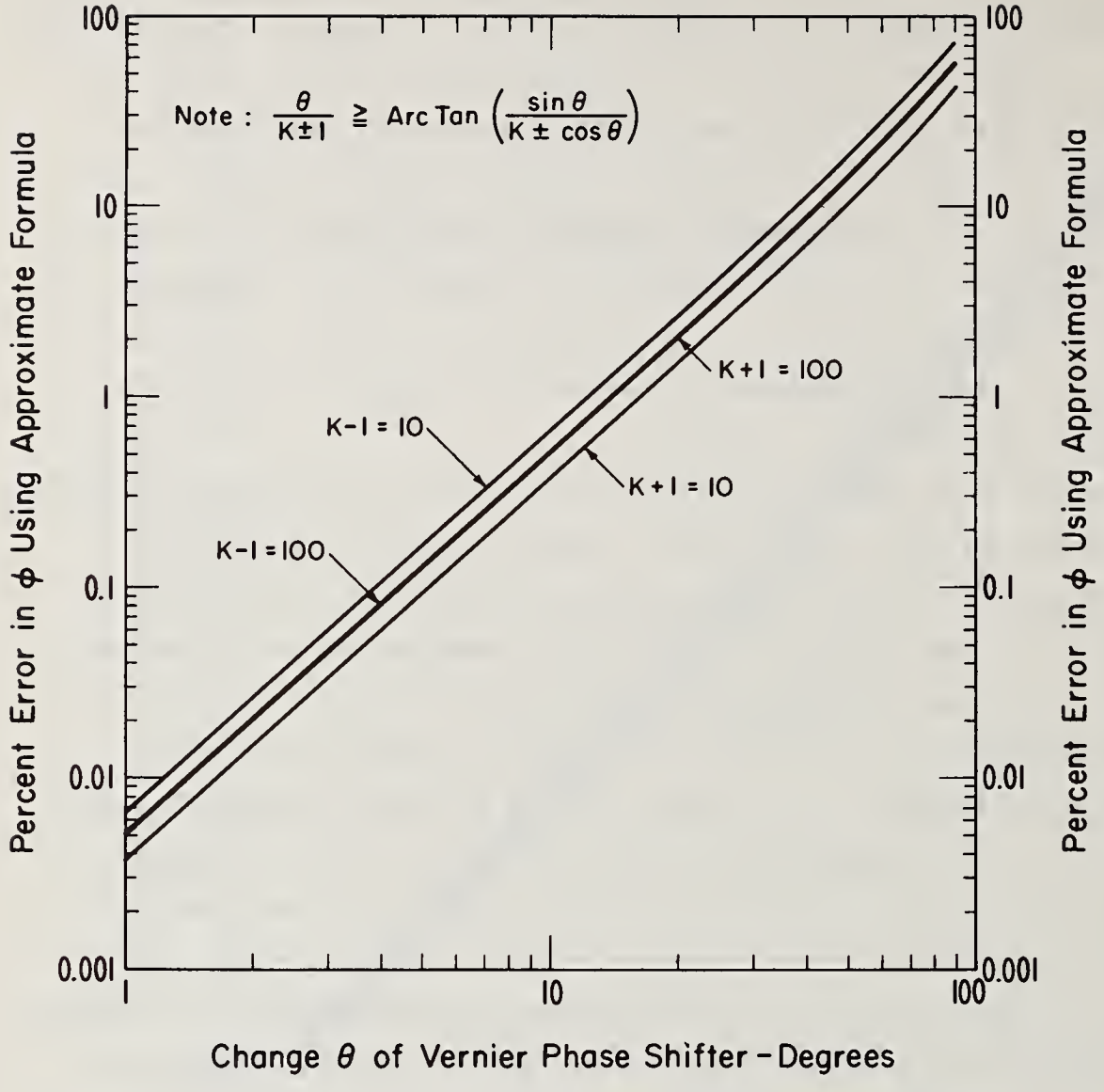

Figure 6-37. Percent error in calculating desired phase shift Φ using approximate formula $\Phi \cong \theta/(K \pm 1)$.

7. Phase Shift

7.1. Introduction

Prior to 1963, little attention was devoted to the subject of phase shift measurements and standards. However, the increased use of phased array antennas led to greater interest and basic microwave phase shift equations were published (Beatty, 1964d). In section 3.10, fundamental definitions of phase shift were briefly given. These are applied to a 2-port model in section 7.2, which is an extended version of the above referenced work.

A standard phase shifter was devised by loading a tuned reflectometer with a sliding short-circuit in a precision section of waveguide. The phase of the reflectometer output tracks the position of the short-circuit and can be accurately calculated for any frequency of operation. Errors due to imperfect tuning, dimensional variations of the waveguide, etc. were analyzed (Schafer and Beatty, 1960). The analysis of errors is described in section 7.3.

The final topic is the development of a standard differential phase shifter (Beatty, 1964e) which consists of two tuned reflectometer phase shift standards having ganged short circuits sliding inside waveguides of different widths. This topic is discussed in section 7.4.

7.2. Phase Shift Equations

a Introduction

In section 3.10, the phase of a sinusoidally varying quantity was defined and the phase shift of voltage, current, or some other quantity associated with a 2-port was discussed. Three kinds of phase shift (1) transmission, (2) substitution, and (3) differential phase shift were defined.

In the following, circuit theory developed in chapter 3 is applied to the development of phase shift equations for 2-ports. Impedances, admittances, and scattering coefficients are used in the equations. By means of these equations, one clearly defines the quantity to be measured and can evaluate some errors due to assumed conditions not being completely satisfied. In addition, the concept of an ideal phase shifter is clearly explained.

The equations are based upon the representation of a phase shifter by a 2-port waveguide junction. As mentioned in section 6.6, the effects of connectors are neglected when using such a simple model. If extremely high accuracy in phase measurements is required in the future, it may be necessary to use a better model.

b General

Several types of phase shift of 2-ports may be considered, as will be shown with reference to figure 7-1.

The usefulness of the different types of phase shift considered will depend upon what types of detectors are used in a measurement of phase difference and whether they respond to wave amplitudes or generalized voltage and current. (An electric field probe in a slotted line would respond to v, for example.)

In figure 7-1, the terminal surfaces 1-1, and 2-2, in the waveguide leads of the 2-port, are the places where the complex amplitudes a and b of the incident and emergent voltage waves, and v and i, the generalized voltage and current, (Kerns, 1967) are to be considered. The assumptions inherent in this representation of a 2-port, such as single-mode propagation in the lossless waveguide leads have been set forth by Kerns, (1967).

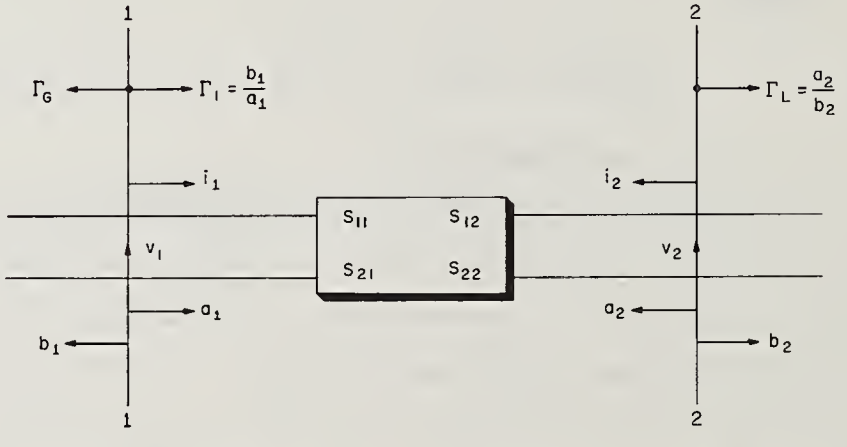

Figure 7-1. Representation of a 2-port, showing two sets of terminal variables.

The relationship between the two sets of terminal variables is as follows

$$\left.\begin{aligned} v &= a + b \\ Z_0 i &= a - b \end{aligned}\right\} \tag{2.33}$$

The amplitude b_G of the generator wave, a_1, b_1, and Γ_G are related by the following equation:

$$a_1 = b_G + b_1\Gamma_G \tag{3.32}$$

One can consider the phase shift of the 2-port to be the difference in phase between v_2 and v_1, between i_2 and i_1, between b_2 and a_1, or between b_2 and b_G, for example. "The phase shift of a 2-port" may, therefore, be a misleading and ambiguous expression, since it seems to imply either that there is only one, or that all phase shifts of a given 2-port are the same. In the following, equations will be given to show how these various phase shifts will differ in general, and under what conditions some of them may be the same.

The equations will be given for the case of a linear 2-port (which may be nonreciprocal) inserted into a system in such a direction that a generator feeds arm 1 and the load terminates arm 2. For simplicity, the symbols such as ψ_v for phase shift do not indicate that this direction has been chosen. One can easily obtain the corresponding phase shift for the opposite direction of energy flow thru the 2-port by interchanging subscripts 1 and 2 in the equations.

If the phase shifter is a reciprocal one, the condition $Z_{01}S_{21} = Z_{02}S_{12}$ will hold, where Z_{01} and Z_{02} are the reference impedances chosen for waveguide leads 1 and 2 of the 2-port. Very often, $Z_{01} = Z_{02}$, and the reciprocity condition is written $S_{21} = S_{12}$. This condition may be substituted into the phase shift equations in order to reduce the number of variables by one for a reciprocal 2-port.

c Phase Shift Equations

The derivation of the following expressions for phase shift will not be given, as they follow from straightforward algebraic manipulation of eqs. (2.33) and (3.32) and the scattering equations of the 2-port.

$$\left.\begin{aligned} b_1 &= S_{11}a_1 + S_{12}a_2 \\ b_2 &= S_{21}a_1 + S_{22}a_2 \end{aligned}\right\} \tag{3.4}$$

(1) Phase Shift of v

The transmission phase shift of v, denoted by ψ_v, may be written as follows

$$\psi_v = \arg \frac{v_2}{v_1} = \arg \frac{S_{21}(1 + \Gamma_L)}{(1 + S_{11})(1 - S_{22}\Gamma_L) + S_{12}S_{21}\Gamma_L} \tag{7.1}$$

This phase shift depends upon the reflection coefficient of the load as well as upon the characteristics of the 2-port. When the load is nonreflecting,

$$[\psi_v]_{\Gamma_L=0} = \arg \frac{S_{21}}{1 + S_{11}}. \tag{7.2}$$

If one employs the impedance matrix instead of the scattering matrix of the 2-port, the equations corresponding to eq. (7.1) and to eq. (7.2) are

$$\psi_v = \arg \frac{Z_{21}Z_L}{Z_{11}(Z_{22} + Z_L) - Z_{12}Z_{21}} \tag{7.3}$$

and

$$[\psi_v]_{Z_L=1} = \arg \frac{Z_{21}}{Z_{11}(Z_{22} + 1) - Z_{12}Z_{21}}, \tag{7.4}$$

where normalized impedances are used. For an open-circuited phase shifter,

$$[\psi_v]_{Z_L=\infty} = \arg \frac{Z_{21}}{Z_{11}}. \tag{7.5}$$

(2) Phase Shift of i

Proceeding in a similar way, the transmission phase shift of i is

$$\psi_i = \arg \frac{-i_2}{i_1} = \arg \frac{S_{21}(1 - \Gamma_L)}{(1 - S_{11})(1 - S_{22}\Gamma_L) - S_{12}S_{21}\Gamma_L}. \tag{7.6}$$

When the load is nonreflecting,

$$[\psi_i]_{\Gamma_L=0} = \arg \frac{S_{21}}{1 - S_{11}}. \tag{7.7}$$

If one employs the admittance matrix instead of the scattering matrix of the 2-port, the equations corresponding to eq. (7.6) and to eq. (7.7) are

$$\psi_i = \arg \frac{-Y_{21}Y_L}{Y_{11}(Y_{22} + Y_L) - Y_{12}Y_{21}}, \tag{7.8}$$

and

$$[\psi_i]_{Y_L=1} = \arg \frac{-Y_{21}}{Y_{11}(Y_{22} + 1) - Y_{12}Y_{21}}, \tag{7.9}$$

where normalized admittances are used. For a short-circuited phase shifter,

$$[\psi_i]_{Y_L=\infty} = \arg\left(-\frac{Y_{21}}{Y_{11}}\right). \tag{7.10}$$

(3) Phase Difference Between b_2 and a_1

One can see by inspection of the scattering equations and figure 7-1 that

$$\psi_{b_2,a_1} = \arg \frac{b_2}{a_1} = \arg \frac{S_{21}}{1 - S_{22}\Gamma_L}. \tag{7.11}$$

When the load is nonreflecting,

$$[\psi_{b_2,a_1}]_{\Gamma_L=0} = \arg S_{21} = \psi_{21}. \tag{7.12}$$

This phase shift is particularly interesting because it is simply the phase ψ_{21} of the scattering coefficient S_{21}, a fundamental characteristic of the 2-port.

(4) Phase Difference between b_2 and b_G

It is clear from eq. (3.32) that the generator wave b_G does not, in general, have the same amplitude as the wave incident upon the 2-port in arm 1. The phase difference between b_2 and b_G is therefore of interest and may be written

$$\psi_{b_2,b_G} = \arg \frac{b_2}{b_G} = \arg \frac{S_{21}}{(1 - S_{11}\Gamma_G)(1 - S_{22}\Gamma_L) - S_{12}S_{21}\Gamma_G\Gamma_L}, \tag{7.13}$$

or

$$\psi_{b_2,b_G} = \arg \frac{S_{21}}{(1 - \Gamma_G\Gamma_1)(1 - S_{22}\Gamma_L)}. \tag{7.14}$$

This phase shift depends upon the reflection coefficients of generator and load as well as upon the scattering coefficients of the 2-port. When only the load is nonreflecting,

$$[\psi_{b_2,b_G}]_{\Gamma_L=0} = \arg \frac{S_{21}}{1 - S_{11}\Gamma_G}. \tag{7.15}$$

When only the generator is nonreflecting,

$$[\psi_{b_2,b_G}]_{\Gamma_G=0} = \arg \frac{S_{21}}{1 - S_{22}\Gamma_L}. \tag{7.16}$$

When both generator and load are nonreflecting,

$$[\psi_{b_2,b_G}]_{\Gamma_G=\Gamma_L=0} = \arg S_{21} = \psi_{21}. \tag{7.17}$$

It is observed that this is the same result as eq. (7.12) and is of special interest for the same reason that eq. (7.12) is of interest.

The phase difference between b_2 and b_G may be expressed in terms of two components, (1) the phase difference between a_1 and b_G, and (2) the phase difference between b_2 and a_1 as follows.

$$[\psi_{b_2,b_G}] = \arg \frac{b_2}{b_G} = \arg\left(\frac{b_2}{a_1} \cdot \frac{a_1}{b_G}\right) = \psi_{b_2,a_1} + \psi_{a_1,b_G}. \tag{7.18}$$

The first of these components is given by eq. (7.11), and the second follows from subsequent inspection of eq. (7.14).

$$\psi_{a_1,b_G} = \arg \frac{a_1}{b_G} = \arg \frac{1}{1 - \Gamma_G\Gamma_1}. \tag{7.19}$$

Thus, one obtains

$$\psi_{b_2,b_G} = \psi_{21} - \arg(1 - S_{22}\Gamma_L) - \arg(1 - \Gamma_G\Gamma_1). \tag{7.20}$$

This latter expression shows clearly how reflections from the generator and load can affect ψ_{b_2,b_G}.

Other phase differences such as between b_2 and b_1, a_2 and a_1, b_2 and v_1, etc., could be considered, but are perhaps of less interest than the above examples. Writing of equations for these phase differences would not be difficult, if they were desired.

(5) Differential Phase Shift

When variable phase shifters are adjusted, one is interested in a change produced in the phase of v_2 or b_2 at the output waveguide lead of the 2-port as shown in figure 7-1.

For the purposes of analysis, it is convenient to regard a variable phase shifter adjustment as though one removed an initial phase shifter and substituted a final phase shifter, even though the variable phase shifter remains in the system at all times. Using front superscripts i and f to denote initial and final conditions, respectively, it can be shown as follows that the change in phase of v_2 produced by

a given change of a variable phase shifter is the same as the corresponding change in phase of b_2. Writing the change in phase

$$\Delta\psi_{v_2} = \arg \frac{f_{v_2}}{i_{v_2}} = \arg \frac{f_{b_2} + f_{a_2}}{i_{b_2} + i_{a_2}} = \arg \frac{f_{b_2}}{i_{b_2}} \left(\frac{1 + f_{\Gamma_L}}{1 + i_{\Gamma_L}} \right). \tag{7.21}$$

If there is no change in the load, $f_{\Gamma_L} = i_{\Gamma_L}$, and

$$\Delta\psi_{v_2} = \arg \frac{f_{v_2}}{i_{v_2}} = \arg \frac{f_{b_2}}{i_{b_2}} = \Delta\psi_{b_2} = \Delta\psi. \tag{7.22}$$

One can now obtain an expression for the differential phase shift, using[1]

$$b_2 = \frac{S_{21} b_G}{(1 - S_{11}\Gamma_G)(1 - S_{22}\Gamma_L) - S_{12}S_{21}\Gamma_G\Gamma_L}, \tag{7.23}$$

and eq. (7.22), and assuming that there is no change in b_G, Γ_G, or Γ_L.

The differential phase shift is

$$\Delta\psi = \arg \left\{ \frac{f_{S_{21}}}{i_{S_{21}}} \cdot \frac{(1 - i_{S_{11}}\Gamma_G)(1 - i_{S_{22}}\Gamma_L) - i_{S_{12}} i_{S_{21}}\Gamma_G\Gamma_L}{(1 - f_{S_{11}}\Gamma_G)(1 - f_{S_{22}}\Gamma_L) - f_{S_{12}} f_{S_{21}}\Gamma_G\Gamma_L} \right\}. \tag{7.24}$$

If only the generator is nonreflecting

$$[\Delta\psi]_{\Gamma_G=0} = \arg \left\{ \frac{f_{S_{21}}}{i_{S_{21}}} \cdot \frac{1 - i_{S_{22}}\Gamma_L}{1 - f_{S_{22}}\Gamma_L} \right\}. \tag{7.25}$$

If only the load is nonreflecting

$$[\Delta\psi]_{\Gamma_L=0} = \arg \left\{ \frac{f_{S_{21}}}{i_{S_{21}}} \cdot \frac{1 - i_{S_{11}}\Gamma_G}{1 - f_{S_{11}}\Gamma_G} \right\}. \tag{7.26}$$

If both generator and load are nonreflecting,

$$[\Delta\psi]_{\Gamma_G=\Gamma_L=0} = \arg \frac{f_{S_{21}}}{i_{S_{21}}} = f_{\psi_{21}} - i_{\psi_{21}}. \tag{7.27}$$

(6) Insertion Phase Shift

When a (final) 2-port is substituted for another (initial) 2-port, a phase shift of v_2 or b_2 occurs at the load. The general expression for the phase shift of b_2 is eq. (7.24). This was shown to be the same for v_2 as for b_2. When both generator and

[1]This follows from manipulation of eqs. (3.32) and (3.4) substituting $a_2 = b_2\Gamma_L$.

load are nonreflecting the substitution phase shift reduces to the difference between the characteristic phase shifts of the initial and final 2-ports.

Consider that the insertion phase shift is a special case of the substitution phase shift, just as it was considered in section 3.8c that the insertion loss is a special case of substitution loss. The special condition is that the initial 2-port is lossless, nonreflecting, and has zero characteristic phase shift. These conditions on the scattering coefficients are

$$ {}^{i}S_{11} = {}^{i}S_{22} = 0, \text{ and } {}^{i}S_{12}\,{}^{i}S_{21} = 1. \tag{7.28} $$

Substitution of these conditions into eq. (7.24) yields

$$ \psi_I = \arg\left(S_{21} \frac{1 - \Gamma_G\Gamma_L}{(1 - S_{11}\Gamma_G)(1 - S_{22}\Gamma_L) - S_{12}S_{21}\Gamma_G\Gamma_L} \right), \tag{7.29} $$

where the front superscript f is no longer needed and has been omitted. When the system is nonreflecting ($\Gamma_G = \Gamma_L = 0$),

$$ [\psi_I]_{\Gamma_G=\Gamma_L=0} = \arg S_{21}, \tag{7.30} $$

the characteristic phase shift of the 2-port.

d. Characteristic Phase Shift

The foregoing equations have served to illustrate that the phase differences considered will in general depend not only upon the characteristics of the 2-port, but also upon the characteristics of the load, and in some cases also upon the characteristics of the generator.

If one is interested in a phase difference which depends only upon characteristics of the 2-port, the eqs. (7.2), (7.7), (7.12), and (7.17) can be considered. Of these eqs. (7.12) and (7.17) are simplest. Thus it would seem desirable to select ψ_{21} as one of the characteristic phase shifts of a 2-port. (The other would be ψ_{12}.) It would be defined[2] as the phase difference between b_2 and b_G when nonreflecting

[2]This definition is in harmony with that given in IRE Standards on Antennas and Waveguides: Waveguide and Waveguide Component Measurements, 1959, Proc. IRE 47 No. 4, 568 582.

generator and load are connected to arms 1 and 2, respectively, of the 2-port.

The differential phase shift of a 2-port in a nonreflecting system as given by eq. (7.27) is then simply the differential characteristic phase difference, as defined above.

When phase differences of 2-ports are measured under different source or load conditions, different results will be expected. The discrepancies can be called mismatch errors, which can be evaluated by reference to the foregoing equations.

e. An Ideal Phase Shifter

The concept of an ideal phase shifter is useful for comparison purposes in evaluating the performance of actual phase shifters. Such a phase shifter is nonreflecting, lossless when terminated by a nonreflecting load, and nonreciprocal. The conditions on its scattering coefficients are

$$S_{11} = S_{22} = S_{12} = 0, \text{ and } S_{21} = e^{j\psi_{21}}, \tag{7.31}$$

assuming that energy is incident upon arm 1 and there is no reflected wave in arm 2.

One notes that the phase shifts of an ideal phase shifter more closely approach ψ_{21}, than one which is not ideal, even if generator and load reflections are present. For example, compare eqs. (7.1), (7.6), (7.13) and (7.11), respectively with

$$\psi_V = \psi_{21} + \arg (1 + \Gamma_L), \tag{7.32}$$

$$\psi_i = \psi_{21} + \arg (1 - \Gamma_L), \tag{7.33}$$

$$\psi_{b_2,b_G} = \psi_{21}, \tag{7.34}$$

and

$$\psi_{b_2,a_1} = \psi_{21}. \tag{7.35}$$

The differential phase shift of an ideal phase shifter is from eq (7.31) and eq. (7.24),

$$\Delta\psi = ({}^{f}\psi_{21} - {}^{i}\psi_{21}). \tag{7.36}$$

It is seen that the use of an ideal phase shifter obviates the need for a nonreflecting system, if the characteristic phase shift is to be produced, in the cases of ψ_{b_2,b_G}, ψ_{b_2,a_1}, and $\Delta\psi$. However in the cases of ψ_V and ψ_I, a nonreflecting load is also required.

In an ideal situation, it can be seen from inspection of eqs. (7.23) and (7.31) that the output level is not changed when the phase shifter is adjusted. However, it

can be seen that if the lossless, nonreflecting phase shifter is reciprocal ($S_{12} = S_{21} = e^{j\psi_{21}}$), the change in level expressed in decibels of either v_2 or b_2 is

$$\Delta L = 20 \log_{10}\left|\frac{{}^{i}b_2}{{}^{f}b_2}\right| = 20 \log_{10}\left|\frac{1 - \Gamma_G\Gamma_L e^{2j\,{}^{f}\psi_{21}}}{1 - \Gamma_G\Gamma_L e^{2j\,{}^{i}\psi_{21}}}\right|. \tag{7.37}$$

The change in level is due to the interaction of reflections between generator and load which would be suppressed by a nonreciprocal phase shifter.

Of course there would be no change in level from a lossless, nonreflecting reciprocal phase shifter in a nonreflecting system ($\Gamma_G = \Gamma_L = 0$).

f. Conclusions

It has been shown that one can reasonably choose ψ_{21}, the argument of S_{21}, and ψ_{12}, the argument of S_{12}, as the characteristic phase shifts of a 2-port. For a variable phase shifter, the characteristic differential phase shift $\Delta\psi$ equals the change in ψ_{21} between initial and final settings.

In measuring these quantities, it is important to insert the phase shifter into nonreflecting systems ($\Gamma_G = \Gamma_L = 0$), and in using the phase shifter thereafter, it is no less important to duplicate these conditions. Any deviation from these conditions will result in a mismatch error, and these have been analyzed (Schafer, 1960) for some types of measurement systems.

The use of an ideal phase shifter which is nonreciprocal, lossless, and nonreflecting obviates the need for a nonreflecting system in phase shift measurements of ψ_{b_2,b_G}, ψ_{b_2,a_1}, and $\Delta\psi$. However, a nonreflecting load would be required in the cases of ψ_V and ψ_I. It was shown that there will be no change in the output level of an ideal variable phase shifter. However, a reciprocal, but otherwise ideal variable phase shifter in general requires either Γ_G or Γ_L to vanish if level changes are to be eliminated.

7.3. Standard Phase Shifter

a. Introduction

A standard microwave phase shifter was proposed (Magid, 1958) which utilizes an adjustable short circuit attached to a tunable three-arm waveguide junction. This

standard is illustrated in figure 7-2. It can be shown (Beatty and Kerns, 1958) that the change of phase of the emergent wave from the third arm can be ideally made to

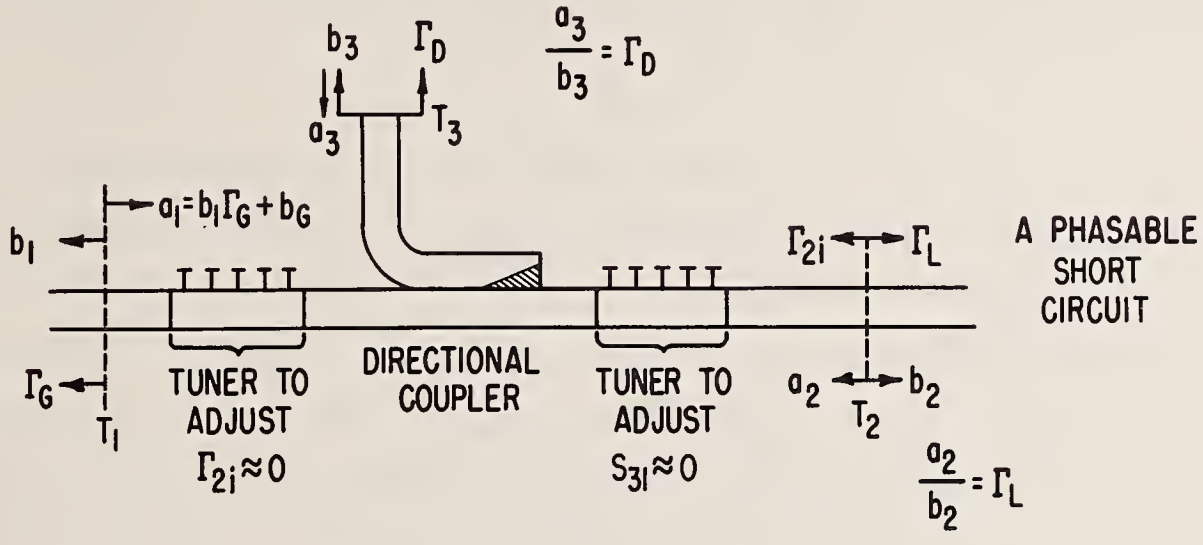

Figure 7-2. A standard microwave phase shifter.

equal the change of phase of the equivalent load attached to the second arm, whether or not $\Gamma_G = \Gamma_D = 0$. Practical limitations in tuning the junction result in departures from this ideal behavior which leaves an error to be evaluated.

The difference between the change of phase of the emergent wave from arm 3 and the change of phase of the load attached to arm 2 because of imperfect tuning is termed the tuning error. This analysis relates the tuning error to amplitude changes which are observed at the detector attached to arm 3 during the tuning procedure. Graphs are presented for determining parameters needed to estimate the limits of tuning error from observations of amplitude variations during the tuning procedure.

Other sources of error which are considered are those which enter in determining the change of phase of the reflection coefficient of the load attached to arm 2. This load is a short circuit whose axial motion in the waveguide can be measured. The change of phase produced depends on the waveguide wavelength and the length of travel of the short circuit. For the dominant mode of propagation in lossless rectangular waveguide, the only dimension which affects the waveguide wavelength is the broad dimension. The difference between the phase shift of the reflection coefficient

of the short-circuit and the calculated phase shift of the load caused by broad dimension nonuniformity, and by inaccuracy in determining the motion of the short circuit is termed dimension error. Limits of dimension errors are calculated for WR-90 waveguide in the recommended frequency range of 8.2 to 12.4 GHz, and presented in graphical form.

b. Tuning Errors

It has been shown (Beatty and Kerns, 1958), (see also section 3.15i) that the amplitude of b_3, the emergent wave from arm 3 (connected to the detector), may be expressed in the form

$$\frac{b_3}{b_G} = \frac{\begin{vmatrix} S_{21} & S_{22} \\ S_{31} & S_{32} \end{vmatrix} \Gamma_L + S_{31}}{\begin{vmatrix} (1-S_{11}\Gamma_G) & S_{13}\Gamma_D \\ S_{31}\Gamma_G & (1-S_{33}\Gamma_D) \end{vmatrix} (1-\Gamma_{2i}\Gamma_L)}, \tag{7.38}$$

The phase of b_3 with respect to an arbitrary reference, b_G, may be defined as θ_{3G}.

Adjustments of the junction are made to render as nearly as possible $S_{31} = 0$ and $\Gamma_{2i} = 0$. Under these ideal conditions, eq. (7.38) reduces to

$$\frac{b_3}{b_G} = \frac{S_{21}S_{32}\Gamma_L}{(1 - S_{11}\Gamma_G)(1 - S_{33}\Gamma_D)} = C\Gamma_L. \tag{7.39}$$

where C is a constant. The change of phase of the emergent wave, ${}^{f}\theta_{3G} - {}^{i}\theta_{3G}$, when the load is changed from intial to final settings, ${}^{i}\Gamma_L$ to ${}^{f}\Gamma_L$, may be determined from the ratio of the final to initial values of b_3 as obtained from eq. (7.39)

$$\frac{{}^{f}b_3}{{}^{i}b_3} = \frac{{}^{f}\Gamma_L}{{}^{i}\Gamma_L}. \tag{7.40}$$

This may be written to show the changes of phase explicitly as

$$\left|\frac{{}^{f}b_3}{{}^{i}b_3}\right| e^{j({}^{f}\theta_{3G} - {}^{i}\theta_{3G})} = \left|\frac{{}^{f}\Gamma_L}{{}^{i}\Gamma_L}\right| e^{j({}^{f}\psi_L - {}^{i}\psi_L)}. \tag{7.41}$$

where ${}^{f}\psi_L$ and ${}^{i}\psi_L$ are the phases of the reflection coefficients of the equivalent load at final and initial settings, respectively. From which it is apparent that the change of phase of the emergent wave is equal to the change of phase of the load attached to arm 2, ${}^{f}\psi_L - {}^{i}\psi_L = {}^{fi}\psi_L$.

If the tuning errors are small, then departures from this ideal response because of $S_{21} \neq 0$ and $\Gamma_{2i} \neq 0$ can be considered separately and the contributions added. The following analysis uses this first order approximation.

(1) Case I

$S_{31} = 0$, but $\Gamma_{2i} \neq 0$. The ratio ${}^{f}b_3/{}^{i}b_3$, for these conditions may be derived from eq. (7.38) and written as

$$\frac{{}^{f}b_3}{{}^{i}b_3} = \frac{{}^{f}\Gamma_L}{{}^{i}\Gamma_L} \frac{1 - \Gamma_{2i}\,{}^{i}\Gamma_L}{1 - \Gamma_{2i}\,{}^{f}\Gamma_L}, \tag{7.42}$$

from which it is apparent that the change of phase of the emergent wave, ${}^{f}\theta_{3G} - {}^{i}\theta_{3G}$ differs from the change in phase of Γ_L by $\varepsilon_{T.I}$, where

$$\varepsilon_{T.I} = \text{argument of } \frac{1 - \Gamma_{2i}\,{}^{i}\Gamma_L}{1 - \Gamma_{2i}\,{}^{f}\Gamma_L} \tag{7.43}$$

= argument of $(1 - \Gamma_{2i}\,{}^{i}\Gamma_L)$ - argument of $(1 - \Gamma_{2i}\,{}^{f}\Gamma_L) + 2n\pi$, where n is an integer. In order to evaluate $\varepsilon_{T.I}$ from eq (7.43), one would need to know Γ_{2i}, ${}^{f}\Gamma_L$ and ${}^{i}\Gamma_L$. It is more convenient to calculate a limit of error assuming that one knows the magnitudes of these quantities and the change in phase of Γ_L, which one controls during the measurement. The phases are then assumed to have the values which would give maximum $\varepsilon_{T.I}$. Referring to figure 7-3, in which the phase of Γ_{2i} and the initial phase of Γ_L are chosen to give the maximum tuning error ($\lim \varepsilon_{T.I}$) for a given ${}^{fi}\psi_L$, one obtains

$$\frac{\sin\left(\frac{\lim \varepsilon_{T.I}}{2}\right)}{\sin\left(\frac{{}^{fi}\psi_L}{2} + n\pi\right)} = \frac{|\Gamma_{2i}||\Gamma_L|}{1 - |\Gamma_{2i}||\Gamma_L|} \leq |\Gamma_{2i}||\Gamma_L|. \tag{7.44}$$

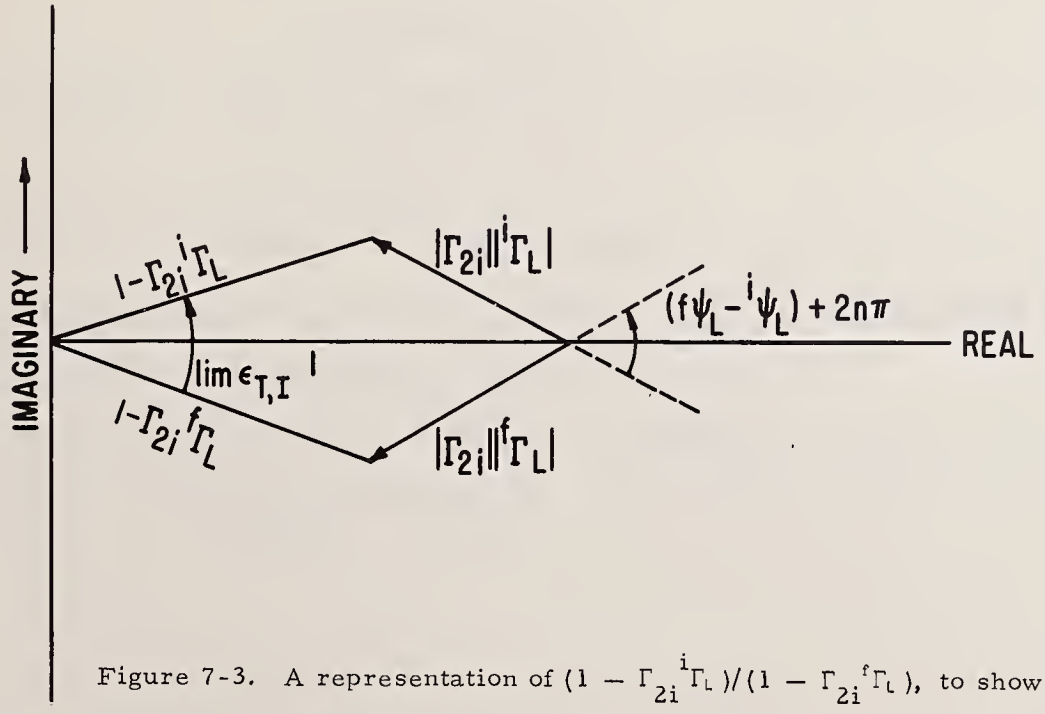

Figure 7-3. A representation of $(1 - \Gamma_{2i}\,{}^{i}\Gamma_L)/(1 - \Gamma_{2i}\,{}^{f}\Gamma_L)$, to show maximum $\epsilon_{T,I}$ for a given ${}^{f}\psi_L - {}^{i}\psi_L$.

Since $\Gamma_L \simeq 1$, and since the errors are assumed small, eq (7.44) yields

$$\lim \varepsilon_{T.I} \simeq 2|\Gamma_{2i}|\left|\sin \frac{fi\psi_L}{2}\right|. \tag{7.45}$$

It is noted that the tuning error from this source cannot exceed $2\ |\Gamma_{2i}|$ radians for any phase measurement.

One can determine $|\Gamma_{2i}|$ as follows. In the tuning procedure for setting $\Gamma_{2i} \simeq 0$, the reflection coefficient of the phasable load which is attached to arm 2, $\Gamma_{T.I}$, is nearly of unit magnitude and $S_{31} \simeq 0$; therefore, the ratio of the maximum to minimum response of the detector as the phase of $\Gamma_{T.I}$ is varied may be obtained from eq (7.38) as approximately,

$$\frac{|b_3|_{max}}{|b_3|_{min}} \simeq \frac{1 + |\Gamma_{2i}|}{1 - |\Gamma_{2i}|} \simeq 1 + 2|\Gamma_{2i}| \tag{7.46}$$

or,

$$20 \log_{10} \frac{|b_3|}{|b_3|_{min}} \simeq 20 \log_{10}(1 + 2|\Gamma_{2i}|) \simeq 17.4|\Gamma_{2i}|. \tag{7.47}$$

(2) Case II

$\Gamma_{2i} = 0$, but $S_{31} \neq 0$. For this case, the ratio of the final emergent wave to the initial emergent wave may be derived from eq. (7.38) as

$$\frac{f_{b_3}}{i_{b_3}} = \frac{f_{\Gamma_L}}{i_{\Gamma_L}} \cdot \frac{1 + \dfrac{S_{31}}{(S_{32}S_{21} - S_{31}S_{22})^{f}\Gamma_L}}{1 + \dfrac{S_{31}}{(S_{32}S_{21} - S_{31}S_{22})^{i}\Gamma_L}}, \tag{7.48}$$

from which it is apparent that the change of phase at the emergent wave differs from the change of phase of the load by $\varepsilon_{T.II}$ where,

$$\varepsilon_{T.II} = \text{argument of } \frac{1 + \dfrac{S_{31}}{(S_{32}S_{21} - S_{31}S_{22})^{f}\Gamma_L}}{1 + \dfrac{S_{31}}{(S_{32}S_{21} - S_{31}S_{22})^{i}\Gamma_L}} \tag{7.49}$$

which for $|S_{31}S_{22}| << |S_{32}S_{21}|$ may be written as

$$\varepsilon_{T.II} \simeq \text{argument of}\left(1 + \frac{S_{31}}{S_{32}S_{21}{}^{f}\Gamma_L}\right)$$

$$- \text{argument of}\left(1 + \frac{S_{31}}{S_{32}S_{21}{}^{i}\Gamma_L}\right) + 2n\pi. \tag{7.50}$$

Since $|\Gamma_L| \simeq 1$, one may write $1/\Gamma_L \simeq e^{-j\psi_L}$. From a derivation similar to that used for $\varepsilon_{T.I}$, it can be shown that, for small errors.

$$\lim \varepsilon_{T.II} \cong 2\left|\frac{S_{31}}{S_{32}S_{21}}\right| \cdot \left|\sin\left(\frac{{}^{fi}\psi_L}{2}\right)\right|. \tag{7.51}$$

Since $|S_{21}|$is of the order of unity, $\lim \varepsilon_{T.II}$ is, to the same approximation, proportional to the inverse of the directivity ratio. One can determine this ratio as follows. The observed amplitude variation of the side arm output when tuning adjustments are made to set $S_{31} \simeq 0$ can be shown to be

$$20 \log_{10} \frac{|b_3|_{max}}{|b_3|_{min}} \cong 20 \log_{10}\left(1 + 2\left|\frac{S_{31}}{S_{32}S_{21}}\right| \cdot \left|\frac{1}{\Gamma_{T.II}}\right|\right) = 17.4\left|\frac{S_{31}}{S_{32}S_{21}\Gamma_{T.II}}\right|. \tag{7.52}$$

where $\Gamma_{T.II}$ is the reflection coefficient of the phasable load, which is attached to arm 2 when tuning for the condition $S_{31} = 0$. The magnitude $|\Gamma_{T.II}|$is small for this adjustment and an estimate of its value must be made in order to evaluate the error.

c. Dimension Errors

Ideally, the change of phase of the standard phase shifter at a single frequency is

$${}^{fi}\psi_L = \frac{4\pi(\ell_f - \ell_i)}{\lambda_g} \text{ radians}, \tag{7.53}$$

where $\ell_f - \ell_i$ is the distance between the final and initial positions of the short circuit within a waveguide in which the waveguide wavelength is λ_g.

The error in the change of phase of Γ_L due to the uncertainty in measurement of the axial motion of the sliding short circuit is termed the motional error, ε_ℓ. A

small motional error is readily evaluated by considering the partial derivative of ${}^{fi}\psi_L$ with respect to ℓ. In terms of this partial derivative.

$$\varepsilon_\ell = \frac{\partial}{\partial \ell} ({}^{fi}\psi_L)\Delta\ell = \frac{4\pi}{\lambda_g} (\Delta\ell_f - \Delta\ell_i) \text{ radians,} \tag{7.54}$$

where the $\Delta\ell$'s are the errors in setting the positions of the load. If the uncertainty in setting the initial and final positions of the load is $|\Delta\ell|$, then the limit of motional error, lim ε_ℓ is

$$\lim \varepsilon_\ell = \frac{8\pi|\Delta\ell|}{\lambda_g} \text{ radians} = 1440 \frac{|\Delta\ell|}{\lambda_g} \text{ degrees.} \tag{7.55}$$

In general, the waveguide wavelength will not be uniform over a particular path between ℓ_f and ℓ_i because of variations in the dimensions. A limit of this error may be established by calculating the difference between the change of phase of Γ_L in a uniform waveguide with the maximum (or minimum) dimension and the change of phase in a uniform waveguide with the nominal dimension. Let this difference be termed the limit of tolerance error. If the tolerance of the waveguide dimension (maximum variation from the nominal value) is given by Δa, then a small limit of tolerance error, lim ε_a, can be obtained from

$$\lim \varepsilon_a = \frac{\partial}{\partial \lambda_g} ({}^{fi}\psi_L) \frac{\partial \lambda_g}{\partial a} \Delta a \text{ radians} \tag{7.57}$$

This error limit is proportional to the total change in phase of Γ_L, and therefore is presented as a fractional error, $\varepsilon_a / {}^{fi}\psi_L$, as

$$\lim \frac{\varepsilon_a}{{}^{fi}\psi_L} = \frac{\lambda_g^2}{4a^3} \Delta a. \tag{7.58}$$

d. Graphical Presentation of Results

It was assumed that the errors in the change of phase were small and therefore the individual contributions to the error could be summed. Two graphs, figures 7-4 and 7-5, present values of $|\Gamma_{2i}|$, and $|S_{31}/S_{32}S_{21}|$, respectively, which are used to estimate the limits of error from the two tuning errors given by eqs. (7.45) and (7.51) respectively. Two more graphs, figures 7-6 and 7-7 present limits of dimensional errors. The graphs of $|\Gamma_{2i}|$and $|S_{31}/S_{32}S_{21}|$ are applicable for any frequency range or waveguide size, while the graphs of limits of dimensional error are only applicable to WR-90 waveguide over the operating range of frequencies noted on the graphs. The equations used to construct these graphs, however, may be used for any size waveguide.

Figure 7-4 is a graph of the value of $|\Gamma_{2i}|$ plotted against the ratio of the maximum to the minimum response of the detector attached to arm 3, in decibels, as the tuning load (a short circuit) is moved along the waveguide. This value of $|\Gamma_{2i}|$ is to be used in eq. (7.45) to estimate lim $\varepsilon_{T.I}$.

Figure 7-5 is a graph of the value of $|S_{31}/S_{32}S_{21}|$ plotted against the ratio of the maximum to the minimum response of the detector attached to arm 3, in decibels, as the tuning load (having small reflection) is moved along the waveguide. This value of $|S_{31}/S_{32}S_{21}|$ is to be used in eq. (7.51) to estimate lim $\varepsilon_{T.II}$. In this portion of the tuning procedure, the magnitude of reflection coefficient of the tuning load usually lies within the range 0.001 to 0.1. Therefore, several curves are plotted for different $|\Gamma_{T.II}|$. It is only necessary to determine an upper limit to the magnitude of $\Gamma_{T.II}$ to estimate limits of error from this source.

Figure 7-6 is a graph of the limit of motional error plotted against the maximum uncertainty of motion imparted by the drive mechanism to the short circuit. Several curves are plotted for various frequencies throughout the recommended frequency range of WR-90 waveguide.

Figure 7-7 is a graph of the limit of tolerance error per degree of change of phase, in degrees error per degree of change of phase, applicable for any value of the change of phase of Γ_L. Several curves are plotted for different frequencies throughout the recommended frequency range of WR-90 waveguide.

As an example of the use of the graphs, assume that a standard phase shifter was made and used as follows. The load attached to arm 2 is made with a short-circuit adjustable with a micrometer of 0.0005-in. maximum uncertainty placed in a WR-90 waveguide of standard tolerance (± 0.003 in.). The tuning procedure for Γ_{2i} was carried out to 0.01-dB variation in the maximum to minimum response. The tuning for S_{31} was carried out to 1.0-dB variation in the maximum to minimum response with a tuning load of maximum VSWR of 1.01. The operating frequency is 9,000 MHz. The change of phase is 60°.

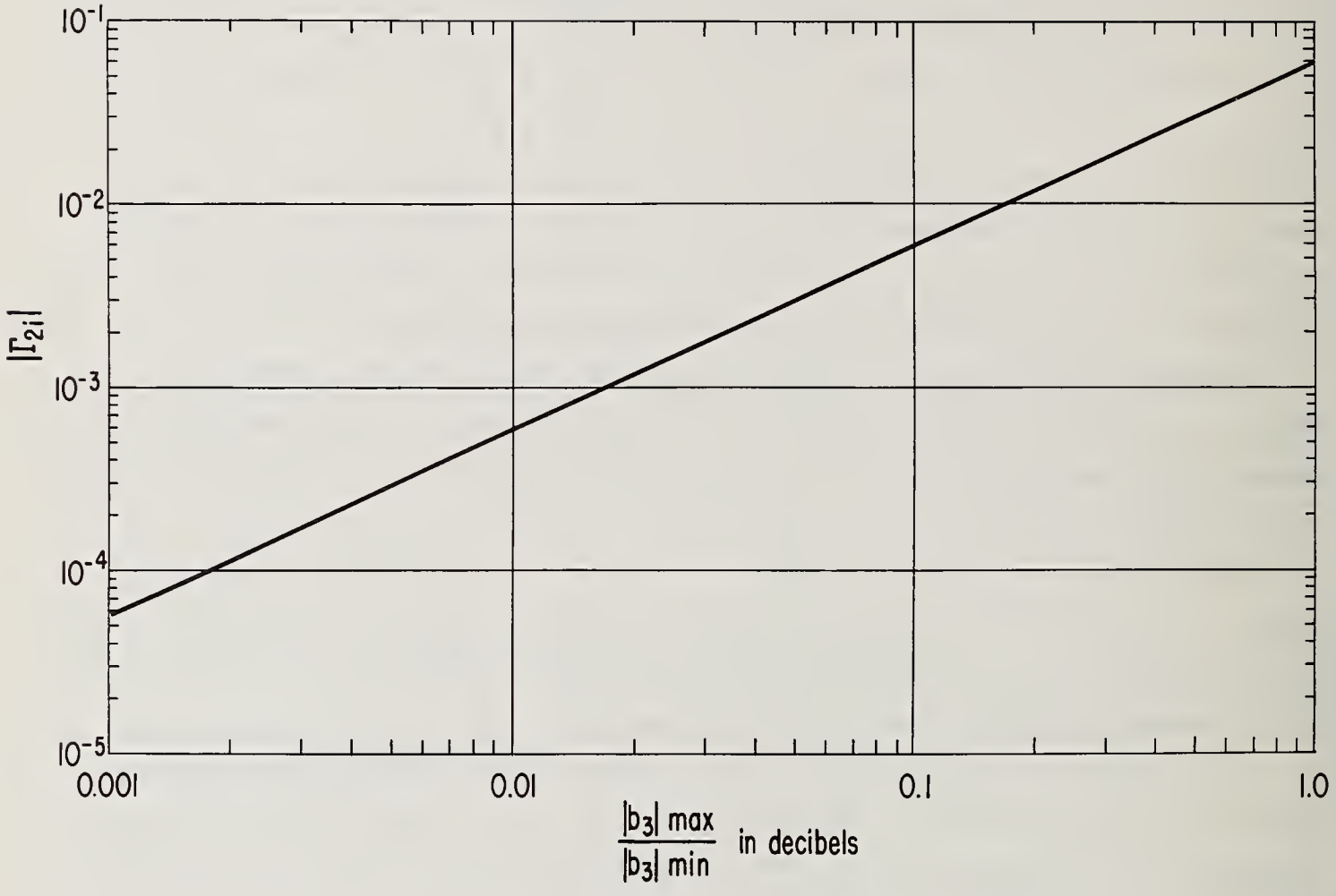

Figure 7-4. Graph for the determination of $|\Gamma_{2i}|$.

From figure 7-4, $|\Gamma_{2i}|$ for a 0.01-dB variation is 0.00058. From eq. (7.45), the limit of tuning error lim $\varepsilon_{T.I}$ is therefore 0.00058 radians or 0.033 deg. From

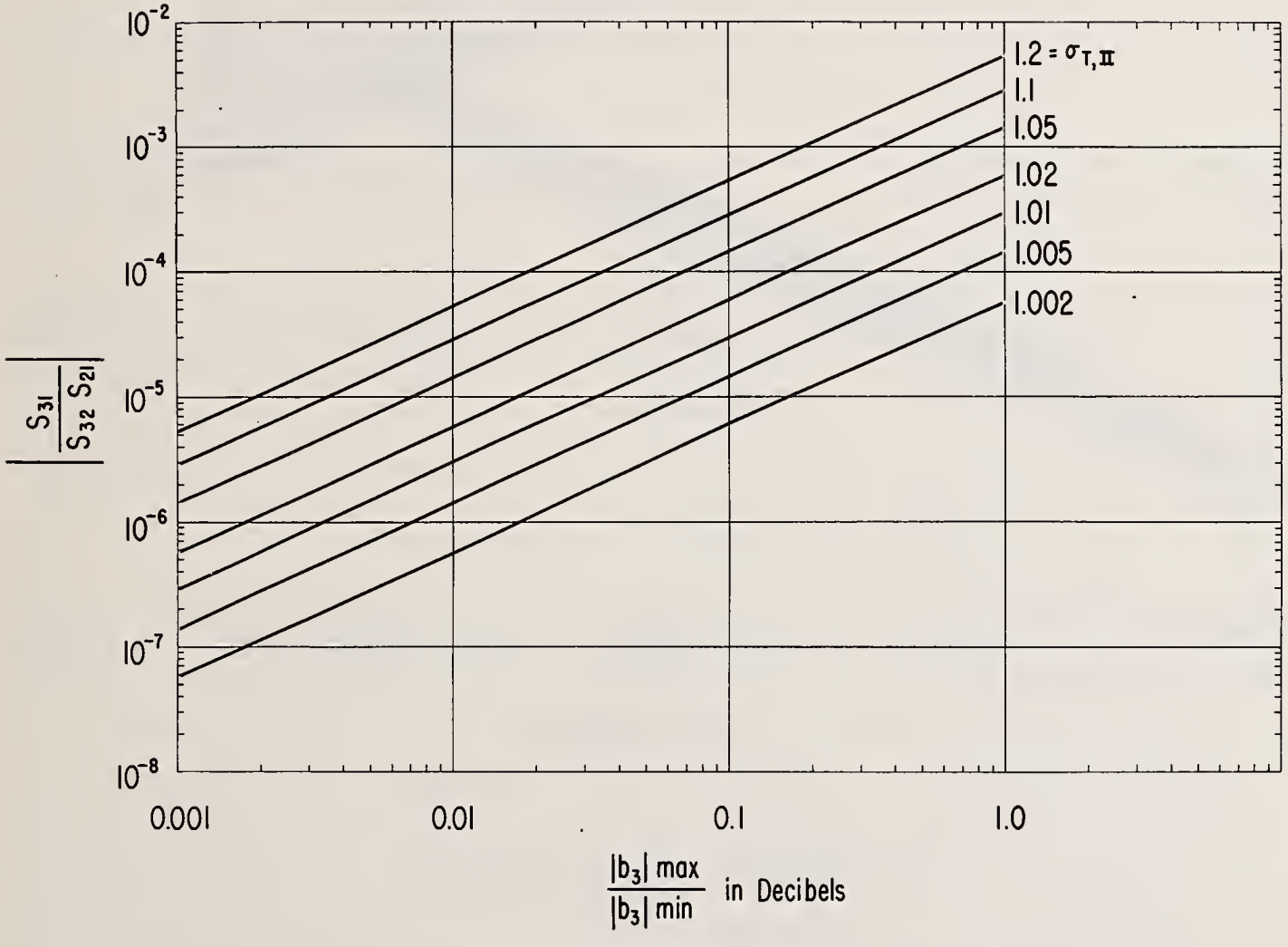

Figure 7-5. Graph for the determination of $|S_{31}/S_{32}S_{21}|$.

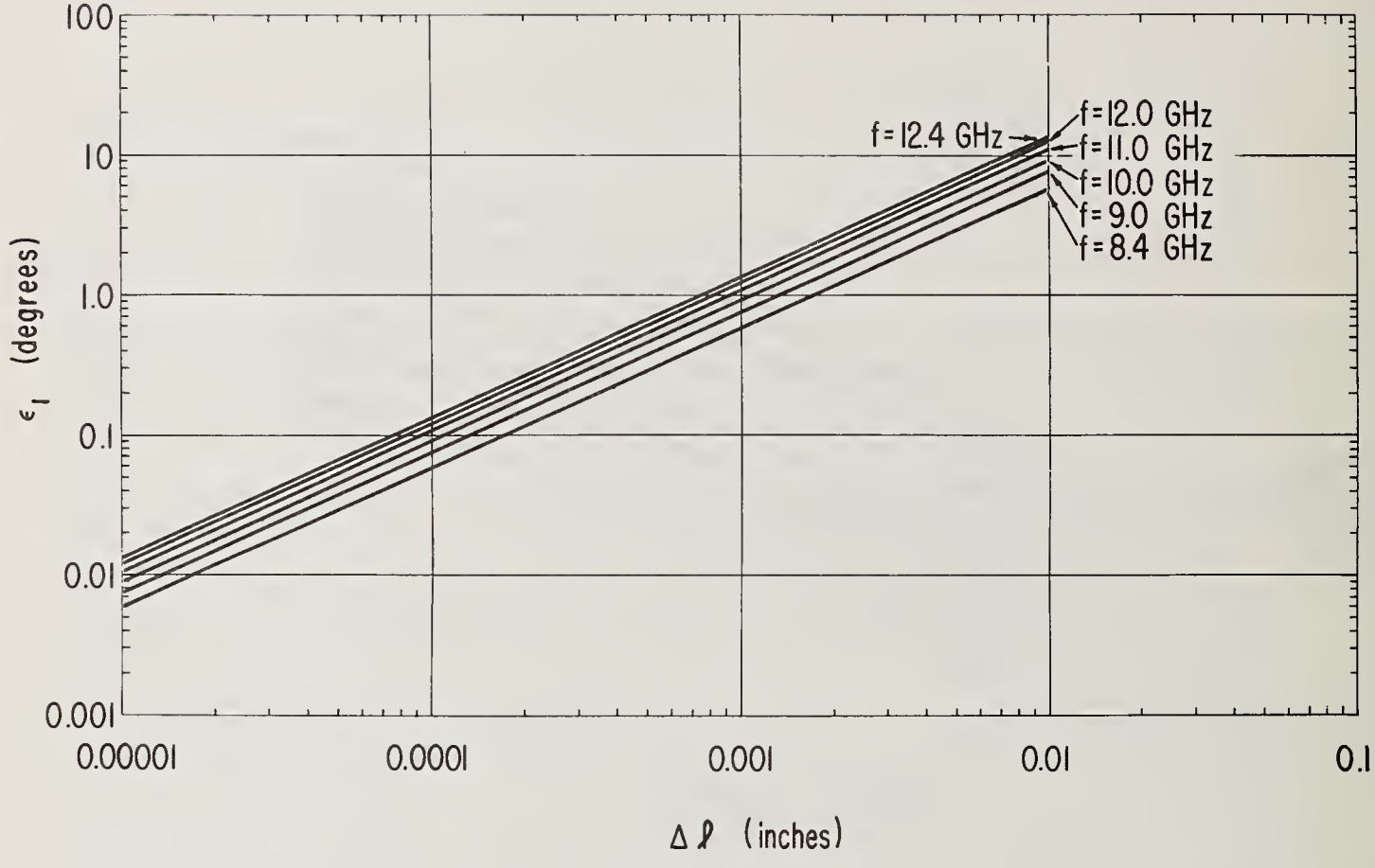

Figure 7-6. Limit of motional error.

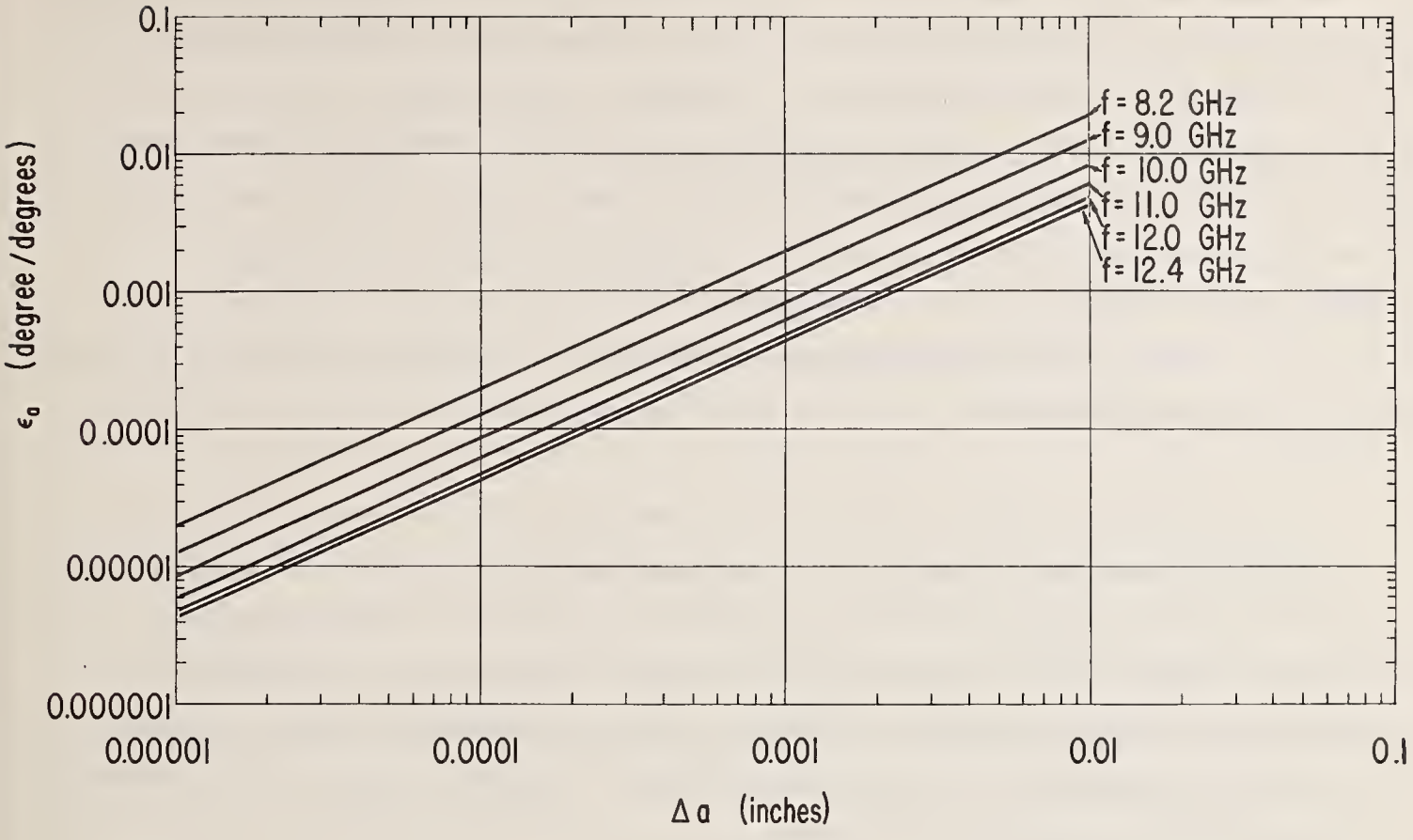

Figure 7-7. Limit of tolerance error.

figure 7-5, $|S_{31}/S_{32}S_{21}|$ for a 1.0-dB variation with a $|\Gamma_{T.II}|$ of 0.005 (VSWR = 1.01) is 0.00029. From eq. (7.51), the limit of tuning error, lim $\epsilon_{T.II}$, is 0.00029 radians or 0.018 deg. The total limit of tuning error is then 0.051 deg. From figure 7-6, for a tolerance of the micrometer of 0.0005 in., the limit of motional error at 9,000 Mc/s is 0.38 deg. From figure 7-7, for a tolerance of 0.003 in. in the dimension of the waveguide at 9,000 MHz, the limit of waveguide dimension error per degree of change of phase is 0.0038 deg/deg. For 60°, this is a limit of waveguide dimension error of 0.228°. The total limit of error from these sources is then 0.66 deg.

The above example is considered to be typical of readily constructed phase shifters since the tolerances were typical (WR-90) commercial tolerances and the tuning variations used can be attained in reasonably stable systems. However, precision waveguide sections, and tuning loads of very small reflection coefficients permit constructing standard phase shifters of extremely high accuracy. For example, the motional error may easily be reduced to 0.038 deg while precision waveguides have been constructed which have 0.00013°/deg limit of dimensional error per degree of change of phase. With such improvement in the dimensional errors, the total limit of error in the phase measurement described in the above example would be only 0.097 deg.

7.4. Differential Phase Shifter

It was mentioned in section 7.3 that a standard phase shifter can be constructed by combining a short-circuited section of uniform waveguide and a tuned, single directional coupler type of reflectometer, as shown in figure 7-2. In operation, the phase of the side arm output tracks the position of the short-circuiting plunger, once the tuning adjustments have been correctly made. The phase change ϕ corresponding to a displacement ℓ of the short circuit is

$$\phi = 2\beta\ell \tag{7.59}$$

where $\beta = 2\pi/\lambda_G$ and λ_G is the "guide wavelength."

In this section (a modified version of Beatty, 1964e) we suggest a method of obtaining a differential phase shifter by combining two phase shifters of the above type with ganged short circuits, as shown in figure 7-8. The phase shifters are

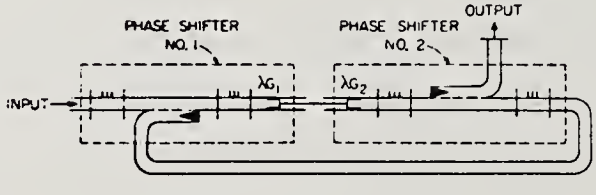

Figure 7-8. Differential phase shifter.

arranged so that the phase shift ψ of the output is the difference of the phase shifts produced by the two units, or $\psi = \phi_2 - \phi_1$. If the uniform waveguide sections in which the short circuits lie have identical cross sections, then $\phi_1 = \phi_2$ and the phase shift, $\psi = 0$. But if one waveguide section has a different cutoff wavelength λ_c from the other, then the phase shift ψ is not equal to zero; instead,

$$\psi = 4\pi\ell\left(\frac{1}{\lambda_{G_2}} - \frac{1}{\lambda_{G_1}}\right) \tag{7.60}$$

where the guide wavelength λ_G is related to the cutoff wavelength λ_c by

$$\frac{1}{\lambda_G{}^2} = \frac{1}{\lambda^2} - \frac{1}{\lambda_c{}^2}. \tag{7.61}$$

The cutoff wavelengths of the two waveguides can be chosen to produce any phase shift ψ between zero and the limiting case when one waveguide is operating below cutoff and the phase shift ψ is that of a single phase shifter alone.

Such a differential phase shifter has a number of potential applications such as the following. As the above standard phase shifter is extended to higher frequencies, say above 30 GHz, it takes a smaller displacement to produce the same phase shift; hence, errors in determining this displacement produce correspondingly larger errors in the phase shift. This situation can be avoided by using a differential phase shifter as described above, with the waveguide cutoff frequencies chosen so that the phase of the output varies more slowly than it would if it were tracking the position of one short circuit.

For example, at an operating frequency of 75 GHz, if one waveguide section is WR-15 and the other is WR-12, $\lambda_{G_1} = 0.5230$ cm, and $\lambda_{G_2} = 0.4719$ cm. A displacement of 0.2615 cm will produce a phase shift of 39 degrees, which is approximatly one ninth of the phase shift that would be produced by a single phase shifter using WR-12 waveguide.

Another application is in the investigation of uniformity of waveguide sections and the suitability of short circuits for phase shift standards. If the arrangement of figure 7-8 is used and the two waveguide sections are nominally identical, there will ideally be zero phase shift of the output as the short circuits are moved. Any phase shift which actually does occur is due to deficiencies in the short circuits or the waveguide sections, or in both.

Another application might consist of the determination of relative displacement from the measurement of phase shift. This would require that the motion of the

two short circuits be independent rather than ganged. The sensitivity of phase shift to relative displacement could be preselected by choosing the cutoff frequencies of the individual waveguides as desired.

If the tuners are dispensed with, the differential phase shifter will still function but with reduced accuracy, due to the finite directivities of the directional couplers and the reflections in the system. Errors in such a phase shifter were investigated (Ellerbruch, 1964) to find that tuning and dimensional errors were greater than with a single phase shifter, while the short-circuit position error was less. Thus, the device works best for small phase changes (less than 60 degrees). However, errors were further reduced in a different design based upon the same principle (Keys, 1968), in which two waveguide line stretchers were used.

8. Conclusions

In precisely defining the quantity to be measured, in developing accurate measuring techniques and standards, and in analyzing errors and evaluating limits of uncertainty, waveguide and circuit theory have been indispensable tools.

Theory deals with idealized concepts and models which approximately represent actual devices, circuits, and systems. The development of accurate measurement methods and standards is often a compromise in which the situation in the real world is controlled and adapted to fit a manageable theory. For example, uniform, cylindrical waveguide is used which has very low loss so that the theory of lossless waveguides will closely represent the actual situation. If losses or non-uniformities had to be rigorously taken into account, a more complicated model would need to be used, and the mathematics might become unwieldy or unmanageable. The use of "terminal invariant parameters," as proposed by Engen, would relieve the requirement of uniformity, but would still require losslessness.

The above point is also illustrated in section 6.6, where a more complicated model is used to represent an attenuator and the connector pairs which connect it into a waveguide circuit. The additional complexity is not justified unless one requires a reduction in the uncertainties in measuring attenuation.

In section 5.3, an impedance standard is described which can be closely approximated by a lossless section of short-circuited waveguide. The effect of small losses is calculated without assuming any change in the wall current distribution due to the losses. Also, the standard has in theory no current flowing across the waveguide joint connecting it to the measurement system. Thus the normal loss in the joint can be safely neglected.

In devising precise definitions of quantitites to be accurately measured, it is necessary to consider all of the assumptions and approximations which are made, then try to specify and control the measurement system and the conditions of measurement to fit the theory. There is always some "fuzziness" in the evaluation of measurement uncertainties. The reduction of this fuzziness begins with the sharpening of the definition of the quantity to be measured and tightly specifying the conditions of measurement.[1] This point is illustrated in section 6.2g with regard to definitions of attenuation. The same principle might also be applied to other quantities if accuracy requirements increase.

---

[1] In Eisenhart (1963) the concept of a "true value" is discussed.

Circuit theory can sometimes be used to explain the operation of a device such as the adjustable sliding termination of section 5.2. The termination is regarded as an attenuator terminated in a short-circuited waveguide of variable length, and design criteria are developed. Instead of using complicated field theory, simpler circuit theory suffices in this instance.

The use of tuners with reflectometers was well known, but the analytical techniques which were developed in section 3.15f, section 5.4, and section 5.5 permitted the analysis and evaluation of limits of uncertainty due to imperfectly adjusted tuners. There is always a limit to how well one can adjust a tuner due to limitations of the equipment used to recognize when the adjustment has been correctly made.

The reduction of errors depends upon how well they are understood. The analysis of mismatch errors in power measurements in section 4.2 led to a large reduction in the errors due to mismatch. It became clear that it was important to reduce the source mismatch, which could be controlled and minimized by the calibrator. Once the source was well-matched, the limit of uncertainty could be calculated from a knowledge of the VSWR's of the power meters. The calibrator could then quote a conservative limit of uncertainty for this measurement.

The examples of applications given here deal only with power, impedance, attenuation and phase shift. They represent only a small portion of the applications of waveguide and circuit theory to the development of accurate measurement methods and standards. There are numerous other applications in the measurement of frequency, noise temperature, antenna and horn gain, etc.

After an accurate measurement method and standard has been developed for a given quantity in a frequency range where none existed before, the need for increased accuracies and ranges of measurement continues, but sometimes at decreased urgency. The theory and techniques described should prove useful in extending the frequency range higher into the millimeter, sub-millimeter, infrared and optical regions.

9. References

[1] Adams, J. W. and R. F. Desch (1968), Experimental confirmation of barretter substitution error, IEEE Trans. on MTT 16, No. 3, 201-202.

[2] Adams, J. W. and S. Jarvis, Jr. (1969), Current distribution in barretters and its application to microwave power measurements, IEEE Trans. on MTT 17, No. 10, 778-785.

[3] AIEE (1942), American Standard Definitions of Electrical Terms, The American Institute of Electrical Engineers, New York, N.Y.

[4] Almassy, G. (1971), A first-order correction to sliding short behaviour with application to the problem of measuring small losses, IEEE Trans. on I & M 20, No. 3, 162-169.

[5] Altschuler, H. M. (1962), The measurement of arbitrary linear microwave two-ports, Proc. IEE (London) 109, Part B, Supplement No. 23, 704-712.

[6] Altschuler, H. M. (1963), Attenuation and Phase Constants, Chapter VI, 1, Handbook of Microwave Measurements, 3rd ed. (Polytechnic Press, Brooklyn,N.Y.).

[7] Andrews, W. A. (1955), U.S. Patent No. 2, 701,861, 2-8-55.

[8] Anson, W. J. (1961), A guide to the use of the modified reflectometer technique of VSWR measurement, J. Res. NBS (U.S.) 65C, No. 4, 217-223.

[9] Barnett, E. F. (1953), More about the HP precision directional couplers, Hewlett-Packard Jour. 4, No. 5-6, 1-4.

[10] Beatty, R. W. (1950), Determination of attenuation from impedance measurements, Proc. IRE 38, No. 8, 895-897.

[11] Beatty, R. W. (1954), Mismatch errors in the measurement of ultrahigh-frequency and microwave variable attenuators, J. Res. NBS (U.S.) 52, No. 1, 7-9.

[12] Beatty, R. W. (1957), An adjustable sliding termination for rectangular waveguide, IRE Trans. on MTT 5, No. 3, 192-194.

[13] Beatty, R. W. (1959), Magnified and squared VSWR responses for microwave reflection coefficient measurements, IRE Trans. on MTT 7, No. 3, 346-350.

[14] Beatty, R. W. (1960), U.S. Patent No. 2,922,963, Jan. 26, 1960.

[15] Beatty, R. W. (1964a), Insertion loss concepts, Proc. IEEE 52, No. 6, 633-671.

[16] Beatty, R. W. (1964b), Effects of connectors and adapters on accurate attenuation measurements at microwave frequencies, IEEE Trans. on Instr. 13, No. 4, 272-284.

[17] Beatty, R. W. (1964c), Intrinsic attenuation, IEEE Trans. on MTT 11, No. 3, 179-182.

[18] Beatty, R. W. (1964d), Some basic microwave phase shift equations, Radio Sci. J. Res., NBS/USNC-URSI 68D, No. 4, 349-353.

[19] Beatty, R. W. (1964e), A differential microwave phase shifter, IEEE Trans. on MTT 12, No. 2, 250-251.

[20] Beatty, R. W. (1965), A two-channel nulling method for measuring attenuation constants of short sections of waveguide and the losses in waveguide joints, Proc. IEEE 53, No. 6, 642-643.

[21] Beatty, R. W. (1967a), Impedance measurements and standards for uniconductor waveguide, Proc IEEE 55, No. 6, 933-941.

[22] Beatty, R. W. (1967b), Microwave attenuation measurements and standards, NBS Monograph 97.

[23] Beatty, R. W. (1971), Short discussion of error reduction in network-parameter measurement through computerized automation, Progress in Radio Science 1966-1969 2, International Union of Radio Science, Brussels, Belgium.

[24] Beatty, R. W. (1972a), Efficiencies of microwave 2-ports from reflection coefficient measurements, IEEE Trans. on MTT 20, No. 5, 343-344.

[25] Beatty, R. W. (1972b), Invariance of the cross ratio applied to microwave network analysis, Nat'l. Bureau of Standards (U.S.) Technical Note 623, 26 p., issued Sept. 1972.

[26] Beatty, R. W. and W. J. Anson (1962), Application of reflectometer techniques to accurate reflection measurements in coaxial systems, Proc. IEE (London) 109, Part B, No. 46, 345-348.

[27] Beatty, R. W., G. F. Engen, and W. J. Anson (1960), Measurements of reflections and losses of waveguide joints and connectors using microwave reflectometer techniques, IRE Trans. on Instr. 9, No. 2, 219-226.

[28] Beatty, R. W. and G. H. Fentress (1968), An attenuation and phase shift divider circuit, Proc. IEEE 56, No. 11, 2063-2064.

[29] Beatty, R. W. and G. H. Fentress (1971), A simple tuning circuit for waveguide and transmission line systems, IEEE Trans. on MTT 19, No. 3, 337-338.

[30] Beatty, R. W., and D. M. Kerns (1958), Recently developed microwave impedance standards and methods of measurement, IRE Trans. on Instr. 7, Nos. 3 and 4, 319-321.

[31] Beatty, R. W., and A. C. MacPherson (1953), Mismatch errors in microwave power measurements, Proc. IRE 41, No. 9, 1112-1119.

[32] Beatty R. W., and F. Reggia (1955), An improved method of measuring efficiencies of ultra-high-frequency and microwave bolometer mounts, J. Res. NBS (U.S.) 54 No. 6, 321-327.

[33] Beatty, R. W., and B. C. Yates (1969) A graph of return loss versus frequency for quarter-wavelength short-circuited waveguide impedance standards, IEEE Trans. on MTT 17, No. 5, 282-284.

[34] Bodway, G. E. (1967), Two port power flow analysis using generalized scattering parameters, Microwave Journal 10, No. 6, 61-69.

[35] Booth, S. F. (1961), Precision Measurement and Calibration, Vol. I, Electricity and Electronics, Nat'l. Bureau of Standards Handbook 77, Vol. I, 695-735.

[36] Brady, M. M. (1967), Worldwide specs on rectangular waveguides and flanges, MicroWaves 6, No. 7, 33-38.

[37] Carlin, H. J., and M. Sucher (1952), Accuracy of bolometric power measurements, Proc. IRE 40, No. 2, 1042-1048.

[38] Crowell, T. Y. Co. staff (1962), Roget's International Thesaurus, 3rd Ed. (Thomas Y. Crowell Co., New York, N.Y.).

[39] Cullen, A. L. (1949), Measurement of microwave transmission efficiency, Wireless Engrg. 26, No. 11, 255-258.

[40] deRonde, F. C. (1957), Un élément simple pour mesurer des impédances en ondes centimétriques et millimétriques: la terminaison variable à réglages indépendants et à lecture directe du module et de l'argument du coefficient de réflexion, Archives des Sciences 10, fasc. spéc., 66-67.

[41] Desch, R. F., and R. E. Larson (1963), Bolometric microwave power calibration techniques at the National Bureau of Standards, IEEE Trans. on I & M 12, No. 1, 29-33.

[42] Deschamps, G. A. (1953), Determination of reflection coefficients and insertion loss of a waveguide junction, J.A.P. 24, No. 8, 1046-1050.
[43] Eisenhart, C. (1963), Realistic evaluation of the precision and accuracy of instrument calibration systems, J. Res. NBS (U.S.) 67C, No. 2, 161-187.
[44] Ellenwood, R. C., and W. E. Ryan (1953), A uhf and microwave matching termination, Proc. IRE 41, No. 1, 104-107.
[45] Ellerbruch, D. A. (1964), Analysis of a differential phase shifter, IEEE Trans. on MTT 12, No. 4, 453-459.
[46] Engen, G. F. (1957), A self-balancing direct-current bridge for accurate bolometric power measurements, J. Res. NBS (U.S.) 59, No. 2, 101-105.
[47] Engen, G. F. (1958), Amplitude stabilization of a microwave signal source, IRE Trans. on MTT 6, No. 2, 202-206.
[48] Engen, G. F. (1961), A bolometer mount efficiency measurement technique, J. Res. NBS (U.S.) 65C, No. 2, 113-124.
[49] Engen, G. F. (1966), Coaxial power meter calibration using a waveguide standard, J. Res. NBS (U.S.) 70C, No. 2, 127-138.
[50] Engen, G. F. (1969), An Introduction to the Description and Evaluation of Microwave Systems Using Terminal Invariant Parameters, NBS Monograph No. 112.
[51] Engen, G. F. (1972), An extension to the sliding short method of connector and adapter evaluation, J. Res. NBS (U.S.) 76C, Nos. 3 & 4, 177-183.
[52] Engen, G. F. and R. W. Beatty (1959), Microwave reflectometer techniques, IRE Trans. on MTT 7, No. 3, 351-355.
[53] Engen, G. F. and R. W. Beatty (1960), Microwave attenuation measurements with accuracies from 0.0001 to 0.06 dB over a range of 0.01 to 50 dB, J. Res. NBS (U.S.) 64C, No. 2, 139-145.
[54] Fairchild's Dictionary of Textiles (1967), Ed. by Isabel B. Wingate (Fairchild Publications, New York, N.Y.).
[55] Funk and Wagnall's New Standard Dictionary of the English Language (1965) (Funk and Wagnall's, New York, N.Y.).
[56] Ginzton, E. L. (1957), Microwave Measurements (McGraw-Hill Book Co. Inc., New York, N.Y.).
[57] Grantham, R. E. (1951), A reflectionless waveguide termination, Rev. Sci. Instr. 22, No. 11, 828-834.
[58] Gray, Peter (1967), The Dictionary of the Biological Sciences (Reinhold Publishing Corp., New York, N.Y.).
[59] Griesheimer, R. N (1947), Microwave power measurements, Chapter 3, Technique of Microwave Measurements, C. G. Montgomery, Ed., 1st Ed., 79-220 (McGraw-Hill Book Co., Inc. New York, N.Y).
[60] Hand, B. P., and N. B. Schrock (1951), Power measurements from 10 to 12,400 megacycles, Hewlett-Packard Jour. 2, No. 7-8, 1-4.
[61] Harris, I. A. (1965), Mode of use and assessment of precision coaxial connectors, Proc. IEE (London) 112, No. 11, 2025-2032.
[62] Hashimoto, S. (1968), A new method for determination of mismatch errors in cascade-connected attenuators, Bull. Electrotechnical Lab., Japan 32, No. 10, 1028-1037 (In Japanese, abstract in English).
[63] Holm, J. D., D. L. Johnson, and K. S. Champlin (1967), Reflections from rotary-vane precision attenuators, IEEE Trans. on MTT 15, No. 2, 123-124.

[64] IRE Dictionary of Electronics Terms and Symbols (1961) (The Institute of Radio Engineers, Inc., New York, N.Y.).

[65] IEEE Standard Dictionary of Electrical and Electronics Terms (1972) (Wiley Interscience, New York, N.Y.).

[66] Jackson, Willis (1951), High Frequency Transmission Lines, 3rd Ed. (John Wiley and Sons, Inc., New York, N.Y.).

[67] Jarvis, S., Jr., and J. W. Adams (1968), Calculation of substitution error in barretters, J. Res. NBS (U.S.) 72C, No. 2, 127-137.

[68] Jordan, E. C. (1950), Electromagnetic Waves and Radiating Systems (Prentice-Hall, Inc., New York, N.Y.).

[69] Kato, N., and T. Sakai (1955), Waveguide type variable impedance circuit and its application to the Rieke diagram, Report of the Microwave Commun. Res. Comm. in Japan, 7.

[70] Kerns, D. M. (1949a), Basis of the application of network equations to waveguide problems, J. Res. NBS (U.S.) 42, No. 5, 515-540.

[71] Kerns, D. M. (1949b), Determination of efficiency of microwave bolometer mounts from impedance data, J. Res. NBS (U.S.) 42, No. 6, 579-585.

[72] Kerns, D. M. (1951), Analysis of symmetrical waveguide junctions, J. Res. NBS (U.S.) 46, No. 4, 267-282.

[73] Kerns, D. M. (1967), Definitions of v, i, Z, Y, a, b, Γ, and S, Proc. IEEE 55, No. 6, 892-900.

[74] Kerns, D. M., and R. W. Beatty (1967), Basic Theory of Waveguide Junctions and Introductory Microwave Network Analysis (Pergamon Press, New York, N.Y.).

[75] Keys, J. E. (1968), Differential microwave phase shifter, Radio Science 3, No. 3, 303-304.

[76] Kienlin U., and A. Kürzl (1958), Reflexionen an Hohlleiter-Flanschverbindungen, Nachr tech. Z. heft. 11, 561-564.

[77] Larson, R. E. (1962), Microwave measurements in the NBS electronic calibration center, Proc. IEE (London) 109, Part B, Supplement No. 23, 644-650.

[78] Leber, A. N. (1964), Method free from mismatching errors from measuring the loss of attenuators, IEEE Trans. on MTT 12, No. 4, 480.

[79] Little, W. E., W. Larson, and B. J. Kinder (1971), Rotary-vane attenuator with an optical readout, J. Res. (U.S.) 75C, No. 1, 1-5.

[80] Magid, M. (1958), Precision microwave phase shift measurements, IRE Trans. on Instr. 7, Nos. 3 and 4, 321-331.

[81] Macpherson, A. C., and D. M. Kerns (1950), Accuracy with which two loads can be matched on a magic T, Electronics 23, No. 9, 190.

[82] Macpherson, A. C., and D. M. Kerns (1956), A new technique for the measurement of microwave standing-wave ratios, Proc. IRE 44, No. 8, 1024-1030.

[83] Mathis, H. F. (1954), Experimental procedures for determining the efficiency of four-terminal networks, J.A.P. 25, No. 8, 982-986.

[84] Mathis, H. F. (1955), Measurements of reflection coefficients through a lossless network, IRE Trans. on MTT 3, No. 5, 58.

[85] Michels, W. C., Ed. (1961), The International Dictionary of Physics and Electronics, 2nd Ed. (D. Van Nostrand Co. Inc., New York, N.Y.).

[86] Mirsky, L. (1955), An Introduction to Linear Algebra (Oxford University Press, Oxford, England).

[87] Rabinovitch, B. E. (1962), Method free from mismatching errors for measuring the loss of attenuators, (In Russian) Izmeritelnaya Tekh., 44-47. Meas. Tech., 238-243 (In English).

[88] Rumfelt, A. Y., and L. B. Elwell (1967), Radio frequency power measurements, Proc. IEEE 55, No. 6, 837-850.

[89] Schafer, G. E. (1960), Mismatch errors in microwave phase shift measurements, IRE Trans. on MTT 8, No. 6, 617-622.

[90] Schafer, G. E., and R. W. Beatty (1958), A method for measuring the directivity of directional couplers, IRE Trans. on MTT 6, No. 4, 419-422.

[91] Schafer, G. E., and R. W. Beatty (1960), Error analysis of a standard microwave phase shifter, J. Res. NBS (U.S.) 64C, No. 4, 261-265.

[92] Schafer, G. E. and A. Y. Rumfelt (1959), Mismatch errors in cascade-connected variable attenuators, IRE Trans. on MTT 7, No. 4, 447-453.

[93] Southworth, G. C. (1950), Principles and Applications of Waveguide Transmission (D. Van Nostrand Co. Inc., New York, N.Y.).

[94] Storer, J.E. et al. (1953), A simple graphical analysis of a two port waveguide junction, Proc. IRE 41, No. 8, 1004-1013.

[95] Townsend, E. J. (1915), Functions of a Complex Variable, 178-182 (Henry Holt and Co., New York, N.Y.).

[96] Tweney, C. F., and L. E. C. Hughes, Ed. (1961), Chamber's Technical Dictionary (The Macmillan Company, New York).

[97] Warner, F. L., D. O. Watton, and P. Herman (1972), A very accurate x band rotary attenuator with an absolute digital angular measuring system, IEEE Trans. on I & M 21, No. 4, 446-450.

[98] Weber, E. (1947), The Measurement of Attenuation, Chapter 13, Technique of Microwave Measurements, MIT Rad. Lab Series, 11, 804-853 (McGraw-Hill Book Co. Inc., New York, N.Y.).

[99] Webster, N. (1806), A Compendious Dictionary of the English Language, facsimile edition, 1970, Bounty Books, Crown Publishers, Inc., New York, N.Y.

[100] Weinschel, B. O. (1960), Development in attenuation measurements and standards, J. Res. NBS (U.S.) 64D, No. 6, 599-600 (URSI U.S. Nat'l. Comm. Reports).

[101] Youla, D. C., and P. M. Paterno (1964), Realizable limits of error for dissipationless attenuators in mismatched systems, IEEE Trans. on MTT 12, No. 3, 288-289.

FORM NBS-114A (1-71)

U.S. DEPT. OF COMM. BIBLIOGRAPHIC DATA SHEET	1. PUBLICATION OR REPORT NO. NBS-MN-137	2. Gov't Accession No.	3. Recipient's Accession No.

4. TITLE AND SUBTITLE

Applications of Waveguide and Circuit Theory to the Development of Accurate Microwave Measurement Methods and Standards

5. Publication Date: August 1973

6. Performing Organization Code

7. AUTHOR(S)

R. W. Beatty

8. Performing Organization

9. PERFORMING ORGANIZATION NAME AND ADDRESS

NATIONAL BUREAU OF STANDARDS, Boulder Labs.
DEPARTMENT OF COMMERCE
Boulder, Colorado 80302

10. Project/Task/Work Unit No.: 2721115

11. Contract/Grant No.

12. Sponsoring Organization Name and Address

Same as Item 9.

13. Type of Report & Period Covered: Final

14. Sponsoring Agency Code

15. SUPPLEMENTARY NOTES

16. ABSTRACT (A 200-word or less factual summary of most significant information. If document includes a significant bibliography or literature survey, mention it here.)

The basic theory and analytical methods used in the development of accurate microwave measurement methods and standards are presented.

Developments at the U. S. National Bureau of Standards during 1948-1968 are described in which the above theory and analytical methods were applied.

These developments were in the fields of power, impedance, attenuation and phase shift, and led to the establishment of National Standards and calibration methods at frequencies from about 300 MHz to 30 GHz.

17. KEY WORDS (Alphabetical order, separated by semicolons) Attenuation definitions; attenuation measurement; barretter mount efficiency; coaxial connectors; impedance measurement; microwave network theory; mismatch errors; phase shift-measurement; power measurement; reflectometers; waveguide joints; waveguide theory.

18. AVAILABILITY STATEMENT

[X] UNLIMITED.

[ ] FOR OFFICIAL DISTRIBUTION. DO NOT RELEASE TO NTIS.

19. SECURITY CLASS (THIS REPORT): UNCLASSIFIED

21. NO. OF PAGES: 322

20. SECURITY CLASS (THIS PAGE): UNCLASSIFIED

22. Price: $5.20

USCOMM-DC 66244-P71

★ U.S. GOVERNMENT PRINTING OFFICE : 1973 O—508-680